

**Mesoporous silica nanoparticle incorporation  
of essential oils onto synthetic textiles for  
tailored antimicrobial activity**

**John Lillie**

**PhD 2016**

**Mesoporous silica nanoparticle incorporation  
of essential oils onto synthetic textiles for  
tailored antimicrobial activity**

**John Lillie**

A thesis submitted in partial fulfilment of the  
requirements of the Manchester Metropolitan  
University for the degree of Doctor of Philosophy

School of Healthcare Science of Manchester  
Metropolitan University

2016

## **Acknowledgements**

Firstly I would like to wholeheartedly thank my Director of Studies Professor Bill Gilmore, without whom, this project, and completion to PhD would not have been possible. In addition, I would like to thank Professor Jo Verran for her insight, expertise, and support over the course of the project. Special thanks is reserved for the final member of my supervisory team, Dr. Christopher Liauw, for guiding and supporting me during the project and in particularly the writing of the thesis. His technical expertise has been invaluable in driving the research forward and the precise manner in which it is now presented. I would also like to thank the Healthcare Science Research Centre, for providing me with a studentship.

In addition to my supervisory team, there have been a number of researchers and technical staff who provided advice and made the research possible. I would like to thank, Lee Harman, Dr. Paul Benson, Elaine Howarth, Dr. Lubomira Tosheva, Hayley Andrews and Dr. Mike Dempsey for their contributions.

I would also like to thank some of my dearest friends for their words of encouragement when I felt as though the wind had faded from my sails, Dr. Warren Flood, Dr. Carmine Circelli and Dr. Andrew James, it is appreciated.

In addition, I would like to thank my cousin, Professor Dean Felsher for his words of advice and constant encouragement, during the course of my academic career, truly an inspiration.

Finally, the rock solid support and love from my family has enabled me to be in this position. Mum, Dad, Sam, thank you, your love and support is fully reciprocated.

## **Declaration**

I declare that this work has not already been accepted for any degree and is not being currently submitted in candidature for any other than the degree of Doctor of Philosophy of the Manchester Metropolitan University

## Table of contents

<b>ABSTRACT .....</b>	<b>I</b>
<b>STRUCTURE OF THESIS .....</b>	<b>II</b>
<b>LIST OF TABLES.....</b>	<b>II</b>
<b>LIST OF FIGURES .....</b>	<b>VI</b>
<b>LIST OF EQUATIONS.....</b>	<b>XV</b>
<b>LIST OF ABBREVIATIONS.....</b>	<b>XV</b>
<b>CHAPTER 1 .....</b>	<b>1</b>
1.1 HEALTHCARE ASSOCIATED INFECTIONS.....	2
<i>Includes infections of bones and joints and the central nervous system. Often linked to surgical or invasive procedures.....</i>	4
1.2 ANTIMICROBIAL RESISTANCE .....	5
1.3 BACTERIAL RESERVOIRS, ENVIRONMENTAL CLEANING AND PERSISTENCE.....	7
<b>CHAPTER 2 .....</b>	<b>14</b>
2.1 INTRODUCTION .....	15
2.1.1 <i>Essential oils .....</i>	15
2.1.2 <i>Mode of action.....</i>	16
2.1.3 <i>Essential oils used in this study.....</i>	19
2.1.4 <i>Screening of essential oils.....</i>	21
2.1.5 <i>The bacterial cell .....</i>	23
2.1.6 <i>Microorganisms.....</i>	24
2.1.6.1 <i>Pseudomonas aeruginosa .....</i>	25
2.1.6.2 <i>Staphylococcus aureus .....</i>	25
2.1.6.3 <i>Methicillin resistant Staphylococcus aureus .....</i>	26
2.1.6.4 <i>Escherichia coli.....</i>	26
2.1.6.5 <i>Candida albicans.....</i>	27
2.1.7 <i>Gas chromatography mass spectroscopy.....</i>	28
2.2 OBJECTIVES.....	31
2.3 EXPERIMENTAL.....	31
2.3.1 <i>Materials.....</i>	31
2.3.1.1 <i>Culture media .....</i>	31
2.3.1.2 <i>Microorganisms.....</i>	32
2.3.1.3 <i>Essential oils .....</i>	32
2.3.2 <i>Methods .....</i>	33
2.3.2.1 <i>Preparation of cell suspensions.....</i>	33
2.3.2.2 <i>Growth curves.....</i>	33
2.3.3 <i>Agar dilution assay .....</i>	34
2.3.4 <i>Disk diffusion assay.....</i>	34
2.3.5 <i>Broth micro-dilution assay .....</i>	35
2.3.6 <i>Time – Kill assay.....</i>	36
2.3.7 <i>Checkerboard blend assay.....</i>	37
2.3.8 <i>GC-MS analysis of essential oils.....</i>	40
2.4 RESULTS AND DISCUSSION.....	41
2.4.2 <i>Disk diffusion of individual essential oils.....</i>	44
2.4.3 <i>Agar dilution of individual essential oils .....</i>	45
2.4.4 <i>Broth micro-dilution of individual essential oils.....</i>	47
2.4.5 <i>Time kill assays.....</i>	52
2.4.6 <i>Checkerboard blending assay.....</i>	60
2.4.7 <i>Gas chromatography – mass spectroscopy (GC-MS) analysis.....</i>	64
2.5 CONCLUSIONS.....	75
<b>CHAPTER 3 .....</b>	<b>76</b>

3.1 INTRODUCTION .....	77
3.1.1 <i>Mesoporous silica nanoparticles</i> .....	77
3.1.2 <i>Characterisation methods</i> .....	80
3.1.2.1 Scanning electron microscopy .....	81
3.1.2.2 Electrophoretic light scattering.....	82
3.1.2.3 Nitrogen adsorption.....	82
3.1.2.4 Thermogravimetric analysis .....	84
3.2 OBJECTIVES.....	86
3.3 MATERIALS.....	87
3.3.1 <i>Chemicals</i> .....	87
3.3.2 <i>Media, microbes and EOs</i> .....	87
3.4 EXPERIMENTAL.....	87
3.4.1 <i>MSN fabrication</i> .....	87
3.4.2 <i>Characterisation of MSN</i> .....	88
3.4.2.1 Zeta potential.....	88
3.4.2.2 SEM.....	88
3.4.2.3 Nitrogen adsorption.....	89
3.4.2.4 Thermal gravimetric analysis.....	90
3.4.3 <i>Loading of EO blend into MSNs</i> .....	90
3.4.4 <i>Release of EO from MSNs</i> .....	91
3.4.5 <i>Molecular modelling of EO antimicrobial components</i> .....	92
3.4.6 <i>Antimicrobial testing of blank and EO loaded MSNs</i> .....	92
3.4.7 <i>Growth inhibition assays of blank MSNs</i> .....	93
3.4.8 <i>Bactericidal assays</i> .....	94
3.4.9 <i>Time-kill assays</i> .....	94
3.5 RESULTS AND DISCUSSION .....	96
3.5.1 <i>Characterisations of MSN</i> .....	96
3.5.1.1 Thermogravimetric analysis (TGA).....	96
3.5.1.2 Zeta potential.....	99
3.5.1.3 Scanning electron microscopy .....	100
3.5.1.4 Nitrogen Adsorption of MSNs.....	103
3.5.2 <i>Molecular modelling of major EO constituents</i> .....	106
3.5.3 <i>Loading of EOs into MSNs, solvent evaporation studies</i> .....	108
3.5.3.1 Solvent evaporation loading .....	108
3.5.3.2 EO immersion loading.....	111
3.5.3.3 EO release from loaded MSNs .....	120
3.5.4 <i>Antimicrobial testing of blank and EO loaded MSNs</i> .....	122
3.5.4.1 Blank MSNs growth inhibition assay .....	122
3.5.4.2 Bactericidal activity of EO loaded MSNs.....	124
3.5.4.3 Time-kill assays.....	125
3.6 CONCLUSIONS.....	131
<b>CHAPTER 4.....</b>	<b>132</b>
4.1 INTRODUCTION .....	133
4.1.1 <i>Organically modified silicates (Ormosils)</i> .....	133
4.1.2 <i>Silane coupling linkers</i> .....	134
4.1.3 <i>Gas chromatography</i> .....	136
4.1.4 <i>Attenuated total reflectance Fourier transform infrared spectroscopy (ATR FTIR)</i> .....	136
4.1.5 <i>Scanning electron microscopy</i> .....	137
4.2 OBJECTIVES.....	138
4.3 MATERIALS.....	138
4.3.1 <i>Chemicals</i> .....	138
4.3.2 <i>Solvents</i> .....	139
4.3.3 <i>Media, microbes and EOs</i> .....	139
4.4 EXPERIMENTAL.....	139
4.4.1 <i>Ormosil synthesis and textile stiffness</i> .....	139
4.4.2 <i>Affixation methods</i> .....	141
4.4.2.1 One pot synthesis .....	141
4.4.2.2 Silane grafted MSNs.....	141
4.4.2.3 Layer by layer treatment .....	142
4.4.2.4 Analysis of optimal MSN coverage of synthetic fibres.....	144

4.4.3	<i>EO release from loaded textiles</i> .....	145
4.4.4	<i>Attenuated total reflectance (ATR) FTIR analysis of affixation layers</i> .....	145
4.4.5	<i>SEM</i> .....	146
4.5	RESULTS AND DISCUSSIONS.....	146
4.5.1	<i>Ormosil treated textile stiffness</i> .....	146
4.5.2	<i>Affixation methods</i> .....	153
4.5.2.1	<i>One pot synthesis</i> .....	154
4.5.2.2	<i>Silane grafted MSNs</i> .....	155
4.5.2.3	<i>Layer-by-layer</i> .....	157
4.5.2.4	<i>Optimal MSN coverage of synthetic fibres analysis</i> .....	158
4.5.3	<i>EO release from loaded textile</i> .....	161
4.5.4	<i>ATR FTIR analysis of affixation layers</i> .....	163
4.6	CONCLUSIONS.....	167
<b>CHAPTER 5</b> .....		<b>168</b>
5.1	INTRODUCTION .....	169
5.1.1	<i>Textiles and the skin</i> .....	169
5.1.2	<i>Challenges faced by the use of natural agents on textiles</i> .....	170
5.1.3	<i>Antimicrobial textile finishes</i> .....	171
5.1.4	<i>Methods commonly used to test antimicrobial textile finishes</i> .....	174
5.2	OBJECTIVES.....	176
5.3	MATERIALS .....	176
5.3.1	<i>Synthetic textile coupons</i> .....	176
5.3.2	<i>Culture media</i> .....	176
5.3.3	<i>Microorganisms</i> .....	176
5.3.4	<i>Essential oils</i> .....	176
5.4	EXPERIMENTAL.....	177
5.4.1	<i>Antibacterial activity assessment of textile materials: Parallel streak method (AATCC 147)</i> .....	177
5.4.2	<i>Zone of inhibition</i> .....	178
5.4.3	<i>Dynamic killing assay</i> .....	179
5.4.4	<i>Wash durability</i> .....	180
5.5	RESULTS AND DISCUSSION .....	181
5.5.1	<i>Antibacterial activity assessment of textile materials: Parallel streak method (AATCC 147)</i> .....	181
5.5.2	<i>Zone of inhibition</i> .....	184
5.5.3	<i>Dynamic kill assessment</i> .....	186
5.5.4	<i>Wash durability testing</i> .....	190
5.5.4.1	<i>Reduction in %CFU/mL for five test microorganisms in static and exponential growth phase exposed to EO MSN and EO IMM in ISB</i> .....	190
5.5.4.2	<i>Reduction in %CFU/mL for five test microorganisms in static and exponential growth phase exposed to EO MSN and EO IMM in PBS</i> .....	194
5.6	CONCLUSIONS.....	199
<b>CHAPTER 6</b> .....		<b>200</b>
6.1	OVERALL CONCLUSIONS.....	201
6.1.1	<i>Chapter 2 Conclusions</i> .....	<b>Error! Bookmark not defined.</b>
6.1.2	<i>Chapter 3 Conclusions</i> .....	<b>Error! Bookmark not defined.</b>
6.1.3	<i>Chapter 4 Conclusions</i> .....	<b>Error! Bookmark not defined.</b>
6.1.4	<i>Chapter 5 Conclusions</i> .....	<b>Error! Bookmark not defined.</b>
6.2	FURTHER WORK.....	203
<b>REFERENCES</b> .....		<b>206</b>
<b>APPENDICES</b> .....		<b>227</b>
APPENDIX I .....		227
APPENDIX II.....		230
APPENDIX III .....		231

## Abstract

Healthcare associated infections (HCAI) impose significant financial and environmental problems for modern healthcare settings, therefore it is important to develop novel strategies to combat HCAs and the causative microorganisms. This study investigates the use of an encapsulated essential oil (EO) antimicrobial coating for textiles in the healthcare environment. The antimicrobial activity of several EOs were studied, individually and in blends, against five microorganisms associated with HCAI (*Staphylococcus aureus*, methicillin resistant *Staphylococcus aureus*, *Candida albicans*, *Escherichia coli*, and *Pseudomonas aeruginosa*). A 1:1 blend of cinnamon (CIN) and clove oils (CLO) containing 94.8 % (v/v) eugenol (by GC-MS) showed the highest antimicrobial efficacy and gave a minimum inhibitory concentration (MIC) of less than 0.25% (v/v). Mesoporous silica nanoparticles (MSN) were used to encapsulate volatile EOs. The MSNs displayed narrow size distribution, high surface area and pore size between 1.8-2.2 nm. MSNs, directly loaded with CIN:CLO blend (72 % by mass of MSN), achieved bactericidal values (25-50 mg/mL) against the test microorganisms. Dynamic killing profiles of the EO loaded MSNs against the test microorganisms were recorded. The highest kill rates were observed during the first 15 minutes of contact. Organically modified silica (ormosil) gels were synthesised to provide thin film coverage of synthetic fibres. Gamma-methacryloxypropyltrimethoxysilane ( $\gamma$ -MPS) was used to attach un-loaded MSNs to the ormosil coating. A layer-by-layer treatment method provided good coverage of synthetic fibres with MSNs, as evidenced by scanning electron microscopy (SEM). Attenuated total reflectance Fourier transform infrared spectroscopy (ATR-FTIR) was used to monitor the layer-by-layer treatment sequence. Head space GC-MS sampling of EO loaded MSN treated textile coupons showed that EO was able to diffuse from the MSN mesopores after being bonded to the synthetic fibres. The EO loaded MSN textile coupons were microbiologically challenged using a method based on AATCC 100. The EO loaded MSN textile coupons displayed good antimicrobial activity over five washing cycles using a method based on (AATCC 61 and 135) thereby indicating a degree of controlled release.

## Structure of Thesis

The thesis details the concept of producing antimicrobial textiles via the chemical affixation of essential oil-loaded mesoporous silica nanoparticles to synthetic fibres. The thesis begins with Chapter 1, which includes a brief overview and introduction to the subject area. The underlying problem is outlined and the project aims and objectives are summarised. Chapters 2 to 5 describe the research contributing towards the thesis. These chapters comprise technique-specific introductions, objectives, materials and methods, results and discussion and conclusions. The final chapter of the thesis includes a summary of the work undertaken, overall conclusions and further work.

## List of Tables

TABLE 1.1. MAIN CAUSES OF HEALTHCARE-ASSOCIATED INFECTIONS IN ENGLAND (NATIONAL AUDIT OFFICE 2009).....	4
TABLE 1.2. THE ASSOCIATED COSTS OF THE NATIONAL INITIATIVES FOR TACKLING HCAI ADAPTED FROM THE NAO'S "REDUCING HEALTHCARE ASSOCIATED INFECTIONS IN HOSPITALS IN ENGLAND" (2009).....	11
TABLE 2.1. DIAMETERS OF INHIBITION ZONES OF INDIVIDUAL OILS AGAINST FIVE MICROORGANISMS (MM). VALUES REPRESENT THE AVERAGE FROM THREE REPLICATES. MIC – MINIMUM INHIBITORY CONCENTRATION, SD – STANDARD DEVIATION ( $\pm$ ), (N=9). .....	44
TABLE 2.2. MIC DATA FOR AGAR DILUTION ASSAY. SEVEN ESSENTIAL OILS (EOs) DISPERSED IN ISA IN A DOUBLING DILUTION SERIES FROM 0.03-2% (v/v) WERE	

INOCULATED WITH FIVE MICROORGANISMS USING A MULTIPOINT REPLICATOR. VALUES REPRESENT THE AVERAGE FROM THREE REPLICATES. SD – STANDARD DEVIATION IN PARENTHESIS, (N=9)..... 45

TABLE 2. 3. MIC AND MBC DATA FOR BROTH MICRODILUTION ASSAY. VALUES REPRESENT THE RANGE FROM THREE REPLICATES. SD – STANDARD DEVIATION, (N=9)..... 48

TABLE 2. 4. CHANGE IN LOG<sub>10</sub> CFU/ML AFTER INCUBATION WITH CINNAMON OIL RELATIVE TO THAT AT TIME ZERO, (N=3) (LOUGHLIN *ET AL* 2008). STANDARD DEVIATION (SD) PRESENTED IN PARENTHESIS..... 53

TABLE 2. 5. CHANGE IN LOG<sub>10</sub> CFU/ML AFTER INCUBATION WITH CLOVE OIL RELATIVE TO THAT AT TIME ZERO, (N=3). STANDARD DEVIATION (SD) PRESENTED IN PARENTHESIS. .... 54

TABLE 2. 6. CHANGE IN LOG<sub>10</sub> CFU/ML AFTER INCUBATION WITH EUCALYPTUS OIL RELATIVE TO THAT AT TIME ZERO, (N=3). STANDARD DEVIATION (SD) PRESENTED IN PARENTHESIS..... 55

TABLE 2. 7. CHANGE IN LOG<sub>10</sub> CFU/ML AFTER INCUBATION WITH GERANIUM OIL RELATIVE TO THAT AT TIME ZERO, (N=3). STANDARD DEVIATION (SD) PRESENTED IN PARENTHESIS..... 56

TABLE 2. 8. CHANGE IN LOG<sub>10</sub> CFU/ML AFTER INCUBATION WITH LEMONGRASS OIL RELATIVE TO THAT AT TIME ZERO, (N=3). STANDARD DEVIATION (SD) PRESENTED IN PARENTHESIS..... 57

TABLE 2. 9. CHANGE IN LOG<sub>10</sub> CFU/ML AFTER INCUBATION WITH LIME OIL RELATIVE TO THAT AT TIME ZERO, (N=3). STANDARD DEVIATION (SD) PRESENTED IN PARENTHESIS. .... 58

TABLE 2. 10. CHANGE IN LOG<sub>10</sub> CFU/ML AFTER INCUBATION WITH TEA TREE OIL RELATIVE TO THAT AT TIME ZERO, (N=3). STANDARD DEVIATION (SD) PRESENTED IN PARENTHESIS..... 59

TABLE 2. 11. FRACTIONAL INHIBITORY CONCENTRATIONS FROM CHECKERBOARD TESTING ESSENTIAL OIL BLENDS. MIC <sub>X</sub> DENOTES THE MIC FOR OIL X IN THE COMBINATION, MIC <sub>Y</sub> DENOTES THE MIC FOR OIL Y IN THE COMBINATION, (N=3). GREEN HIGHLIGHT DENOTES MOST EFFECTIVE BLENDS. ....	62
TABLE 3.1. SHOWING MASS LOSS BETWEEN KEY TEMPERATURE RANGES FOR FIVE MSN SAMPLES. WITH TEMPLATE (WT) AND WITHOUT TEMPLATE (WOT).....	97
TABLE 3.2. SUMMARY OF MESOPOROUS SILICA NANOPARTICLE SAMPLE CHARACTERISATIONS.....	106
TABLE 3.3. LOADING LEVELS FOR EO EVAPORATION AND SUBSEQUENT SOLVENT WASHING (METHANOL).....	110
TABLE 3. 4. RESIDUE FRACTIONS OF BLANK MSN SAMPLES AND % EO LOAD VIA IMMERSION AND SHAKING FOR SAMPLES 1-5.....	120
TABLE 3.5. BACTERICIDAL ACTIVITY OF EO LOADED MSNs AT FOUR CONCENTRATIONS. 'G' REPRESENTS THE OCCURRENCE OF GROWTH, 'NG' REPRESENTS THE OCCURRENCE OF NO GROWTH (N=3). ....	124
TABLE 3.6. THE BACTERICIDAL CONCENTRATIONS (MG/ML) FOR EACH TEST MICROORGANISM.....	125
TABLE 4.1. FTIR ADSORPTION FREQUENCIES OF NOTE FOR THE ORGANO-SILICON SPECIES USED IN THIS STUDY (ESTELLA <i>ET AL</i> 2007, PARDAL <i>ET AL</i> 2009).....	137
TABLE 4.2. SUMMARY OF THE REACTANT VOLUMES (ML) FOR ORMOSIL SYNTHESIS AT VARIOUS PRECURSOR RATIOS.....	140
TABLE 4.3. SUMMARY OF THE AMOUNT OF MSN AND TIME OF EXPOSURE TEXTILE SAMPLES ENCOUNTERED TO DETERMINE OPTIMAL COVERAGE OF SYNTHETIC FIBRES. ....	144

TABLE 4.4. DISPLAYING THE FIVE SYNTHETIC TEXTILE SAMPLES AND THEIR RESPECTIVE LAYER-BY-LAYER TREATMENT, FOR ATR FTIR ANALYSIS..... 146

TABLE 4.5. RESULTS OF STIFFNESS TESTING OF SYNTHETIC TEXTILE COUPONS TREATED WITH ORMOSIL GELS RANGING IN MTEOS:TEOS CONCENTRATION. DROOP RESULTS AN AVERAGE OF THREE REPEATS (N=3)..... 148

TABLE 5.1. SUMMARY TABLE OF TEST COUPON OUTCOMES FOR THE PARALLEL STREAK METHOD ..... 182

## List of Figures

FIGURE 2. 1. THE LOCATIONS AND MECHANISMS IN THE BACTERIAL CELL THOUGHT TO BE SITES OF ACTION FOR ESSENTIAL OIL ACTIVE COMPONENTS (AHMED & AQIL 2009)..	19
FIGURE 2. 2. A DIAGRAM SHOWING GAS CHROMATOGRAPHY ANALYSIS. ....	29
FIGURE 2.3. A DIAGRAM SHOWING MASS SPECTROMETRY ANALYSIS. ....	30
FIGURE 2.4. GROWTH CURVE FOR <i>C.ALBICANS</i> , DEMONSTRATING THAT THE YEAST ENTERS EXPONENTIAL GROWTH PHASE AT APPROXIMATELY 5-6 HOURS.....	41
FIGURE 2.5. GROWTH CURVE FOR <i>E.COLI</i> DEMONSTRATING THAT THE BACTERIUM ENTERS EXPONENTIAL GROWTH PHASE AFTER 1-2 HOURS. ....	41
FIGURE 2.6. GROWTH CURVE FOR <i>P.AERUGINOSA</i> , SHOWING THAT THE BACTERIUM ENTERS EXPONENTIAL GROWTH PHASE AFTER APPROXIMATELY 2.5-3 HOURS.....	42
FIGURE 2.7. GROWTH CURVE FOR <i>S.AUREUS</i> SHOWING THAT THE BACTERIUM ENTERS EXPONENTIAL GROWTH PHASE AFTER 2.5-3 HOURS. ....	42
FIGURE 2.8. GROWTH CURVE FOR <i>MRSA</i> DEMONSTRATING THAT THE BACTERIUM ENTERS EXPONENTIAL GROWTH PHASE AFTER 3 HOURS. ....	43
FIGURE 2.9. 96 WELL MICROTITRE PLATE, DEMONSTRATING WELL LAYOUT. ....	36
FIGURE 2.10. AN INOCULATED CHECKERBOARD MICRO-TITRE PLATE CONTAINING A BLEND OF CINNAMON AND TEA TREE OIL IN VARIOUS CONCENTRATIONS AGAINST <i>S.AUREUS</i> . CINNAMON DESCENDING IN CONCENTRATION ACROSS THE X-AXIS, TEA TREE OIL DESCENDING IN CONCENTRATION DOWN THE Y-AXIS (2% - 0.03%). THE RED COLOURING OF THE TTC DYE IN THE BOTTOM RIGHT CORNER INDICATES METABOLIC ACTIVITY (GROWTH) OF THE BACTERIUM. ....	38
FIGURE 2.11. GRAPHICAL REPRESENTATION OF METHOD DESCRIBED IN SECTION 2.3.7, WHERE EACH ESSENTIAL OIL HAD A STARTING CONCENTRATION OF 2% (V/V). EO (X) BEING ADDED IN DESCENDING CONCENTRATIONS ACROSS THE X AXIS LEFT TO RIGHT. EO (Y) BEING ADDED IN DESCENDING CONCENTRATIONS DOWN THE Y AXIS TOP TO BOTTOM. ....	38

FIGURE 2.12. BROTH MICRODILUTION ASSAY OF CINNAMON OIL. COLUMN 1 CONTAINING POSITIVE GROWTH CONTROLS. COLUMN 2 CONTAINING CINNAMON OIL AT 2%, DECREASING IN DOUBLING CONCENTRATIONS ACROSS THE PLATE FROM LEFT TO RIGHT TO 0.03% IN COLUMN 8. ROW A CONTAINING <i>S.AUREUS</i> , B – <i>E.COLI</i> , C – <i>MRSA</i> , D – <i>P.AERUGINOSA</i> , AND E – <i>C.ALBICANS</i> . .....	49
FIGURE 2.13. COMPARISON OF ESSENTIAL OIL MIC % (V/V) RESULTS FOR THE AGAR DILUTION (AD) AND BROTH MICRO-DILUTION (BD)METHOD .....	51
FIGURE 2.14. THE MAJOR COMPONENTS OF CINNAMON OIL, AS DETERMINED BY GC-MS. THE NUMBERS IN RED REPRESENT THE % COMPOSITION OF THE CHEMICAL COMPONENT. THE LABELS ON THE X-AXIS ARE THE NAMES OF EACH CHEMICAL COMPONENT.....	65
FIGURE 2.15. THE MAJOR COMPONENTS OF CLOVE OIL, AS DETERMINED BY GC-MS. THE NUMBERS IN RED REPRESENT THE % COMPOSITION OF THE CHEMICAL COMPONENT. THE LABELS ON THE X-AXIS ARE THE NAMES OF EACH CHEMICAL COMPONENT.....	68
FIGURE 2.16. THE MAJOR COMPONENTS OF EUCALYPTUS OIL, AS DETERMINED BY GC-MS. THE NUMBERS IN RED REPRESENT THE % COMPOSITION OF THE CHEMICAL COMPONENT. THE LABELS ON THE X-AXIS ARE THE NAMES OF EACH CHEMICAL COMPONENT.....	69
FIGURE 2.17. THE MAJOR COMPONENTS OF GERANIUM OIL, AS DETERMINED BY GC-MS. THE NUMBERS IN RED REPRESENT THE % COMPOSITION OF THE CHEMICAL COMPONENT. THE LABELS ON THE X-AXIS ARE THE NAMES OF EACH CHEMICAL COMPONENT.....	70
FIGURE 2.18. THE MAJOR COMPONENTS OF LEMONGRASS OIL, AS DETERMINED BY GC-MS. THE NUMBERS IN RED REPRESENT THE % COMPOSITION OF THE CHEMICAL COMPONENT. THE LABELS ON THE X-AXIS ARE THE NAMES OF EACH CHEMICAL COMPONENT.....	71

FIGURE 2.19. THE MAJOR COMPONENTS OF LIME OIL, AS DETERMINED BY GC-MS. THE NUMBERS IN RED REPRESENT THE % COMPOSITION OF THE CHEMICAL COMPONENT. THE LABELS ON THE X-AXIS ARE THE NAMES OF EACH CHEMICAL COMPONENT.....	72
FIGURE 2.20. THE MAJOR COMPONENTS OF TEA TREE OIL, AS DETERMINED BY GC-MS. THE NUMBERS IN RED REPRESENT THE % COMPOSITION OF THE CHEMICAL COMPONENT. THE LABELS ON THE X-AXIS ARE THE NAMES OF EACH CHEMICAL COMPONENT.....	73
FIGURE 2.21. THE MAJOR COMPONENTS OF CINNAMON-CLOVE OIL BLEND IN A 1:1 RATIO, AS DETERMINED BY GC-MS. THE NUMBERS IN RED REPRESENT THE % COMPOSITION OF THE CHEMICAL COMPONENT. THE LABELS ON THE X-AXIS ARE THE NAMES OF EACH CHEMICAL COMPONENT. ....	74
FIGURE 3.1. SCHEMATIC SHOWING THE FORMATION OF ORDERED MESOPOROUS MATERIALS;.....	77
FIGURE 3.2. IUPAC ADSORPTION ISOTHERM CLASSIFICATION (DONOHUE AND ARANOVICH1998).....	84
FIGURE 3.3. THERMOGRAVIMETRIC ANALYSIS (SOLID LINE) AND DERIVATIVE THERMOGRAVIMETRIC CURVE (DOTTED LINE) OF SURFACTANT INTACT MSN SAMPLE 1 (A) AND MSN SAMPLE 1 POST CALCINATION (B). ....	98
FIGURE 3.4. ZETA POTENTIAL FOR THE FIVE MSN SAMPLES USED FOR FURTHER EXPERIMENTATION.....	99
FIGURE 3.5. SCANNING ELECTRON MICROSCOPE IMAGES OF CALCINED MSNs (SAMPLE 1). ....	100
FIGURE 3.6. SCANNING ELECTRON MICROSCOPE IMAGES OF CALCINED MSNs, B AND C, SAMPLES 2 AND 3, RESPECTIVELY.....	101
FIGURE 3.7. SCANNING ELECTRON MICROSCOPE IMAGES OF CALCINED MSNs, D AND E, SAMPLES 4 AND 5, RESPECTIVELY.....	102

FIGURE 3.8. NITROGEN SORPTION ISOTHERM FOR GAS ADSORPTION (BLUE LINE) AND DESORPTION (MAROON LINE) AT 77K AND PORE SIZE DISTRIBUTION GRAPH (SAMPLE 1).....	103
FIGURE 3.9. NITROGEN SORPTION ISOTHERM FOR GAS ADSORPTION (BLUE LINE) AND DESORPTION (MAROON LINE) AT 77K AND PORE SIZE DISTRIBUTION GRAPH B AND C, (SAMPLE 2 AND 3, RESPECTIVELY).....	104
FIGURE 3.10. NITROGEN SORPTION ISOTHERM FOR GAS ADSORPTION (BLUE LINE) AND DESORPTION (MAROON LINE) AT 77K AND PORE SIZE DISTRIBUTION GRAPH D AND E (SAMPLE 4 AND 5, RESPECTIVELY).....	105
FIGURE 3.11. EUGENOL (REPRESENTED AS A SPACE FILLING MOLECULAR MODEL WITH STICK MODEL OVERLAID) IS THE MAJOR CONSTITUENT OF CLOVE OIL AND CINNAMON OIL.....	107
FIGURE 3.12. TGA TRACE OF BLANK MSNS BEFORE OIL LOADING. (RED LINE) PERCENTAGE MASS LOSS PLOTTED AGAINST INCREASING TEMPERATURE °C, (BLUE LINE) DERIVATIVE OF MASS LOSS.....	108
FIGURE 3.13. TGA OF CLO-CIN LOADED MSN SAMPLE AFTER EVAPORATION OF MEOH. NO SUBSEQUENT SOLVENT WASHING. (RED LINE) PERCENTAGE MASS LOSS PLOTTED AGAINST INCREASING TEMPERATURE °C, (BLUE LINE) DERIVATIVE OF MASS LOSS.	109
FIGURE 3.14. TGA OF CLO-CIN LOADED MSN SAMPLE AFTER PRIMARY MEOH WASHING AND EVAPORATION. (RED LINE) PERCENTAGE MASS LOSS PLOTTED AGAINST INCREASING TEMPERATURE °C, (BLUE LINE) DERIVATIVE OF MASS LOSS. ....	109
FIGURE 3.15. TGA OF CLO-CIN LOADED MSN SAMPLE AFTER SECOND ROUND OF WASHING WITH MEOH. (RED LINE) PERCENTAGE MASS LOSS PLOTTED AGAINST INCREASING TEMPERATURE °C, (BLUE LINE) DERIVATIVE OF MASS LOSS. ....	110
FIGURE 3.16. SAMPLE 1 TGA TRACE OF EO LOADED MSNS. (RED LINE) PERCENTAGE MASS LOSS PLOTTED AGAINST INCREASING TEMPERATURE °C, (BLUE LINE) DERIVATIVE OF MASS LOSS.....	111

FIGURE 3.17. SAMPLE 2 TGA TRACE OF EO LOADED MSNS. (RED LINE) PERCENTAGE MASS LOSS PLOTTED AGAINST INCREASING TEMPERATURE °C, (BLUE LINE) DERIVATIVE OF MASS LOSS.....	112
FIGURE 3.18. SAMPLE 3 TGA TRACE OF EO LOADED MSNS. (RED LINE) PERCENTAGE MASS LOSS PLOTTED AGAINST INCREASING TEMPERATURE °C, (BLUE LINE) DERIVATIVE OF MASS LOSS.....	113
FIGURE 3.19. SAMPLE 4 TGA TRACE OF EO LOADED MSNS. (RED LINE) PERCENTAGE MASS LOSS PLOTTED AGAINST INCREASING TEMPERATURE °C, (BLUE LINE) DERIVATIVE OF MASS LOSS.....	113
FIGURE 3.20. SAMPLE 5 TGA TRACE OF EO LOADED MSNS. (RED LINE) PERCENTAGE MASS LOSS PLOTTED AGAINST INCREASING TEMPERATURE °C, (BLUE LINE) DERIVATIVE OF MASS LOSS.....	114
FIGURE 3.21. A EUGENOL MOLECULE MODELLED USING SCIGRESS SOFTWARE, IN THE TWO POSSIBLE ORIENTATIONS OF ADSORPTION, (A) VERTICALLY AND (B) FLAT.....	116
FIGURE 3.22. THE ANTICIPATED ORIENTATIONS OF ATTACHMENT TO THE MSN SURFACE FOR EUGENOL. (I) VERTICAL, DUAL-POINT ATTACHED, (II) FLAT, MULTI-POINT ATTACHED.....	119
FIGURE 3.23. CHROMATOGRAPHS OF MEOH EXTRACT FROM THREE EO LOADED MSN SAMPLES AFTER INCREASING SOLVENT WASHING WITH MEOH. (I) AFTER 10 ML, (II) 20 ML AND (III) 30 ML OF WASHING WITH MEOH. PEAKS ASSIGNED AS FOLLOWS: (A) EUGENOL (B) BETA CARYOPHYLENE (C) EUGENYL ACETATE (D) BENZYL BENZOATE. EUGENOL PEAK MAX HEIGHT (I) $1.1 \times 10^8$ , (II) $9 \times 10^7$ , (III) $8 \times 10^7$ .....	121
FIGURE 3.24. THE CAPACITY OF BLANK MSNS AT 12.5, 25, 50 AND 100 MG/ML TO PREVENT GROWTH OF FIVE TEST MICROORGANISMS OVER A 24 HOUR PERIOD BASED ON OPTICAL DENSITY READINGS. RESULTS ARE EXPRESSED AS A PERCENTAGE OF 'TIME 0' OD VALUES. STANDARD DEVIATION BARS ARE DISPLAYED (N=3).....	123

FIGURE 3.25. CFU/ML VERSUS TIME PLOTS FOR <i>S.AUREUS</i> IN THE STATIC (S) AND EXponential GROWTH (E) PHASES, BOTH WITH AND WITHOUT 25 MG/ML OF EO LOADED MSNS. STANDARD DEVIATION BARS ARE SHOWN (N=3). .....	126
FIGURE 3.26. CFU/ML VERSUS TIME PLOTS FOR <i>E.COLI</i> IN THE STATIC (S) AND EXponential GROWTH (E) PHASES, BOTH WITH AND WITHOUT 25 MG/ML OF EO LOADED MSNS. STANDARD DEVIATION BARS ARE SHOWN (N=3). .....	126
FIGURE 3.27. CFU/ML VERSUS TIME PLOTS FOR <i>C.ALBICANS</i> IN THE STATIC (S) AND EXponential GROWTH (E) PHASES, BOTH WITH AND WITHOUT 50 MG/ML OF EO LOADED MSNS. STANDARD DEVIATION BARS ARE SHOWN (N=3). .....	127
FIGURE 3.28. CFU/ML VERSUS TIME PLOTS FOR <i>MRSA</i> IN THE STATIC (S) AND EXponential GROWTH (E) PHASES, BOTH WITH AND WITHOUT 25 MG/ML OF EO LOADED MSNS. STANDARD DEVIATION BARS ARE SHOWN (N=3). .....	127
FIGURE 3. 29. CFU/ML VERSUS TIME PLOTS FOR <i>P.AERUGINOSA</i> IN THE STATIC (S) AND EXponential GROWTH (E) PHASES, BOTH WITH AND WITHOUT 50 MG/ML OF EO LOADED MSNS. STANDARD DEVIATION BARS ARE SHOWN (N=3). .....	128
FIGURE 4.1. THE SILANE COUPLING LINKER TRIMETHOXYSILYLPROPYLMETHACRYLATE ( $\gamma$ - MPS), CONTAINS AN ACRYLIC CARBON-CARBON DOUBLE BOND (C=C) AND METHOXYSILANE GROUPS (SiOCH <sub>3</sub> ). .....	135
FIGURE 4.2. THE INTERNAL INSTRUMENT SETUP FOR SINGLE REFLECTION ATR FTIR ANALYSIS. ....	136
FIGURE 4.3. SCHEMATIC REPRESENTATION OF THE ANTICIPATED STRUCTURE PRODUCED USING THE LAYER-BY-LAYER METHOD FOR CHEMICALLY AFFIXING MSNS TO SYNTHETIC FIBRES. ....	143
FIGURE 4.4. SEM IMAGES OF UNTREATED SYNTHETIC TEXTILE (65% POLYESTER, 35% COTTON). ....	147

FIGURE 4.5. SEM IMAGES OF ORMOSIL TREATED SYNTHETIC TEXTILE SAMPLES AT DIFFERING PRECURSOR RATIOS MTEOS:TEOS A) 1:1.....	149
FIGURE 4.6. SEM IMAGES OF ORMOSIL TREATED SYNTHETIC TEXTILE SAMPLES AT DIFFERING PRECURSOR RATIOS MTEOS:TEOS, B) 2:1 C) 3:1.....	150
FIGURE 4.7. SEM IMAGES OF ORMOSIL TREATED SYNTHETIC TEXTILE SAMPLES AT DIFFERING PRECURSOR RATIOS MTEOS:TEOS, D) 1:2 E) 1:3.....	151
FIGURE 4.8. ORMOSIL TREATED SAMPLE 3:1 MTEOS:TEOS 1 HOUR STIR, AIR DRIED.	152
FIGURE 4.9. SEM IMAGE OF ONE POT SYNTHESIS ON SYNTHETIC TEXTILE. ....	154
FIGURE 4.10. GRAFTING OF SILANE COUPLING LINKERS ONTO MSNS BASED ON (PARDAL <i>ET AL</i> 2009, BARTHOLOME <i>ET AL</i> 2003). IMAGE REPRODUCED FROM PARDAL <i>ET AL</i> 2009. ....	155
FIGURE 4.11. TMSPMA GRAFTED MSNS ATTACHED TO ORMOSIL COATING ON SYNTHETIC TEXTILE FIBRES. ....	156
FIGURE 4.12. SEM IMAGE SHOWING MSNS AFFIXED TO SYNTHETIC TEXTILE FIBRES AFTER LAYER-BY-LAYER TREATMENT.....	158
FIGURE 4.13. SEM IMAGES OF MSN COVERAGE ON INDIVIDUAL SYNTHETIC FIBRES, REPRESENTATIVE OF COVERAGE ON TEXTILE COUPONS TREATED WITH THREE DIFFERENT CONCENTRATIONS OF BLANK MSNS (0.1, 0.5 AND 1G). WITH THREE DIFFERENT LENGTHS OF EXPOSURE (0.167, 1 AND 18 HOURS). ....	159
FIGURE 4. 14. EXTRACTS FROM GCMS SPECTRA SHOWING EO RELEASE AT THREE DIFFERENT TIME POINTS FROM EO LOADED MSNS AFFIXED TO SYNTHETIC FIBRES. (A) EUGENOL, (B) EUGENYL ACETATE. GAS SAMPLES WERE TAKEN AT 1 HOUR (I), 12 HOURS (II), AND 24 HOURS (III). Y AXIS SCALES (I) AND (II) (COUNTS (AU x 10 <sup>4</sup> )), (III) (COUNTS (AU x 10 <sup>3</sup> )).....	161
FIGURE 4.15. FTIR SPECTRA FOR TEXTILE COUPON SAMPLES AT THE FIRST STAGE OF TREATMENT. UNTREATED (BLUE) AND ORMOSIL TREATED (RED),.....	163

FIGURE 4.16. FTIR SPECTRA FOR TEXTILE COUPON SAMPLES AT EACH STAGE OF TREATMENT. ORMOSIL TREATED (BLUE) AND SILANE TREATED (RED).....	164
FIGURE 4.17. FTIR SPECTRA FOR TEXTILE COUPON SAMPLES AT EACH STAGE OF TREATMENT. TMSPMA TREATED (BLUE) AND BLANK MSN TREATED (RED).....	165
FIGURE 4.18. FTIR SPECTRA FOR TEXTILE COUPON SAMPLES AT EACH STAGE OF TREATMENT. BLANK MSN TREATED (BLUE) AND EO LOADED MSNs (RED). ....	166
FIGURE 5.1. SHOWING AN EO MSN TREATED TEXTILE COUPON INOCULATED WITH <i>S.AUREUS</i> AFTER 24 HOUR INCUBATION. THE GREY CIRCLE DENOTES THE ZONE OF INHIBITION AROUND THE EO MSN TREATED SYNTHETIC TEXTILE COUPON. ....	183
FIGURE 5.2. ZONES OF INHIBITION FOR UNTREATED, EO MSN TREATED AND EO IMMERSSED SYNTHETIC TEXTILE COUPONS AGAINST FIVE TEST MICROORGANISMS..	184
FIGURE 5.3. SHOWING AN EO MSN TEXTILE COUPON INOCULATED WITH <i>S.AUREUS</i> AFTER 24 HOURS INCUBATION.....	185
FIGURE 5.4. % CFU/ML REDUCTION FOR UNWASHED EO MSN AND EO IMMERSSED COUPONS (EO IMM) AFTER 24 HOURS CONTACT TIME IN ISB, WITH TEST MICROORGANISMS IN STATIC (S) AND EXPONENTIAL (E) PHASES OF GROWTH. ....	187
FIGURE 5.5. CFU/ML % REDUCTION FOR UNWASHED EO MSN AND EO IMMERSSED COUPONS (EO IMM) AFTER 24 HOURS CONTACT TIME IN PBS, WITH TEST MICROORGANISMS IN STATIC (S) AND EXPONENTIAL (E) PHASES OF GROWTH. ....	187
FIGURE 5.6. CFU/ML % REDUCTION FOR TEST MICROORGANISMS IN STATIC GROWTH PHASE, EXPOSED TO EO MSN COUPONS AFTER 1, 2, 5 AND 10 WASH CYCLES, AFTER 24 HOURS CONTACT TIME IN ISB.....	191
FIGURE 5.7. CFU/ML % REDUCTION FOR TEST MICROORGANISMS IN STATIC GROWTH PHASE, EXPOSED TO EO IMM COUPONS AFTER 1, 2, 5 AND 10 WASH CYCLES, AFTER 24 HOURS CONTACT TIME IN ISB.....	191

FIGURE 5.8. CFU/ML % REDUCTION FOR TEST MICROORGANISMS IN EXPONENTIAL GROWTH PHASE, EXPOSED TO EO MSN COUPONS AFTER 1, 2, 5 AND 10 WASH CYCLES, AFTER 24 HOURS CONTACT TIME IN ISB..... 192

FIGURE 5.9. CFU/ML % REDUCTION FOR TEST MICROORGANISMS IN STATIC GROWTH PHASE, EXPOSED TO EO IMM COUPONS AFTER 1, 2, 5 AND 10 WASH CYCLES, AFTER 24 HOURS CONTACT TIME IN ISB..... 192

FIGURE 5.10. CFU/ML % REDUCTION FOR TEST MICROORGANISMS IN STATIC GROWTH PHASE, EXPOSED TO EO MSN COUPONS AFTER 1, 2, 5 AND 10 WASH CYCLES, AFTER 24 HOURS CONTACT TIME IN PBS. .... 194

FIGURE 5.11. CFU/ML % REDUCTION FOR TEST MICROORGANISMS IN STATIC GROWTH PHASE, EXPOSED TO EO IMM COUPONS AFTER 1, 2, 5 AND 10 WASH CYCLES, AFTER 24 HOURS CONTACT TIME IN PBS. .... 195

FIGURE 5.12. CFU/ML % REDUCTION FOR TEST MICROORGANISMS IN EXPONENTIAL GROWTH PHASE, EXPOSED TO EO MSN COUPONS AFTER 1, 2, 5 AND 10 WASH CYCLES, AFTER 24 HOURS CONTACT TIME IN PBS..... 196

FIGURE 5.13. CFU/ML % REDUCTION FOR TEST MICROORGANISMS IN EXPONENTIAL GROWTH PHASE, EXPOSED TO EO IMM COUPONS AFTER 1, 2, 5 AND 10 WASH CYCLES, AFTER 24 HOURS CONTACT TIME IN PBS..... 196

## List of Equations

EQUATION 2.1. FIC CALCULATION, CONSIDERING MIC VALUES FOR EOs INDIVIDUALLY AND IN COMBINATION.	39
EQUATION 3.1. RESIDUE FRACTION CALCULATION, ALLOWING EO LOADING PERCENTAGES TO BE DETERMINED.	91
EQUATION 3.2. THEORETICAL MONOLAYER COVERAGE FOR EUGENOL ON MSN SURFACTANT IN PROPOSED ORIENTATIONS OF ADSORPTION.	117
EQUATION 5.1. CALCULATION TO DETERMINE THE PERCENTAGE REDUCTION IN BACTERIAL VIABILITY, AFTER 24 HOURS EXPOSURE TO ANTIMICROBIAL TEXTILE.	179

## List of Abbreviations

<b>AATCC</b>	American association of textile chemists and colorists
<b>AITC</b>	Antimicrobial allylthiocyanate
<b>AMR</b>	Antimicrobial resistance
<b>a.m.u.</b>	atomic mass units
<b>ASTM</b>	American society for testing and materials
<b>ATR</b>	Attenuated total reflectance
<b>ATP</b>	Adenosine triphosphate
<b>BET</b>	Brunauer, Emmett and Teller
<b>BJH</b>	Barret, Joyner and Halenda
<b>BSAC</b>	British society for Antimicrobial Chemotherapy
<b>CFU</b>	Colony forming unit
<b>CIN</b>	Cinnamon
<b>CLO</b>	Clove
<b>CTAB</b>	Cetyltrimethylammonium bromide
<b>DH</b>	Department of health
<b>DLS</b>	Dynamic light scattering
<b>DNA</b>	Deoxyribose nucleic acid

<b>EARS-Net</b>	European antimicrobial resistance surveillance network
<b>EIEC</b>	Enteroinvasive
<b>EO</b>	Essential oil
<b>EO IMM</b>	Essential oil immersed
<b>EO MSN</b>	Essential oil mesoporous silica nanoparticles
<b>EPEC</b>	Enteropathogenic
<b>ETEC</b>	Enterotoxigenic
<b>ETEOS</b>	Ethyltriethoxysilane
<b>EUC</b>	Eucalyptus
<b>FIC</b>	Fractional inhibitory concentration
<b>FTIR</b>	Fourier transform infrared spectroscopy
<b><math>\gamma</math>-MPS</b>	Gamma-methacryloxypropyltrimethoxysilane
<b>GC</b>	Gas chromatography
<b>GC-MS</b>	Gas chromatography – mass spectrometry
<b>GER</b>	Geranium
<b>HAI</b>	Hospital acquired infection
<b>HCl</b>	Hydrochloric acid
<b>HCAI</b>	Healthcare associated infection
<b>HEPA</b>	High-efficiency particulate air
<b>HIS</b>	Hospital infection society
<b>HIV</b>	Human immunodeficiency virus
<b>HPA</b>	Health protection agency
<b>ISA</b>	Isosensitest agar
<b>ISB</b>	Isosensitest broth
<b>IR</b>	Infrared
<b>IUPAC</b>	International union of pure and applied chemistry
<b>LCT</b>	Liquid crystal templating

<b>LDE</b>	Laser Doppler electrophoresis
<b>LEM</b>	Lemongrass
<b>LIM</b>	Lime
<b>MCM-41</b>	Mobil composition of matter-No.41
<b>MeOH</b>	Methanol
<b>MHA</b>	Mueller-Hinton agar
<b>MIC</b>	Minimum inhibitory concentration
<b>MRSA</b>	Methicillin resistant <i>Staphylococcus aureus</i>
<b>MSD</b>	Mass selective detector
<b>MS</b>	Mass spectrometry
<b>MSN</b>	Mesoporous silica nanoparticle
<b>MTEOS</b>	Methyltriethoxysilane
<b>MTP</b>	Micro-titre plate
<b>NA</b>	Nutrient agar
<b>NAO</b>	National audit office
<b>NaOH</b>	Sodium hydroxide
<b>NB</b>	Nutrient broth
<b>NHS</b>	National health service
<b>NPSA</b>	The national patient safety agency
<b>OD</b>	Optical density
<b>Ormosil</b>	Organically modified silica
<b>PBS</b>	Phosphate buffered saline
<b>PPE</b>	Personal protective equipment
<b>QAC</b>	Quaternary ammonium compound
<b>QS</b>	Quorum sensing
<b>RF</b>	Residue fraction
<b>SBA-15</b>	Santa Barbara amorphous-15

<b>SD</b>	Standard deviation
<b>SEM</b>	Scanning electron microscope
<b>TEOS</b>	Tetraethoxysilane
<b>TG</b>	Thermogravimetric
<b>TGA</b>	Thermogravimetric analysis
<b>TSA</b>	Tryptone soya agar
<b>TTC</b>	Trimethyltetrazolium chloride
<b>TTO</b>	Tea tree oil
<b>UTI</b>	Urinary tract infection
<b>UV</b>	Ultra violet
<b>VTEC</b>	Vero cytotoxigenic
<b>WHO</b>	World health organisation
<b>WOT</b>	Without template
<b>WT</b>	With template
<b>ZOI</b>	Zone of inhibition

## **Chapter 1**

### **Introduction to healthcare associated infections**

## 1.1 Healthcare associated infections

The term Healthcare-associated Infection (abbreviated as HCAI) has largely replaced others such as Hospital-acquired Infection (HAI), nosocomial infection and hospital-onset infection. HCAI is a more modern reflection of the range of settings in which people receive health-related attention. The term HCAI is defined as any infectious agent acquired as a consequence of a person's treatment by a healthcare provider, or which is acquired by a healthcare worker in the course of their duties (From National Audit Office (NAO) report *Reducing Healthcare-associated Infections in Hospitals in England*, 2009, quoting from the Health Act 2006: *Code of Practice for the Prevention and Control of Healthcare-associated Infections*). This has replaced the previous definition of an infection that was neither present nor incubating at the time of entering a hospital environment (NAO, 2009) (Table 1.1). HCAs are an important worldwide health problem, posing a major problem to patient safety. The economic burden of HCAI is significant in terms of resources, including extended hospital stays, staff time and treatment costs. Additional requirements, such as isolation and sterilisation of facilities and instruments used for these patients also significantly increase healthcare costs (Warnke, 2009). Reported hospital costs for a patient with HCAI are 2.9 times higher than for an uninfected patient, equating to an increase of over £3000 per patient, with HCAI costing the NHS at least £1bn annually and causing 5000 deaths (NAO 2004; NAO, 2009). However, the indirect costs of HCAI are more difficult to quantify. These include costs for cleaning, additional clinical waste, microbiology and surveillance (Damani 2003). The Hospital Infection Society released the results of the third national prevalence survey in March 2007. This survey of 190 acute hospitals in England was conducted in 2006 and involved 58,000 patients. It was reported, in the latter, that 8.2% of patients have an HCAI, a reduction from 9.2%, as reported in

the first national prevalence survey conducted in 1980 Hospital Infection Society (HIS) Press Release 8<sup>th</sup> March 2007 (HIS, 2007).

The Health Protection Agency (HPA) conducted a survey of 99 NHS acute trusts and five private-sector care organisations between September and November 2011. In total, data from 52,433 patients was analysed and presented in the report. The survey included data on the type of infection (the microorganism involved), the location of the infection, patient characteristics and hospital characteristics. Based on results from a selection of hospitals across England, the report indicates that there have been large reductions in both MRSA and *C. difficile* rates since the last survey was conducted in 2006. *C. difficile* infections fell from 2% of patients becoming infected in 2006 to 0.4% in the 2012 report. Methicillin resistant *Staphylococcus aureus* (MRSA) fell even more sharply, from 1.8% of patients affected to less than 0.1% (HPA, 2011)

Table 1.1. Main Causes of Healthcare-associated Infections in England (National Audit Office 2009).

Type of Infection	Percentage of all HCAI	Risk Factors	Main Causative Organisms
<b>Urinary Tract Infections (UTI)</b>	20%	80% of HCAI UTI are associated with urinary catheters (method and duration of catheterisation and susceptibility of patient.)	Gram negative bacteria especially <i>E. coli</i>
<b>Lower Respiratory Tract Infections</b>	20%	Mechanical ventilation; cumulative duration of ventilation.	<i>Acinetobacter</i> species, <i>S. aureus</i>
<b>Gastrointestinal</b>	22%	The gut may become colonised with <i>C. difficile</i> which may establish an infection if normal gut flora is disrupted by broad spectrum antibiotics. The elderly are at particular risk.	70% of HCAI gastro- intestinal infections were caused by <i>C. difficile</i>
<b>Surgical Site Infection</b>	14%	Duration of surgery, surgical technique, preparation, presence of foreign material, length of hospital stay and antibiotic prophylaxis.	<i>S. aureus</i> ~50%, <i>P. aeruginosa</i> Other Gram negative bacteria
<b>Bacteraemia</b>	7%	Approx. 44% associated with invasive devices.	<i>E. coli</i> and other Gram negative bacteria, <i>S. aureus</i>
<b>Skin &amp; Soft Tissue</b>	10%	Management of open wounds and pressure sores.	<i>S. aureus</i>
<b>Other</b>	7%	Includes infections of bones and joints and the central nervous system. Often linked to surgical or invasive procedures.	

Bacteria cause the majority of HCAs, with the public being mainly aware of MRSA bloodstream infections and the gastrointestinal infection caused by *Clostridium difficile* (CDI). The July – September 2011 HPA quarterly epidemiology report providing mandatorily reportable MRSA bacteraemia, and *C. difficile* infection data, reported 86.2% decrease in incidences of these two infections, (HPA, 2011c). The report suggests that recent efforts to tackle MRSA transmission in hospitals have been effective at driving down the prevalence of these infections. Many of these are simple yet effective and include; emphasis of the importance of regular, thorough hand-washing and swabbing patients to test for MRSA as they are being admitted to hospital. Despite these improvements, the HPA still emphasises there needs to be continued focus on preventative efforts in order to keep the number of infections low. Considering the incidence and costs implications of HCAI (roughly £1 billion per annum for the NHS), it is not surprising that healthcare authorities around the world are continuously seeking new ways to control HCAs.

## 1.2 Antimicrobial resistance

A golden age of antibiotic drug discovery occurred between the 1930's and the 1960's. However, the advent of antibiotic resistance rapidly followed the introduction of all classes of antibiotics into clinical practice (Hogberg *et al*, 2010). The need for new antibiotics to combat the threat of antimicrobial resistance (AMR), contrasts sharply with the lack of research and development of new antimicrobial compounds by pharmaceutical companies (Talbot *et al*, 2006).

Pharmaceutical companies have reduced their focus on research and development of new antibiotics for the following reasons (Hogberg *et al*, 2010):

- Long time lines for development;
- Spread of antibiotic and antimicrobial resistance (that can limit the market life of a product);
- Low profit margins as a result of short treatment times and the effects of stewardship programmes to restrict the use of new agents.

The misuse of antimicrobials is one of the major driving forces in the emergence of antimicrobial resistance. A high level of antimicrobial consumption in a specific geographic region is perhaps the biggest driving force behind the emergence of antimicrobial resistance. In light of this, the World Health Organisation (WHO) compiled an antimicrobial surveillance report, raising awareness of AMR and the need for appropriate surveillance systems. The European Antimicrobial Resistance Surveillance Network – EARS-Net is an international surveillance system that includes all 28 EU countries. The network includes surveillance of antibacterial susceptibility of eight indicator pathogens causing bloodstream infections and meningitis. It also monitors variations in AMR over time and place (WHO 2014).

Exposure to sub-inhibitory antimicrobial concentrations can select for a hypermutation phenotype, leading to the rapid accumulation of resistance mutations (Laureti *et al*, 2013). A sub-inhibitory concentration is a concentration of antimicrobial that is not sufficient to kill bacteria, but may alter cellular processes. Whether these newly acquired resistance mechanisms persist and disseminate within the bacterial population is dependent on the extent of damage to cell viability imposed. Another major driving force in the emergence of antimicrobial resistance in a specific geographic region is the level of antimicrobial consumption in that area. Comparison of antimicrobial consumption levels from 15 European countries from 1998 to 2004 and 2004 to

2005, showed that there was a significant association between antimicrobial resistance and antimicrobial consumption in all of the countries studied (Riedel 2007). As a consequence, more aggressive antibiotics are used to treat the infection, such as vancomycin. These drugs tend to cause more risk to the patient due to increased side effects, and in general a full course of the antibiotic tends to be more expensive than the original drug of choice. Bacterial resistance to antibiotics also increases the risk of fatality due to HCAI. Therefore it is of vital importance to discover ways to reduce incidence of HCAI in patients, rather than treating them when they occur. Cross-resistance of disinfectant-resistant bacteria to antibiotics has also developed. This can occur as a result of quaternary ammonium compound (QAC) resistance genes being located within conserved regions of integrons, which have been shown to carry multiple antibiotic resistance genes (Zhang *et al* 2011, Zou *et al* 2014).

Antibiotic resistance is either acquired through mutation, via gene exchange or is inherent, as seen in many environmental bacteria. Selective pressures upon the organisms from the hospital environment are also a factor in the acquisition of resistance. Antibiotic resistance has been designated as an 'emerging' infectious disease and is now considered a major public health issue. This has come as a result of 'bacterial evolution finally surpassing the human capacity to create new antimicrobial agents' (Rahal *et al*, 2002).

### 1.3 Bacterial reservoirs, environmental cleaning and persistence

Infection prevention and control are seen as the responsibility of all within the healthcare setting and has a level of high importance within the National Health Service (NHS). The latter have produced (or have had produced on their behalf) numerous policies and guidance documents. National evidence-based

guidelines for the prevention of HCAI within the NHS were commissioned by the Department of Health (DH) and published in 2001. These standard principles for prevention of HCAI include, among others, guidance on hospital environmental hygiene, hand hygiene and the use of personal protective equipment. Other aids to HCAI prevention include surveillance, for example, mandatory reporting of MRSA bacteraemia in England since 2001 and *Clostridium difficile* in over 65's since 2004 with enhanced surveillance from 2007 in all patients aged  $\geq 2$  years, along with auditing compliance with key policies and procedures for preventing HCAI.

The regular domestic cleaning of inanimate surfaces in a healthcare environment is vitally important. In addition, the behaviours of healthcare workers daily routine activities, such as hand washing (animate surfaces) to block or minimise the colonisation by microorganism strains that can cause nosocomial infection are equally important. The routes of transmission for microorganisms are varied. Bacteria may come from endogenous sources, from the patients themselves, or exogenously from others or the environment. Bacteria can be dispersed from these reservoirs (coughs and sneezes from colonised or infected patients or from water outlets) to susceptible hosts. In addition to the duration of persistence of microorganisms in the environment, other factors influencing persistence of microbes have been identified. Low temperature and high humidity were both associated with longer persistence for most bacteria, fungi and some viruses (Boyce, 2007). It has been shown that healthcare workers' gloved hands may become contaminated, and that on removal of gloves the hands may also be contaminated.

*P. aeruginosa* can also survive on inanimate surfaces for long periods of  $\leq 16$  months, and on a dry floor,  $\leq 5$  weeks. This fact is in contrast to many other Gram-negative bacteria, which are often highly susceptible to desiccation in dry

environments (Kramer *et al*, 2006). Hospital surfaces such as curtains, mattress covers, bed linen, staff uniforms and chair covers have been reported as a possible reservoir of microorganisms causing HCAI. The most common HCAI pathogens such as MRSA and *C.difficile* can survive on inanimate hospital surfaces for months and can therefore be a continuous source of transmission if no regular preventative surface disinfection is performed (Kramer *et al*, 2006). Although patients are especially vulnerable due to their existing conditions, they are not the only people at risk of contracting infection in a healthcare environment. Healthcare workers are frequently exposed to infectious agents via airborne, droplet and person-to-person transmission. The current work will focus on five microorganisms associated with HCAI, namely *S.aureus*, MRSA, *E.coli*, *P.aeruginosa* and *C.albicans*. Chosen to provide a range of microorganisms, including Gram-positive, Gram-negative and a yeast.

The importance of *P. aeruginosa* as a HCAI pathogen is underlined by multi-drug resistance. The bacterium may possess a number of inherent or acquired resistance mechanisms including drug exclusion and enzymatic inactivation. Exclusion of antibiotics was long considered to be due to the impermeability of the cell, however three-component efflux pumps, comprising the pump in the cytoplasmic membrane, a linker lipoprotein in the periplasm and an exit portal in the outer membrane appear to contribute (Avrain *et al* 2013). Within the hospital, *P. aeruginosa* is found in numerous reservoirs including disinfectants (Lanini *et al*, 2011), bath basins (Johnson *et al*, 2009), water-baths used to thaw frozen plasma (Muyldermans *et al*, 1998), contaminated nebulizers (Cobben *et al*, 1996) and bronchoscopes (Diaz-Granados *et al*, 2009). As can be seen from these examples, many of the reservoirs are aqueous or associated with high moisture content. The long-term survival of potential pathogens on surfaces, together with increasing resistance development to disinfectants and antibiotics

used in treatment, highlights the need to ensure surfaces including medical textiles (curtains, mattress covers, sheets, uniforms, chair covers) do not pose a potential transmission route for the spread of HCAI. Both water and air harbour microorganisms and there are strategies to prevent transmission via these routes. Hospital patients are frequently exposed to waterborne microorganisms as they can exist in many moist reservoirs. Persistence of these microorganisms within the hospital environment, poses a significant risk for their transmission to susceptible patients. Owing to the risk of patient acquisition of pathogenic bacteria from the hospital environment much emphasis has been placed on hospital cleanliness and a number of initiatives launched as a result (Table 1.2). Hand hygiene has very much been the focus of government and NHS guidance to health care workers and visitors alike. The National Patient Safety Agency (NPSA) launched the national “clean your hands” campaign in 2004 to improve hand hygiene practiced by NHS staff. The process of hand washing has evolved to include alcohol-based gel products along with hand washing using soap and water in an attempt to interrupt the transmission of infection cycle from health care workers to patients. Personal Protective Equipment (PPE) such as gloves, aprons and face masks are also available for health care workers as routine for many procedures and also when attending to patients nursed in source isolation, known as barrier nursing.

Table 1.2. the associated costs of the national initiatives for tackling HCAI adapted from the NAO's "Reducing Healthcare Associated Infections in Hospitals in England" (2009).

<b>Initiative</b>	<b>Aims</b>	<b>Cost</b>
<b>Modern Matrons</b> (2004)	The improvement of clinical care	Approximately £56 million per year (Infection control is 30 per cent of their workload)
<b>Cleanyourhands Campaign</b> (2004)	To improve the availability of alcoholhand rub at the point of patient care, increase compliance with hand hygiene and also auditing of hand hygiene.	£2.5 million
<b>Saving Lives</b> (2006)	To provide the tools and resources for hospital trusts to embed robust infection prevention and control measures across their organisation	Not possible to separately identify
<b>The Code of Practice</b> (part of the Health Act 2006)	This sets out statutory criteria by which managers of NHS organisations are to ensure that patients are cared for in a clean environment, where the risk of HCAI is kept as low as possible.	Not possible to separately identify
<b>The Improvement Teams</b> (2006)	Provide support to trusts in achieving reductions in MRSA bloodstream infections. Including support that ranges from visits to telephone advice.	£3 million per year
<b>The Deep Clean</b> (2008)	Improvements in cleanliness and patient confidence.	£62.6 million
<b>Technology Programme</b> (2008) including the Rapid Review Panel (2004)	Speed up the process of assessment and adoption of technologies to further help prevent HCAI.	£25,000 for the panel and £10 million per year from 2008-09 onwards
<b>MRSA Screening</b> (from April 2009)	To reduce the carriage of MRSA in patients admitted electively or acutely to hospital.	Approximately £130 million per year from 2010-11

Alongside the personal hygiene responsibilities of individual healthcare workers and the encouragement for a similar attitude for both patients and visitors, is attention to the cleanliness of the hospital environment itself. In NHS environments, cleaning staff are issued with cleaning schedules, which list areas, rooms and frequencies of clean, as specified in (National specifications for cleanliness in the NHS 2007) which are initialed daily on completion by domestic staff. Domestic Supervisors undertake routine monitoring audits, and required frequency of cleaning. Clinical staff undertake cleaning of patient related equipment and clinical equipment. Identified areas with infections are cleaned using 'Deep Clean' or 'Chlor Clean' (1000 ppm Chlorine with cold water) procedures. Many novel approaches have been developed to augment traditional 'domestic' cleaning methods. These include ultra microfibre cloths, mops containing biocides, ultra violet UV irradiation, impregnation of materials with heavy metals and ionisation (Veerabadran 2010). Other interventions involve patient care such as cohort nursing, isolation rooms, ventilation, screening of patients for carriage of pathogens such as MRSA, ensuring good nutrition and, for prevention of *C. difficile* infection, administration of probiotics (Plummer *et al* 2004, Cepeda *et al* 2005). Interventions to reduce acquisition of water-borne pathogens include point-of-use filters, thermal shock, UV-light and copper-silver ionisation. High-efficiency particulate air (HEPA) filtration and optimised ventilation can reduce the number of air-borne pathogens such as the fungus *Aspergillus*, as well as bacteria such as MRSA and *P. aeruginosa* (Curtis, 2008). However, it is very difficult to validate or instigate a risk-assessed method for hospital cleanliness.

The primary objective of this thesis was to investigate the potential for the use of natural antimicrobials to add antimicrobial efficacy to synthetic textiles. It was envisaged that mesoporous silica nanoparticles could be used to provide a slow release of the antimicrobial from the textile, with any successful product being used in healthcare environments against the spread of healthcare associated infections.

## **Chapter 2**

### **Screening of essential oils for antimicrobial properties**

## 2.1 Introduction

The initial stage of this study was to select a range of essential oils (EO) and assess their antimicrobial efficacy against a number of microorganisms associated with healthcare associated infections. The EOs were tested individually and in blends. The most effective blend was then tested against the microorganisms. The most effective EOs and blends were analysed using gas chromatography mass spectrometry to determine if there were any chemical differences between them, and their respective antimicrobial efficacies.

### 2.1.1 Essential oils

Essential oils are complex mixtures of plant secondary metabolites, mostly comprising volatile chemical constituents, such as terpenoids. These chemical compounds are responsible for the characteristic odour, pigments and flavours in many plants. They act as a defence against microbes, herbivores, plant disease and other ecological factors (Wallace 2004). There are approximately 4500 individual constituents known to occur in essential oils: such chemical diversity does not allow a common structural definition for them. However, monoterpenes, sesquiterpenes and their derivatives are the predominant chemical constituents. Additional components include aliphatic hydrocarbons, acids, alcohols, aldehydes, acyclic esters, lactones, nitrogen and sulphur containing compounds, coumarins and phenylpropanoids (Giordini *et al* 2001). It is known that many oil constituents display antimicrobial activity, with olive oil and virgin olive oil containing polyphenol groups displaying some antimicrobial activity (Brenes *et al* 2007). Essential oils can be obtained from plants by expression, fermentation, enfleurage or extraction, but the steam distillation method is the most commonly used for commercial production (Van de Braak

and Leijten, 1999). Evidence exists for the production of 'fragrant waters' from boiling plant material as far back as the Indus Valley civilisation, 5000 years ago (Williams, 1989). The use of tea tree oil for medical remedies has been documented since the colonisation of Australia (Carson and Riley, 1993). Currently, the heaviest use of essential oils in the EU is in food, as flavourings, perfumes and pharmaceuticals. The antibacterial properties of essential oils and their components are also exploited in commercial products, such as dental root canal sealers and antiseptics (Cox *et al* 2000). This project focuses on the antimicrobial bioactivities displayed by many essential oils.

#### 2.1.2 Mode of action

To date, research has shown EO bacterial cell targets include the cell wall and membrane, consequently disrupting Adenosine tri-phosphate (ATP) production and pH homeostasis in the cell. EOs can also affect the bacterial cells transcriptome, proteome and the cell signalling (quorum-sensing) system (Szabo 2010). For a bacterial cell, a series of vital functions rely on an intact working membrane, including the energy production, nutrient uptake and processing, synthesis of macromolecules and secretion. Once the cell membrane is disrupted by EOs, those processes will be compromised. In prokaryotes, ATP production takes place in the membrane and the cytosol by glycolysis. Intracellular and extracellular energy production is therefore disrupted by the EO activity on the cell membrane. Disruption of pH homeostasis by EOs is a consequence of their action on bacterial membranes, which become incapable of blocking proton entry. Bacterial cells adopt a series of strategies to achieve the most vital of processes, when exposed to conditions that compromise their survival. In particular, deoxyribose nucleic acid (DNA) transcription, protein synthesis and enzymatic activity (Fux *et al*, 2005). Intracellular pH maintenance

is crucial to these processes (Iwami *et al*, 2002). Reduction in intracellular pH has been reported in bacterial cells that are exposed to EOs (Oussalah 2006). Proton influx can occur in bacterial cells exposed to EOs, if proton levels exceed the cytoplasmic buffering capacity or overwhelm proton efflux pumps, the intracellular pH level decreases and essential cellular functions are subsequently compromised (Foster 2004).

Quorum sensing (QS) describes the capacity of bacterial communities to modulate their population density via cell-cell communication and the use of small signalling molecules to assess the outside environment and their physiologic response (Camilli 2006). Central cellular processes such as motility, biofilm production, stress resistance, swarming and virulence are regulated by QS (Gobetti *et al* 2007). EOs have been studied as anti-QS products, with many EO molecules similar in structure to QS molecules (Szabo 2010). The technique of monitoring transcription levels of QS molecules in *E.coli* was used. Amongst those oils reported to be most active against QS were clove and geranium oil (Khan *et al* 2009).

Diminished enzymatic activity and the appearance of coagulated material within the cell have been reported to result from EO activity. Cinnamon EO has been reported to effect intracytoplasmic changes to *E.coli* and *S.aureus* (Derakhshan 2008).

Much research has been carried out on the antimicrobial mechanism of action of essential oils, with more than 20,000 journal articles published on the topic since the year 2000, [www.sciencedirect.com](http://www.sciencedirect.com) (keywords, essential oil, antimicrobial, mechanism, mode of action). Considering the large number of different groups of chemical compounds found in essential oils, it is likely their antibacterial activity is not solely attributed to one specific mechanism, but that there are several different targets in the cell (Figure 2.1). The chemical structure of the individual

essential oil constituent affects their precise mode of action and antibacterial activity (Dorman and Deans 2000). The lipophilicity of essential oil constituents, lipid composition of bacterial membranes and their net surface charge are the major factors deciding the membrane permeability of oil constituents. Their hydrophobicity enables them to incorporate into the lipid layers of the bacterial cell membrane, disturbing the structures and rendering them more permeable. Essential oil constituents may also cross the bacterial cell membrane, penetrating the interior of the cell and interacting with intracellular sites critical for antibacterial activity (Trombetta *et al* 2005).

Gram-negative bacteria are less susceptible to the action of essential oils, compared to Gram-positive bacteria. This is due to the presence of the outer membrane surrounding the cell wall, which restricts the diffusion of lipophilic compounds through the lipopolysaccharide covering (Mann *et al* 2000). The seven essential oils used in this study (cinnamon, clove, eucalyptus, geranium, lemongrass, lime and tea tree) were selected after reviewing the literature for their varying reported antimicrobial activities against microorganisms reported to cause HCAs.

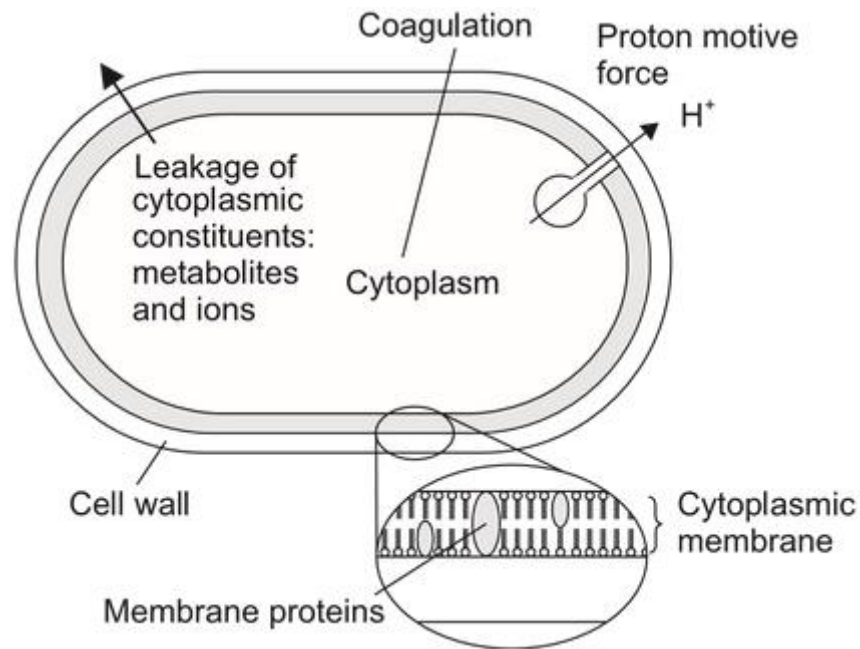


Figure 2. 1. The locations and mechanisms in the bacterial cell thought to be sites of action for essential oil active components (Ahmed & Aqil 2009).

### 2.1.3 Essential oils used in this study

Cinnamon leaf oil is extracted from plants belonging to the *Cinnamomum* genus. The oil is native to Indonesia, but often cultivated in India and Sri Lanka. The main chemical components of the oil distilled from the leaves are eugenol, eugenol acetate, cinnamic aldehyde and benzyl benzoate. Cinnamon leaf oil has been shown to display antimicrobial activity against *P.larvae* (Gende 2008, Prabuseenivasan 2006).

Clove oil (Upadhyay 2010) is extracted from the clove plant, *Syzygium aromaticum*. Clove oil contains a very high proportion of eugenol that has been shown to be highly antimicrobial (Chaieb 2007). Clove oil was reported to have inhibited growth of the yeast *C.albicans* at 0.12 (v/v), (Hammer 1999).

Eucalyptus oil is distilled from leaves of the eucalyptus tree, belonging to the genus *Eucalyptus* of the plant family *Myrtaceae* that is native to Australia.

Eucalyptus oil has been shown to display antimicrobial activity with MICs of 1% (v/v) against *C.albicans* and *E.coli* (Hammer 1999).

Geranium oil is isolated from plants of the genus *Pelargonium* and is most commonly produced in Algeria, Egypt and Morocco. Geranium oil contains over 50 % (v/v) geraniol and citronellol. Interestingly, a study by Khalaj and Farzin has shown that geranium oil has antidepressant activity (Khalaj and Farzin 2006). Geranium oil also exhibits well-known antimicrobial properties (Rosato 2007).

Lemongrass oil is extracted from the plant *Cymbopogon citratus* and its main chemical constituent is citral at 50-80% (Naik 2010). Lemongrass has displayed antimicrobial activity, with MICs of 0.06% (v/v) against *C.albicans* and 0.06% against *E.coli* (Hammer 1999). Native to India, where it has traditionally been used to treat fever and infectious illnesses. Skin sensitisation can occur when the oil is applied topically to the skin, this is due to the large proportion of citral, which can be an irritant.

Lime oil extracted from the fruit of the *Citrus aurantifolia* tree has been reported to show antimicrobial effects (Prabuseenivasan 2006). Lime oil was reported to inhibit growth of *E.coli* at 1% (v/v) and *C.albicans* and *S.aureus* at 2% (v/v) (Hammer 1999).

Tea tree oil has been shown to disrupt the permeability barrier of microbial membrane structures (Cox *et al* 2000). The study showed enhanced permeability of bacterial cytoplasmic and yeast plasma membranes at minimum inhibitory levels of tea tree oil. Leakage of potassium ions was also observed upon adding tea tree oil to these microbial suspensions of *E.coli*, *S.aureus* and *C.albicans*. Although a certain amount of leakage from bacterial cells may be tolerated without loss of viability, extensive loss of cell contents or the exit of critical molecules and ions will lead to cell death.

#### 2.1.4 Screening of essential oils

It is apparent that evaluation of the antimicrobial activities of EOs is a difficult task as they are complex mixtures, poorly soluble in water and in the main volatile (Lahlou 2004).

While there has been an abundance of studies carried out, the use of essential oils in antimicrobial research has been hampered by the lack of reliable and standardised *in vitro* screening methods. The lack of standardised methods also makes direct comparison of results between studies difficult. The various methods of note in the literature include disc diffusion, well diffusion, agar dilution and broth dilution, with surfactants, such as Tween 20 and 80 used to create a better dispersion of the hydrophobic EOs in broth or agar. For most commonly isolated bacterial and fungal pathogens, antimicrobial susceptibility testing can be performed by routine hospital laboratories. The most common methods utilised are the disc diffusion susceptibility test method (also known as Kirby-Bauer) and minimal inhibitory concentration (MIC) determination. In 2001 the British Society for Antimicrobial Chemotherapy (BSAC) published a standardised disc diffusion method, seen as the gold standard for antibiotic and antiseptic screening (Andrews 2001). It should be noted that the substances normally tested by these methods are generally hydrophilic in nature and therefore the assays have been optimised for this specific condition (Burt, 2004). This is in contrast to the hydrophobic nature of EOs.

Most studies investigating the antibacterial properties of essential oils have incorporated two or more antimicrobial assays, the most popular methods being disc and well diffusion (Hammer *et al* 1999). However, there were widespread differences in incubation times, materials used and the formulation of the systems. Antimicrobial activity from broth dilution assays displayed enormous

variation in technique, methodology and choice of surfactants (necessary for emulsification of the hydrophobic essential oils) (Flamini *et al* 1999).

The major difficulties associated with the use of essential oils seem to be:

- The viscosity or hydrophobicity of the oil creates difficulty in obtaining a stable aqueous dispersion or suspension,
- The problems associated with the diffusion of lipophilic oil components through agar media,
- The need for neutralising agents post-incubation with EO for the determination of colony forming units (CFU)/mL.

Among all the methods described, the broth dilution method is seemingly the most widely used (Prabuseenivasan *et al* 2006). Most researchers cite the minimum inhibitory concentration (MIC) as a measure of the antibacterial performance of EOs. The method to define MIC differs between publications, (Hammer *et al* 1999, Prabuseenivasan *et al* 2006) defines MIC as the lowest concentration of oil inhibiting visible growth, whereas (Kon and Rai 2012) state MICs were determined by measuring optical density at 570 nm and defined as the concentration of oil at which there was a sharp decline in the absorbance value. In addition, (Loughlin *et al* 2008) stated MIC was read as the lowest concentration of antimicrobial at which no colour change occurred, indicating the trimethyl tetrazolium chloride was not reduced to a red colour by bacterial growth. For the purposes of this project, the MIC will be defined as the lowest concentration inhibiting visible growth of the test organism. Essential oils are volatile, insoluble in water, viscous and complex substances. Pauli *et al* reviewed results from three antimicrobial tests; agar diffusion, dilution test and vapour phase test) on 28 EOs (Pauli and Schilcher 2010). There was great

variability in the results, which may be explained by the following factors: natural variability in the composition of the EOs, natural variability in the susceptibility of the microorganisms, different parameters in the microbiological testing methods, the unknown history of the EO tested (their production, age and storage conditions), and insufficient knowledge about exact phytochemical composition.

#### 2.1.5 The bacterial cell

All bacterial cells have an inner bi-layer membrane, comprised of phospholipids, which are encased in a peptidoglycan cell wall. They reproduce by binary fission (Tortora *et al* 2007).

Bacteria are separated into two groups, differentiated by their reaction to a procedure containing dyes and stains. In 1884 the Danish scientist Hans Christian Gram discovered that certain bacterial cells retained crystal violet dye when washed with alcohol, whilst in others the dye was washed away.

Initially, a bacterial sample is heat-fixed on a glass slide. The slide is flooded with crystal violet, colouring all cells in the sample purple. After 1 minute, the excess crystal violet is drained off and the sample is washed with distilled water. The sample is then covered with Gram's iodine, which acts as a mordant to fix the purple colouring of the crystal violet dye. When the iodine is washed off, both Gram-positive and Gram-negative cells appear deep purple. The sample is then washed with 95% ethanol, acting as a decolourising agent, removing the crystal violet stain from some cells, but not others. The sample is washed with distilled water again, then exposed to safranin, a basic red dye, which acts as the counter stain. Once washed for a final time with distilled water, the sample is heat dried and examined.

The physico-chemistry of the cell wall is therefore the differentiating factor. The crystal violet dye and iodine combine in the cytoplasm of each bacterium to colour it dark violet or purple. The bacteria that retain this colour after the alcohol has attempted to decolourise them are referred to as Gram-positive, while the bacteria that lose the purple colouring after the alcohol treatment are referred to as Gram-negative.

Gram-positive bacteria have a rigid cell wall, which is between 30 nm and 100 nm in thickness. The peptidoglycan grows with new layers formed on the inside of the cell wall, next to the cell membrane, with the oldest layers at the outer edge. Gram-positive cell walls also contain teichoic acids that provide rigidity, and act as cell growth regulators (Singleton 2004). Crystal violet and iodine readily enter both Gram-positive and Gram-negative cells, combining to form a crystal violet-iodine (CV-I) complex, that is a larger molecule than the crystal violet or iodine entering the cells. Due to its size, this (CV-I) complex can not be washed out of the thick peptidoglycan layer of Gram-positive cells by alcohol. Gram-negative bacteria, in contrast, have a thin peptidoglycan layer. The alcohol disrupts the outer lipopolysaccharide layer and the CV-I complex is washed out of the Gram-negative cells. As a result, Gram-negative cells are colourless, until counter stained with safranin, after which they appear pink.

#### 2.1.6 Microorganisms

Five microorganisms were selected as challenges for screening the antimicrobial activity of the EOs. Two Gram-positive, two Gram-negative bacteria and one yeast were selected to provide a range of microorganisms, reported to cause HCAI, and are described briefly below.

#### 2.1.6.1 *Pseudomonas aeruginosa*

*P.aeruginosa* is a Gram-negative bacillus with cell dimensions of approximately 0.5 – 0.8 µm by 1.5 – 3.0 µm. A high proportion of *P.aeruginosa* strains are motile via a single polar flagellum. *P.aeruginosa* grows well at a variety of temperatures (25 - 37°C) and is resistant to relatively high concentrations of salt, dyes, weak antiseptics and most commonly used antibiotics (Krishnan *et al* 2015). These robust characteristics allow it to survive well in many environments resulting in prolific transfer and contamination.

The Health Protection Agency (HPA) described *P.aeruginosa* as an opportunistic pathogen that can cause a wide range of infections, particularly against the immunocompromised. A study conducted by the HPA showed *P.aeruginosa* accounted for approximately 93% of all identified *Pseudomonas spp.* Infections reported in UK healthcare facilities (HPA 2009).

The frequency of *P.aeruginosa* HCAs make it an ideal target for any technology aimed at reducing the incidence of HCAI. In a survey of most frequently associated microorganisms associated with HCAI, *P.aeruginosa* accounted for 6% of the 3,506 cases (HPA 2011).

#### 2.1.6.2 *Staphylococcus aureus*

*S.aureus* is a non-sporulating, non-motile, Gram-positive cocci with an average diameter of 1 µm. They occur in grape like clusters, tetrads and sometimes in short chains. *S.aureus* is a facultative anaerobe that is coagulase and catalase positive. *S.aureus* occurs naturally on the skin and is part of the human mucosal membrane flora (Stevens 2006).

Of all staphylococci species, *S.aureus* is the most important human pathogen, causing a wide range of infections due to its ability to produce a wide variety of cellular and extracellular proteins associated with virulence of the bacterium.

These range from skin and soft tissue infection, cellulitis, folliculitis, impetigo, post-operative wound infection, osteomyelitis, endocarditis and haemolytic pneumonia (Blomquist 2006).

#### 2.1.6.3 Methicillin resistant *Staphylococcus aureus*

Methicillin resistant *Staphylococcus aureus* (MRSA) are strains of *S.aureus* which have acquired resistance to the antibiotic methicillin. Due to increasing antimicrobial resistance, efforts are being made to ensure the correct antibiotics are only administered when necessary. Important actions include preventing infections from happening in the first place, through better hygiene, access to clean water, infection control in health-care facilities, and vaccination to reduce the need for antibiotics. The development of new diagnostics, antibiotics and other tools are necessary to allow healthcare professionals to stay ahead of emerging resistance. MRSA are described as opportunistic pathogens, about 0.5 – 1 µm in diameter gram positive cocci. Commonly found in skin infections, MRSA can cause osteomyelitis, septicaemia and abscesses (Cohen 1986). MRSA infections are difficult to treat and accounts for a 64% higher mortality rate in comparison to methicillin susceptible *Staphylococcus aureus* infection (WHO 2014).

#### 2.1.6.4 *Escherichia coli*

*E.coli* is a Gram-negative rod-shaped bacterium that resides in the lower intestine, usually motile by peritrichous flagella. *E.coli* is the most common cause of acute urinary tract infections as well as urinary tract sepsis. It has also been known to cause neonatal meningitis and sepsis and also abscesses in a number of organ systems. *E.coli* may also cause acute enteritis in humans as well as

animals and is a general cause of 'traveller's diarrhoea', a dysentery-like disease affecting humans, and haemorrhagic colitis often referred to as 'bloody diarrhoea'. Virulence types of *E.coli* include enterotoxigenic (ETEC), enteroinvasive (EIEC), enteropathogenic (EPEC), and Vero cytotoxigenic (VTEC) (Curtis and Lawley 2003). Moreover, *E. coli* are introduced into water bacteriology because it is a useful marker of faecal pollution and thus became an important marker in food and water hygiene (Percival *et al* 2004).

#### 2.1.6.5 *Candida albicans*

*Candida albicans* is an opportunistic human fungal pathogen, which causes disease mainly in immuno-compromised patients. Activity of hydrolytic enzymes is essential for virulence of *C.albicans* and so is the capacity of these cells to undergo transition from yeast to mycelial form of growth. It can grow as yeast cells, pseudohyphae and hyphae, and this dimorphic switching is required for full virulence (Yang 2003). *C.albicans* cells can adhere to and colonise certain human tissues and prostheses, eventually leading to biofilm formation. This subsequently reinforces adhesion, infection and resistance to antifungals (Tangarife-Castano *et al* 2011). Secretion of hydrolytic enzymes such as proteinases and phospholipases contribute to infections such as oral candidosis, where overgrowth of cells of the resident microflora occurs in the mouth. These enzymes are responsible for adhesion, tissue damage and invasion of host tissues. The production of a range of extracellular hydrolases has been attributed to *C.albicans* pathogenicity (Tangarife-Castano *et al* 2011). Candidiasis ranges from superficial infections such as oral thrush to deeply invasive disease, such as the *Candida* bloodstream infection, candidaemia. Bloodstream infections are the most common form of invasive candidiasis.

Systemic candidiasis is a common fungal infection worldwide and associated with high rates of morbidity and mortality in certain groups of patients. *C. albicans* infections remain as the top source of fungal infections in immunocompromised people. For example, in human immunodeficiency virus (HIV) patients, over 48% will develop a case of candidiasis (Khan *et al* 2012).

Although it is known that antifungal resistance imposes a substantial burden on health-care systems in industrialised countries, the global burden of antifungal-resistant *Candida* is unknown. Resistance to fluconazole, a common antifungal drug, varies widely by country and species. Resistance to the newest class of antifungal agents, the echinocandins, is already emerging in some countries (WHO 2014). *C.albicans* was added to the test microorganisms as a yeast in addition to four bacteria, providing an array of microbes that cause HCAs.

#### 2.1.7 Gas chromatography mass spectroscopy

Gas chromatography-mass spectrometry (GC-MS) is a combination of two distinct techniques used to analyse mixtures of chemicals. The initial part of the analysis is to isolate the individual components of the EO samples. In gas chromatography (GC) the chemical mixture is injected into an inert carrier gas, often helium, which is the mobile phase. The mobile phase and the sample then pass through the GC column, containing chemically receptive particles (the stationary phase). The components in the mixture interact with these particles at varying rates as they pass through the GC column (Figure 2.2). Molecules which have a weaker interaction with the column particle surface will elute first, while molecules that interact strongly will take longer to pass through the stationary phase. In this way the molecular components of the sample are separated out. Further separation can be achieved by adjusting temperature with low boiling

point molecules eluting faster at low temperature and high boiling point molecules eluting faster at higher temperatures. Once the molecule has passed through the stationary phase it is fed into a detector, which creates an electronic signal. The greater abundance of a molecule the larger the signal. The signal is plotted on a linear time graph with abundance of molecules on the y-axis and time on the x-axis. The area of the peak generated by the signal is a measure of the amount of that molecule detected and can be rationalised by the use of an internal standard of known concentration.

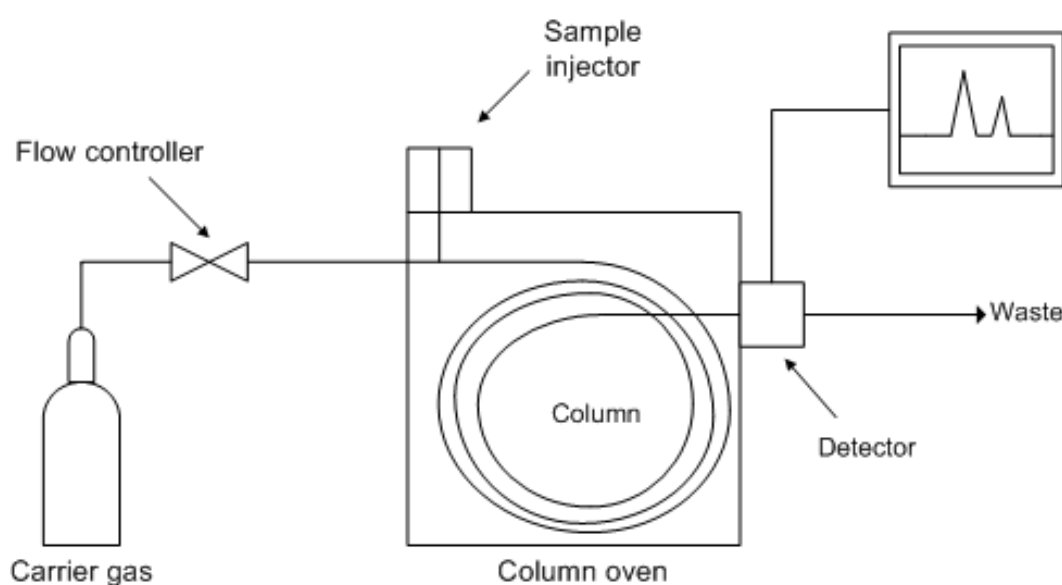


Figure 2. 2. A diagram showing gas chromatography analysis.

While GC allows for determination of the number of molecular components and their abundance, the mass spectrometer (MS) can detect the chemical makeup of the molecule, allowing it to be identified. Once the molecules have passed through the GC they are fed into the electron ionisation mass detector of the MS. Here they are bombarded with electrons, breaking them into ionised fragments of the original molecule. The ionised fragments are passed through a magnet which focuses them onto a detector (Figure 2.3). By varying the strength of the magnet, fragments of differing molecular mass can be focused onto the detector. The detector generates a signal for each fragment, which is plotted on a graph,

with molecular mass on the x-axis and abundance on the y-axis. This graph is the mass spectrum of the molecule which is often unique, and by comparing the mass spectrum of an unknown sample to a database it is possible to identify the molecule (Derwich *et al* 2010).

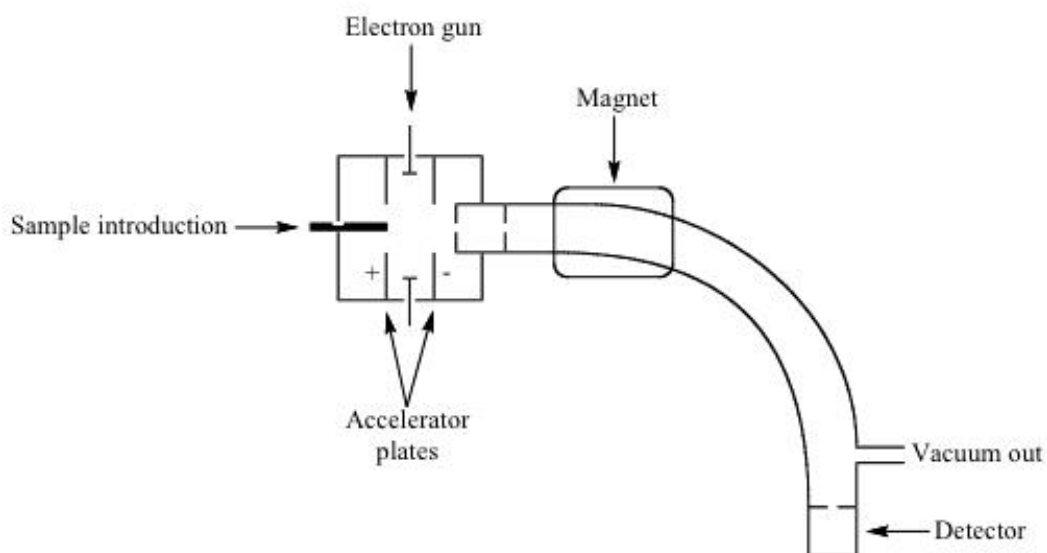


Figure 2.3. A diagram showing mass spectrometry analysis.

For this part of the project, GC-MS was used to analyse the chemical components of individual oils and then their respective blends to see if any changes occurred chemically and if these changes have an impact on antimicrobial efficacy.

## 2.2 Objectives

- Select a number of EOs for their range of antimicrobial activity against microorganisms associated with HCAs.
- Screen oils alone against microorganisms associated with HCAI at <2% to avoid skin sensitisation, considering potential end use.
- Test for synergy between the EOs in blends against the microorganisms.
- Record efficacy for contact kill against the microorganisms.
- Analyse EOs and the most potent blend using gas chromatography mass spectrometry to identify major chemical constituents.

## 2.3 Experimental

### 2.3.1 Materials

#### 2.3.1.1 Culture media

Nutrient agar (Oxoid CM0003, Basingstoke, UK), Iso-Sensitest agar (Oxoid CM0471, Basingstoke, UK), Mueller-Hinton agar (Oxoid CM0337, Basingstoke, UK), Tryptone soya agar (Oxoid CM0131, Basingstoke, UK) and Columbia agar (Oxoid CM0331, Basingstoke, UK) were made as per manufacturer's instructions and autoclaved at 121°C for 15 minutes in glass durans, then cooled to 50°C, before adding 5% (v/v) defibrinated horse blood for Columbia blood agar plates. Agar was then dispensed in 20 mL volumes in each petri dish. All agar plates were stored at 4°C, any unused agar plates were discarded after 4 weeks. Nutrient broth (Oxoid CM0001, Basingstoke, UK) and Iso-sensitest broth (Oxoid CM0473, Basingstoke, UK) were made as per manufacturer's instructions and dispensed in 500 mL glass bottles.

### 2.3.1.2 Microorganisms

*Escherichia coli* NCIMB9001, *Staphylococcus aureus* NCIMB8625, *Candida albicans* NCYC1363, *Pseudomonas aeruginosa* NCTC 6749, MRSA MMU T4. Stock cultures of all microorganisms were stored at -80°C. Subcultures were prepared from frozen isolates by streaking onto fresh agar plates. Nutrient agar (NA) was used for *S.aureus*, MRSA, *E.coli* and *P.aeruginosa*. Tryptone soya agar (TSA) was used for *C.albicans*. All streaked plates were incubated at 37°C for 24 hours, and stored in a refrigerated cabinet at 4°C prior to use. These streaked plates were replaced every four weeks, with fresh cultures being made before each experiment.

### 2.3.1.3 Essential oils

Tea Tree oil (*Melaleuca alternifolia*), clove oil (*Syzygium aromaticum*), cinnamon oil (*Cinnamomum zeylanicum*), lime oil (*Citrus aurantifolia*), eucalyptus oil (*Eucalyptus polybractea*), lemongrass oil (*Cymbopogon citratus*) and geranium oil (*Pelargonium graveolens*) (100 mL of each) were obtained from the on-line supplier [www.essentialoilsdirect.co.uk](http://www.essentialoilsdirect.co.uk). All oils were stored away from sunlight, at room temperature. Sterility was checked periodically by streaking a 2% (v/v) dilution of the oils onto a nutrient agar plate and incubating for 24 hours, with no signs of microbial growth apparent.

## 2.3.2 Methods

### 2.3.2.1 Preparation of cell suspensions

Prior to each experiment an overnight suspension was prepared for each microbial culture. Three well isolated colonies were taken from the streaked agar plate, inoculated into 10 mL of sterile Nutrient broth (NB) and incubated for 18 hours at 37°C. The optical density (OD) of the cell suspensions were adjusted to 0.1 at 600 nm and a count performed in order to determine CFU/mL.

### 2.3.2.2 Growth curves

Growth curves for the five chosen test organisms were undertaken to provide information on the stationary and exponential phases of growth, in order to determine appropriate incubation times when using test organisms in different stages of growth during time – kill assays.

An overnight culture of each microorganism was diluted to OD 0.1 at 600 nm. A 1:10 dilution of this culture was made, and 5 mL was added to 100 mL of Nutrient broth, or Sabouraud dextrose liquid medium for *C.albicans* and incubated at 37°C on a shaker at 120 rpm. Finally, 1 mL aliquots were taken at timed intervals ranging from 0 minutes to 24 hours and the OD at 600 nm was tracked over time.

### 2.3.3 Agar dilution assay

The agar dilution assay used in this study was based on a previously published method (Hammer 1999). Tween-20 was incorporated into Isosensitest agar (ISA) at a final concentration of 0.5% (v/v) to enhance dispersion of the oil within the media (Loughlin *et al* 2008). Cinnamon, clove, eucalyptus, lime, tea tree, lemongrass and geranium essential oils were used. A series of two-fold dilutions for each oil, ranging from 2% (v/v) to 0.03% (v/v) was prepared in ISA, with 0.5% Tween-20. A multi-point replicator was used to inoculate the plates with one spot of 1-2  $\mu$ L of the standardised cell suspension of each microorganism. Three ISA plates, with 0.5% (v/v) Tween-20 but no essential oil were used as positive growth controls. Inoculated plates were incubated at 37°C for 24 hours. The experiment was run in triplicate and repeated three times (n=9), with MICs determined as the lowest concentration of oil inhibiting visible growth of each microorganism on the nutrient agar plate.

### 2.3.4 Disk diffusion assay

Microbial suspensions were prepared as previously described and 30  $\mu$ L spread over the plates (standard 85 mm in diameter) containing 20 mL of Mueller Hinton agar (MHA) using a sterile plate spreader. Under aseptic conditions sterile paper disks were impregnated with 5  $\mu$ L of EO and left on paper towels for 5 minutes at room temperature to allow excess oil to soak out. Disks were then placed on the inoculated MHA surface, three on each plate. A disk with no absorbed EO was used as a control. The Petri dishes were left for 30 minutes at room temperature (20-22°C) to encourage oil diffusion prior to bacterial growth and were then placed in an incubator at 37°C for 24 hours. After the incubation period diameters of inhibition zones around the disks with EOs were measured in mm

using a ruler. The experiment was run in triplicate on three separate occasions (n=9).

#### 2.3.5 Broth micro-dilution assay

The method for this assay was based on that previously published (Loughlin 2008). Iso-Sensitest Broth (ISB) was autoclaved with double strength Tween-80 0.5% (v/v) with a final concentration of 0.25% to enhance oil distribution in the broth. The ISB Tween-80 mix was then used to dilute neat essential oil in doubling dilution for a final range of 2% (v/v) to 0.03% (v/v). Clove, cinnamon, tea tree, lemongrass, eucalyptus, lime and geranium oil were used for this assay. To overcome the problem of turbidity due to emulsified essential oil, trimethyltetrazolium chloride (TTC) was added post autoclaving (to ISB) using a sterile syringe to give a final concentration of 0.005% (v/v). TTC is a tetrazolium salt which is reduced by metabolically active cells to a coloured water-soluble formazan derivative, allowing visual identification of metabolic activity by a deep red colour indicating growth (Brady *et al* 2006). The microorganisms to be tested were then added to sterile 25 mL glass bottles containing 10 mL ISB-TTC mix, for a final concentration of approximately  $10^6$  CFU/mL.

Using a 96 well micro-titre plate (MTP), the ISB-TTC mix (75  $\mu$ L) was added to column 1 wells A-E and the ISB-Tween-80 mix (75  $\mu$ L) was added to column 2 wells A-E as controls (Figure 2.9). The ISB-Tween80-EO mix (75  $\mu$ L) was then added to the appropriate wells. Column 9 wells A-E containing the lowest concentration (0.03%), ascending to column 3 wells A-E containing the highest concentration (2%). The ISB-TTC-microorganism mix (75  $\mu$ L) was then added to all test wells apart from the negative control wells.

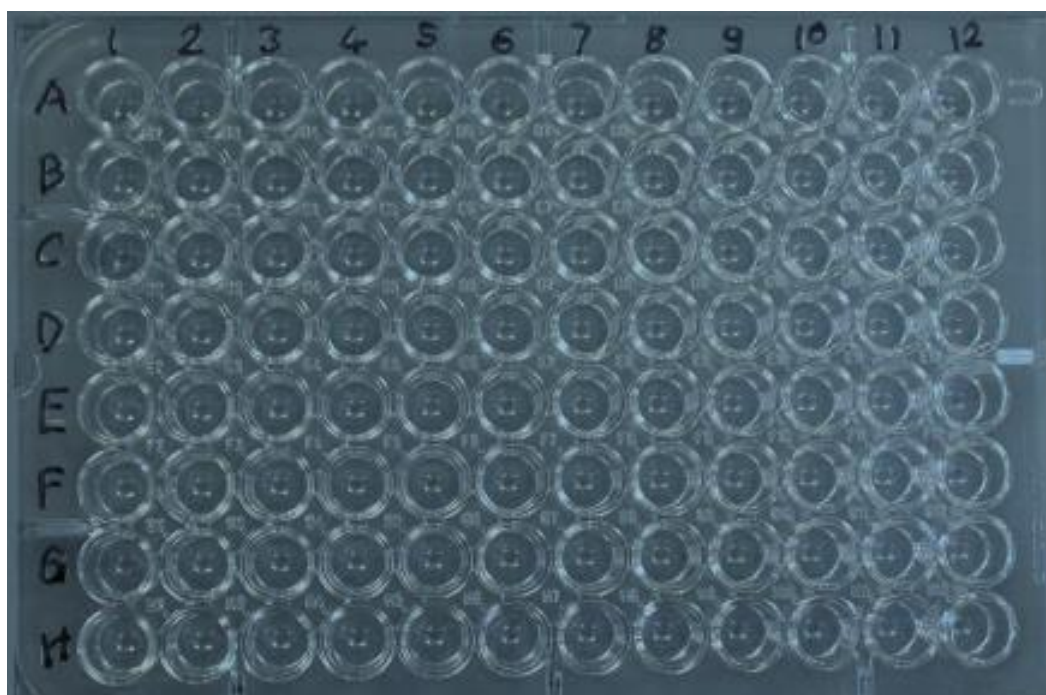


Figure 2.4. 96 well microtitre plate, demonstrating well layout.

Once inoculated, the MTPs were covered using Parafilm and aerobically incubated at 37°C for 24 hours. Post incubation, bacterial growth was indicated by TTC reduction and development of a red colour in the wells. MICs were taken to be the lowest concentration of essential oil at which no visible colour change occurred. The minimum bactericidal concentrations (MBCs) were determined by taking 10  $\mu$ L aliquots using an auto pipette, from each well that showed no growth in the MIC test and sub culturing onto nutrient agar. The 10  $\mu$ L drops were left to absorb into the agar and the plates were then aerobically incubated at 37°C for 24 hours. The first concentration which rendered no growth was taken to be the MBC. The experiment was run in triplicate, three times (n=9).

#### 2.3.6 Time – Kill assay

To provide a profile of the killing efficacy of the EOs, *S.aureus* MRSA, *P.aeruginosa*, *C.albicans* and *E.coli* were taken from an overnight culture in stationary phase. In addition, the microorganisms were also prepared in

exponential growth phase, by diluting overnight bacterial cultures in fresh broth and incubating at 37°C until they reached exponential growth phase according to the growth curves (Figures 2.1 to 2.5). In 5 mL glass bottles, 1 mL of cell suspension was added to 20 or 1.25 µL of EO to give final concentrations of 0.125% and 2% (v/v), respectively. Tween 80 was used as a surfactant, added to the broth containing cell cultures at a final concentration of 0.05% (v/v). A 10 µL aliquot was taken from the 0% EO test tube immediately after mixing to be used as a 'time 0' control. Test tubes were then incubated at 37°C, and after 15, 30 and 60 minutes 10 µL of suspension was removed and spread on ISA using a sterile plastic spreader, recording CFU/mL over time. The experiment was run in triplicate (n=3).

#### 2.3.7 Checkerboard blend assay

The method to assess the interaction between two EOs in a blend was carried out much in the same way as described previously in (Section 2.3.5), the difference being that instead of 75 µL of ISB-Tween80-EO mix being added to the appropriate wells, 37.5 µL of EO (X) and 37.5 mL of EO (Y) were added separately then mixed thoroughly using an auto pipette. EO (X) was added in descending concentrations across the X axis left to right. EO (Y) was added in descending concentrations down the Y axis top to bottom, as shown in Figure 2.10 and 2.11. The seven oils used previously were combined in equal volumes. 75 µL of ISB-TTC-microorganism mix was then added to the appropriate wells, with one microorganism being tested with each MTP. Once inoculated, the MTPs were aerobically incubated at 37°C for 24 hours. Post incubation, microbial growth was indicated by the development of a red colour in the wells. Therefore, MICs were taken to be the lowest concentration of essential oil at which no colour change occurred. The experiment was run in triplicate (n=3).

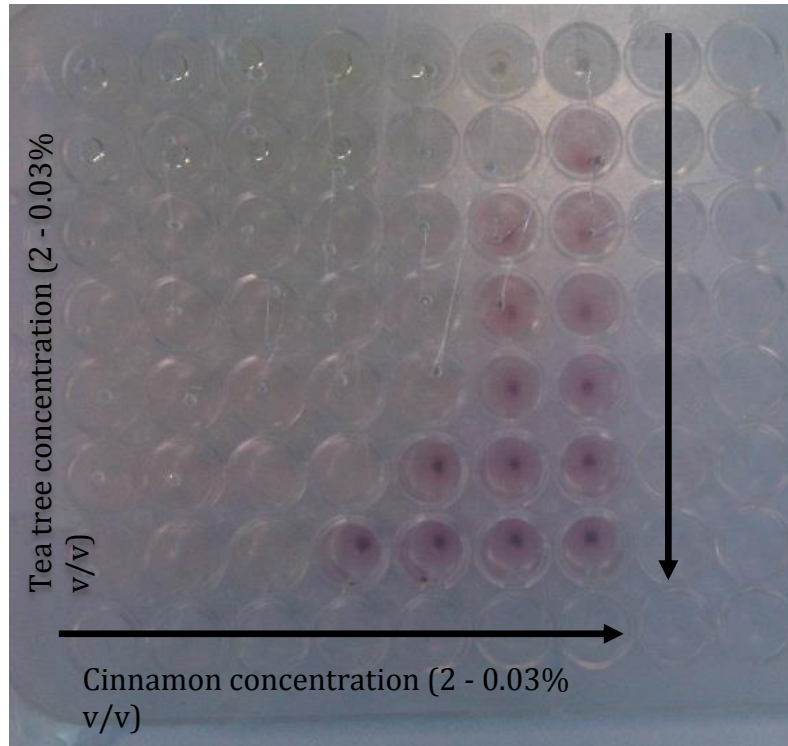


Figure 2.5. An inoculated checkerboard micro-titre plate containing a blend of cinnamon and tea tree oil in various concentrations against *S.aureus*. Cinnamon descending in concentration across the X-axis, tea tree oil descending in concentration down the Y-axis (2% - 0.03%). The red colouring of the TTC dye in the bottom right corner indicates metabolic activity (growth) of the bacterium.

	2%	1%	0.5%	0.25%	0.125%	0.06%	0.03%
2%	↓	↓	↓	↓	↓	↓	↓
1%	↓	↓	↓	↓	↓	↓	↓
0.5%	↓	↓	↓	↓	↓	↓	↓
0.25%	↓	↓	↓	↓	↓	↓	↓
0.125%	↓	↓	↓	↓	↓	↓	↓
0.06%	↓	↓	↓	↓	↓	↓	↓
0.03%	↓	↓	↓	↓	↓	↓	↓

Figure 2.6. Graphical representation of method described in Section 2.3.7, where each essential oil had a starting concentration of 2% (v/v). EO (X) being added in descending concentrations across the X axis left to right. EO (Y) being added in descending concentrations down the Y axis top to bottom.

The level of synergistic activity was assessed using fractional inhibitory concentration (FIC) calculations, shown in equation 2.1:

Equation 2.1. FIC calculation, considering MIC values for EOs individually and in combination.

FIC = X + Y where

$$X = \frac{(\text{MIC of } X \text{ in combination})}{(\text{MIC of } X \text{ alone})}$$
$$Y = \frac{(\text{MIC of } Y \text{ in combination})}{(\text{MIC of } Y \text{ alone})}$$

When X is the first EO and Y is the second EO in the blend.

If  $\text{FIC} \leq 0.5$  the relationship is synergistic

If  $0.5 < \text{FIC} \leq 1$  the relationship is additive

If  $1 < \text{FIC} \leq 4$  the relationship is indifferent

If  $\text{FIC} \geq 4$  the relationship is antagonistic (Meletiadis *et al* 2010).

The aim of using EO blends is to reduce the concentration of each oil while retaining an increasing antimicrobial potential. Synergism was defined as a positive interaction between the two EOs such that the combined effect of the two EOs was significantly greater than the expected additive result. Antagonism was defined as a negative interaction between the two EOs such that the combined effect of the two EOs was significantly less than the expected additive result. An additive relationship occurred when the sum of the separate effects was the same as the effect of EOs used in combination. Indifference indicated that the effect of the EOs in combination was the same as that of the most potent EO individually (Meletiadis *et al* 2010).

### 2.3.8 GC-MS analysis of essential oils

GC-MS analysis of the seven individual EOs and selected EO blends were performed using an HP 5890 Series 2 GC interfaced with a 5972 series mass selective detector (MSD) (Hewlett Packard co., Palo Alto, USA).

For each EO, 1  $\mu\text{L}$  was added to 10 mL of hexane solvent and vortexed for 20 seconds. As this EO concentration is too strong for the MSD, the method was setup to include a split of 20 to 1 resulting in 19 parts being discarded for every 1 part that reaches the detector. This way saturation of the detector is avoided and the MSD lifespan is increased. Helium at a flow rate of 1 mL/min and 69,000 Pa was used as the carrier gas. Sample injection volume was 1  $\mu\text{L}$ .

Temperature programmes were used to allow GC runs to be completed within an appropriate timescale. The initial oven temperature was 60°C for 3 minutes, then increased to 230°C at a rate of 4°C/min and held for 20 minutes. After running all EOs with this programme it was noted that a number of peaks eluted around 110°C. The GC method was subsequently altered to include an initial temperature ramp from 60°C to 112°C at a rate of 4°C/min, followed by a second temperature ramp from 112°C to 230°C at a rate of 10°C/min. Before any test samples were run the injection needle was flushed several times with hexane and the column was run with hexane using a 16 minute programme to ensure the column was ready to use. The injector and detector temperatures were 275°C and 250°C respectively. The MSD operating conditions were as follows: ionisation energy 70 eV, mass range 50 to 550 atomic mass units (a.m.u.) scanning rate 1.52 scans/s. Peaks were positively identified using the Wiley 275 mass spectral database.

## 2.4 Results and discussion

### 2.4.1 Growth Curves

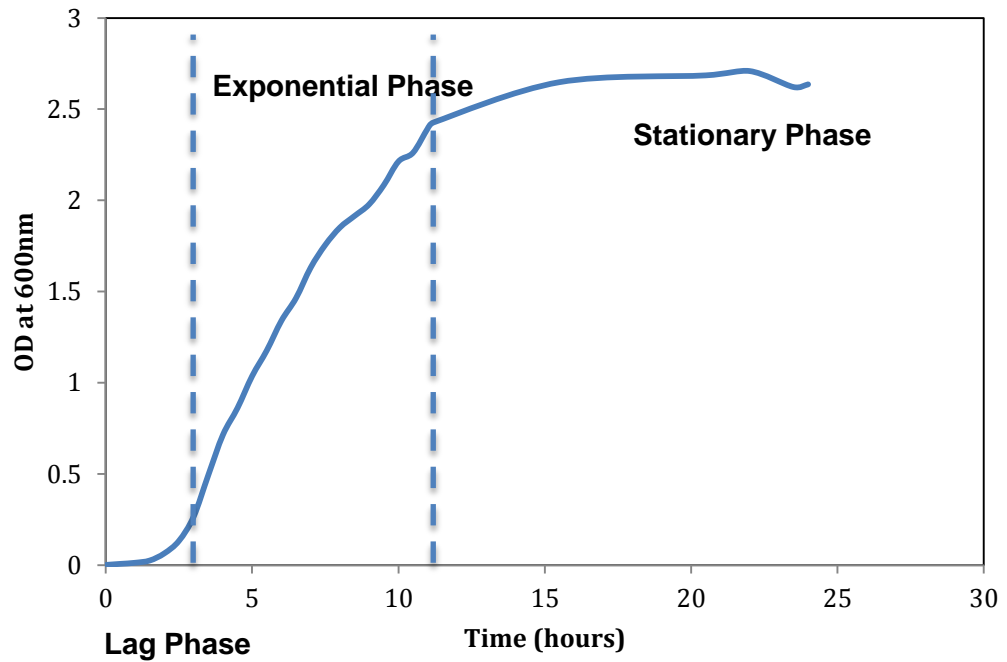


Figure 2.7. Growth curve for *C.albicans*, demonstrating that the yeast enters exponential growth phase at approximately 3 hours.

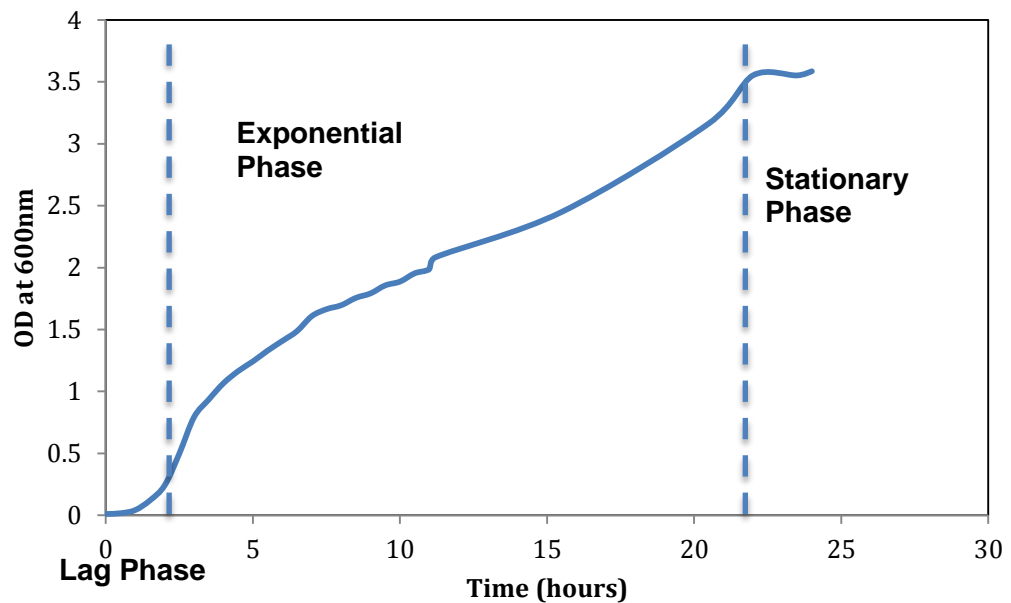


Figure 2.8. Growth curve for *E.coli* demonstrating that the bacterium enters exponential growth phase after 1-2 hours.

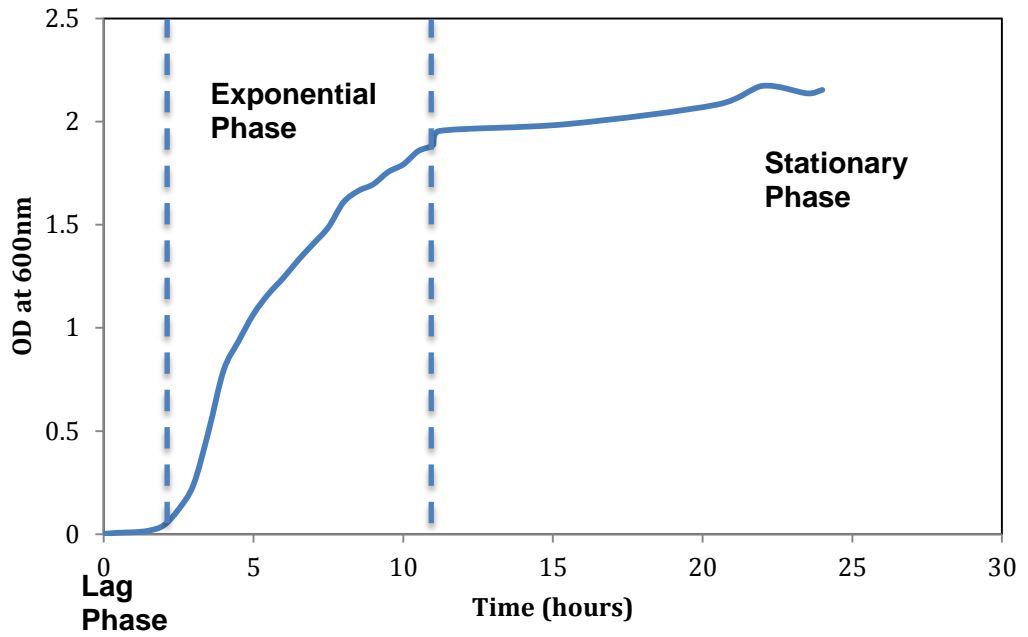


Figure 2.9. Growth curve for *P.aeruginosa*, showing that the bacterium enters exponential growth phase after approximately 2.5-3 hours.

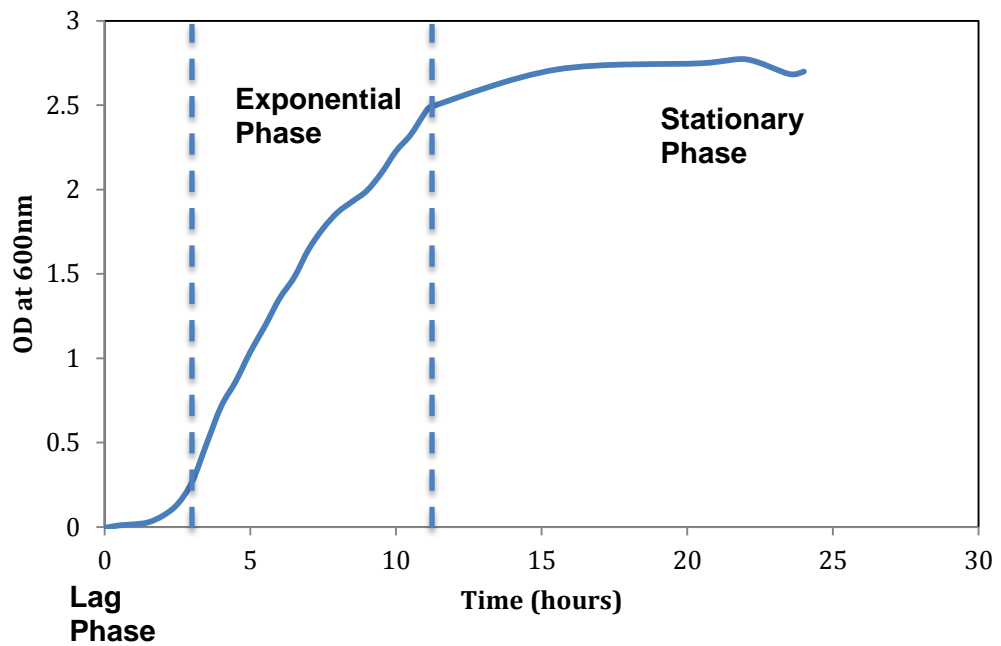


Figure 2.10. Growth curve for *S.aureus* showing that the bacterium enters exponential growth phase after 2.5-3 hours.

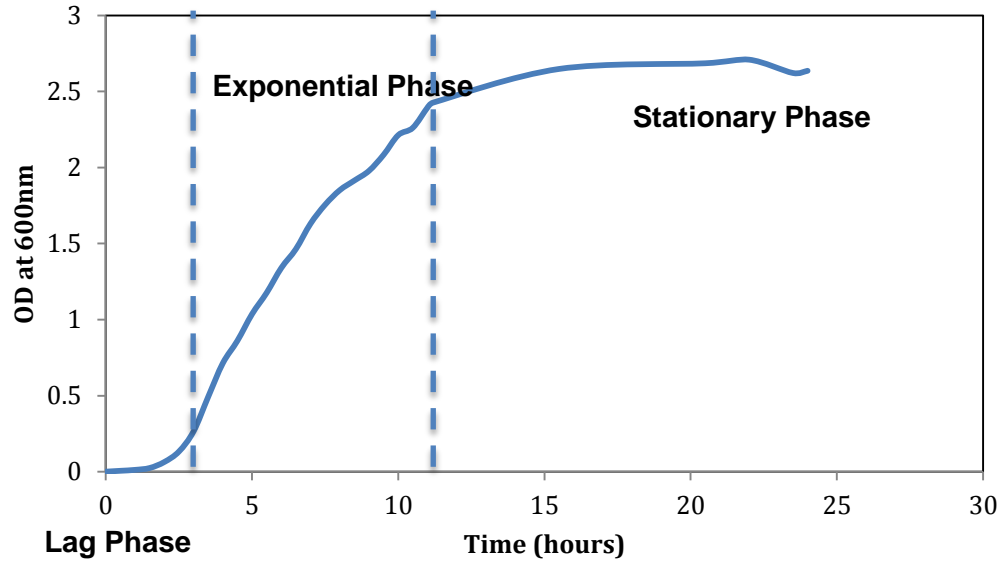


Figure 2.11. Growth curve for MRSA demonstrating that the bacterium enters exponential growth phase after 3 hours.

## 2.4.2 Disk diffusion of individual essential oils

Each of the seven oils was initially screened for antimicrobial activity against *S.aureus*, *MRSA*, *E.coli*, *P.aeruginosa* and *C.albicans*. The disk diffusion method was used and the zone of inhibition data are presented in (Table 2.1).

Table 2.1. Diameters of inhibition zones of individual oils against five microorganisms (mm). Values represent the average from three replicates. MIC – Minimum inhibitory concentration, SD – Standard deviation ( $\pm$ ), (n=9).

Essential oil	<i>S.aureus</i>		<i>MRSA</i>		<i>E.coli</i>		<i>P.aeruginosa</i>		<i>C.albicans</i>	
	ZOI	SD	ZOI	SD	ZOI	SD	ZOI	SD	ZOI	SD
Cinnamon	51.0	4.0	53.1	4.4	41.1	2.8	17.1	0.5	24.8	3.0
Clove	22.4	2.5	25.0	0.9	22.0	3.4	13.9	2.1	17.1	0.7
Eucalyptus	7.9	3.0	11.1	2.5	12.4	0.8	n/a	n/a	3.4	1.0
Geranium	21.4	2.3	27.4	1.8	12.3	1.1	10.1	1.2	16.8	2.2
Lemongrass	34.3	0.4	39.3	2.4	20.4	0.3	11.3	0.9	12.9	1.1
Lime	4.2	0.7	5.5	0.3	5.1	0.8	na	na	4.0	0.3
Tea tree	22.5	4.0	20.5	1.4	22.6	4.0	10.9	1.7	22.1	2.0

The disk diffusion results show cinnamon to be the most potent oil, recording the largest zone of inhibition (ZOI) for each microorganism tested, with the largest ZOI being against *MRSA* at  $53.1 \pm 4.4$  mm. Both lime and eucalyptus oils failed to achieve a ZOI against *P.aeruginosa*. However, this gram-negative bacterium proved to be the most robust of the five microorganisms tested.

Having confirmed the antimicrobial nature of the oils, agar dilution assays were conducted to obtain MICs for the individual oils.

### 2.4.3 Agar dilution of individual essential oils

The seven EOs were tested for antimicrobial efficacy against *P.aeruginosa*, *E.coli*, *S.aureus*, *MRSA* and *C.albicans* in agar. The minimum inhibitory concentration (MIC) data are presented in (Table 2.2).

Table 2.2. MIC data for agar dilution assay. Seven essential oils (EOs) dispersed in ISA in a doubling dilution series from 0.03-2% (v/v) were inoculated with five microorganisms using a multipoint replicator. Values represent the average from three replicates. SD – Standard deviation in parenthesis, (n=9).

	<i>S.aureus</i>	<i>MRSA</i>	<i>E.coli</i>	<i>P.aeruginosa</i>	<i>C.albicans</i>
	MIC (%) (SD)	MIC (%) (SD)	MIC (%) (SD)	MIC (%) (SD)	MIC (%) (SD)
Cinnamon	0.50 (0.00)	0.33 (0.14)	0.50 (0.00)	>2 (0.00)	0.41 (0.14)
Clove	0.83 (0.29)	0.50 (0.00)	0.50 (0.00)	>2 (0.00)	0.21 (0.07)
Eucalyptus	2.00 (0.00)	2.00 (0.00)	1.00 (0.00)	>2 (0.00)	1.00 (0.00)
Geranium	1.00 (0.00)	2.00 (0.00)	1.00 (0.00)	>2 (0.00)	1.00 (0.00)
Lemongrass	0.33 (0.14)	0.25 (0.00)	0.16 (0.07)	>2 (0.00)	0.50 (0.00)
Lime	2.00 (0.00)	2.00 (0.00)	2.00 (0.00)	>2 (0.00)	>2 (0.00)
Tea tree	0.83 (0.29)	0.50 (0.00)	0.41 (0.14)	>2 (0.00)	0.50 (0.00)

Of the seven oils tested, lemongrass exhibited the greatest antimicrobial efficacy against three of the five test microorganisms; MICs of 0.33%, 0.25% and 0.16% (v/v) for *S.aureus*, *MRSA* and *E.coli* respectively. Lime oil registered the least antimicrobial efficacy, recording MICs of 2% (v/v) or above for all the test microorganisms. Of the five bacteria tested, *P.aeruginosa* displayed the most resistance to the oils, with no inhibition of growth at the highest oil concentration tested. The least resistant was *E.coli*, with growth being inhibited at less than 2% (v/v) for all oils tested, disregarding lime oil.

The MIC values recorded for lime and eucalyptus in (Table 2.2) correlate well with those in the literature, with Hammer (1999) reporting an MIC of 2% (v/v) for *S.aureus* and over 2% for *P.aeruginosa*.

The MIC values for lemongrass however do not match well with those reported in the literature, with Hammer (1999) reporting much lower MICs for *S.aureus*, *E.coli* and *C.albicans*, all 0.06% (v/v). This compared to 0.33, 0.16 and 0.5% respectively, for this study. Some of the results for tea tree oil corresponded well to those found in the literature, (Carson *et al* 2006) published MICs of 0.08-2% (v/v) for tea tree against *E.coli* and 0.5-1.25% (v/v) against *S.aureus*. Hammer (1999) obtained an MIC of 0.25% (v/v) for *E.coli* in comparison to 0.41% (v/v) for this study and an MIC of 0.5% for *S.aureus* as opposed to 0.83%, found in the present study. However, agreement was found on 0.5% (v/v) for *C.albicans* and an MIC of >2% (v/v) for *P.aeruginosa*. Due to, among other factors, the varying composition of the EO, differences in MICs found in the literature and those obtained in this study are to be expected. Variation in the chemical composition of plant extracts and oils is related to Local climatic and environmental conditions the plants are grown in. Further factors which can impact on the oil composition include, soil acidity, rainfall, and the time of day at which the plants are harvested (Janssen *et al* 1987, Sivropoulou *et al* 1995). Therefore, batches of essential oil harvested from individual plants can show variation in antimicrobial activity. Previous research has also demonstrated the existence of multiple chemotypes amongst plant extracts, producing different chemical compositions of an essential oil (Thompson *et al* 2002, Chizzola *et al* 2008). Hammer 1999, did not include the chemotype of the oils used in their study. If the oils used in this study are of a different chemotype, this could explain the differences in MICs observed. Different strains of bacteria may also have different susceptibilities (Tenover 2006).

#### 2.4.4 Broth micro-dilution of individual essential oils

The seven EOs were tested for antimicrobial efficacy against *P.aeruginosa*, *E.coli*, *S.aureus*, *MRSA* and *C.albicans* in broth. The MIC data are presented in (Table 2.3). An image taken of the micro-titre plate of cinnamon oil inoculated against the test microorganisms is given (Figure 2.12).

Table 2. 3. MIC and MBC data for broth microdilution assay. Values represent the range from three replicates. SD – Standard deviation, (n=9)

	<i>S.aureus</i>		MRSA		<i>E.coli</i>		<i>P.aeruginosa</i>		<i>C.albicans</i>	
	MIC (SD)	MBC (SD)	MIC (SD)	MBC (SD)	MIC (SD)	MBC (SD)	MIC (SD)	MBC (SD)	MIC (SD)	MBC (SD)
Cinnamon	0.17 (0.07)	0.50 (0.00)	0.17 (0.07)	0.67 (0.29)	0.21 (0.07)	0.50 (0.00)	2.00 (0.00)	>2 (na)	0.25 (0.00)	1.00 (0.00)
Clove	0.13 (0.00)	0.42 (0.14)	0.33 (0.14)	1.00 (0.00)	0.17 (0.07)	0.42 (0.14)	2.00 (0.00)	>2 (na)	0.21 (0.07)	0.67 (0.29)
Eucalyptus	2.00 (0.00)	>2 (na)	2.00 (0.00)	2.00 (0.00)	1.00 (0.00)	2.00 (0.00)	>2 (0.00)	>2 (na)	2.00 (0.00)	>2 (na)
Geranium	0.33 (0.14)	0.50 (0.00)	1.67 (0.58)	2.00 (0.00)	0.25 (0.00)	0.67 (0.29)	>2 (0.00)	>2 (na)	1.00 (0.00)	2.00 (0.00)
Lemongrass	0.33 (0.14)	0.67 (0.29)	0.17 (0.07)	0.50 (0.00)	0.21 (0.07)	0.50 (0.00)	>2 (0.00)	>2 (na)	0.25 (0.00)	0.50 (0.00)
Lime	2.00 (0.00)	>2 (na)	2.00 (0.00)	>2 (na)	1.33 (0.00)	>2 (na)	>2 (0.00)	>2 (na)	2.00 (0.00)	>2 (na)
Tea tree	0.25 (0.00)	0.50 (0.00)	0.33 (0.14)	1.00 (0.00)	0.25 (0.00)	0.50 (0.00)	2.00 (0.00)	>2 (na)	0.50 (0.00)	1.00 (0.00)

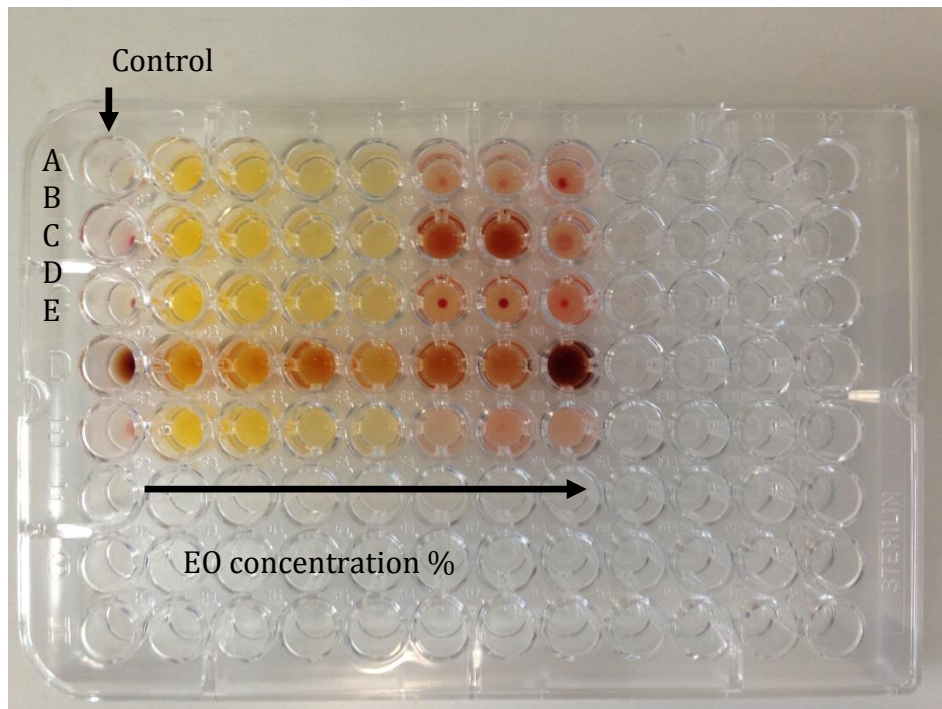


Figure 2.12. Broth microdilution assay of cinnamon oil. Column 1 containing positive growth controls. Column 2 containing cinnamon oil at 2%, decreasing in doubling concentrations across the plate from left to right to 0.03% in column 8. Row A containing *S.aureus*, B – *E.coli*, C – *MRSA*, D – *P.aeruginosa*, and E – *C.albicans*.

For the seven oils tested, clove oil displayed the strongest antimicrobial effect, recording the lowest MIC for three of the five microorganism tested. The lowest MIC for the experiment was 0.13% (v/v), for clove against *S.aureus*. Lime oil was the least efficacious, only inhibiting one microorganism, *E.coli* with an MIC of 1.3% (v/v). The most robust microorganism was again *P.aeruginosa*, with all seven oils failing to inhibit growth of this gram negative bacterium at concentrations below 2% (v/v). This high level of resistance was considered to be associated with the lipopoly-saccharide outer membrane, which protects the cytoplasmic phospholipid based membrane against antimicrobial attack, by the EO (Livermore 2002). The other gram-negative bacterium, *E.coli* was the only microbe to be inhibited by all seven oils at less than 2% (v/v). Therefore, the oils must be able to permeate the outer membrane and an alternative defence mechanism must be causing the relatively high resistance of *P.aeruginosa* to EO

action. The loss of membrane integrity and function is characteristic of treatment with such oils. The results obtained by agar and broth dilution (Figure 2.13) are likely to vary due to many factors differing between assays. Microbial growth, solubility of essential oil, the use and concentration of an emulsifier, exposure of the microorganism to the oil all contribute to variability.

The aim was to identify an essential oil that displayed antimicrobial efficacy against the five test microorganisms at less than 2% (v/v) in order to minimise the chance of skin irritation if the eventual oil laden textile were to contact and sensitise upper dermal layers. The data contained in this chapter indicate that none of the seven oils tested inhibits *P.aeruginosa* below the desired concentration of 2% (v/v). In order to identify an antimicrobial oil effective at concentrations below 2% (v/v), blends of the oils were tested using a modified version of the broth microdilution assay.

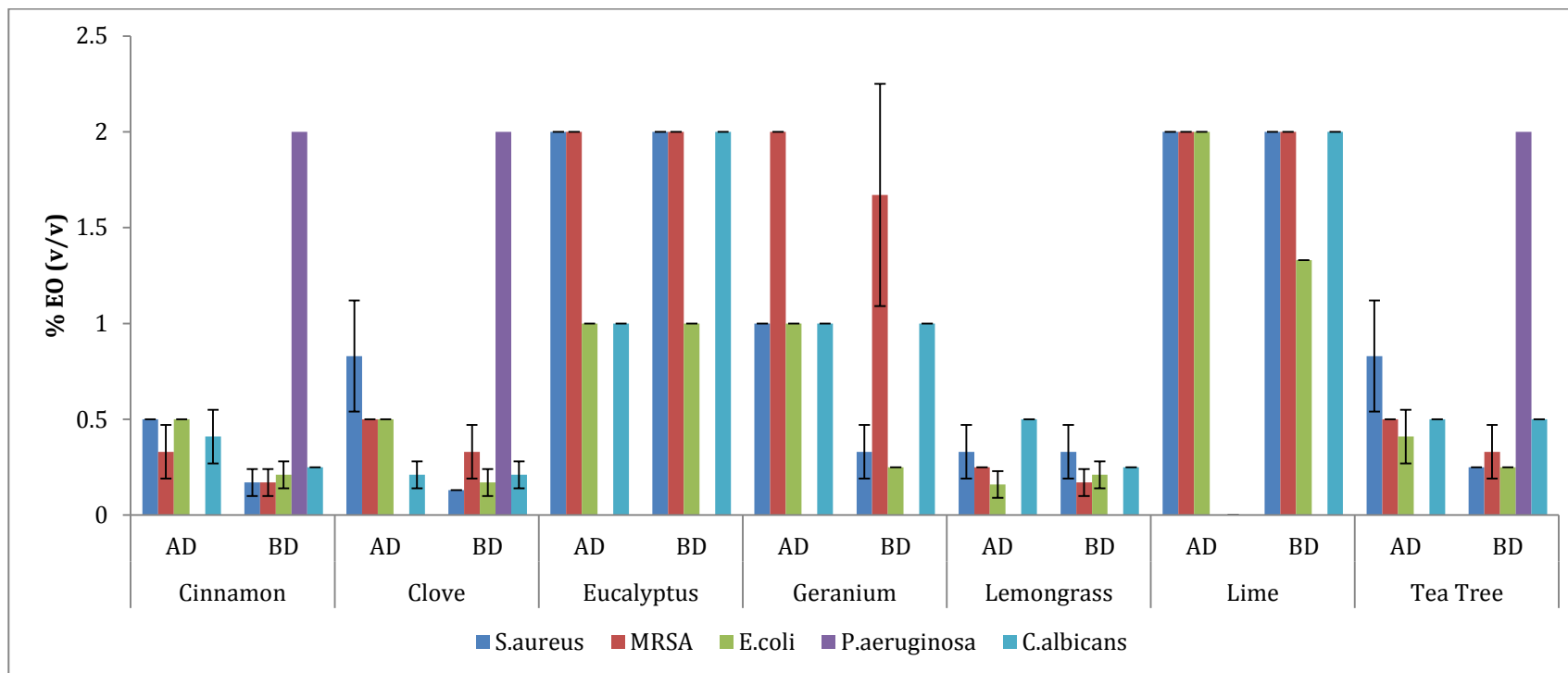


Figure 2.13. Comparison of essential oil MIC % (v/v) results for the agar dilution (AD) and broth micro-dilution (BD)method

#### 2.4.5 Time kill assays

The seven essential oils were tested for their dynamic killing characteristics, results shown in (Tables 2.4-2.10). For this assay, *S.aureus*, *E.coli* and *C.albicans* were used as model gram-positive, gram-negative bacteria and yeast respectively.

The number of viable microorganisms in the exponential growth phase (E in table 2.4) was reduced, after 60 minutes, by 2.63, 3.30 and 1.04 ( $\log_{10}$ ) for *S.aureus*, *E.coli* and *C.albicans*, respectively with 0.125% (v/v) cinnamon oil. However, addition of 2% (v/v) oil produced a reduction by 4.03, 3.77 and 1.52 ( $\log_{10}$ ) for the same respective microorganisms. In addition, *S.aureus* in the stationary growth phase (S in Table 2.4), was reduced by 1.5 ( $\log_{10}$ ) after 60 minutes in the presence of 0.125% (v/v) cinnamon oil, and by 2.67 ( $\log_{10}$ ) in the presence of 2% (v/v) cinnamon oil. A slower rate of killing for stationary phase microorganisms was observed for all three test species. When entering the stationary growth phase, cell membrane fluidity, surface charge and hydrophobicity change. These alterations may account for the changed tolerance of the test microorganisms to EO, as the cell membrane is the main target of EO antimicrobial activity (Kwiecinski 2009).

Table 2. 4. Change in log<sub>10</sub> CFU/mL after incubation with cinnamon oil relative to that at time zero, (n=3) (Loughlin *et al* 2008). Standard deviation (SD) presented in parenthesis.

Time (mins)	Microbe	0.125%(S)	2%(S)	0.125%(E)	2%(E)
15	<i>S.aureus</i>	-0.71 (0.29)	-1.00 (0.30)	-1.03 (0.51)	-1.69 (0.41)
15	<i>E.coli</i>	-0.40 (0.32)	-0.66 (0.22)	-0.77 (0.55)	-1.41 (0.64)
15	<i>C.albicans</i>	-0.21 (0.30)	-0.59 (0.18)	-0.43 (0.56)	-0.97 (0.45)
30	<i>S.aureus</i>	-1.17 (0.25)	-1.98 (0.41)	-1.87 (0.40)	-2.51 (0.45)
30	<i>E.coli</i>	-0.72 (0.17)	-1.41 (0.23)	-1.31 (0.22)	-2.38 (0.29)
30	<i>C.albicans</i>	-0.34 (0.20)	-1.05 (0.41)	-0.87 (0.45)	-1.34 (0.32)
60	<i>S.aureus</i>	-1.50 (0.30)	-2.67 (0.32)	-2.63 (0.35)	-4.03 (0.64)
60	<i>E.coli</i>	-1.17 (0.25)	-2.29 (0.35)	-3.30 (0.30)	-3.77 (0.74)
60	<i>C.albicans</i>	-0.51 (0.19)	-1.31 (0.35)	-1.04 (0.31)	-1.52 (0.57)

For clove oil, the patterns of killing for *S.aureus*, *E.coli* and *C.albicans* were similar to those recorded for cinnamon oil. Clove oil at 0.125% and 2% (v/v) produced a greater kill against the microorganisms in exponential growth phase compared to stationary phase. However, *S.aureus* proved to be more susceptible to clove oil in exponential growth phase, with 2.09 (log<sub>10</sub>) reduction after 60 minutes in the presence of 0.125% clove oil and 3.57 for 2% (v/v). This result correlates well with those in (Section 2.4.3) where clove oil recorded an average MIC score of 0.13%.

Table 2. 5. Change in log<sub>10</sub> CFU/mL after incubation with clove oil relative to that at time zero, (n=3). Standard deviation (SD) presented in parenthesis.

Time (mins)	Microbe	0.125%(S)	2%(S)	0.125%(E)	2%(E)
15	<i>S.aureus</i>	-0.18 (0.38)	-0.30 (0.53)	-0.54 (0.40)	-1.23 (0.48)
15	<i>E.coli</i>	0.06 (0.24)	-0.27 (0.30)	-0.47 (0.50)	-0.74 (0.59)
15	<i>C.albicans</i>	-0.20 (0.38)	-0.30 (0.30)	-0.38 (0.41)	-0.69 (0.54)
30	<i>S.aureus</i>	-0.38 (0.24)	-0.87 (0.31)	-1.45 (0.39)	-3.09 (0.50)
30	<i>E.coli</i>	-0.25 (0.18)	-1.29 (0.29)	-1.27 (0.49)	-1.60 (0.22)
30	<i>C.albicans</i>	-0.46 (0.17)	-1.00 (0.23)	-0.72 (0.37)	-1.06 (0.22)
60	<i>S.aureus</i>	-0.82 (0.28)	-1.65 (0.25)	-2.09 (0.34)	-3.57 (0.41)
60	<i>E.coli</i>	-0.43 (0.18)	-2.02 (0.30)	-1.82 (0.27)	-3.39 (0.28)
60	<i>C.albicans</i>	-0.80 (0.16)	-1.38 (0.24)	-1.52 (0.43)	-2.00 (0.49)

Eucalyptus oil produced a much slower rate of killing in comparison to cinnamon and clove oil. This was consistent with the results for the agar and broth dilution assays. *S.aureus* in exponential phase was most susceptible to eucalyptus oil, with a 1.92 (log<sub>10</sub>) reduction in viable cells seen after 60 minutes with 2% (v/v) eucalyptus oil. Once again, *C.albicans* was least susceptible, producing a 0.97 and 1.28 (log<sub>10</sub>) reduction in viable cells after 60 minutes in the presence of 2% for stationary and exponential phase cells respectively.

Table 2. 6. Change in log<sub>10</sub> CFU/mL after incubation with eucalyptus oil relative to that at time zero, (n=3). Standard deviation (SD) presented in parenthesis.

Time (mins)	Microbe	0.125%(S )	2%(S)	0.125%(E )	2%(E)
15	<i>S.aureus</i>	-0.23 (0.35)	-0.45 (0.49)	-0.39 (0.55)	-0.88 (0.98)
15	<i>E.coli</i>	0.12 (0.23)	-0.18 (0.38)	-0.20 (0.41)	-0.48 (0.55)
15	<i>C.albicans</i>	-0.28 (0.23)	-0.29 (0.32)	-0.32 (0.44)	-0.38 (0.55)
30	<i>S.aureus</i>	-0.32 (0.35)	-0.58 (0.38)	-0.80 (0.23)	-1.22 (0.44)
30	<i>E.coli</i>	-0.26 (0.49)	-0.49 (0.43)	-0.56 (0.48)	-1.07 (0.49)
30	<i>C.albicans</i>	-0.24 (0.50)	-0.25 (0.49)	-0.50 (0.45)	-0.70 (0.40)
60	<i>S.aureus</i>	-0.72 (0.27)	-0.98 (0.23)	-1.22 (0.52)	-1.92 (0.60)
60	<i>E.coli</i>	-0.66 (0.40)	-1.00 (0.45)	-1.10 (0.52)	-1.14 (0.95)
60	<i>C.albicans</i>	-0.38 (0.39)	-0.97 (0.27)	-0.77 (0.21)	-1.28 (0.46)

Geranium oil produced similar results for all three test organisms at the various oil concentrations after 60 minutes exposure. A log<sub>10</sub> reduction between 0.95-1.38 was seen at 0.125% for microorganisms in stationary phase, and 1.38-1.66 when in exponential phase. Likewise, a log<sub>10</sub> reduction of 1.83-1.95 was at 2% and 2.54-3.03 was observed in stationary and exponential phases respectively.

Table 2. 7. Change in log<sub>10</sub> CFU/mL after incubation with geranium oil relative to that at time zero, (n=3). Standard deviation (SD) presented in parenthesis.

Time (mins)	Microbe	0.125%(S)	2%(S)	0.125%(E)	2%(E)
15	<i>S.aureus</i>	-0.40 (0.43)	-0.77 (0.55)	-0.67 (0.64)	-0.99 (0.38)
15	<i>E.coli</i>	-0.33 (0.19)	-0.59 (0.20)	-0.53 (0.32)	-0.79 (0.25)
15	<i>C.albicans</i>	-0.25 (0.09)	-0.48 (0.29)	-0.76 (0.33)	-0.90 (0.30)
30	<i>S.aureus</i>	-0.60 (0.26)	-1.29 (0.12)	-0.82 (0.29)	-1.76 (0.23)
30	<i>E.coli</i>	-0.83 (0.17)	-1.20 (0.10)	-0.83 (0.20)	-1.68 (0.26)
30	<i>C.albicans</i>	-0.62 (0.17)	-0.96 (0.18)	-1.00 (0.21)	-1.98 (0.10)
60	<i>S.aureus</i>	-0.95 (0.08)	-1.91 (0.15)	-1.38 (0.15)	-2.67 (0.21)
60	<i>E.coli</i>	-1.38 (0.07)	-1.83 (0.20)	-1.66 (0.15)	-2.54 (0.12)
60	<i>C.albicans</i>	-1.16 (0.16)	-1.95 (0.31)	-1.51 (0.28)	-3.03 (0.48)

The number of viable microorganisms in exponential growth phase was reduced by 2.03, 1.55 and 1.26 (log<sub>10</sub>) for *S.aureus*, *E.coli* and *C.albicans* respectively with 0.125% (v/v) lemongrass oil after 60 minutes. While addition of 2% (v/v) oil produced a reduction by 2.56, 2.46 and 1.89 (log<sub>10</sub>) for the same microorganisms. In addition, *S.aureus* and *E.coli* cells in stationary growth phase were reduced by 1.63 and 1.62 (log<sub>10</sub>) after 60 minutes in the presence of 2% (v/v) lemongrass oil, with *C.albicans* reduced by 1.27 (log<sub>10</sub>).

Table 2. 8. Change in log<sub>10</sub> CFU/mL after incubation with lemongrass oil relative to that at time zero, (n=3). Standard deviation (SD) presented in parenthesis.

Time (mins)	Microbe	0.125%(S)	2%(S)	0.125%(E)	2%(E)
15	<i>S.aureus</i>	-0.49 (0.19)	-0.83 (0.58)	-0.56 (0.18)	-1.03 (0.40)
15	<i>E.coli</i>	-0.32 (0.20)	-0.58 (0.14)	-0.83 (0.40)	-1.11 (0.60)
15	<i>C.albicans</i>	-0.37 (0.21)	-0.71 (0.35)	-0.69 (0.42)	-0.83 (0.25)
30	<i>S.aureus</i>	-0.91 (0.35)	-1.09 (0.10)	-1.32 (0.17)	-1.43 (0.16)
30	<i>E.coli</i>	-0.59 (0.10)	-1.09 (0.20)	-1.25 (0.23)	-1.51 (0.17)
30	<i>C.albicans</i>	-0.27 (0.23)	-0.88 (0.18)	-0.89 (0.08)	-1.27 (0.30)
60	<i>S.aureus</i>	-1.00 (0.17)	-1.63 (0.12)	-2.03 (0.11)	-2.56 (0.23)
60	<i>E.coli</i>	-1.13 (0.17)	-1.62 (0.14)	-1.55 (0.13)	-2.46 (0.21)
60	<i>C.albicans</i>	-0.68 (0.33)	-1.27 (0.30)	-1.26 (0.26)	-1.89 (0.66)

As with previous assays, lime oil produced lower levels of killing in 60 minutes exposure to the test microorganisms. A log<sub>10</sub> reduction of 1.07 for *E.coli* in exponential phase at 60 minutes with 2% (v/v) lime oil was the least observed.

Table 2. 9. Change in log<sub>10</sub> CFU/mL after incubation with lime oil relative to that at time zero, (n=3). Standard deviation (SD) presented in parenthesis.

Time (mins)	Microbe	0.125%(S)	2%(S)	0.125%(E)	2%(E)
15	<i>S.aureus</i>	-0.40 (0.52)	-0.43 (0.40)	-0.32 (0.21)	-0.80 (0.75)
15	<i>E.coli</i>	-0.34 (0.41)	-0.60 (0.51)	-0.61 (0.51)	-0.95 (0.66)
15	<i>C.albicans</i>	-0.26 (0.29)	-0.44 (0.41)	-0.55 (0.43)	-0.89 (0.56)
30	<i>S.aureus</i>	-0.36 (0.29)	-0.66 (0.21)	-0.57 (0.29)	-0.85 (0.56)
30	<i>E.coli</i>	-0.50 (0.34)	-0.81 (0.42)	-0.66 (0.38)	-1.06 (0.38)
30	<i>C.albicans</i>	-0.39 (0.18)	-0.52 (0.25)	-0.78 (0.45)	-0.99 (0.15)
60	<i>S.aureus</i>	-0.53 (0.32)	-1.03 (0.40)	-1.07 (0.72)	-1.40 (1.04)
60	<i>E.coli</i>	-0.64 (0.29)	-0.93 (0.22)	-1.09 (0.41)	-1.07 (0.46)
60	<i>C.albicans</i>	-0.60 (0.17)	-0.80 (0.12)	-1.21 (0.34)	-1.61 (0.47)

*S.aureus* cells in stationary growth phase were reduced by 1.56 (log<sub>10</sub>) after 60 minutes in the presence of 0.125% and 2.44 (log<sub>10</sub>) in the presence of 2% (v/v) tea tree oil. The slower rate of killing for stationary phase microorganisms was again observed for all three test species. These findings compare well with results previously published by (Gustafson *et al* 1998) who reported *E.coli* in stationary growth phase were killed by TTO at a much slower rate than cells from the exponential growth phase.

Table 2. 10. Change in log<sub>10</sub> CFU/mL after incubation with tea tree oil relative to that at time zero, (n=3). Standard deviation (SD) presented in parenthesis.

Time (mins)	Microbe	0.125%(S)	2%(S)	0.125%(E)	2%(E)
15	<i>S.aureus</i>	-0.75 (0.54)	-1.31 (0.53)	-1.33 (0.72)	-2.22 (0.42)
15	<i>E.coli</i>	-0.31 (0.44)	-0.64 (0.35)	-0.48 (0.40)	-1.39 (0.49)
15	<i>C.albicans</i>	-0.25 (0.31)	-0.58 (0.40)	-0.56 (0.51)	-0.75 (0.20)
30	<i>S.aureus</i>	-1.27 (0.67)	-1.83 (0.87)	-1.60 (0.48)	-2.62 (0.60)
30	<i>E.coli</i>	-0.65 (0.34)	-1.35 (0.68)	-1.16 (0.67)	-1.94 (0.30)
30	<i>C.albicans</i>	-0.45 (0.24)	-0.96 (0.29)	-0.77 (0.24)	-1.46 (0.45)
60	<i>S.aureus</i>	-1.56 (0.80)	-2.44 (0.63)	-2.22 (0.67)	-2.86 (0.56)
60	<i>E.coli</i>	-1.17 (0.58)	-1.75 (0.29)	-1.73 (0.78)	-2.82 (0.84)
60	<i>C.albicans</i>	-1.00 (0.20)	-1.53 (0.64)	-1.63 (0.79)	-2.21 (0.81)

Kwiecinski (2009) reported a 2 (log<sub>10</sub>) reduction in viable *S.aureus* cells in exponential growth phase after incubation with 0.5% (v/v) tea tree oil after 60 minutes. Furthermore, a 4 (log<sub>10</sub>) reduction in viable *S.aureus* cells after 60 minutes was reported, with tea tree oil at 8%.

The results for this experiment show that bacteria in the stationary growth phase are more tolerant to antimicrobials, in this case essential oils compared to bacteria in the exponential growth phase (Gustafson *et al* 1998, Cox *et al* 1998). When entering the stationary growth phase, cell membrane protein composition, fluidity, surface charge and hydrophobicity of bacterial cells change. These physical alterations might account for the relative tolerance to essential oils when in stationary growth phase, as the cell membrane is the main target of essential oil antimicrobial activity (Kwiecinski 2009).

#### 2.4.6 Checkerboard blending assay

Using the method described in (Section 2.3.6) the seven oils were tested for their antimicrobial efficacy in blends. Twenty-one blends were tested against the five microorganisms previously used in the MIC assays for the individual oils. However, for checkerboard assays fractional inhibitory concentrations (FICs) are used to determine the relationship between the two oils in a given blend. Blends were classified synergistic if they had an FIC of  $\leq 0.5$ , and FIC of between 0.99 and 0.5 was indicative of an additive relationship. Between 3.99 and 1, the relationship was said to be indifferent and finally an FIC of  $\geq 4$  showed the blend to be antagonistic. The results of the checkerboard assays are presented in (Table 2.11).

Oil blends containing cinnamon were most effective against the five microorganisms tested. According to the FIC values obtained, the blend with the lowest FIC index for each microorganism contained cinnamon, these were: cinnamon-lemongrass (0.95) and cinnamon-tea tree (0.97) for *S.aureus*, cinnamon-clove (0.63) for *MRSA*, cinnamon-clove (0.76) and cinnamon-eucalyptus (0.75) for *E.coli*, cinnamon-geranium (0.17) for *P.aeruginosa* and cinnamon-tea tree (0.85) for *C.albicans*. Due to the doubling dilutions used in the checkerboard method, it is difficult to interpret synergy using FIC indices, due to the doubling gradient of well concentrations. The majority of blends for this experiment for *S.aureus*, *MRSA*, *E.coli* and *C.albicans* recorded MICs between 1 and 4, indicative of indifference. However, many of these blends recorded lower MICs in combination than the oils individually, meaning less oil was needed to inhibit the growth of the microbe in combination compared to when tested individually. For instance, the individual MICs for cinnamon and clove against *MRSA* in broth were found to be 0.17 and 0.33% (v/v), for the cinnamon-clove

blend, the MICs for the two oils decreased to an average of 0.07%(v/v), providing an FIC index of 0.63 for the blend.

From the results, although a number of blends provided a reduced level of oil concentration (v/v) to inhibit growth in comparison to the individual oils, there were no blends that scored a synergistic FIC index for all the test microorganisms, although there was a reduced amount of oil concentration required to inhibit growth. It is logical the reduction would decrease the cost of the antimicrobial and therefore it would be beneficial to use one of the blends which produced a reduction in MIC scores for the oils in the blend and produced a synergistic FIC index against the most robust test microbe (*P.aeruginosa*). On this basis, the cinnamon-clove blend was selected for further study.

Table 2. 11. Fractional inhibitory concentrations from checkerboard testing essential oil blends. MICx denotes the MIC for oil X in the combination, MICy denotes the MIC for oil Y in the combination, (n=3). Green highlight denotes most effective blends, the least effective in red.

	S.aureus			MRSA			E.coli			P.aeruginosa			C.albicans		
	MICx	MICy	FIC	MICx	MICy	FIC	MICx	MICy	FIC	MICx	MICy	FIC	MICx	MICy	FIC
CIN-CLO	0.12	0.12	1.62	0.07	0.07	0.63	0.07	0.07	0.76	0.19	0.24	0.21	0.23	0.12	1.45
CIN-EUC	0.13	0.57	1.06	0.12	0.19	0.79	0.12	0.19	0.75	0.38	0.37	0.24	0.20	0.24	0.93
CIN-GER	0.13	0.29	1.67	0.23	0.24	1.51	0.14	0.19	1.45	0.19	0.29	0.17	0.28	0.32	1.44
CIN-LEM	0.10	0.12	0.95	0.10	0.12	1.27	0.12	0.12	1.10	0.38	0.38	0.29	0.17	0.23	1.61
CIN-LIM	0.18	0.57	1.36	0.25	0.57	1.77	0.34	0.65	2.11	>2	>2	n/a	0.54	0.73	2.51
CIN-TTO	0.09	0.12	0.97	0.12	0.12	1.04	0.11	0.11	0.99	0.12	0.12	0.23	0.14	0.14	0.85
CLO-EUC	0.20	0.57	1.85	0.30	0.57	1.19	0.14	0.19	1.04	0.58	0.58	0.36	0.47	0.64	2.59
CLO-GER	0.12	0.60	2.73	0.19	0.29	0.75	0.19	0.19	1.92	0.87	0.92	0.66	0.19	0.24	1.16
CLO-LEM	0.12	0.42	2.19	0.12	0.36	2.49	0.14	0.39	2.70	0.45	0.45	0.34	0.24	0.48	3.10
CLO-LIM	0.12	0.81	1.33	0.34	0.18	1.09	0.35	0.41	2.41	>2	>2	n/a	0.38	0.37	2.01
CLO-TTO	0.12	0.19	1.68	0.18	0.18	1.06	0.12	0.22	1.56	0.76	0.77	0.77	0.23	0.18	1.43
EUC-GER	>2	>2	n/a	1.16	1.16	1.28	0.72	0.94	4.47	>2	>2	n/a	1.17	1.17	1.76
EUC-LEM	>2	>2	n/a	1.67	1.67	10.86	0.92	0.92	5.32	1.50	1.50	0.56	1.50	1.50	6.75
EUC-LIM	>2	>2	n/a	1.67	1.67	1.67	1.16	1.16	2.03	>2	>2	n/a	>2	>2	n/a
EUC-TTO	0.57	0.29	1.43	0.69	0.94	3.15	0.37	0.28	1.49	1.13	1.00	0.64	0.87	1.17	2.78
GER-LEM	0.19	0.31	1.52	0.21	0.41	2.59	0.21	0.33	2.41	0.72	0.94	0.41	0.29	0.29	1.45
GER-LIM	>2	>2	n/a	1.16	1.16	1.28	1.16	1.08	5.45	>2	>2	n/a	1.50	1.50	2.25
GER-TTO	0.57	0.23	2.63	0.57	0.43	1.62	0.57	0.54	4.42	0.92	1.17	0.81	0.91	0.84	2.59
LEM-LIM	>2	>2	n/a	1.50	1.50	9.75	1.16	1.16	6.44	>2	>2	n/a	>2	>2	n/a
LEM-TTO	0.19	0.16	1.23	0.19	0.16	1.63	0.24	0.19	1.93	0.76	0.77	0.58	0.38	0.39	2.29
LIM-TTO	0.57	0.46	2.14	0.47	0.50	1.73	0.57	0.54	2.57	>2	>2	na	1.08	1.33	3.20

The mechanism of action as well as EO composition deserves to be studied in more detail in order to elucidate why combinations of EOs with a strong individual antimicrobial efficacy such as cinnamon and clove, did not show synergistic effects overall even though the concentrations of each oil in the combination required to inhibit the test microorganism decreased. On this basis, the 1:1 clove and cinnamon oil combination was selected for further study. Lambert *et al* (2001), reported that carvacrol and thymol in combination had an additive effect against *S. aureus* and *P. aeruginosa*. Nazer *et al* (2005), found that thymol in combination with other aromatic compounds improved inhibition, but no real synergistic effect was demonstrated between compounds. As EOs are of similar composition, combinations may exhibit additive rather than a synergistic effect. As a result, combinations with other compounds and antimicrobials, containing different chemical structures may improve the antimicrobial efficacy. For example, synergism between carvacrol and its precursor p-cymene was noted by (Ultee *et al* 2000), or synergy between antibiotics and EOs (Langeveld *et al* 2014).

It is not fully understood why certain EO blends display synergy when others do not. Theories have included receptor or site modification, enzymatic degradation, accumulation of antimicrobial within bacterial cell, decreased outer membrane permeability, and attenuation of efflux pumps (Lambert *et al* 2001). Classification of synergistic interactions should be more conservatively evaluated taking into account inherent doubling dilutions in MIC methodology.

#### 2.4.7 Gas chromatography – mass spectroscopy (GC-MS) analysis

The seven individual EOs and blend chosen from the checkerboard assay were analysed by GC-MS to quantify the major chemical constituents of the oils (Figures 2.14 – 2.20). The definition of a major constituent for this analysis was a component >1% of the oil. All percentages of EO constituents are expressed as (v/v).

Cinnamon oil comprised nine major components (Figure 2.14). The most abundant molecule was eugenol, which accounts for over 70% of the oil. Eight other components account for over 1% of the oil, these were:  $\alpha$ -pinene, para-cymene,  $\beta$ -caryophyllene, terpinen-4-ol, cinnamic alcohol, benzyl benzoate, eugenyl acetate and Caryophyllen Epoxyde. Eugenol has been shown to have antimicrobial properties (Gayoso *et al* 2005, Nazer *et al* 2005) and is likely to be responsible for the antimicrobial efficacy of cinnamon oil.

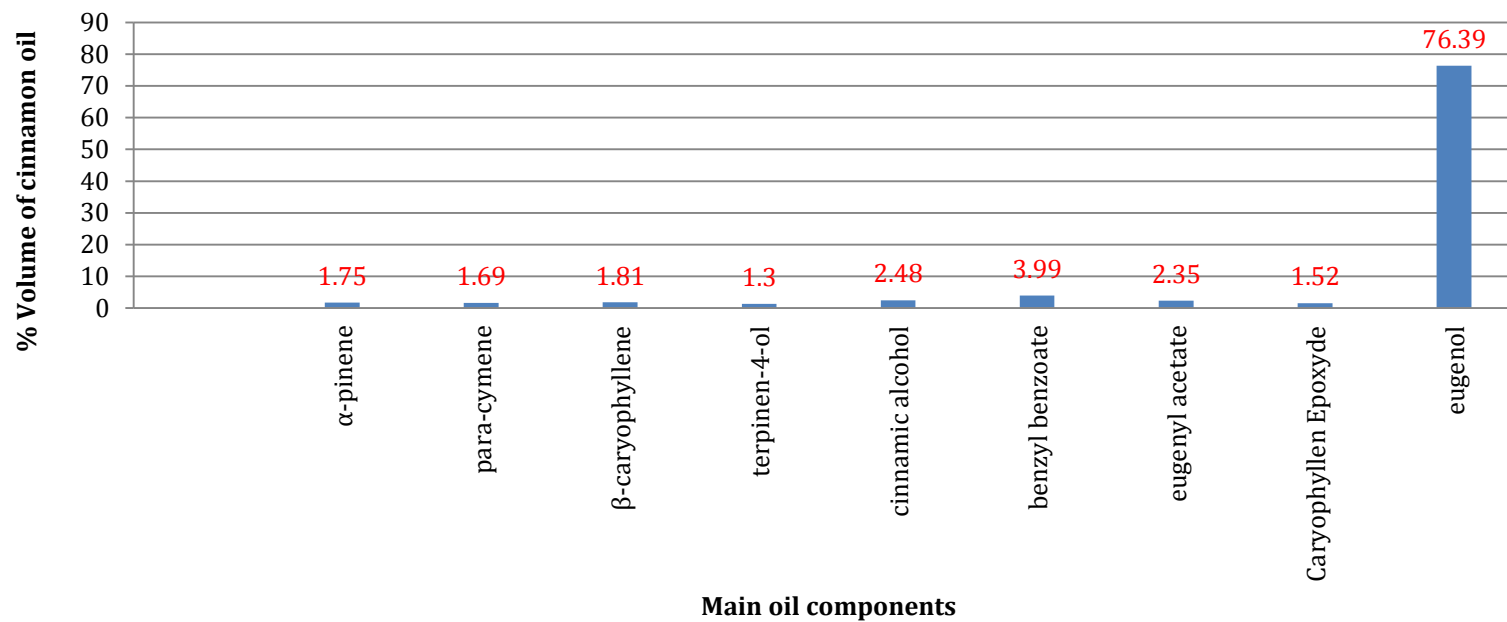


Figure 2.14. The major components of cinnamon oil, as determined by GC-MS. The numbers in red represent the % composition of the chemical component. The labels on the X-axis are the names of each chemical component.

The GC-MS data for clove oil revealed three chemical components that accounted for more than 1% of the oil (Figure 2.15). These were  $\beta$ -caryophyllene (2.65%), eugenyl acetate (11.47%) and as with cinnamon oil, eugenol was the most abundant component (82.85%).

Eucalyptus oil was found to have five major components. The most prevalent being 1,8-cineole, at 80.6% of the oil. The four other major components were:  $\alpha$ -pinene (3.33%),  $\beta$ -myrcene (1.09%), d-limonene (8.62%) and para-cymene (3.61%).

The Geranium oil analysed was shown to be the most complex, with thirteen major components. With four components accounting for approximately 50% of the oil, citronellol (22.7%), geraniol (10.71%), citronellylformate (11.62%) and 6,9-guaiadiene (8.62%).

The data shows the lemongrass oil used in this study to contain eight major components (Figure 2.18). Approximately 80% of the oil is comprised of four molecules, citronellol (9.29%), citronellal (15.05%), geraniol (32.81%) and neral (24.51%). There were four other molecules which account for over 1% of the oil, these were:  $\beta$ -myrcene, geraniol, isopulegol and linalool.

The GC-MS data revealed eleven major components for the lime oil used. The most abundant component was d-limonene (49.39%), with three other components over 5% of the oil:  $\gamma$ -terpinene (11.7%), terpinolene (8.61%) and  $\alpha$ -terpineol (5.88%).

The proportion of each main constituent for tea tree oil was determined (Figure 2.20). Terpinen-4-ol was determined to be the most abundant constituent at 41.8%, correlating well with GC-MS analysis of tea tree oil in the literature (Brophy 1989). There were eleven other components over 1%, combining to account for roughly a further 50% of the oil. Terpinen-4-ol has been reported to show antimicrobial properties (Cox 2001).

Finally, the EO blend chosen for further study was cin-clo in a 1:1 ratio. The EO blend was analysed using GC-MS to determine if the main constituents of the respective oils had changed. The main constituent for both cinnamon and clove oils was confirmed to be eugenol, at 76.39 and 82.85% respectively. The GC-MS report for the EO blend shows eugenol to contribute 94.84% of the blend, with eugenyl acetate being the only other constituent above the cut off of >1%, accounting for 4.75% of the EO blend (Figure 2.21). This increase in concentration of the main antimicrobial constituent may explain the increased antimicrobial efficacy displayed by the blend against the respective microorganisms used in this study.

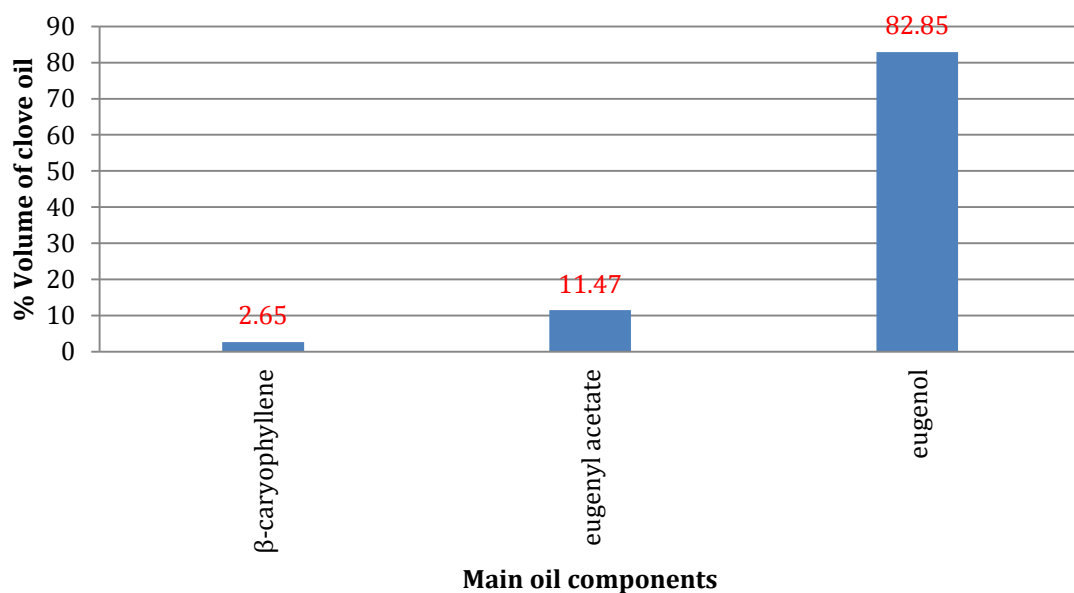


Figure 2.15. The major components of clove oil, as determined by GC-MS. The numbers in red represent the % composition of the chemical component. The labels on the X-axis are the names of each chemical component.

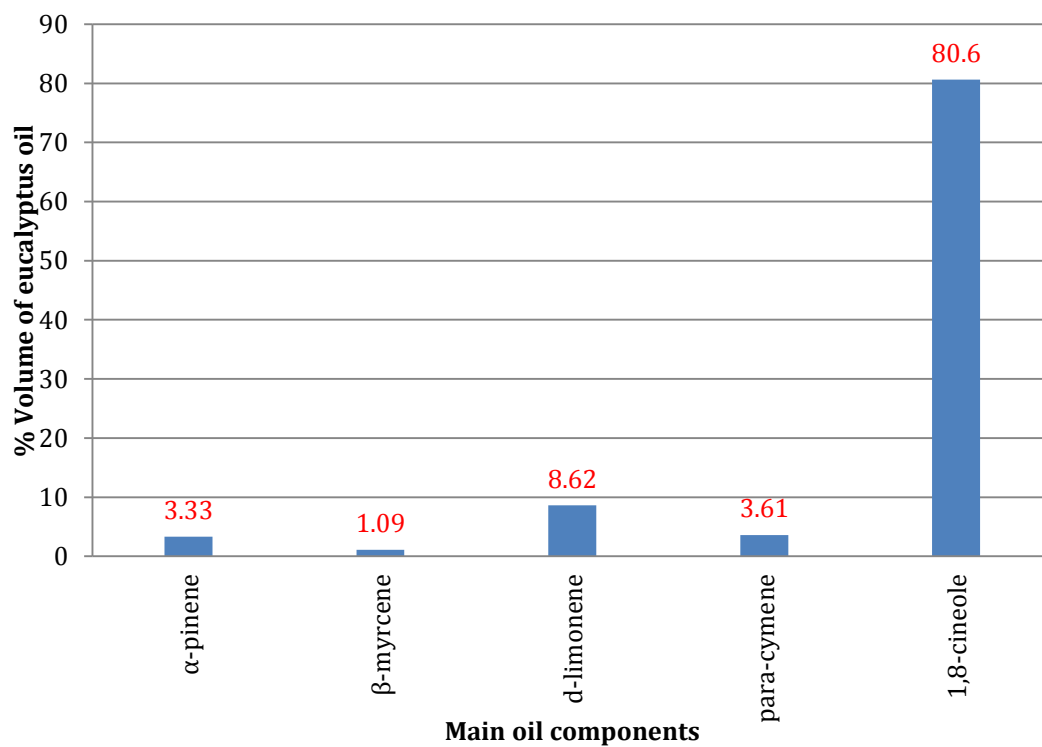


Figure 2.16. The major components of eucalyptus oil, as determined by GC-MS. The numbers in red represent the % composition of the chemical component. The labels on the X-axis are the names of each chemical component.

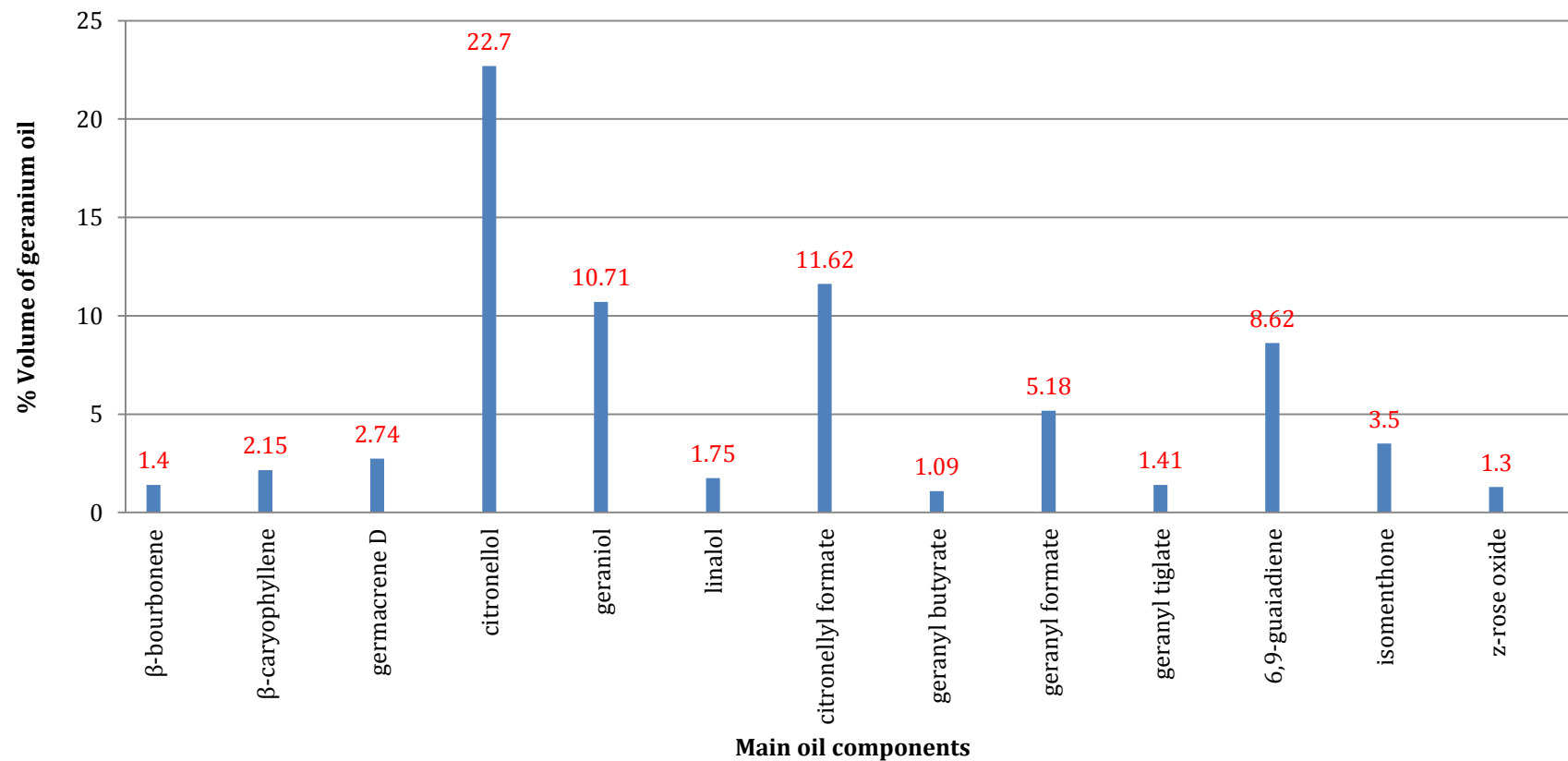


Figure 2.17. The major components of geranium oil, as determined by GC-MS. The numbers in red represent the % composition of the chemical component. The labels on the X-axis are the names of each chemical component.

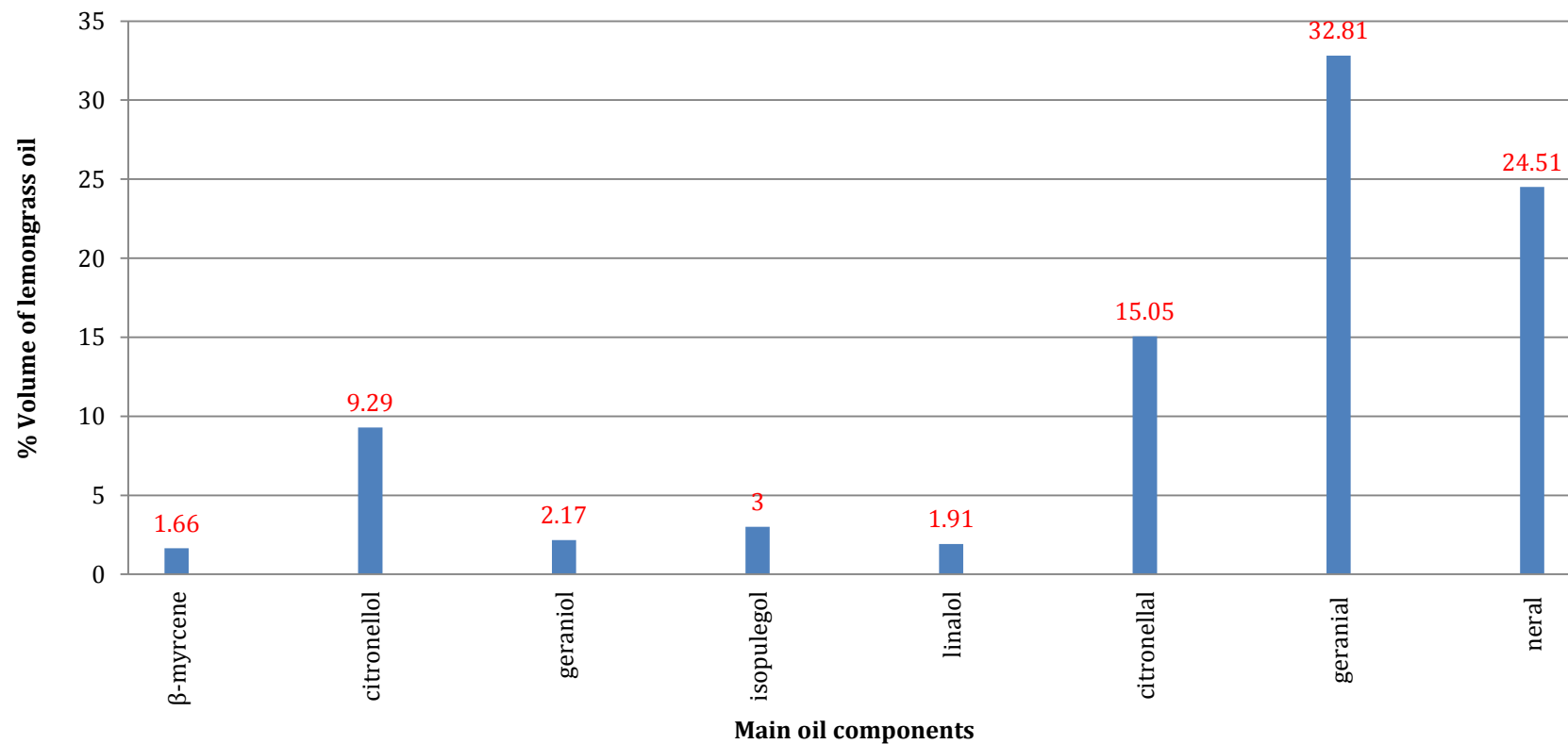


Figure 2.18. The major components of lemongrass oil, as determined by GC-MS. The numbers in red represent the % composition of the chemical component. The labels on the X-axis are the names of each chemical component.

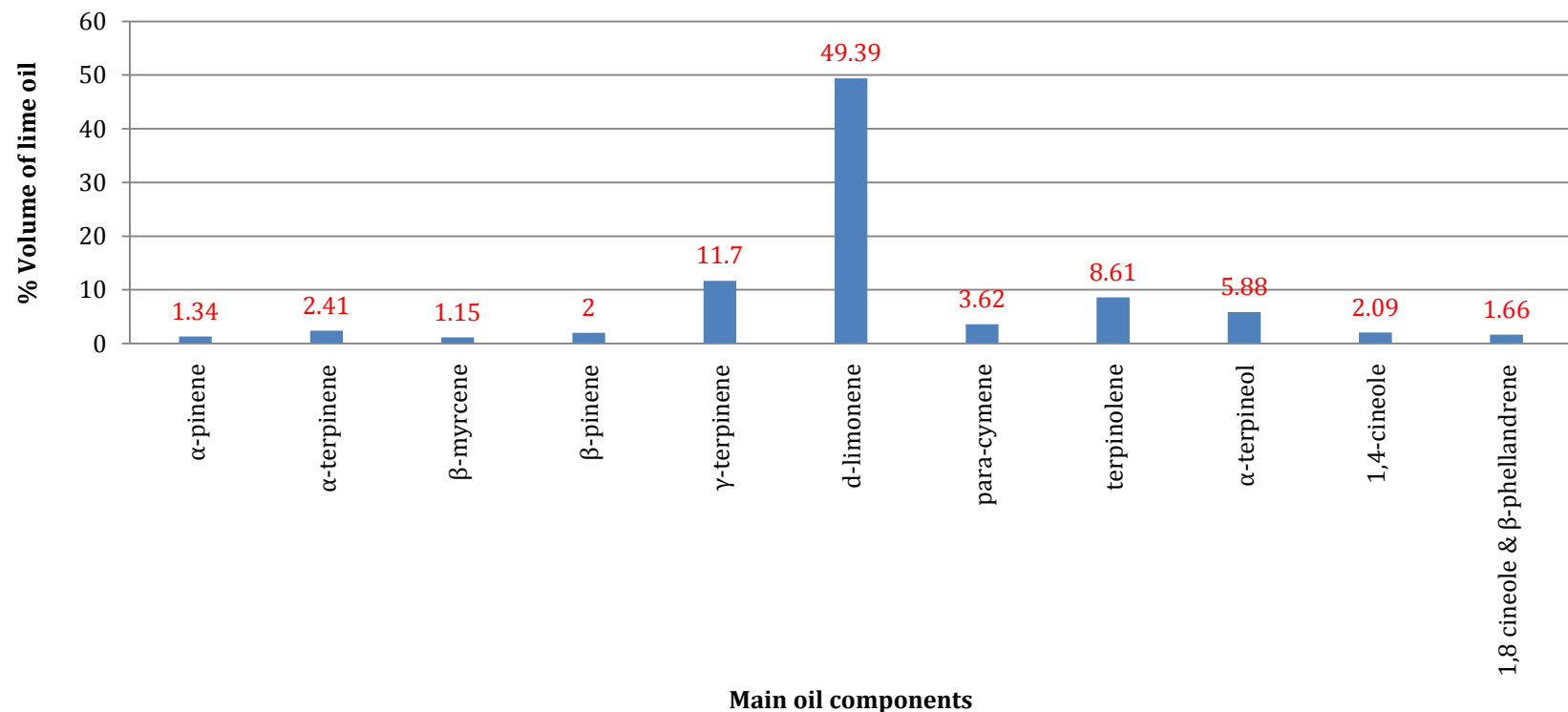


Figure 2.19. The major components of lime oil, as determined by GC-MS. The numbers in red represent the % composition of the chemical component. The labels on the X-axis are the names of each chemical component.

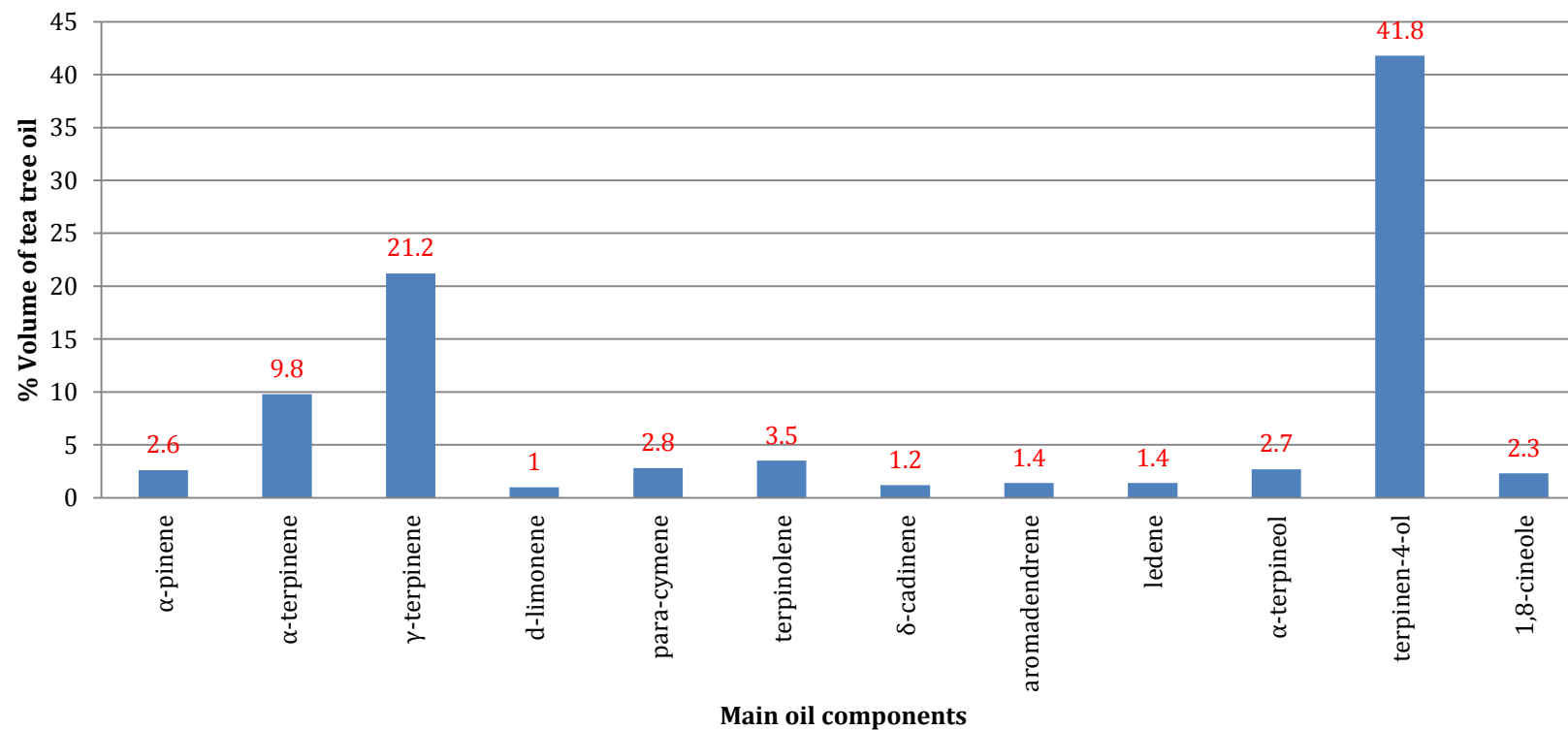


Figure 2.20. The major components of tea tree oil, as determined by GC-MS. The numbers in red represent the % composition of the chemical component. The labels on the X-axis are the names of each chemical component.

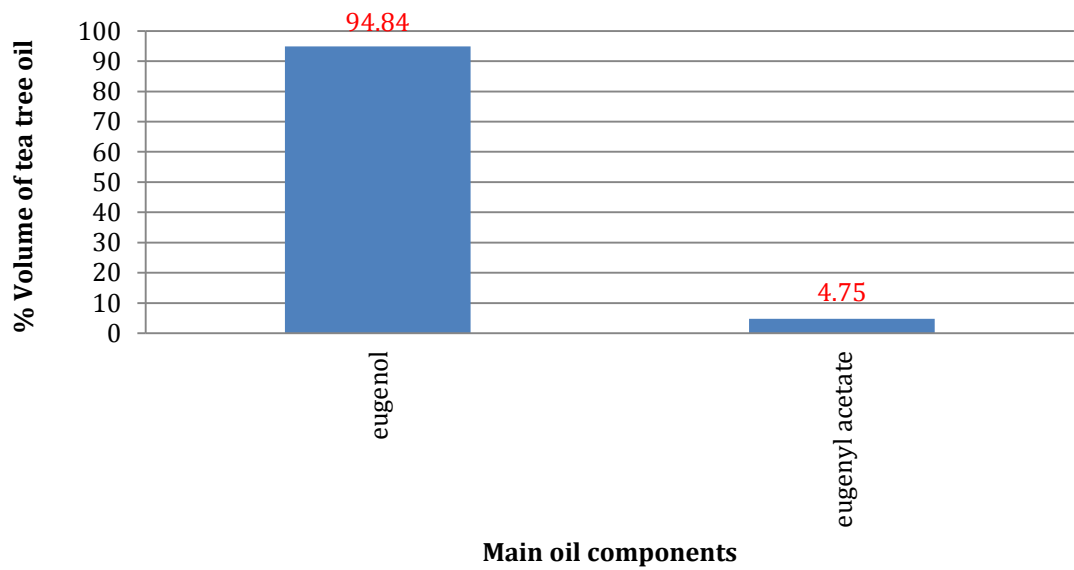


Figure 2.21. The major components of cinnamon-clove oil blend in a 1:1 ratio, as determined by GC-MS. The numbers in red represent the % composition of the chemical component. The labels on the X-axis are the names of each chemical component.

## 2.5 Conclusions

- Seven EOs were selected as antimicrobials on the basis of the initial literature review to provide a range of reported antimicrobial efficacy; cinnamon, clove, eucalyptus, geranium, lemongrass, lime and tea tree oil.
- Cinnamon, clove and lemongrass demonstrated good antimicrobial efficacy individually against most of the panel of microorganisms tested, while *P.aeruginosa* was the most robust test microorganism against individual EOs.
- Blending the EOs allowed identification of numerous blends which displayed a reduction in the concentration (v/v) of oil necessary to inhibit microbial growth, and several blends that displayed synergy against *P.aeruginosa*, which has shown poor results with individual EOs.
- Cinnamon-clove registering the best FIC results across the five microorganisms tested and produced the lowest MIC against the most robust microorganism, *P.aeruginosa* and was therefore selected for further investigation.
- EO constituents >1% were identified using GCMS, with the major antimicrobial constituents changing in % total of the oil when analysing the most efficacious blend from the checkerboard assay.
- For the selected blend of clove and cinnamon (1:1), the percentage of the main antimicrobial constituent increased from 82.85 and 76.39, respectively, to 94.84 when in combination.

### **Chapter 3**

**Synthesis and characterisation of mesoporous silica nanoparticles (MSNs)**

**Loading and release of essential oils from MSNs and antimicrobial testing**

**of blank and essential oil loaded MSNs**

### 3.1 Introduction

#### 3.1.1 Mesoporous silica nanoparticles

Mesoporous silica nanoparticles (MSNs) as encapsulants for bioactive compounds are currently of great interest. Mesoporous silicates, feature an ordered lattice structure of pores and are fabricated in the presence of surfactant or polymer that serves as a template for the polymerising tetraalkoxysilane. After polymerisation of the silica, the organic template can be removed by heating at elevated temperatures (calcination), resulting in a porous structure (Figure 3.1). The term mesoporous describes materials that exhibit pores with a diameter in the range (2 – 50 nm). Attractive features of MSNs include high surface area (up to  $1200 \text{ m}^2 \text{ g}^{-1}$ ), ordered pore structure and modifiable surfaces (Trewyn *et al* 2007). The latter are likely to enable the adsorption of substantial amounts of antimicrobial.

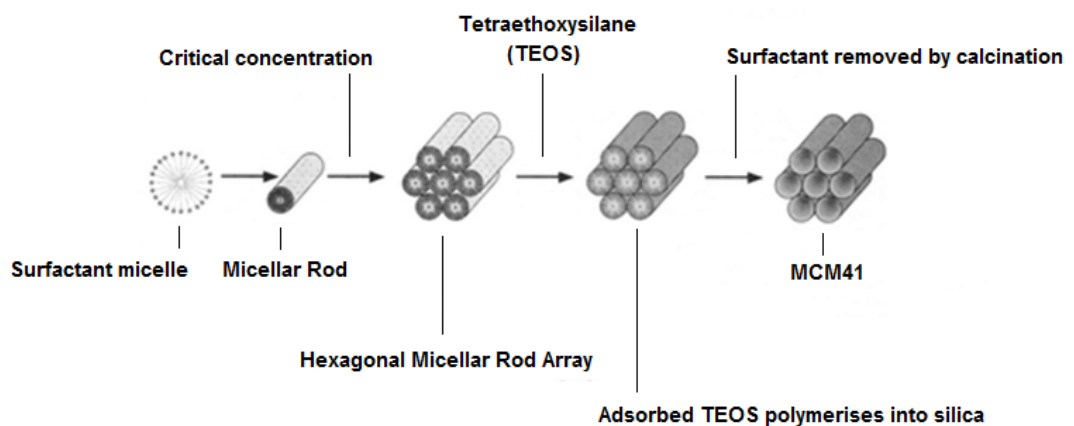


Figure 3.1. Schematic showing the formation of ordered mesoporous materials; At a critical concentration the rod-shaped micelles self-assemble into the hexagonal array. The tetraethoxysilane (TEOS) then adsorbs on the accessible

surfaces of this array, then polymerises into silica. The surfactant array is then removed by calcination leaving the Mobil Composition of Matter No. 41 (MCM-41) (Beck *et al* 1992). The synthesis of mesoporous materials is a development that is of great interest due to the large number of potential applications, such as sustained drug delivery (Salonen *et al* 2008).

For this study, MCM41 silica nanoparticles were synthesised using Liquid Crystal Templating (LCT) procedure. Figure 3.1 shows three main steps that result in mesoporous silica and its characteristic uniformly ordered mesopore channels. The surfactant used here was cetyltrimethylammonium bromide (CTAB), which consists of a long hydrophobic carbon chain with a hydrophilic ammonium end, giving the molecule a positive charge. These micelles then organise themselves into a hexagonal mycellar rod array. TEOS adsorbs on the accessible surfaces of this array, then polymerises into silica resulting in a silica matrix surrounding the rods. The surfactant template can then be removed via calcination, a process in which the surfactant is thermal oxidatively degraded (i.e. burnt away), leaving a porous end product.

The synthesis of mesoporous silica is based on the formation of liquid-crystalline mesophases of amphiphilic molecules (surfactants) that serve as templates for the *in situ* polymerisation of TEOS. The synthesis of MSNs is performed at a low surfactant concentration to make the assembly of the ordered mesophases strongly dependent upon the interaction between the cationic surfactant and the growing anionic oligomers of orthosilicic acid, which in turn limits the assembly of mesophases to small sizes. Once the TEOS is added to the colloidal dispersion, where the anionic silicates electrostatically interact with the cationic surface and are adsorbed on to the now regular array of micelle rods (Trewyn *et al* 2007).

Following filtration and washing of the precipitated particles, the surfactant template must be removed. The template removal can be done one of two ways. If the particles have not been functionalised, calcination can be carried out. This involves heating the particles to 550°C for several hours. The other method of template removal consists of an acid extraction under reflux for 18 hours. Unlike calcination, this technique would preserve any modifications to the nanoparticles that may have been incorporated into the synthesis process (Yanagisawa *et al* 1990).

The resulting mesoporous material will have a structure of well-ordered, uniform pores with large surface areas and pore volume. Additionally, by altering the reaction conditions and substrates used, the morphology and characteristics of the material can be tailored to the specific application the particles are intended for. For example, the pore size can be tuned using surfactants with different chain length during synthesis (Horcajada *et al* 2004). This can enable tuning of the pore size to the molecular size of the antimicrobial and / or tuning the rate of antimicrobial release.

The controlled release of the natural antimicrobial allyl isothiocyanate (AITC) via two different mesoporous silica structures (MCM-41 and Santa Barbara 15 (SBA-15)) was tested for capacity and feasibility of slow release (Park and Pendleton 2012). Pore filling by vapour phase AITC approached 100%, and controlled release was observed as 90% of the available AITC desorbed over 96 hours. The release from SBA-15 silicates occurred as a 'burst release' with 65% desorbed in the first 12 hours compared with only 20% from the MCM-41 silicates.

Reduction of rate of release of active molecules from MSNs can be accomplished relatively easily by decreasing the pore diameter of the silica

material, as demonstrated in previous studies looking at drug release rates from ordered silicates (Lu *et al* 2007). The mesophases based on micelles as the building blocks vary in structure depending on many factors with the surfactant geometry. Therefore, based on the orientation of surfactant templates, a variety of mesophases can be obtained by using different surfactant molecules or changing the packing parameters of a surfactant, adjusting the composition or introducing an additive. For example, the addition of hydrophobic organic molecules increases the hydrophobic volume of the surfactant, and increases the pore size. The retention of active molecules is likely influenced by the surface chemistry of the pores, which could be affected by the high temperatures associated with removal of the surfactant during calcining (Deng *et al* 2013).

### 3.1.2 Characterisation methods

A number of different techniques were used to characterise the nanoparticles. Nanoparticle size and morphology were investigated using electron microscopy. The hydrodynamic size and dispersion stability were examined using a Malvern Zetasizer. The porous silica nanoparticles used in this study were also analysed by nitrogen (N<sub>2</sub>) adsorption that provides particle surface area and pore size distribution. It is vitally important to comprehensively characterise nanoparticles before using them for a specific application as it allows for a greater understanding of the underlying factors that may affect potential applications.

### 3.1.2.1 Scanning electron microscopy

SEM produces highly detailed images with wide depth of focus of conductive and non-conductive materials. Magnification can be up to  $10^5$  times with a maximum resolution of ca. 3 nm. Non-conductive samples are usually coated with a sputtered / vapour deposited conductive film of metal or carbon to prevent electric charge building up in the sample and deflecting the electron beam, resulting in a phenomena known as charging. In order to enable unimpeded electron travel SEM is usually carried out in a high vacuum which prevents imaging of moist and oily samples. Modern SEMs, however, can image such samples, as they are able to operate under lower vacuum conditions.

The high-energy electron beam is often created using a tungsten filament. The electrons produce a signal relating to the surface topography by interacting with the atoms in the sample. The two types of signal produced by this SEM are secondary electron and backscattered electrons. Backscattered electrons consist of high-energy electrons originating in the electron beam, which are reflected or backscattered out of the specimen interaction volume by elastic scattering interactions with specimen atoms. The most common detection is secondary electron imaging, where electrons are produced by the ionisation of the atoms in the sample. The term 'secondary' refers to the electrons not being generated by the primary source of radiation. The primary source of radiation is from the electron beam generated by the tungsten filament, which ionises the surface atoms on the sample to produce secondary electrons. Back-scattered electrons are detected by deflection of electron wave into the direction they originated from. As the electrons are scattered the reflection is diffused (Pennycook and Nellist 2011).

### 3.1.2.2 Electrophoretic light scattering

A Malvern Zetasizer Nano ZS was used to record the electrophoretic Zeta potential of the MSNs in MeOH solution. The fundamental physical principle is that of electrophoresis. A dispersion is introduced into a cell containing two electrodes. An electrical field is applied to the electrodes, and particles or molecules that have a net charge, or more strictly a net zeta potential will migrate towards the oppositely charged electrode with a velocity, known as the mobility, that is related to their zeta potential in millivolts (mV). The greater the zeta potential from 0 mV, the less likely the sample will aggregate (Shaw 1992).

### 3.1.2.3 Nitrogen adsorption

Gas adsorption is usually the method of choice for determination of specific surface area and pore characteristics of particulate materials, the technique measures the amount of gas adsorbed and desorbed onto the particulate solid and thus gives a measure of the surface area. The difference between the adsorption and desorption behaviour can be used to determine pore size distribution (Groen *et al* 2003)(Othman, 2012).

The surface area analyses of particulate solid materials are measured using the Brunauer-Emmett-Teller (BET) isotherm, characterised by a type II isotherm shown in Figure 3.2. To determine the surface area, solid samples are pretreated by applying a vacuum, or flowing gas to remove adsorbed contaminants acquired (typically water and carbon dioxide) from atmospheric exposure. The solid is then cooled, under vacuum, usually to cryogenic temperature (77 K). An adsorptive (in this case nitrogen) is dosed to the solid in controlled increments. After each dose of adsorptive, the pressure is allowed to

equilibrate and the quantity adsorbed is calculated. The quantity adsorbed at each pressure, and temperature defines an adsorption isotherm, from which the quantity of gas required to form a monolayer over the external surface of the solid is determined. With the area covered by each adsorbed gas molecule known, the surface area can be calculated. The N<sub>2</sub> adsorption analysis was conducted using a Micromeritics ASAP 2020 BET surface area and porosity instrumentation.

Pore size can be calculated using the Barret, Joyner and Halenda (BJH) method, using adsorption isotherms and the Kelvin model of pore filling. It applies only to the mesopore and small macropore size range. Surface area determinations involve creating the conditions required to adsorb an average monolayer of molecules onto a sample. By extending this process so that the gas is allowed to condense in the pores, the sample's fine pore structure can be evaluated. As pressure increases, the gas condenses first in the pores with the smallest dimensions. The pressure is increased until saturation is reached, at which time all pores are filled with liquid. The adsorptive gas pressure then is reduced incrementally, evaporating the condensed gas from the system. Evaluation of the adsorption and desorption branches of these isotherms and the hysteresis between them reveals information about the size, volume, and area. The Isotherms produced can be classified using the International Union of Pure and Applied Chemistry classification (IUPAC), mesoporous materials usually fall into the class IV isotherm which can be seen in Figure 3.2 (Donohue and Aranovich, 1998).

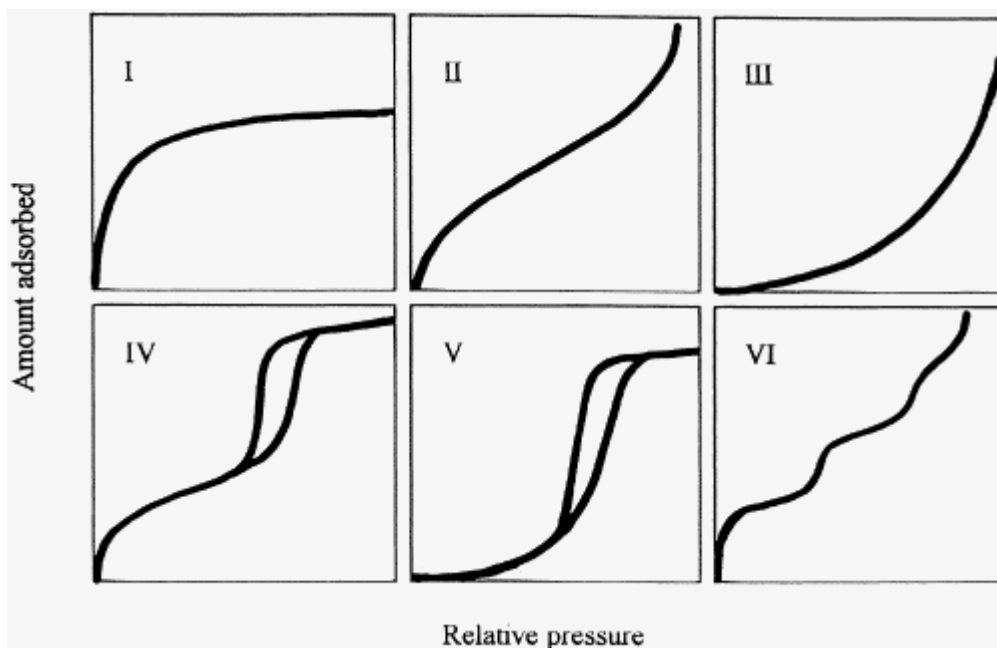


Figure 3.2. IUPAC adsorption isotherm classification (Donohue and Aranovich 1998).

#### 3.1.2.4 Thermogravimetric analysis

Thermogravimetric analysis (TGA) is a thermal analytical method used to determine mass loss as a function of increasing temperature. The thermogravimetric (TG) instrumentation usually consists of four major components; the furnace, sample holder, the data acquisition system and the sensors which detect the samples properties dependent on temperature. These components produce a TG curve, representative of mass change against temperature, where the temperature usually increases uniformly or is kept constant. The TG curve for a sample that displays single stage decomposition will contain two characteristic temperatures,  $T_i$  and  $T_f$ .  $T_i$  is the lowest temperature at which the mass change is detectable by the thermobalance at the selected settings.  $T_f$  is the temperature once the decomposition has been completed. The difference between  $T_i$  and  $T_f$  is defined as the reaction interval. The mass change of a sample due to increasing temperature is defined as dynamic thermogravimetry. Alternatively, when temperature is kept constant and

the change of mass is measured it is defined as isothermal or static thermogravimetry. This analytical technique provides information on the purity of a sample and its specific modes of transformation, dependent on the temperature range (Kealey and Haines 2002).

### 3.2 Objectives

- Synthesis of mesoporous silica nanoparticles (MSN).

To achieve MSNs of high surface area and mono-disperse size, with uniform pores for release of essential oils.

- Characterisation of nanoparticles.

The size and characteristics of nanoparticles will be determined using specialist analytical apparatus, such as electrophoretic light scattering and nitrogen adsorption.

- Determination of the level of essential oil (EO) adsorption on MSNs and the rate of release of essential oil from MSNs.

MSN will be loaded with a 1:1 blend of cinnamon (CIN) and clove (CLO) EOs via deposition from solution in a volatile solvent and by immersion of MSN in the EO blend followed by solvent washing. Thermal gravimetric analysis will be used to determine the loading level of EO. Gas chromatography coupled with mass spectrometry will be used to analyse the oil release from the MSN.

- To determine the antimicrobial activity of MSNs loaded with EO and whether blank MSNs exhibit any antimicrobial action.

Bacteriostatic, bactericidal and time – kill assays will be set up using blank nanoparticles and nanoparticles loaded with essential oil to determine if they display contact kill against microorganisms associated with HCAs.

### 3.3 Materials

#### 3.3.1 Chemicals

Tetraethoxysilane (TEOS) and Methyltriethoxysilane (MTEOS) were purchased from Sigma – Aldrich (UK). Cetyltrimethyl ammonium bromide (CTAB), sodium hydroxide (NaOH), and methanol (MeOH) were purchased from Fisher-Scientific (UK). Purified water from a Millipore Elix<sup>®</sup> 5 bench-top treatment unit was used throughout the study. The water treatment system was maintained according to manufacturer guidelines.

#### 3.3.2 Media, microbes and EOs

*Vide supra* Section 2.3.1.1 – 3, all five test microorganisms were used, along with cinnamon and clove essential oils, in a 1:1 blend.

### 3.4 Experimental

#### 3.4.1 MSN fabrication

Initially, CTAB (1.00g) was dissolved in distilled water (480 mL). To which, 2.0M NaOH (3.5 mL) was pipetted into the solution and the temperature was raised to 80°C. Tetraethyl orthosilicate (TEOS) (4 mL) was pipetted into a small beaker then added drop wise to the solution, using a Pasteur pipette. This solution was stirred continuously for 2 hours at 80°C, producing a white dispersion of MSNs. The MSNs were isolated from the dispersion by centrifuging for 15 minutes at 14,000 rpm, using a Beckman J2-21 Series centrifuge and 250 mL centrifuge bottles. The resulting supernatant was stored and the pellet was washed three

times with methanol. To remove the CTAB surfactant template from the MSNs, the product was dried at 60°C until the methanol had evaporated. The sample was then calcined in air for 5 hours at 550°C.

### 3.4.2 Characterisation of MSN

#### 3.4.2.1 Zeta potential

The particle size and Zeta – potential measurement (surface charge) of the MSNs were measured using a Malvern Zetasizer Nano ZS. Zeta – potential was calculated by Laser Doppler Electrophoresis (LDE) and size by dynamic light scattering (DLS). Before analysis, the samples were sonicated for 15 minutes to adequately disperse the nanoparticles. The sample was then diluted with methanol (ratio 1:10) and added to the cuvette for DLS or the micro-electrophoresis cell for LDE.

#### 3.4.2.2 SEM

To assess the morphology of the MSNs, the samples were observed using a JEOL JSM-5600LV scanning electron microscope (SEM) with a 20 kV acceleration voltage. Before analysis, the samples were sonicated for 15 minutes to adequately disperse the nanoparticles. The sample was then diluted with methanol (ratio 1:10) and a drop from a Pasteur pipette was added to a SEM metal stud. Once dry, the metal studs were coated with gold using an EMITECH SC7460 sputter coater. The SEM studs were placed in the sputter chamber, with the argon gas supply set at 0.7 bar. The chamber was evacuated

to a pressure of < 0.06 mbar, voltage set to 800 V and current at 20 mA. The studs were then gold sputtered for 2 minutes. Images of the MSNs were taken at 20,000 – 50,000x.

#### 3.4.2.3 Nitrogen adsorption

A Micromeritics ASAP 2020 surface area and porosity analyser was used to evaluate the surface area of the MSNs using an automated nitrogen adsorption-desorption method. The calcined samples were placed in an analysis tube, weighed, dehydrated and finally degassed at 300°C for 12 hours. The samples were then re-weighed and the difference between the two masses recorded. Commonly, for gas adsorption measurements of solid materials they must initially undergo a process whereby the majority of previously adsorbed gases and vapours are removed. This process is referred to evacuation where the solid is outgassed to c.  $10^{-4}$  Torr for several hours in order to remove the physical adsorbed gas and majority of the chemisorbed gas. The adsorption of gas or vapour onto the sample is measured by introducing a known volume of adsorbate, which is then determined using volumetric or gravimetric analysis. The gas is held within a burette and the pressure is measured using a manometer. The volumes within the apparatus are calibrated in order for the amount of gas adsorbed by the absorbent sample to be determined via the pressure at equilibrium. The adsorption isotherm is calculated from a progression of readings obtained at different pressures. The cumulative surface area, average pore diameter and mesopores were obtained from pore size distribution curves. This allowed the calculation of the surface area using BET volumetric analysis. The porous sample was degassed and exposed to known volume of nitrogen. The amount of gas absorbed by the sample can be quantified by subtracting the volume of gas once the pressure is equilibrated

from the initial volume of gas injected within the system. Pore size was also calculated via the BJH procedure.

#### 3.4.2.4 Thermal gravimetric analysis

A Perkin Elmer TGA 4000 instrument was used to confirm the absence of surfactant template in post calcined MSNs (temperature increase of 10°C/min under nitrogen) and to produce residue fraction (RF) values for subsequent calculation of EO blend loading. The TG instrumentation normally consists of four components; the furnace, sample holder, sensors which detect the sample properties dependent on temperature and the data acquisition system. Commonly, the furnace is operated electrically and upon sample analysis it is purged with appropriate gases to allow the sample to decompose as it reacts and/ or burns. The temperature is either measured by a thermocouple or resistance sensor, while mass is measured by a thermobalance. The thermobalance is a highly sensitive electrical device that is capable of measuring small changes in mass (1 µg). The sample is placed in an inert crucible, such as aluminium, platinum or ceramic. The percentage weight and derivative TGA data was then recorded as a function of increasing temperature .

#### 3.4.3 Loading of EO blend into MSNs

Two methods were utilised for loading of EO blend (CIN:CLO 1:1) into the nanoparticle mesopores. Initially, a solvent evaporation method was used, whereby 0.1g of MSN sample was placed in a crucible along with 0.1g of EO and 5 mL of MeOH. The crucible was placed in a fume cupboard (flow rate 0.77 m/sec<sup>-1</sup>) and the solvent was allowed to evaporate.

Secondly, 0.1g of MSN sample was immersed in 2 mL of EO and placed in a glass bottle on a table top shaker for 24 hours at 200 rpm. The excess EO was drained from the sample and all samples were lightly washed with MeOH and allowed to dry before use, to ensure the nanoparticles were free of surface EO. TGA was used to produce residue fractions for blank MSN samples and percentage load of EO on dry MSN was calculated for EO loaded MSN samples to discern the loading level relative to a blank MSN sample, using equation 3.1.

Equation 3.1. Residue fraction calculation, allowing EO loading percentages to be determined.

$$(i) \text{Amount of MSN minus EO} = \frac{\% \text{ weight residue at } 900^{\circ}\text{C}}{\text{EO free MSN residue fraction}}$$

$$(ii) \text{Amount of EO in sample} = \% \text{ weight at } 110^{\circ}\text{C} - \text{Amount of MSN minus EO}$$

$$(iii) \% \text{ EO on dry MSN} = \frac{\text{Amount of EO in sample}}{\% \text{ weight at } 110^{\circ}\text{C}}$$

Subsequent MSN samples (EO loaded or blank as required) were prepared at four different MSN concentrations in ISB at double strength allowing for subsequent dilution by the test culture in broth, as follows; 200 mg/mL by adding 0.2g of the EO loaded MSNs to 10 mLs of ISB, 100, 50 and 25 mg/mL EO loaded MSN concentrations by adding 0.1, 0.05 and 0.025g to 10 mLs of ISB, respectively.

#### 3.4.4 Release of EO from MSNs

EO blend loaded MSNs (0.1g) were placed on filter paper in a Buchner funnel, attached to a flask under vacuum and washed with MeOH (3 x 10 mL). After each washing, the solvent was recovered and an aliquot (1 mL) was taken for subsequent GC-MS analysis to assess EO release from the MSN.

#### 3.4.5 Molecular modelling of EO antimicrobial components

Scigress software (Fujitsu) was used to model the main chemical constituents of the EOs attributed with antimicrobial action. The molecular structure was computed using molecular mechanics calculations (MM3 and Scigress version 3.1.9). Geometry labels were assigned to determine the size or length of the molecules to confirm if they would fit in the nanoparticle mesopores. The area of contact for eugenol with the MSN surface was also assigned using geometry labels allowing an estimated monolayer coverage to be calculated.

#### 3.4.6 Antimicrobial testing of blank and EO loaded MSNs

The MSNs were tested for their antimicrobial properties. The microorganisms were challenged with blank and EO loaded MSNs, growth inhibition, and time-kill assays were performed using the method described in (Section 2.3.6).

Growth inhibition studies aim to determine the minimum inhibitory concentration of an antimicrobial agent that will suppress the capacity of a given microorganism to divide and propagate, without causing cell death. With these experiments it was intended to elucidate the potential bacteriostatic activity of the blank MSNs, and what concentrations of 2% (v/v) CIN-CLO blend loaded MSNs, were capable of preventing the growth and multiplication of the microorganisms tested.

### 3.4.7 Growth inhibition assays of blank MSNs

The OD of the ISB bacterial cultures were adjusted to 0.1 at 540 nm with ISB, and 10 mL of each were added to 20 mL glass bottles. Four concentrations of blank MSNs (10 mL) were inoculated into the broth suspended microorganisms (12.5, 25, 50 and 100mg/mL). Immediately after inoculation, a 'time 0' OD reading was recorded for all control and test bottles. In order to ensure an intimate contact between the microorganisms and the nanoparticles, each test bottle was incubated at 37°C with shaking (200 rpm) for 24 hours, at which time 1 mL of sample was removed and OD was recorded for this sample against that of a control culture with no blank MSNs present. The experiment was run in triplicate (n=3).

For this type of growth inhibition study, the principle is based upon the increase in optical density that results from an increase in bacterial cell numbers due to multiplication. If growth occurs, the OD will increase, however if it does not, the OD will remain in-line with the 'time 0' OD values. A decrease in optical density is not expected. Suppression of bacterial cell division capability, or even cell death, still leaves the dormant / dead cells in suspension such that their contribution to increasing optical density remains. Only in the case of cell lysis would the OD decrease. An increase in the OD is therefore indicative of bacterial growth with no bacteriostatic effect being observed, as indicated by the growth curve experiments (Section 2.3.2.2). No change in OD would suggest, bacteriostatic or bactericidal action.

#### 3.4.8 Bactericidal assays

Essential oil (2% CIN-CLO blend) loaded MSN suspensions at 12.5, 25, 50 and 100mg/mL of MSNs were prepared using ISB. Samples were sonicated for 15 minutes before use and appeared uniform. The five test microorganisms were grown overnight in 10 mL of ISB. After ensuring that no growth had occurred in the negative control tube (non-inoculated ISB), the optical density of the cultures was adjusted to 0.1 at 540 nm. Then, 10 mL of culture were added to test bottles containing 10 mL of each of the corresponding nanoparticle suspensions containing EO loaded MSNs. These were then incubated with agitation (200 rpm) overnight at 37°C. A test bottle containing 1 mL of nanoparticle free ISB was inoculated and a blank MSN control was used. Following the overnight incubation, 10 µL of each culture was removed to be inoculated on nanoparticle free ISA plates. These were put in the incubator overnight and finally growth was checked. The bactericidal concentrations were determined based upon a growth/no growth basis. The experiment was run in triplicate (n=3).

#### 3.4.9 Time-kill assays

The dynamic killing capacity of the EO loaded MSNs was investigated (based on Hetrick *et al* 2007). The MSN concentrations that produced no growth in the bactericidal assay were used for this experiment. They were as follows;

*S.aureus*, MRSA and *E.coli* 25 mg/mL

*P.aeruginosa* and *C.albicans* 50 mg/mL

Overnight cultures were taken and adjusted to 0.1 OD at 540 nm using ISB as diluents if necessary. In addition, the microorganisms were also prepared in exponential growth phase, by diluting overnight bacterial cultures in fresh broth

and incubating at 37°C until they reached exponential growth phase (as shown previously in Section 2.3.2.2).

Then, 1 mL of uninoculated ISB was added to 1 mL of the stock EO loaded MSNs and sonicated until dispersed. The broth-MSN suspension was then transferred into the respective test bottle containing 100 µL of each microorganism at exponential or stationary phase and incubated at 37°C while shaking (200 rpm). In addition, at time 0, 100 µL of the OD adjusted cultures were mixed with 1 mL of the control (nanoparticle free ISB). Aliquots of 10 µL were taken from test and control mixtures at time 0, 15, 30 and 60 serially diluted in PBS and 10 µL pipetted onto ISA incubated at 37°C for 24 hours, enabling tracking of CFU/mL over time.

The determination of bacteriostatic and bactericidal concentrations disregard the time required for the antimicrobial agent to demonstrate an effect. With the use of time-kill assays it was intended to obtain an understanding of how the EO loaded MSNs exert their antimicrobial effects over time. The experiment was run in triplicate (n=3).

## 3.5 Results and Discussion

### 3.5.1 Characterisations of MSN

Initially, MSNs were prepared using the method of Trewyn *et al* (2007), which reported nanoparticles of roughly 100-200 nm diameter and mesopores of 2 nm in diameter. Using this method, nanoparticles were characterised, with five samples subsequently used in experiments. Ideally, mono-dispersed MSNs of roughly 100-200 nm in diameter, with high surface area and uniform mesopores large enough to accommodate the main constituents of the EOs used would be fabricated for release of the antimicrobial. In order to produce a surfactant free MSN, the CTAB template must be removed, the template can be removed via calcination and confirmed via TGA.

#### 3.5.1.1 Thermogravimetric analysis (TGA)

TGA was used to confirm the removal of the surfactant template post calcination (Figure 3.3). For each MSN batch, a small sample pre and post calcination was analysed to show the thermal decomposition of the template in the pre-calcined sample. Any fluctuations in the derivative data at room temperature to 110 °C was due to water molecules evaporating from the pores of the nanoparticles. The mass loss between 110°C - 400°C was due to the decomposition of the surfactant template molecules that are still within the MSNs. The mass loss above 400°C may be due to condensation of water from the silanol groups (Verhaegh *et al* 1994). The % mass loss between key temperature ranges for the five MSN samples are displayed in (table 3.1).

Table 3.1. Showing mass loss between key temperature ranges for five MSN samples. With template (WT) and without template (WOT).

Sample No.	Mass % loss between 110-400 (WT)	Mass % loss between 110-900 (WT & WOT)	% surfactant on dry MSN
1 WT	46.5	50.89	46.41
1 WOT		6.61	
2 WT	47.5	54.56	40.60
2 WOT		17.14	
3 WT	46.5	50.89	46.41
3 WOT		6.61	
4 WT	46.5	50.89	44.31
4 WOT		9.71	
5 WT	47.5	54.56	46.19
5 WOT		9.27	

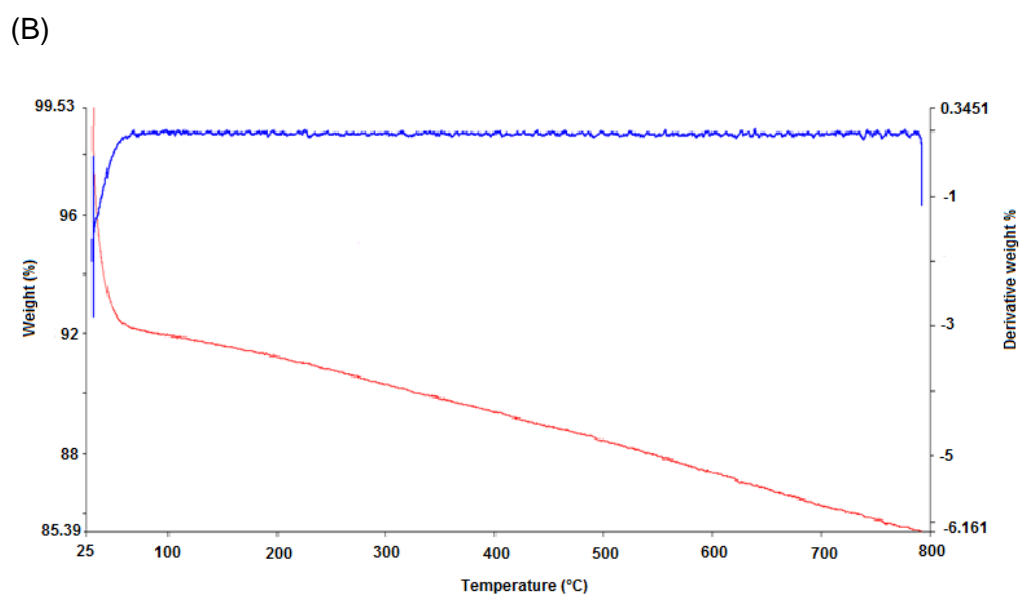
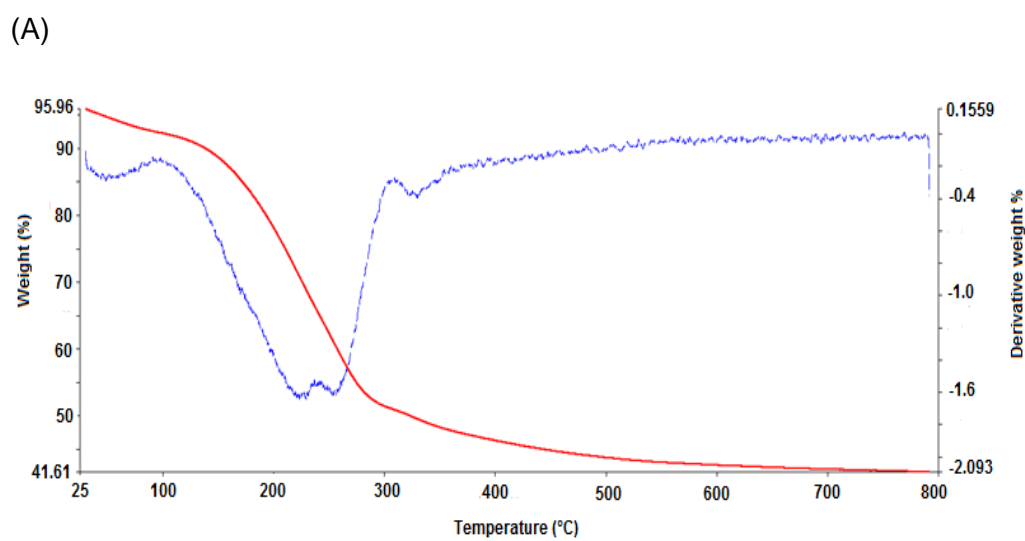


Figure 3.3. Thermogravimetric analysis (solid line) and derivative thermogravimetric curve (dotted line) of surfactant intact MSN sample 1 (A) and MSN sample 1 post calcination (B).

### 3.5.1.2 Zeta potential

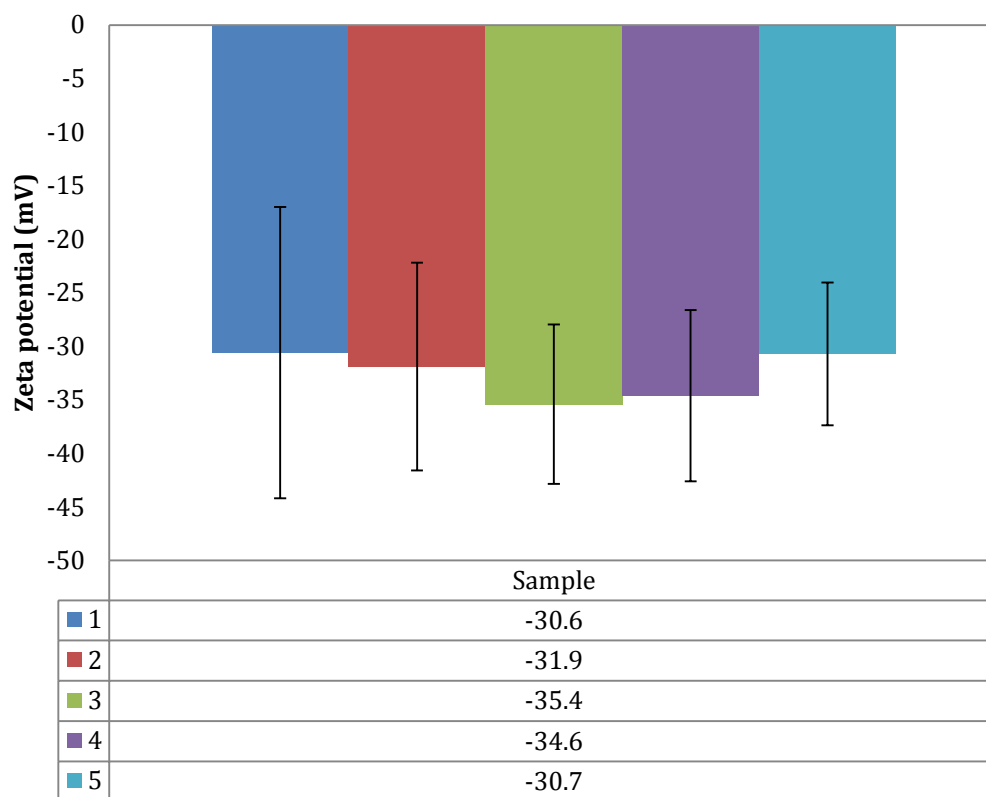


Figure 3.4. Zeta potential for the five MSN samples used for further experimentation.

The Zeta potential of the MSNs (Figure 3.4) displayed good electrophoretic potential in methanol. The five MSN samples recorded Zeta potentials between -30.6 – -35.4 (mV), indicating that the samples will have good aqueous dispersion stability.

### 3.5.1.3 Scanning electron microscopy

The SEM analysis (figure 3.5 – 3.7) confirmed the desired size and dispersion of the MSN samples. ImageJ was used to record nanoparticle diameter, a sample of 100 nanoparticles were measured for each batch of MSNs. Sample 1 recorded an average size of  $94.58 \pm 11.72$  nm and values of  $102.63 \pm 14.79$ ,  $101.35 \pm 10.8$ ,  $109.71 \pm 9.76$ ,  $95.36 \pm 13.83$  were obtained for samples 2-5 respectively.

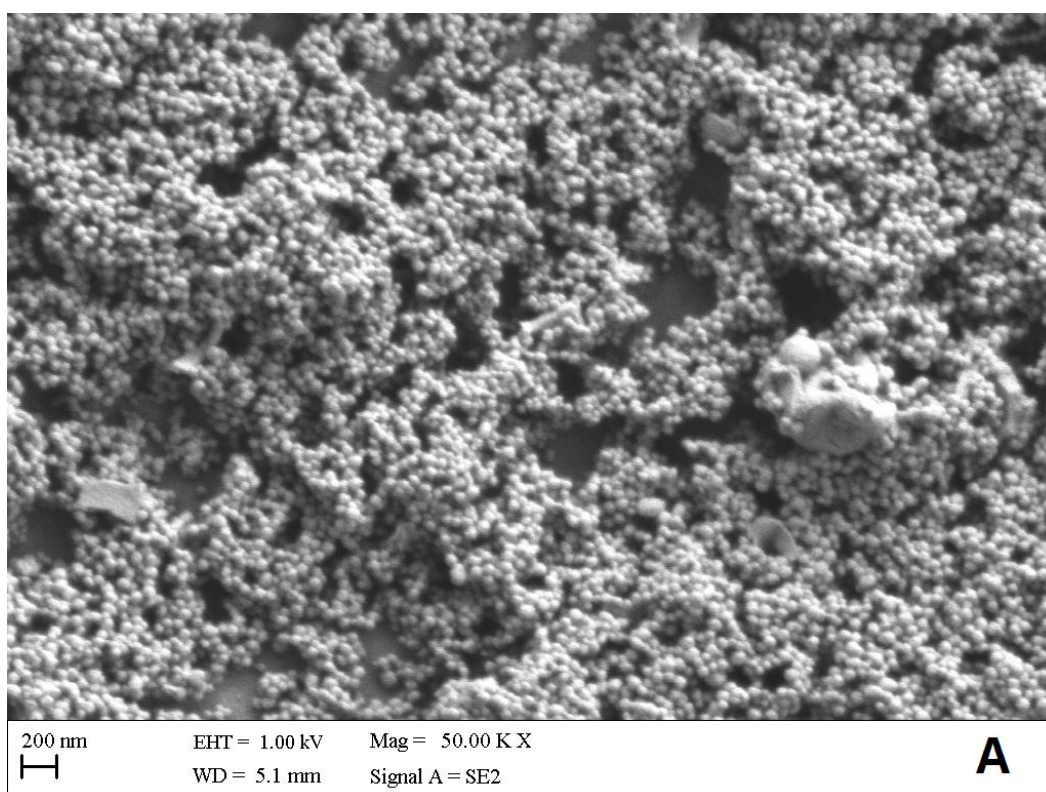


Figure 3.5. Scanning electron microscope images of calcined MSNs (Sample 1).

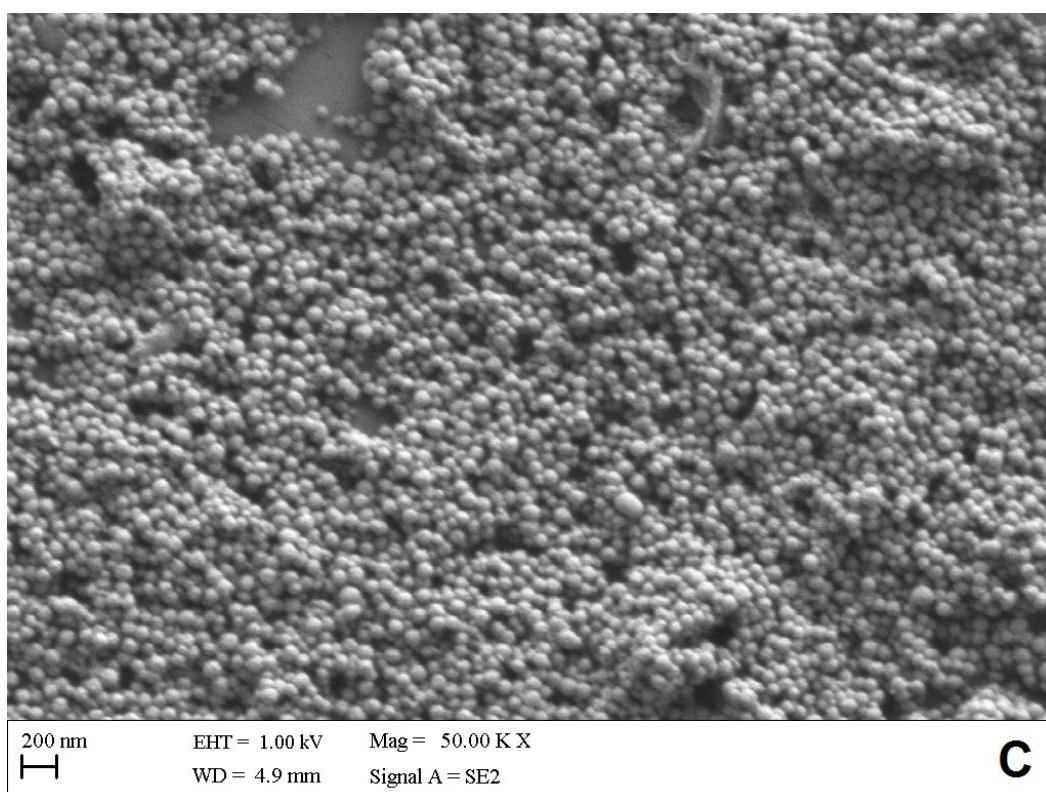
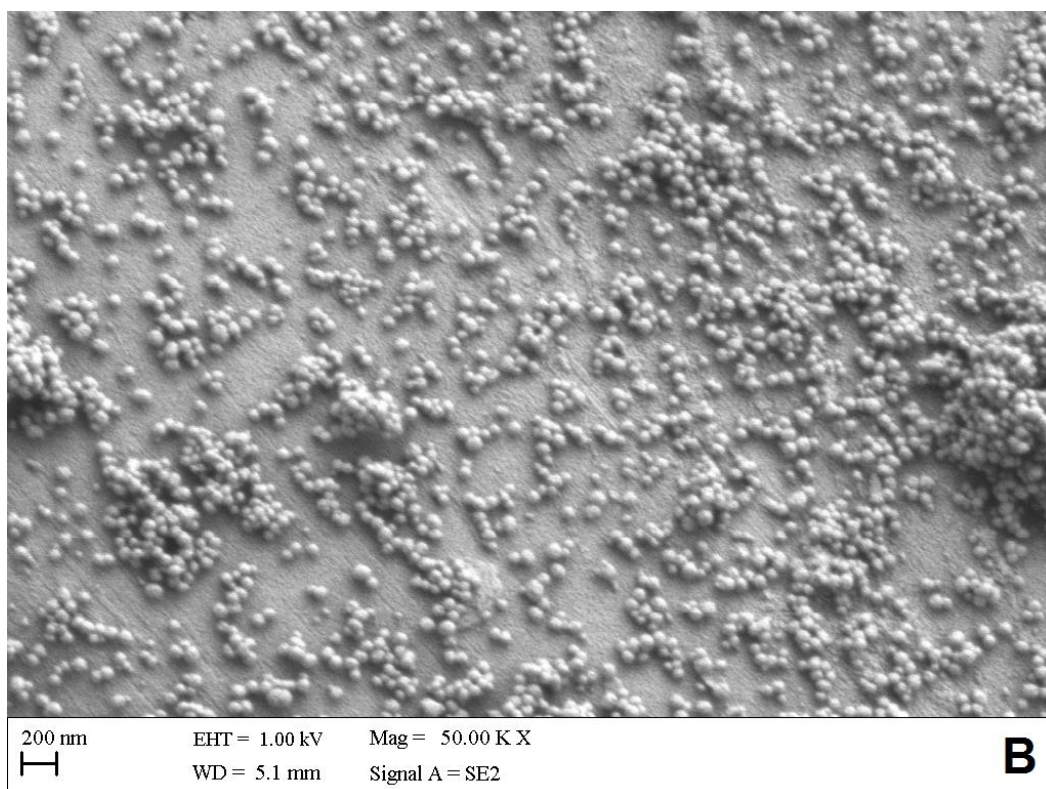


Figure 3.6. Scanning electron microscope images of calcined MSNs, B and C, samples 2 and 3, respectively.

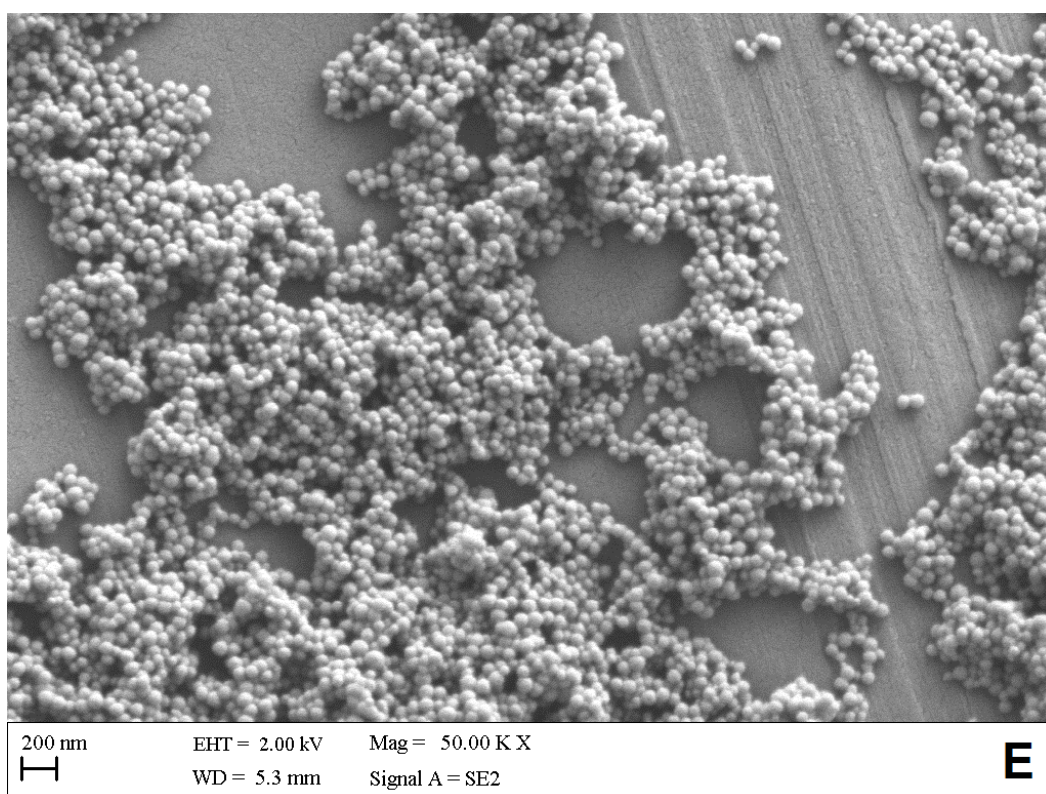
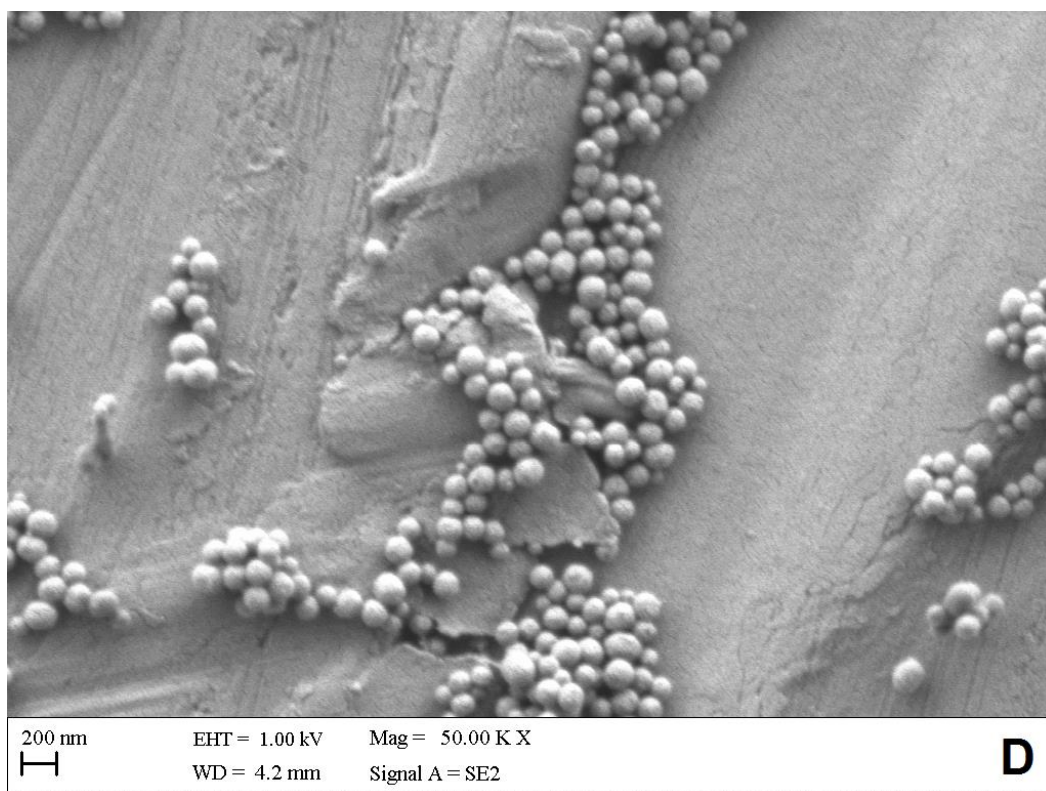


Figure 3.7. Scanning electron microscope images of calcined MSNs, D and E, samples 4 and 5, respectively.

### 3.5.1.4 Nitrogen Adsorption of MSNs

Nitrogen adsorption analysis was conducted to confirm the porosity of the MSN samples. (Figure 3.8 – 3.10) displays the N<sub>2</sub> sorption of MSN samples 1-5. The isotherm curves follow the general type-IV classification of mesoporous materials.

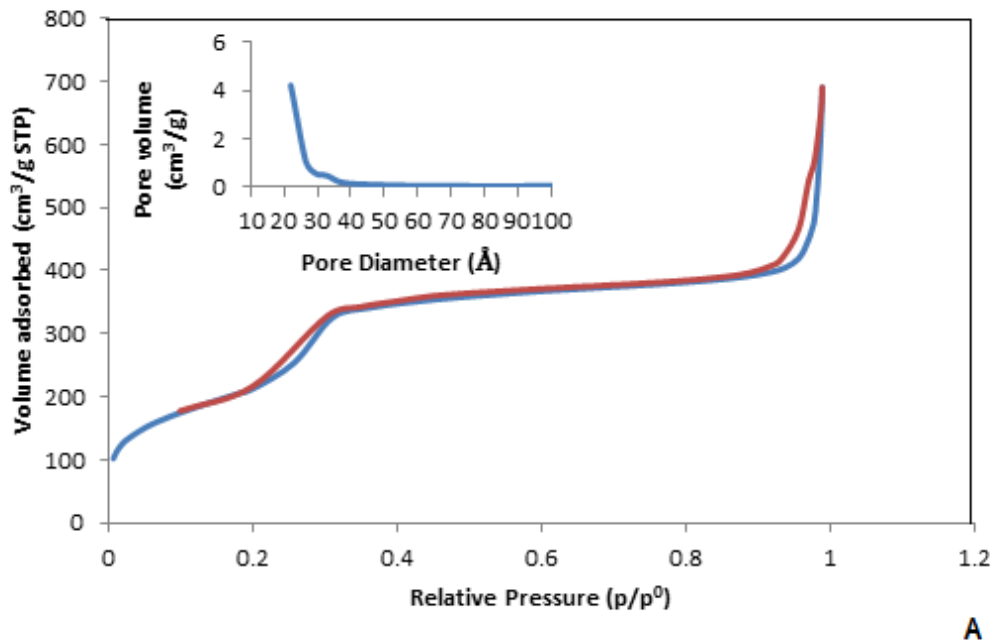


Figure 3..8. Nitrogen sorption isotherm for gas adsorption (blue line) and desorption (maroon line) at 77K and pore size distribution graph (Sample 1).

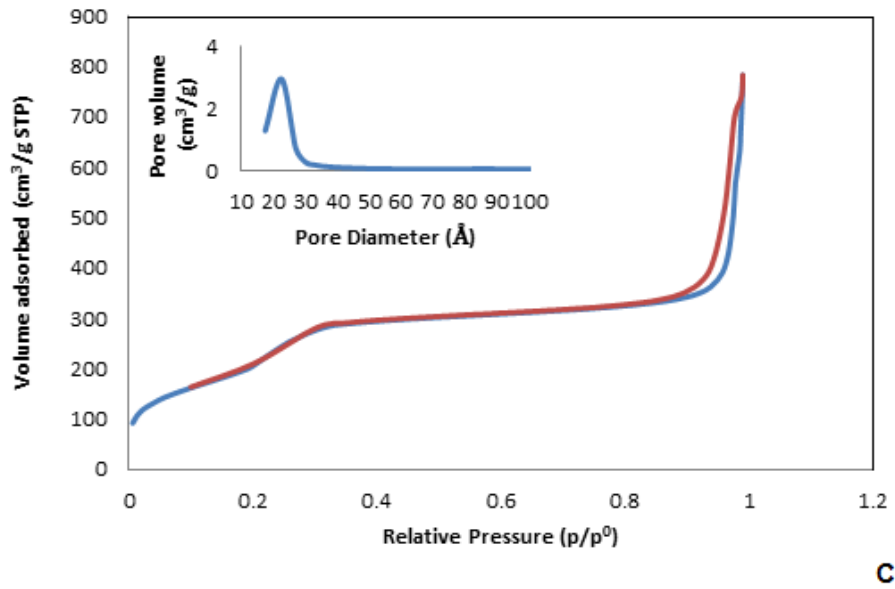
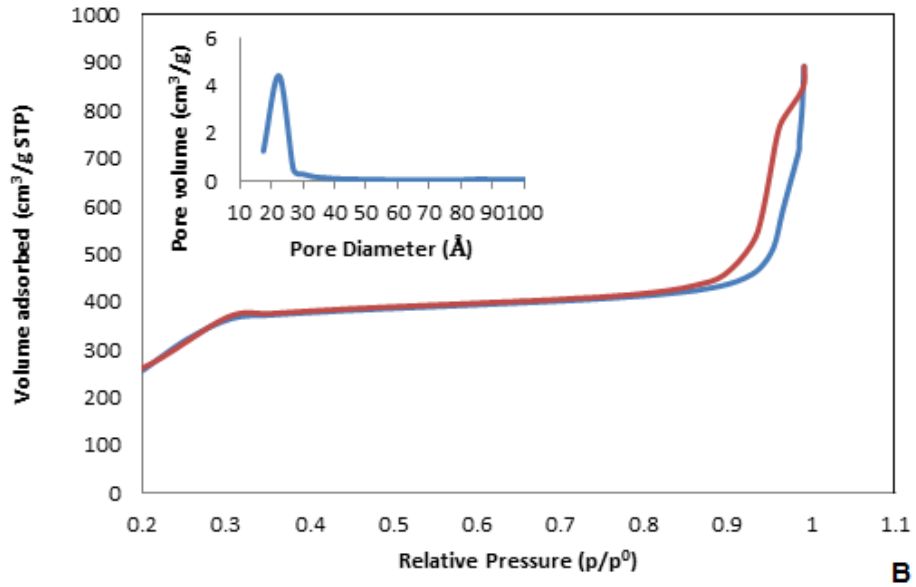


Figure 3.9. Nitrogen sorption isotherm for gas adsorption (blue line) and desorption (maroon line) at 77K and pore size distribution graph B and C, (Sample 2 and 3, respectively).

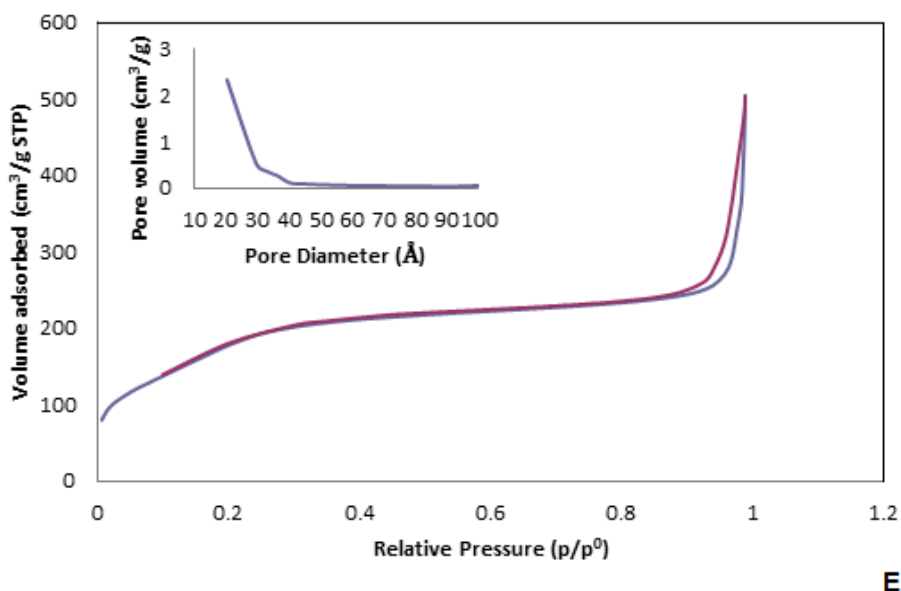
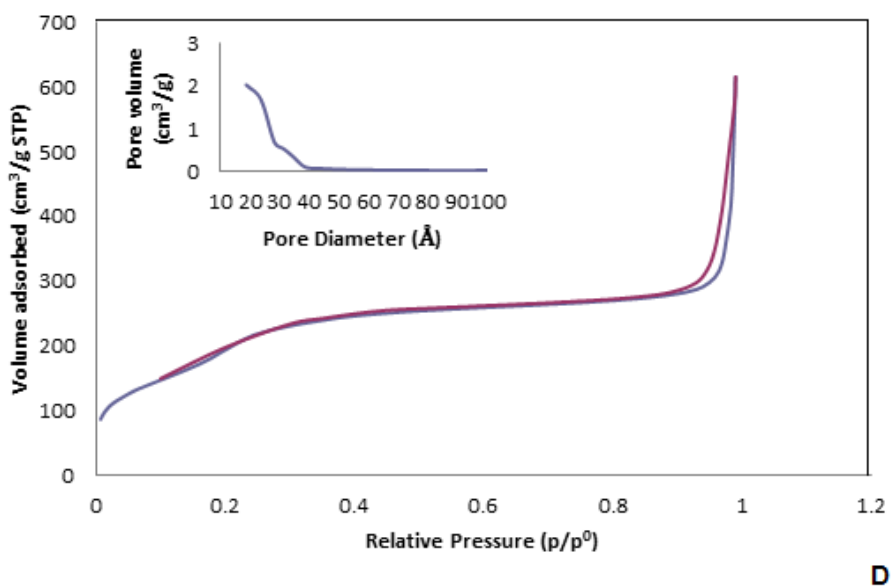


Figure 3.10. Nitrogen sorption isotherm for gas adsorption (blue line) and desorption (maroon line) at 77K and pore size distribution graph D and E (Sample 4 and 5, respectively).

The objective of synthesising porous nanoparticles was achieved. The MSN samples 1-5 have a pore diameter between 1.8-2.2 nm as shown in the pore size distribution graphs (Figure 3.8 – 3.10). The sharp peaks confirm that the ordered mesoporous nanoparticles have a narrow size distribution around 2 nm (Trewyn *et al* 2007, Deng *et al* 2013, Hong *et al* 2007). For the intended MSN

application, the large surface area along with narrow pore size confers the desired characteristics (Table 3.2)

Table 3.2. Summary of mesoporous silica nanoparticle sample characterisations.

MSN sample	Diameter (nm) (SEM images)	Surface area (m <sup>2</sup> /g)	Pore size (nm)	Zeta potential (mV)
1	94.58 ± 11.72	980 ± 77	2.2	-30.6
2	102.63 ± 14.79	1161 ± 76.	2.2	-31.9
3	101.35 ± 10.8	894 ± 44	2.2	-35.4
4	109.71 ± 9.76	759 ± 19	1.8	-34.6
5	95.36 ± 13.83	654 ± 12	2.1	-30.7

### 3.5.2 Molecular modelling of major EO constituents

Scigress software was used to model the main antimicrobial constituents to determine their length and enable assessment as to whether they would physically fit in the nanoparticle mesopores. The molecular model presented in (Figure 3.11) shows that the major EO constituent of the CIN:CLO blend (eugenol) is 0.922 nm in length, for ball and stick and space filling models respectively and would therefore fit in the MSN pores, which ranged from 1.8-2.2 nm in diameter.

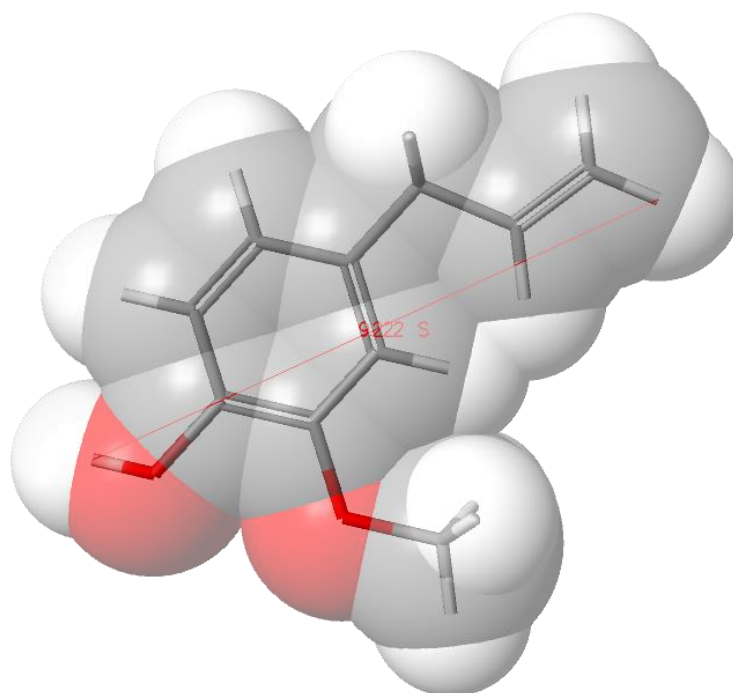


Figure 3.11. Eugenol (represented as a space filling molecular model with stick model overlaid) is the major constituent of clove oil and cinnamon oil.

### 3.5.3 Loading of EOs into MSNs, solvent evaporation studies.

#### 3.5.3.1 Solvent evaporation loading

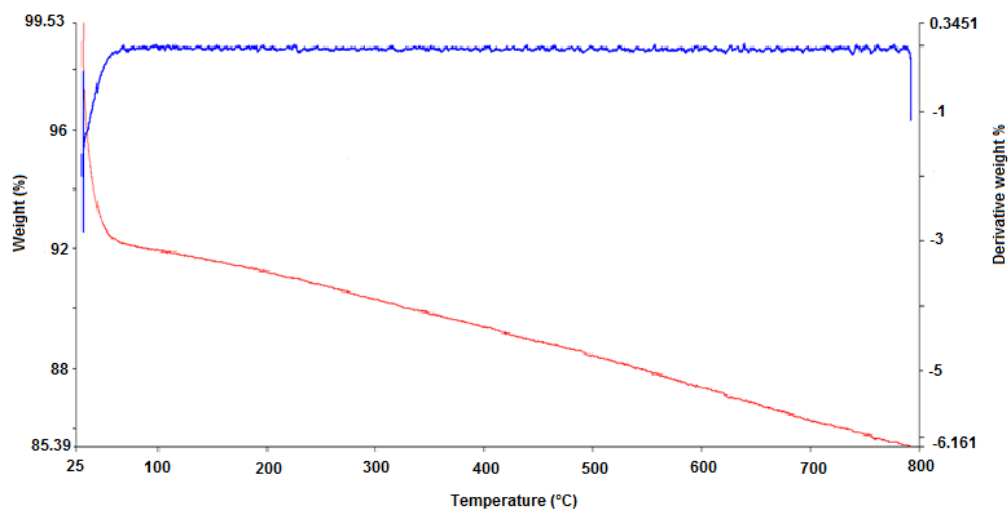


Figure 3.12. TGA trace of blank MSNs before oil loading. (Red line) Percentage mass loss plotted against increasing temperature °C, (Blue line) derivative of mass loss.

There were two separate instances of mass loss for the blank MSN samples used in this study. Mass loss from 0°C to 110°C was the loss of water absorbed by the mesopores. Mass loss in the temperature range 110°C - 900°C is associated with the structural decomposition of the silica nanoparticles. The percentage mass remaining at 900°C for the blank MSN sample which was used to determine the residue fraction, would be used to determine the loading levels of EO via evaporation and immersion using Equation 3.1 (Section 3.4.3). The residue fraction for sample 1 (Figure 3.12) was determined by dividing the % mass residue (85.39) by the % mass after water loss (92), providing a residue fraction of 0.928. The TGA traces for EO loaded samples treated with solvent evaporation are shown in (figures 3.13 – 3.15).

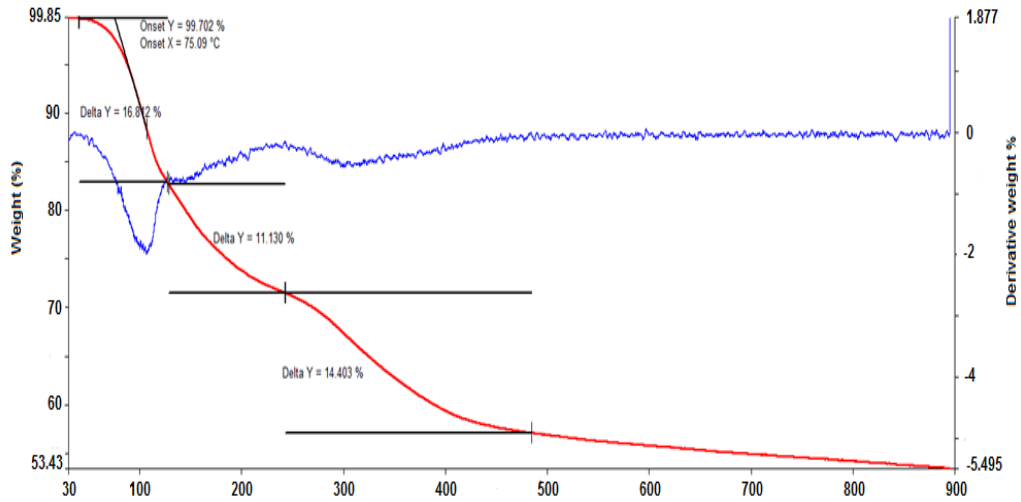


Figure 3.13. TGA of CLO-CIN loaded MSN sample after evaporation of MeOH. No subsequent solvent washing. (Red line) Percentage mass loss plotted against increasing temperature °C, (Blue line) derivative of mass loss.

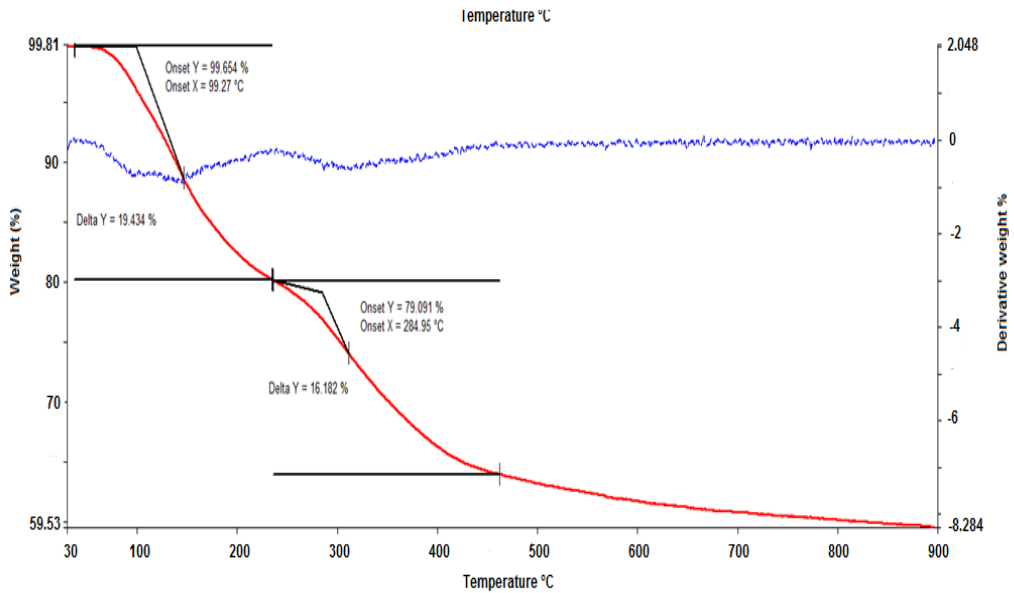


Figure 3.14. TGA of CLO-CIN loaded MSN sample after primary MeOH washing and evaporation. (Red line) Percentage mass loss plotted against increasing temperature °C, (Blue line) derivative of mass loss.

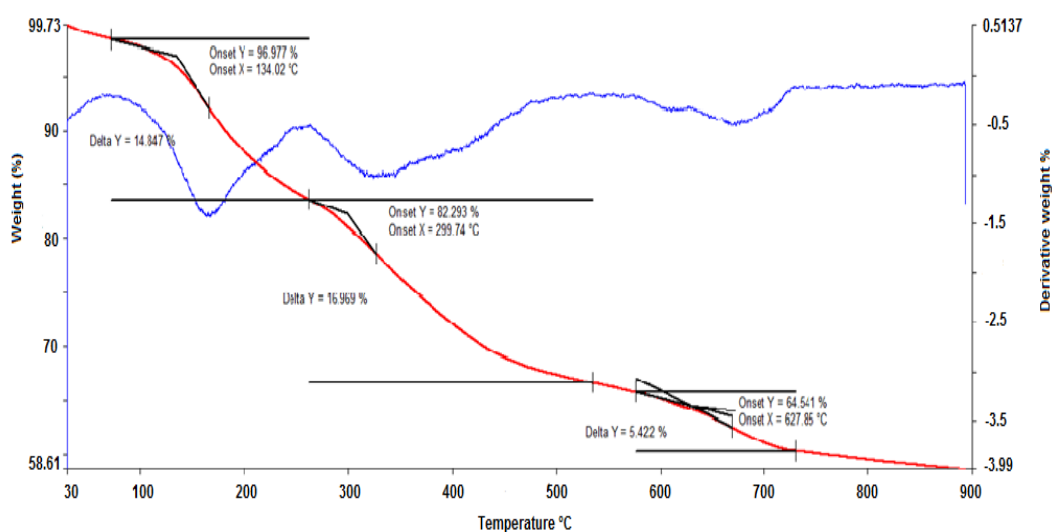


Figure 3.15. TGA of CLO-CIN loaded MSN sample after second round of washing with MeOH. (Red line) Percentage mass loss plotted against increasing temperature °C, (Blue line) derivative of mass loss.

It is significant that the MeOH did not actually wash any EO from the samples and may reflect the strength of the EO – MSN interactions relative to MeOH – MSN interaction. The % loading levels for the EO evaporation and subsequent solvent washing are shown in (Table 3.3)

Table 3.3. Loading levels for EO evaporation and subsequent solvent washing (methanol)

Experimental condition	% EO load
EO evaporation	33.64
1 <sup>st</sup> solvent wash	35.40
2 <sup>nd</sup> solvent wash	38.19

It was decided the solvent evaporation method for EO loading was not providing a high enough oil loading percentage and therefore anticipated EO concentration available at the textile surface, to justify further experimental investigation in this study. An alternative method for loading the EO into the MSNs was sought, Lu showed the potential for MSNs as a viable carrier for hydrophobic anti-cancer drugs (camptothecin) that are similar to essential oils, as camptothecin is isolated from the bark and stem of the *Camptotheca acuminata* tree. Both camptothecin and EO molecules are hydrophobic and contain hydrocarbon structures (Lu *et al* 2007). Using this method, blank MSNs were immersed in essential oils, with agitation and stirring, before draining excess essential oil and lightly washing the sample with MeOH and allowing to dry before use. The TGA traces for the five MSN samples are presented in (figures 3.16 – 3.20).

### 3.5.3.2 EO immersion loading

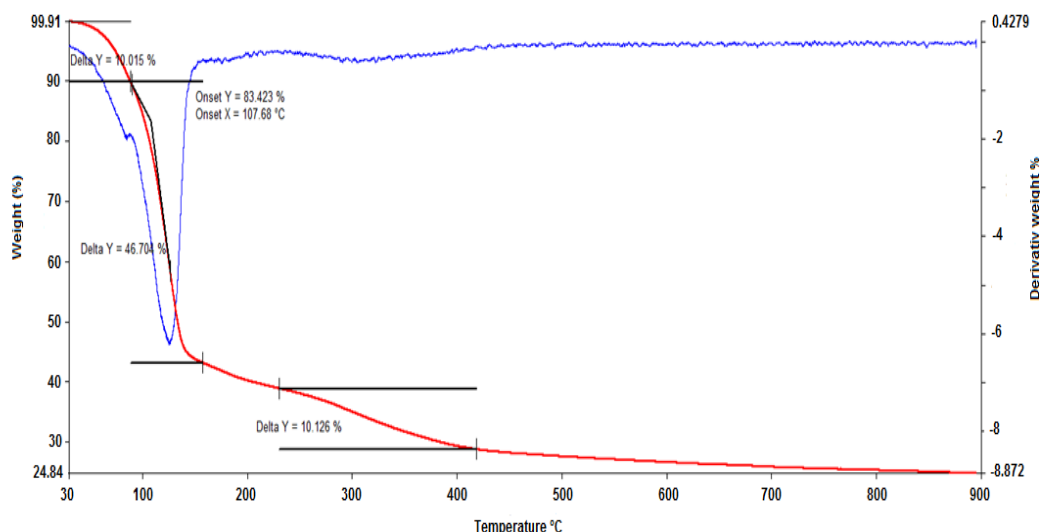


Figure 3.16. Sample 1 TGA trace of EO loaded MSNs. (Red line) Percentage mass loss plotted against increasing temperature °C, (blue line) derivative of mass loss.

There were three instances of mass loss from the EO loaded MSN sample during the TGA heating process. For mass loss occurring up to 110°C, as with the blank MSN samples, this was loss of molecular water. The mass remaining at this point was the mass post free water loss used in Equation 3.1.

The second mass loss occurred between 110°C and 254°C, the boiling point for eugenol which constitutes >90% of the CIN-CLO blend used. The rate of % mass loss between 110°C - 160°C was greater than % mass loss between 160°C - 254°C, this could be explained by the relative strength of interaction of the EO molecules with the MSN surface.

The final mass loss occurred between 254°C - 900°C and was attributable to the loss of structural water in the silica nanoparticles. The mass remaining at the end of the TGA heating program is taken as the mass after volatile loss used in (Equation 3.1).

The TGA traces for EO loading via solvent evaporation (Section 3.5.3.1) and EO immersion, display the same mass loss events over the three temperature ranges described above.

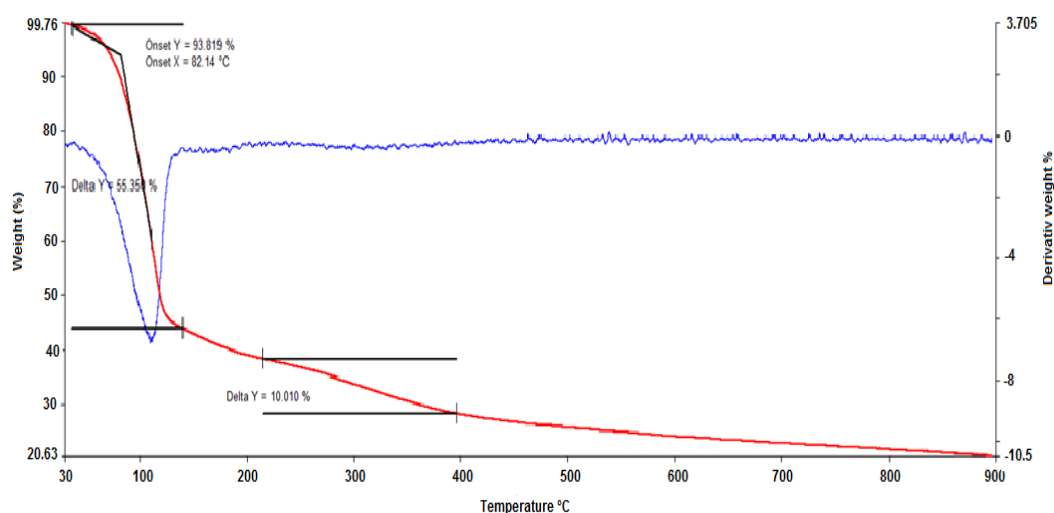


Figure 3.17. Sample 2 TGA trace of EO loaded MSNs. (Red line) Percentage mass loss plotted against increasing temperature °C, (blue line) derivative of mass loss.

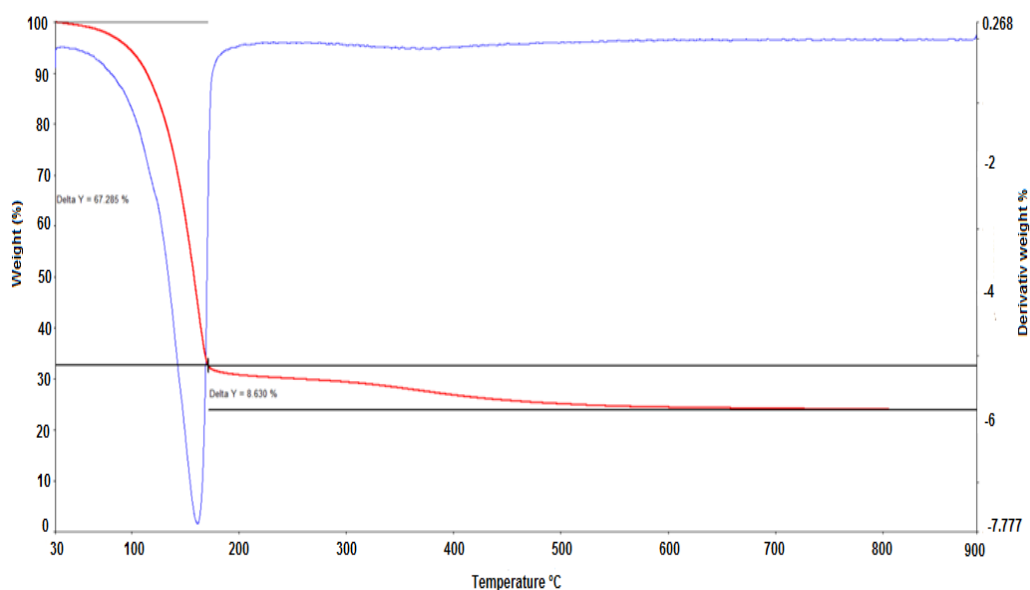


Figure 3.18. Sample 3 TGA trace of EO loaded MSNs. (Red line) Percentage mass loss plotted against increasing temperature °C, (blue line) derivative of mass loss.

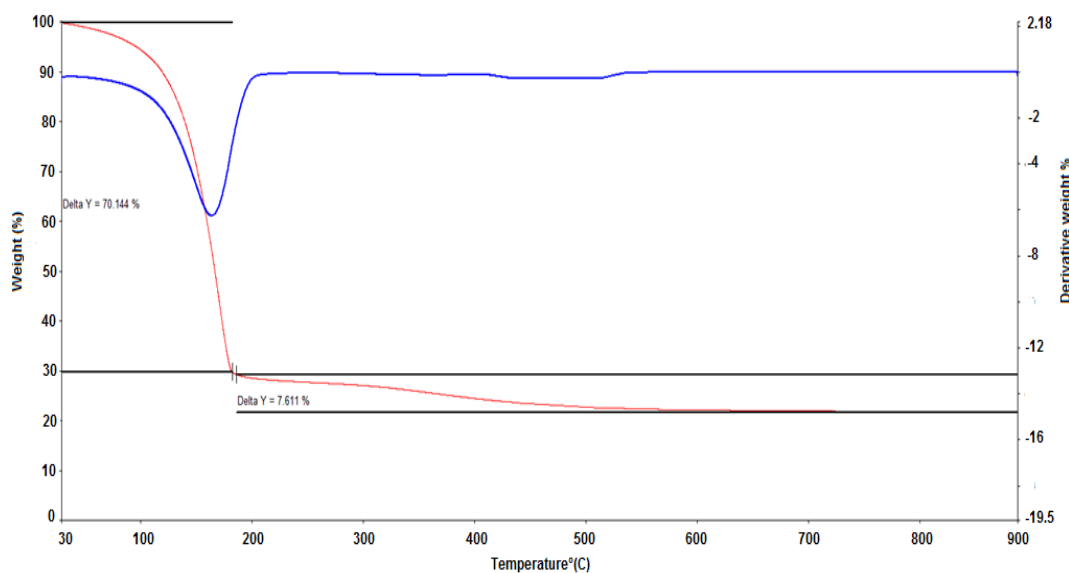


Figure 3.19. Sample 4 TGA trace of EO loaded MSNs. (Red line) Percentage mass loss plotted against increasing temperature °C, (blue line) derivative of mass loss.

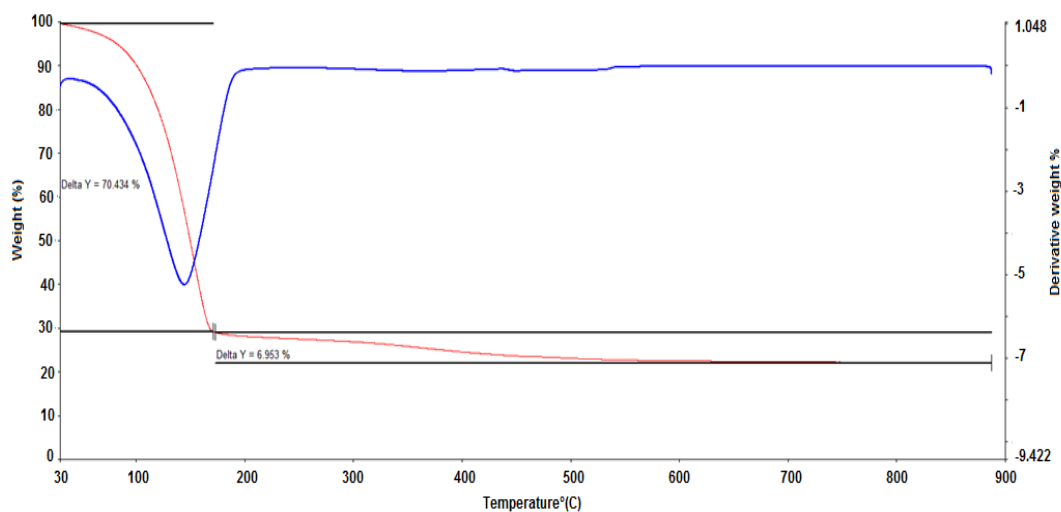


Figure 3.20. Sample 5 TGA trace of EO loaded MSNs. (Red line) Percentage mass loss plotted against increasing temperature °C, (blue line) derivative of mass loss.

TGA was used to determine the level of oil present in the mesopores of the nanoparticles. Fernandes *et al* have shown in some cases, the relative levels of weakly bound and strongly bound surfactants can be highlighted via the use of mass loss data (Fernandes *et al* 2015). The strongly bound surfactant is attributed to the EO molecules bound to the substrate via hydrogen bonding, dipole-dipole interactions and possibly pi-electron interactions, whereas the weakly bound surfactant is attributed to bonding to other surfactant molecules. It follows, that strongly bound oil molecules will release from the sample at a higher temperature than the weakly bound. The blank MSN RFs and their respective loading levels are presented in (Table 3.4). It is interesting to consider theoretical monolayer coverage of the main EO blend constituent (eugenol) on the MSNs. The area of a molecules footprint on a substrate can be used to calculate the theoretical number of molecules adsorbing onto a given substrate surface area (Liauw *et al* 1995). The area of the footprint for a eugenol molecule

in the anticipated orientations for adsorption were calculated (0.42 and 1.11 nm<sup>2</sup> for vertical and flat adsorption, respectively) using a rectangle enclosing the molecule and is shown in (Figure 3.21). In the proposed vertical adsorption orientation of eugenol, there would be interaction between the phenolic OH group and possibly the ether oxygen with the MSN surfaces. In the flat adsorption orientation of eugenol, there would be interaction between the  $\pi$  electron cloud of the phenyl ring, the phenolic OH group and the  $\pi$  electrons of the double bond, with the MSN surfaces. The eugenol molecules would project 0.927 nm into the mesopores in the vertical adsorption mode, as shown in (Section 3.5.2). Assuming adsorption is radial in the pores, the tails of the molecules would not collide, considering the mesopores for MSN samples 1,2,3 and 5 were measured to be 2.1 – 2.2 nm in diameter. The mesopores for sample 4 were measured to be 1.8 nm, leading to possible altered adsorption orientation or packing of coverage in the pores.

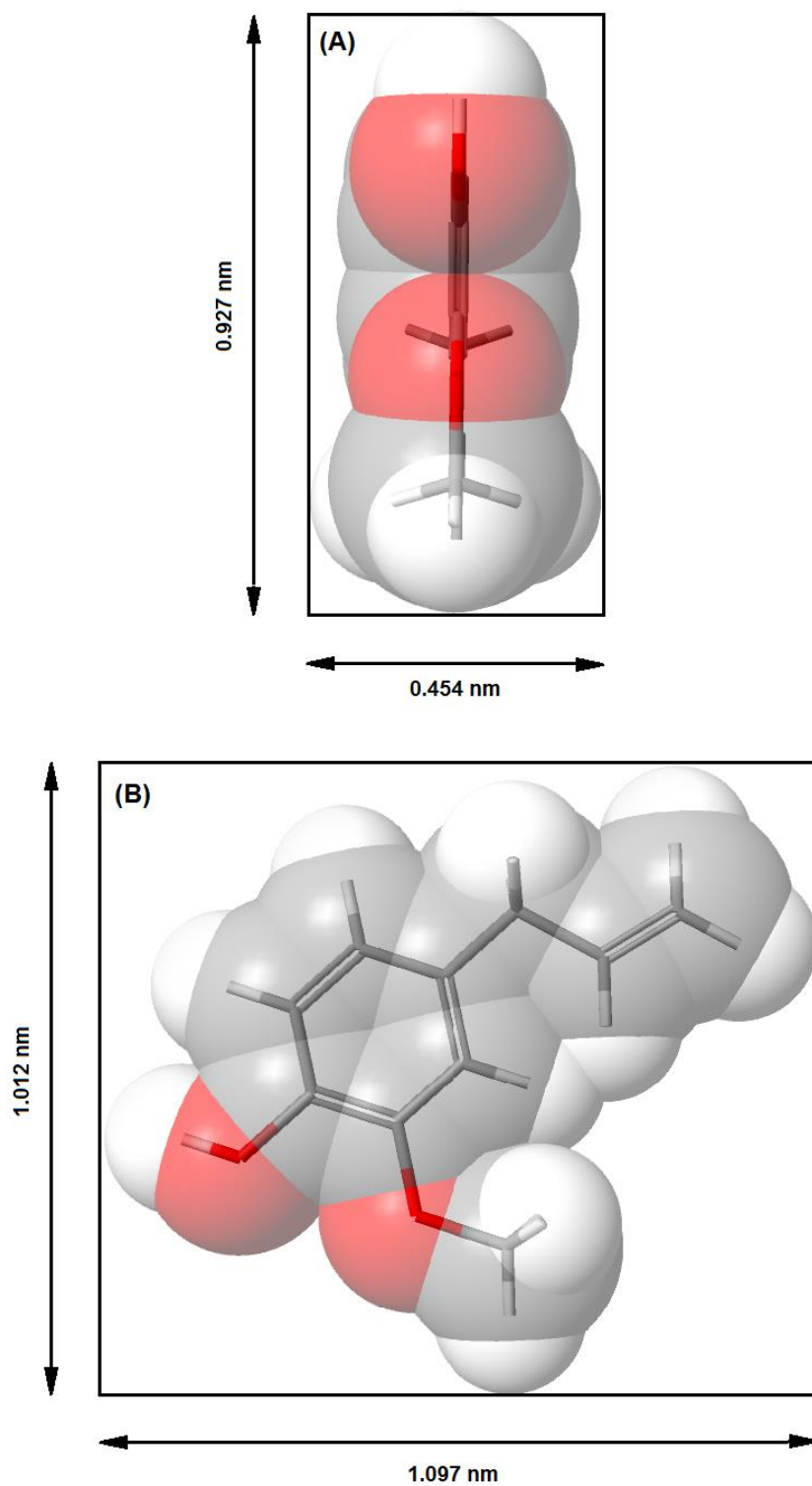


Figure 3.21. A eugenol molecule modelled using Scigress software, in the two possible orientations of adsorption, (A) vertically and (B) flat.

The theoretical monolayer coverage in the vertical adsorption orientation was calculated using equation 3.2 as follows:

Equation 3.2. Theoretical monolayer coverage for eugenol on MSN surfactant in proposed orientations of adsorption.

$$\begin{aligned} \text{Theoretical number of molecules adsorbing per gram of MSN} &= \frac{980 \text{ (m}^2\text{g}^{-1}\text{)}}{4.208 \times 10^{-19} \text{ (m}^2\text{)}} \\ &= 2.329 \times 10^{21} \text{ molecules} \end{aligned}$$

Theoretical number of moles of molecules adsorbing per gram of MSN

$$\begin{aligned} &= \frac{2.329 \times 10^{21}}{6.022 \times 10^{23}} \\ &= 3.867 \times 10^{-3} \text{ moles} \end{aligned}$$

As

$$\text{Number of moles} = \frac{\text{mass}}{\text{relative molar mass}}$$

$$\begin{aligned} \text{The theoretical mass of Eugenol adsorbed per gram of MSN} &= \text{molar mass of} \\ \text{eugenol} \times \text{the number of moles estimated to adsorb} &= 164.2 \times (3.867 \times 10^{-3}) \\ &= 0.635 \text{ g} \end{aligned}$$

Therefore the theoretical adsorption level for Eugenol on MSN is 635 mg g<sup>-1</sup>. Or about 63.5 wt.%, based on initial mass of MSN.

The theoretical monolayer coverage in the flat adsorption orientation was calculated as follows:

$$\begin{aligned} \text{Theoretical number of molecules adsorbing per gram of MSN} &= \frac{980 \text{ (m}^2\text{g}^{-1}\text{)}}{1.110 \times 10^{-18} \text{ (m}^2\text{)}} \\ &= 8.828 \times 10^{20} \text{ molecules} \end{aligned}$$

Theoretical number of moles of molecules adsorbing per gram of MSN

$$\begin{aligned} &= \frac{8.828 \times 10^{20}}{6.022 \times 10^{23}} \\ &= 1.466 \times 10^{-3} \text{ moles} \end{aligned}$$

As

$$\text{Number of moles} = \frac{\text{mass}}{\text{relative molar mass}}$$

$$\begin{aligned} \text{The theoretical mass of Eugenol adsorbed per gram of MSN} &= \text{molar mass of} \\ \text{eugenol} \times \text{the number of moles estimated to adsorb} &= 164.2 \times (1.466 \times 10^{-3}) \\ &= 0.241 \text{ g} \end{aligned}$$

Therefore the theoretical flat adsorption level for Eugenol on MSN is 241 mg g<sup>-1</sup>.

Or about 24.1 wt.%, based on initial mass of MSN.

Theoretical monolayer coverage was estimated to be 635 mg/ 1 g MSN and 241 mg/ 1 g MSN for vertical and flat adsorption, respectively. The two projected areas indicate the upper bound and lower bound estimates for the theoretical monolayer level of loading. The results were based on a MSN surface area of 980 m<sup>2</sup>/g<sup>-1</sup> (sample 1), and the assumptions that the EO blend reaches all parts of the MSN and all surfaces of the MSN sample have equal reactivity. Considering the tacky nature of the EO evaporation and EO immersion samples that were analysed for EO loading level, it can be speculated that some of the EO molecules had adsorbed on the external surfaces of the MSNs. It follows that the loading levels obtained did not represent true monolayer coverage, borne out by the theoretical monolayer calculations. It is interesting that the theoretical loading level for flat adsorption is close to the EO loading level result for EO evaporation and the theoretical loading level for vertical adsorption is close to the EO loading level result for EO immersion (Table 3.4). It was

speculated from this, at lower EO loading levels (solvent evaporation), the flat orientation for adsorption was favoured. While at higher EO loading levels (EO immersion) there could be some vertically adsorbed eugenol molecules on the external surfaces of the MSNs, with the remainder adsorbed on top of this (Figure 3.22).

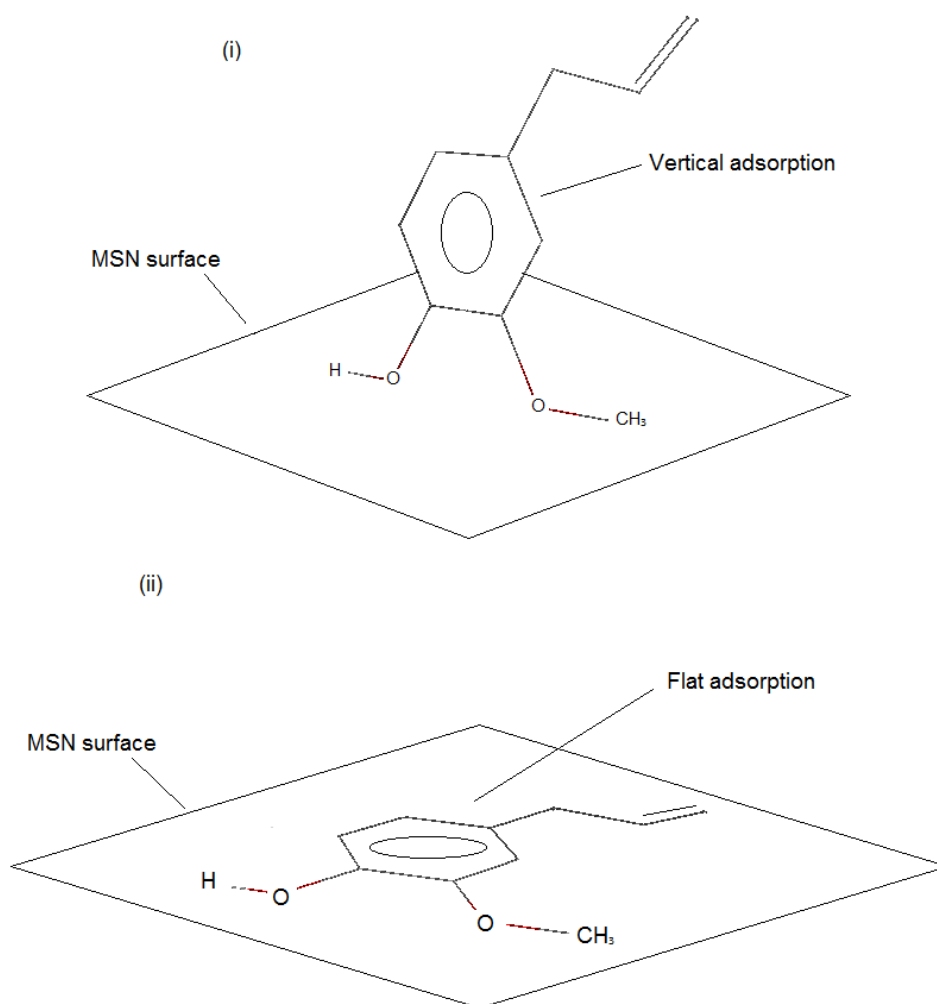


Figure 3.22. The anticipated orientations of attachment to the MSN surface for eugenol. (i) Vertical, dual-point attached, (ii) flat, multi-point attached.

Table 3. 4. Residue fractions of blank MSN samples and % EO load via immersion and shaking for samples 1-5.

MSN sample	Blank MSN Rf	% EO load	Surface area (m <sup>2</sup> /g <sup>-1</sup> )	Pore size (nm)
1	0.97	71.24	980 ± 77	2.2
2	0.819	66.89	1161 ± 76.	2.2
3	0.928	73.38	894 ± 44	2.2
4	0.893	74.4	759 ± 19	1.8
5	0.904	72.65	654 ± 12	2.1

### 3.5.3.3 EO release from loaded MSNs

MSN sample 1 (0.5g) was loaded with CIN:CLO EO blend using the immersion method described in (Section 3.4.3). The sample was washed with 3 x 10 mL MeOH using a Buchner filtration setup. The aliquots taken after each wash were analysed using GCMS to ensure the antimicrobial constituents were able to release from the mesopores (Figure 3.23).

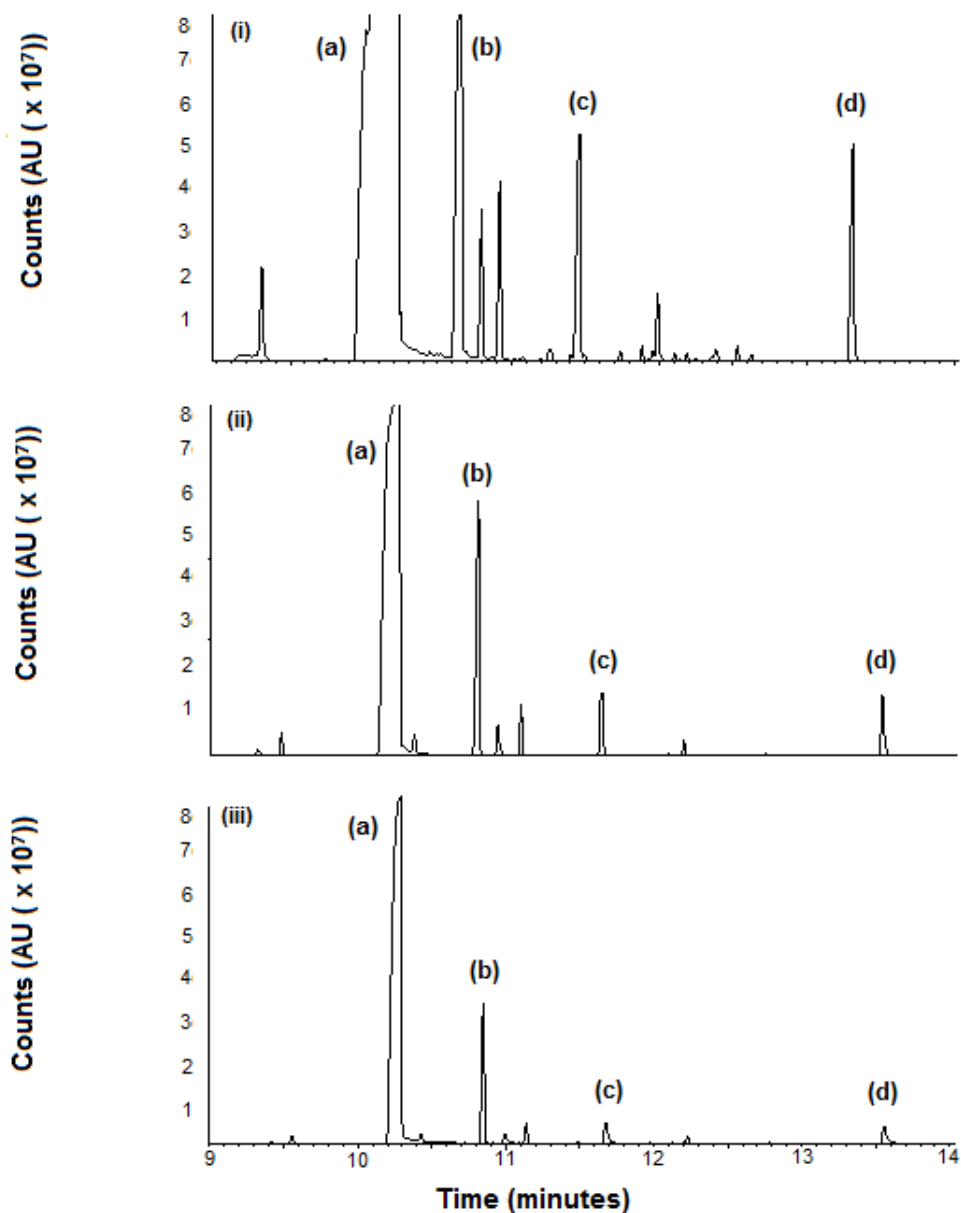


Figure 3.23. Chromatographs of MeOH Extract from three EO loaded MSN samples after increasing solvent washing with MeOH. (i) After 10 mL, (ii) 20 mL and (iii) 30 mL of washing with MeOH. Peaks assigned as follows: (a) eugenol (b) beta caryophyllene (c) eugenyl acetate (d) benzyl benzoate. Eugenol peak max height (i)  $1.1 \times 10^8$ , (ii)  $9 \times 10^7$ , (iii)  $8 \times 10^7$ .

The data obtained from these experiments indicated that the mesoporous silica nanoparticles could be used as an encapsulant for the EOs. The MSN batches used in this study and for further experimentation displayed a high surface area,

with pores large enough in diameter to allow the antimicrobial constituents of the EOs to be accommodated. The TGA of EO loaded MSN samples displayed the loading level of oil in the mesopores relative to the residue fraction of the blank MSNs. Finally, GCMS analysis of solvent washed EO immersion loaded MSNs confirmed the ability of the EOs to leave the mesopores. Interestingly, with each round of solvent washing of the EO evaporation method, sample 1 recorded a slightly increased level of EO composition when TGA was conducted (33.64, 35.40 and 38.19%, respectively). This is in contrast to the EO release observed with solvent washing of the EO immersed sample (originally 70.28% EO load) via GCMS analysis. It is possible at higher loading levels in the MSN pores, some EO molecules are not interacting with the MSN surface and are therefore more easily washed from the MSN sample.

#### 3.5.4 Antimicrobial testing of blank and EO loaded MSNs

##### 3.5.4.1 Blank MSNs growth inhibition assay

The following graph (Figure 3.24) shows the effect of the blank MSNs at varying concentrations on the growth of the five test microorganisms after 24 hour exposure.

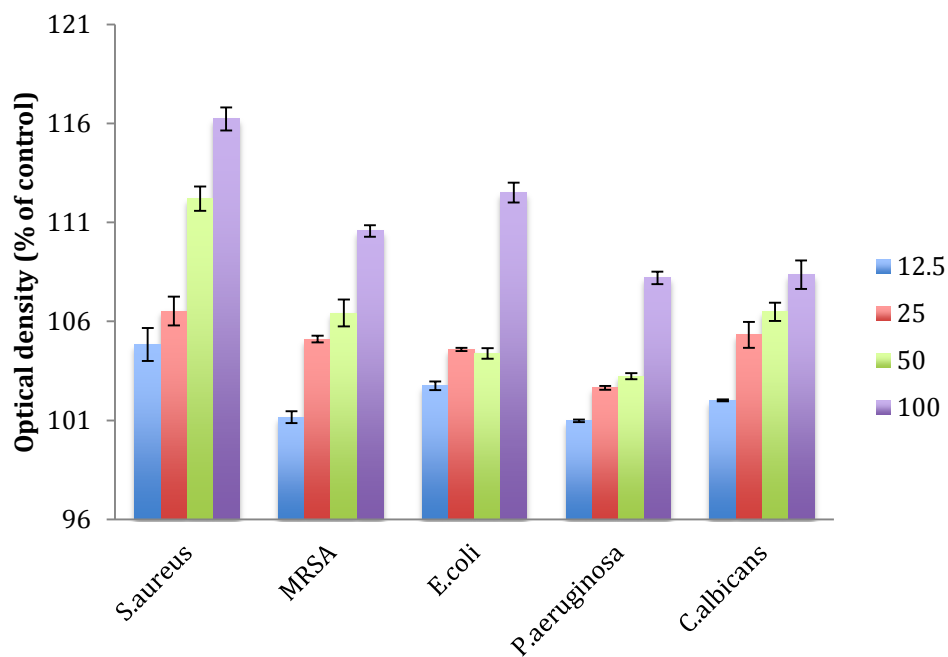


Figure 3.24. The capacity of blank MSNs at 12.5, 25, 50 and 100 mg/mL to prevent growth of five test microorganisms over a 24 hour period based on optical density readings. Results are expressed as a percentage of 'time 0' OD values. Standard deviation bars are displayed (n=3).

The optical density of the negative control (nanoparticle free ISB) did not vary throughout the experiment, whereas it increased in the positive growth control bottles (not included in figure 3.24). Also, the blank (uninoculated) MSN suspensions were shown to be uncontaminated as no colonies grew on the ISA plates inoculated with 10  $\mu$ L of each after overnight incubation at 37°C.

At all four concentrations of blank MSN suspensions, there was no inhibition of microbial growth, relative to the OD values recorded at the beginning of the experiment for each test bottle. However, the increasing OD shown with increasing blank MSN concentration could be due, partly to turbidity of the suspension due to the light scattering effect of aggregated MSNs. As a result, 10  $\mu$ L of each test sample was plated on ISA and incubated overnight at 37°C to check for growth. All samples returned growth, therefore it can be said the blank MSNs do not exert an antimicrobial effect on the test microorganisms. Any

antimicrobial effect shown by EO loaded MSNs can be considered solely to be the action of the oils.

#### 3.5.4.2 Bactericidal activity of EO loaded MSNs

Table 3.5 shows the minimum EO loaded MSN concentration necessary to cause cell death, which was verified by the absence of growth on agar plate after overnight incubation at different nanoparticle concentrations (12.5, 25, 50 and 100 mg/mL).

Table 3.5. Bactericidal activity of EO loaded MSNs at four concentrations. 'G' represents the occurrence of growth, 'NG' represents the occurrence of no growth (n=3).

MSN conc (mg/mL)	S.aureus	E.coli	C.albicans	MRSA	P.aeruginosa
100	NG	NG	NG	NG	NG
50	NG	NG	NG	NG	NG
25	NG	NG	G	NG	G
12.5	G	G	G	G	G

All positive control bottles produced growth, while the negative controls free of MSNs and microorganisms produced no growth when plated. At 12.5 mg/mL all five test microorganisms produced growth when plated, while at 25 mg/mL the microorganisms previously shown to be less robust (*S.aureus*, *E.coli*, and *MRSA*) did not grow. Above this concentration, at 50 and 100 mg/mL there was no growth, demonstrating bactericidal capacity at these concentrations. In such cases, a bactericidal value can be assigned, shown in (table 3.6).

Table 3.6. The bactericidal concentrations (mg/mL) for each test microorganism.

Microorganism	EO loaded MSN concentration (mg/mL)
<i>S.aureus</i>	25
<i>E.coli</i>	25
<i>C.albicans</i>	50
<i>MRSA</i>	25
<i>P.aeruginosa</i>	50

The determination of bactericidal concentrations of the EO loaded MSNs was important as a lower nanoparticle concentration implies reduced cost, and a minimisation of potential irritation to the epidermis if the final product is to be worn or come into contact with the skin. The antimicrobial capacity of nanoparticles is concentration-dependent; i.e. the higher the nanoparticle concentration, the greater the volume of EO blend available, the greater the bactericidal activity. The antimicrobial activity of nanoparticles is also dependent on initial bacterial concentration (Sondi and Salopek-Sondi 2004, Pal *et al* 2007, Nair *et al* 2009).

#### 3.5.4.3 Time-kill assays

The five test microorganisms were tested against EO loaded MSNs at the given bactericidal concentrations for each microbe (Section 3.5.4.2). The microorganisms were prepared in both stationary and exponential growth phases (Section 3.4.9). The following Figures (3.25 – 3.29) display the CFU/mL decrease over time when treated with 2% CIN:CLO 1:1 blend, EO loaded MSNs at the determined bactericidal concentrations for each microorganism.

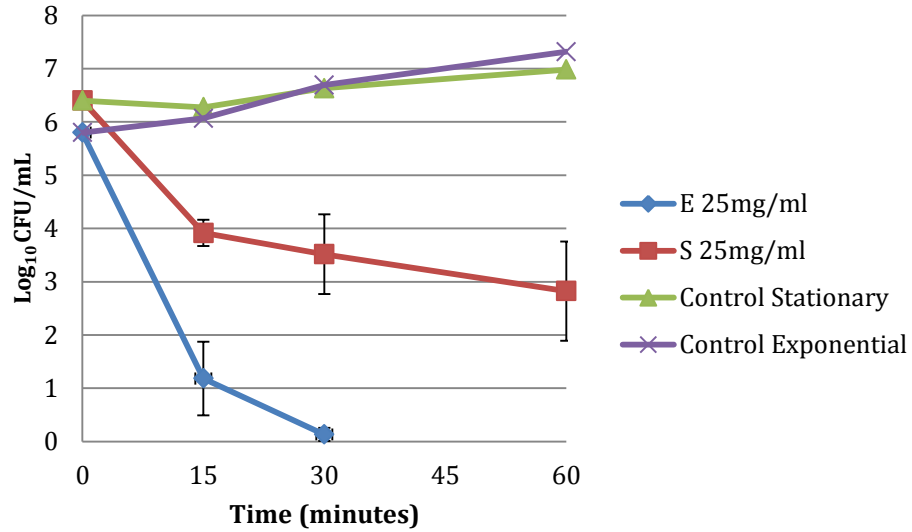


Figure 3.25. CFU/mL versus time plots for *S.aureus* in the static (S) and exponential growth (E) phases, both with and without 25 mg/mL of EO loaded MSNs. Standard deviation bars are shown (n=3).

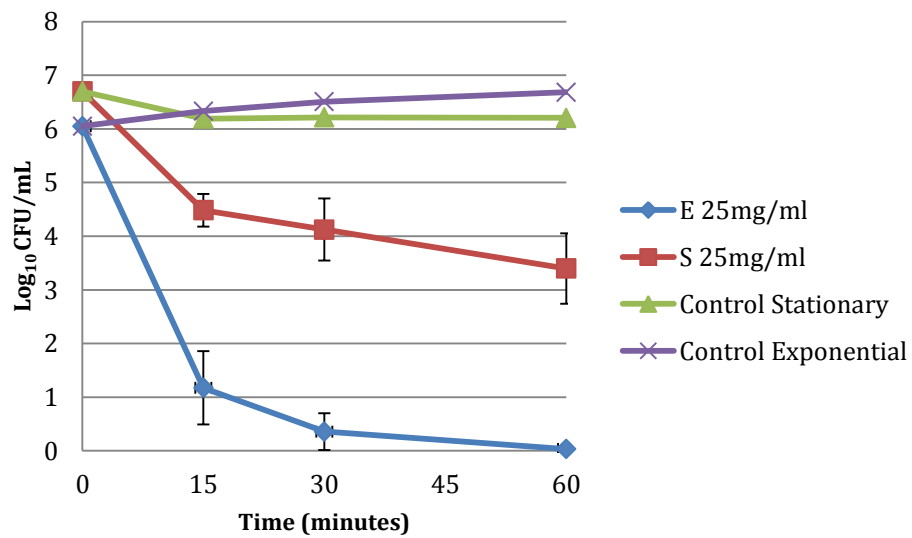


Figure 3.26. CFU/mL versus time plots for *E.coli* in the static (S) and exponential growth (E) phases, both with and without 25 mg/mL of EO loaded MSNs. Standard deviation bars are shown (n=3).

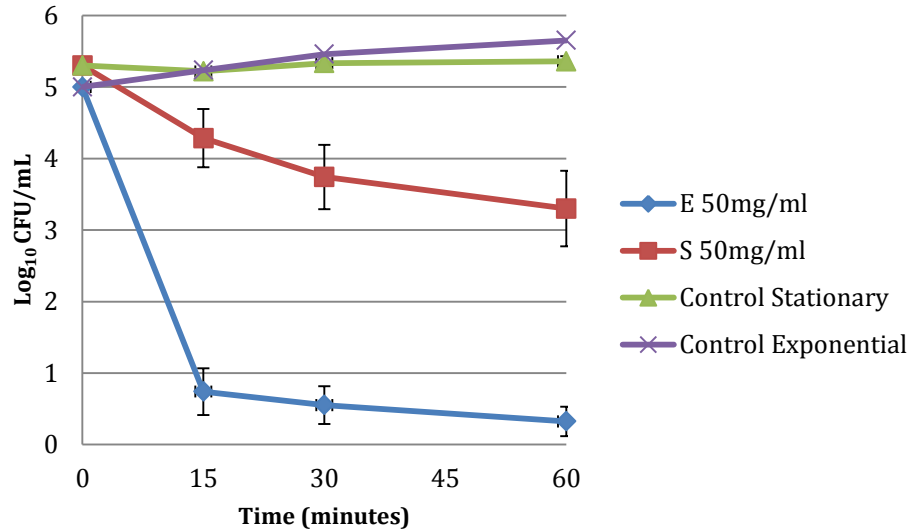


Figure 3.27. CFU/mL versus time plots for *C.albicans* in the static (S) and exponential growth (E) phases, both with and without 50 mg/mL of EO loaded MSNs. Standard deviation bars are shown (n=3).

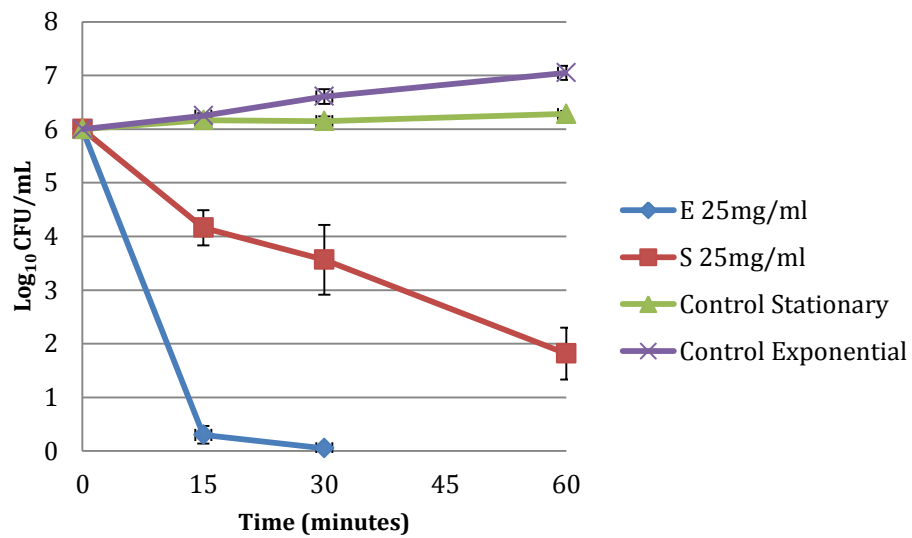


Figure 3.28. CFU/mL versus time plots for *MRSA* in the static (S) and exponential growth (E) phases, both with and without 25 mg/mL of EO loaded MSNs. Standard deviation bars are shown (n=3).

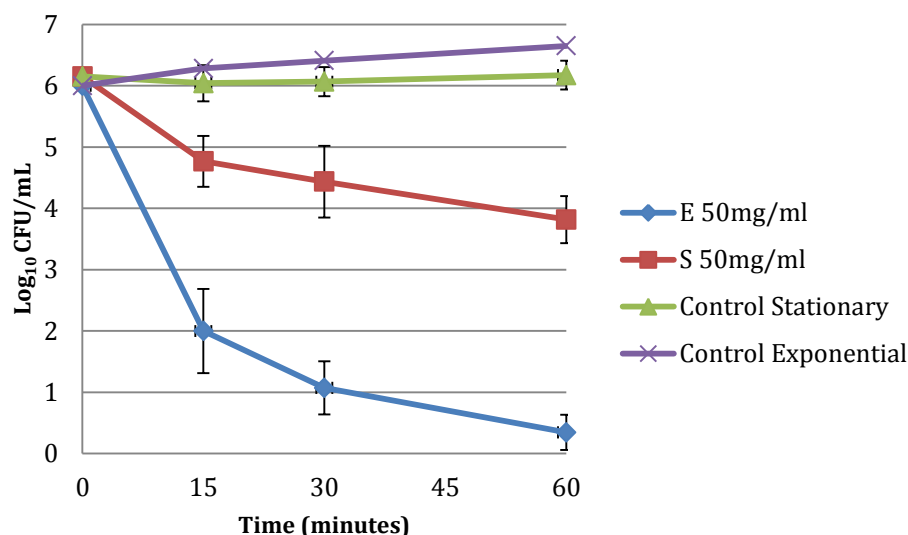


Figure 3. 29. CFU/mL versus time plots for *P.aeruginosa* in the static (S) and exponential growth (E) phases, both with and without 50 mg/mL of EO loaded MSNs. Standard deviation bars are shown (n=3).

At bactericidal concentrations determined using the method described in (Section 3.4.8), the time – kill graphs show the effect of EO loaded MSNs to be time dependent, with the highest rate of killing occurring during the first 15 minutes of exposure. As seen previously, the gram – positive bacteria are more susceptible to the antimicrobial action of the main constituent in the CIN: CLO 1:1 EO blend (eugenol). In addition, the gram – negative *P.aeruginosa* and the yeast *C.albicans* displayed a more robust response to the antimicrobial, with a slower rate of killing and still demonstrating viability after 60 minutes of exposure. From these results, it is clear the loading of EO into the mesopores of the nanoparticles does not attenuate the antimicrobial efficacy of the oil. These are interesting findings, as is the fact that the EO loaded into MSNs retain their potent antimicrobial capacity in a nutrient – rich environment. It is therefore reasonable to propose that this activity would not be hampered in an environment conducive to bacterial or fungal growth.

Interestingly, it has been reported that gram-negative species are more readily killed by the nanoparticles than the gram-positive, reinforcing the extended idea

that the thicker cell wall of this second group of bacteria provides a defence mechanism against silver nanoparticles that the gram-negative lack (Feng *et al* 2000). Although silver nanoparticles and silver ions are capable of entering bacterial cells, membranes are the first barrier with which interaction is established. Consequently, it is easy to hypothesise that the greater thickness of the cell wall in gram-positive bacteria constitutes a defence mechanism against silver nanoparticles (Kim *et al* 2007). This is in contrast to results published for the effect of essential oils on gram-positive and negative bacteria. Gram-negative bacteria are less susceptible to the action of essential oils, compared to Gram-positive bacteria. This is due to the presence of the outer membrane surrounding the cell wall, which restricts the diffusion of lipophilic compounds through the lipopolysaccharide covering (Mann *et al* 2000).

Despite the relatively slim chance of bacterial resistance developing to nanoparticles loaded with antimicrobials (particularly EO), the possibility should not be ignored, particularly if such approaches are to be widely and routinely used. However, it is widely known the natural variance in essential oil chemical composition (particularly an EO blend), even for the same type of oil batch to batch, is the reason bacteria, fungi and viruses cannot easily develop resistance to these natural plant derived antimicrobials (Becerril *et al* 2012). In addition, these complex mixtures display antimicrobial activity by more than one mechanism (Cox *et al* 2000). Treatments and medical equipment, such as wound dressings and urinary catheters impregnated with silver nanoparticles are already being used. In order to minimise the possibility of resistance developing, nanoparticles should be used only when necessary, and ensure a rapid killing of microorganisms. For example, Yamanaka *et al* (2005) challenged *E. coli* with 0.9 – 112 µg/mL silver ion solutions, and although a significant rate of killing was documented, it required over 14 hours. Due to the controlled release behaviour, this long length of time would only encourage resistance to develop, using a

single agent at possibly sub-lethal concentrations. Throughout the course of this investigation, the variation in methods used to assess the performance of nanoparticle based antimicrobials has hampered comparison of data from diverse studies. A standardised method for the latter is urgently needed if the data from research groups active in this field are to be meaningfully compared.

### 3.6 Conclusions

The conclusions are written below in the context of the initial objectives:

- Synthesis of nanoparticles.

Mesoporous silica nanoparticles of high surface area and largely mono-disperse size distribution, with uniformly dimensioned pores, were successfully synthesised, with five samples being used for further study.

- Characterisation of nanoparticles.

The size and characteristics of nanoparticles were successfully determined by the use of specialist analytical apparatus. Image J was used to confirm the MSN samples were roughly 100 nm in diameter, while nitrogen adsorption measurements confirmed the high surface area of the nanoparticles (654 – 1161 m<sup>2</sup>/g<sup>-1</sup>) and mesopore diameter (1.8 – 2.2 nm).

- Loading level and release rate of essential oil from nanoparticles.

TGA was used to determine the loading level of essential oil (66.89 – 74.40%) using the EO immersion method. While gas chromatography coupled with mass spectrometry was used to confirm the major antimicrobial molecules could release from the nanoparticle mesopores.

- To determine the antimicrobial activity of MSNs loaded with EO and whether blank MSNs exhibit any antimicrobial action.

The blank MSNs were shown to have no antimicrobial effect on the test microorganisms. Bactericidal concentrations of EO loaded MSNs for each test microorganism were determined (25 mg/mL for *S.aureus*, MRSA and *E.coli*, 50 mg/mL for *P.aeruginosa* and *C.albicans*). The dynamic killing profiles for these bactericidal values were investigated for all five test microorganisms (*S.aureus* and MRSA in exponential growth phase being killed in 30 minutes exposure).

## **Chapter 4**

### **Affixation of mesoporous silica nanoparticles to synthetic textiles**

## 4.1 Introduction

### 4.1.1 Organically modified silicates (Ormosils)

Ormosils have applications in coating, adsorption, separation media, sensors, drug-delivery supports, and oil-spill clean-up (Brinker and Scherer 1990). Another attractive property is that they are relatively easy to make and highly cost effective (Mackenzie and Bescher, 1998). It was speculated that an ormosil covering the synthetic fibres would provide a matrix conducive to the chemical affixation of the MSNs to the textiles.

Ormosils are produced via the sol-gel method and many different type of ormosils can be produced, ranging from tough and durable to rubbery and bendable films (Hench and West, 1990) (Bescher and Mackenzie, 2003) (McDonagh *et al*, 1998). The sol-gel process involves the evolution of inorganic networks through the formation of a colloidal suspension of solid species in a liquid sol, which is converted into a gel through polycondensation of the sol. A gel is an interconnected, rigid network with polymeric chains, whose average length is greater than a micrometre, and pore width of nanometer dimensions. Hydrogels are formed from aqueous solutions, whereas alcogels are formed from alcoholic solutions. The most widely used silanes are the alkoxysilanes, such as tetraethoxysilane (TEOS) and methyltriethoxysilane (MTEOS). The first step in the synthesis is hydrolysis of the precursor followed by condensation of the hydrolysed species. The hydrolysis reaction that initiates the process may be acid or base catalysed and the rate of hydrolysis is pH dependant (Curran and Stiegman 1999). Drying of the gel is also a critical step. During drying, shrinkage of the gel occurs due to capillary pressure. When the pore liquid is removed at or near ambient pressure by thermal evaporation and shrinkage occurs, the material is termed a xerogel. When the pore liquid is removed as a

gas phase from the interconnected solid gel network under supercritical conditions, the network does not collapse and a low density aerogel is produced. The type of silica produced is solely dependent on the composition (i.e. structures (functionalities) of the components and the molar ratios) (Hench and West, 1990)(McDonagh *et al*, 1998). The structure and porous texture of xerogels synthesised using TEOS as a precursor is dependent on synthesis conditions, namely, pH, temperature, and the precursor:solvent:water molar ratio (Echeverria *et al* 2010, Estella *et al* 2007, Musgo *et al* 2009). The amount of porosity and the size distribution of the latter is also affected by ageing and drying conditions (Estella *et al* 2007). Many studies on the production of ormosils with a wide range of targeted properties have been carried out. These mainly involve mixing the TEOS with other silane precursors such as MTEOS and ethyltriethoxysilane (ETEOS) at different ratios with the addition of water and hydrochloric acid to adjust the pH (McDonagh *et al*, 1998) (Wencel *et al*, 2007).

#### 4.1.2 Silane coupling linkers

Organo-functional silanes such as 3-(trimethoxysilyl)propylmethacrylate ( $\gamma$ -MPS) (Figure 4.1) are widely used for grafting into ormosil structures as they contain silicon-alkoxy functionality and a double-bond end-group (Pardal *et al* 2009). The latter will interact with a variety of addition polymerisation systems (including free radical), thereby producing strong interaction between the ormosil particles and an addition polymerised matrix. For this study, it was hoped a silane could be used to allow the MSNs to be chemically bound to the ormosil matrix covering the synthetic fibers

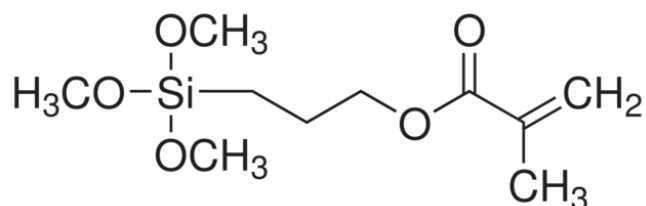


Figure 4.1. The silane coupling linker trimethoxysilylpropylmethacrylate ( $\gamma$ -MPS), contains an acrylic carbon-carbon double bond (C=C) and methoxysilane groups (SiOCH<sub>3</sub>).

Silica-polymer nanocomposites are a promising new class of materials that have many possible applications in aerospace materials, structural materials electronics, sensors, and other areas (Xiangling *et al* 2003). Three main synthetic routes have been developed for the production of such nanocomposites. The first approach involves mixing polymers with silica particles or silica precursors directly. For example, composites containing silica nano-particles that are produced in-situ. Such composites are often based on poly(methylmethacrylate), poly(ethyleneglycol), and polyurethane and have been prepared by mixing these polymers with silica precursors, such as tetraalkoxysilanes that hydrolyse and condense to form silica within the polymer matrix (Petrovic *et al* 2000). The second synthesis approach usually involves direct mixing of the polymer monomers with silica particles followed by polymerisation of the monomers (Lu and Huang 2002). For example, silica colloids in solution have been mixed with organic monomers such as styrene, methylmethacrylate, ethylacrylate, and 2-hydroxyethylmethacrylate. Subsequent polymerisation of these monomers led to the formation of silica nanocomposites. The third synthesis approach involves mixing both silica precursors, such as TEOS and MTEOS with addition polymerisable monomers, followed by simultaneous polymerisation of the precursors and monomers (Hajji *et al* 1999).

### 4.1.3 Gas chromatography

*Vide supra* Section 2.1.7

### 4.1.4 Attenuated total reflectance Fourier transform infrared spectroscopy (ATR FTIR)

Once an affixation technique was chosen, it was hoped the different chemical environments of the affixation technique could be analysed and profiled using ATR FTIR. In ATR sampling the IR beam is directed into a crystal of relatively higher refractive index. ATR FTIR speeds up the analysis of samples, as little preparation is needed. The IR beam reflects from the internal surface of the crystal, with a single bounce and creates an evanescent wave, which projects orthogonally into the sample in intimate contact with the ATR crystal (Figure 4.2). Some of the energy of the evanescent wave is absorbed by the sample and the reflected radiation (some now absorbed by the sample) is returned to the detector. As the infrared (IR) beam reaches the detector it is analysed by the Fourier transform mathematical operation, producing a spectrum of the wavelengths absorbed.

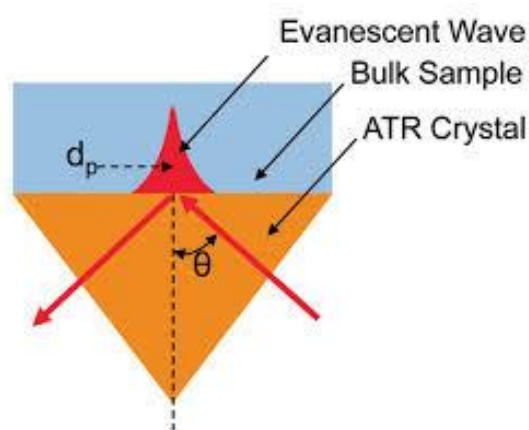


Figure 4.2. The internal instrument setup for single reflection ATR FTIR analysis.

The wavelength of IR absorption is unique to the vibration frequency of a specific chemical group, therefore the FTIR spectrum can be used to determine the chemical make-up of a sample. As a result, FTIR can be used to analyse the interactions between molecules and substrates (Estella *et al* 2007). Furthermore, FTIR can be used to record shifts in peaks due to changes in the chemical environment of a sample. Such peak shifts could potentially be used to monitor the layer-by-layer treatment of textiles (Table 4.1).

Table 4.1. FTIR adsorption frequencies of note for the organo-silicon species used in this study (Estella *et al* 2007, Pardal *et al* 2009).

Wavenumber $\text{cm}^{-1}$	Bond
1100 – 900	Si-O-Si stretch
1760 – 1665	C=O stretch
2900	C-H stretch

#### 4.1.5 Scanning electron microscopy

*Vide supra* Section 3.1.3.1

## 4.2 Objectives

- To investigate the use of organically modified silicates (ormosils) and silane coupling linkers to provide thin film coating of synthetic fibres and thence chemical affixation of MSNs.
- To determine conditions that achieve optimal coverage of synthetic fibres with MSNs.
- To analyse the release of EO from MSNs attached to synthetic fibres.
- To profile synthetic textile coupons in order to identify any chemical / chemical environment changes occurring at each stage of treatment using FTIR.

## 4.3 Materials

### 4.3.1 Chemicals

Tetraethoxysilane (TEOS) 99%, Methyltriethoxysilane (MTEOS) 90% and 3-(Trimethoxysilyl)propyl methacrylate ( $\gamma$ -MPS) 98% were purchased from Sigma Aldrich (UK). Hydrochloric acid (HCl) was used in the synthesis of organically modified silicates (Fisher-Scientific UK). Purified water from a Millipore Elix<sup>®</sup> 5 bench-top treatment unit was used throughout the study. The water treatment system was maintained according to manufacturer guidelines.

#### 4.3.2 Solvents

MeOH, toluene and acetone were purchased from Fisher-Scientific (UK). Hexane was used for all GC-MS analyses of EO release from the treated textile coupons and was purchased from Sigma Aldrich (UK).

#### 4.3.3 Media, microbes and EOs

*Vide supra* Section 2.3.1.1 – 3, all five test microorganisms were used, along with cinnamon and clove essential oils, in a 1:1 blend.

### 4.4 Experimental

#### 4.4.1 Ormosil synthesis and textile stiffness

The required amounts of precursors (TEOS and MTEOS), reactant volumes are summarised in (Table 4.2), and MeOH (25 mL) were mixed in a glass beaker (250 mL) using a magnetic stirrer. Whilst stirring, distilled water (5 mL) was added drop-wise, and the solution was adjusted to pH 2 by drop-wise addition of 0.1 M Hydrochloric acid (HCl). Once the desired pH was achieved, the solution was left to stir for 1 hour at ambient temperature. Finally, samples were decanted into 250 mL screw top glass bottles and placed in an oven at 70°C for 18 hours. Hydrolysis and condensation polymerisation forming the ormosil should occur over this time period.

Three synthetic textile coupons (65% polyester 35% cotton, supplied by Alexandra®) measuring 200 mm x 50 mm were immersed in each ormosil sol (42 mLs), containing different precursor ratios (presented in Table 4.2) and stirred continuously for 1 hour. The coupons were removed, flattened and left to

dry on a plastic tray at ambient temperature before further treatment. Once dry the fifteen coupons were tested for stiffness, relative to an untreated control. The method was based on the (BS 3356 Method for Determination of Bending Length and Flexural Rigidity of Fabrics, British Standards Institution, London, UK, 1990) (Perera *et al* 2013). A synthetic textile coupon was placed on the laboratory bench, with one (50mm) edge at the end of the bench. A ruler was placed over the sample and pushed forward until 10 cm of the sample was unsupported by the bench. The distance between the still horizontal ruler and the end of the sample was measured as the droop from horizontal. The average values of the droop from horizontal were recorded.

Table 4.2. Summary of the reactant volumes (mL) for ormosil synthesis at various precursor ratios.

MTEOS:TEOS	MTEOS	TEOS	pH	MeOH	H <sub>2</sub> O
Control (untreated textile)	0	0	0	0	0
1:1	6	6	2	25	5
2:1	8	4	2	25	5
3:1	9	3	2	25	5
1:2	4	8	2	25	5
1:3	3	9	2	25	5

#### 4.4.2 Affixation methods

##### 4.4.2.1 One pot synthesis

Ormosil gel was prepared using the method described in (Section 4.4.1), with a 3:1 MTEOS:TEOS precursor ratio. Three synthetic textile coupons (65% polyester 35% cotton, supplied by Alexandra®) measuring 20 mm x 20 mm were immersed in the ormosil sol (42 mLs) and stirred continuously for 1 hour. The coupons were removed, flattened and left to dry on a plastic tray at ambient temperature before further treatment.

The coupons were then immersed in a continuously stirred dispersion of blank MSNs (0.1 g) in MeOH (100 mL). The silane coupling agent,  $\gamma$ -MPS, (2 mL) was then added to the dispersion. The immersed coupons were left to stir for 1 hour, before removal and drying at ambient temperature. The treated textile coupons were washed three times by immersion in methanol with stirring for five minutes, to ensure the MSNs were tightly bound to the fibres and then allowed to dry for 1 hour before SEM analysis. Samples were cut into circles of 10 mm diameter to fit the SEM sample stubs, and fixed to the latter using 12 mm diameter conductive carbon loaded double-sided adhesive tabs (Agar Scientific). Finally, samples were gold sputtered in preparation for SEM analysis (as described in Section 3.1.3.1).

##### 4.4.2.2 Silane grafted MSNs

Instead of adding the reactants into one pot, this method was used to initially expose the MSNs to  $\gamma$ -MPS before the synthetic textile coupons. Initially, ormosil gel was prepared using the method described in Section 4.4.1, with 3:1 precursor ratio (MTEOS:TEOS). Three synthetic textile coupons (65% polyester

35% cotton supplied by Alexandra®) measuring 20 mm X 20 mm were immersed in the ormosil sol (42 mL) and stirred continuously for 1 hour. The coupons were left to dry on a plastic tray at ambient temperature before further treatment.

$\gamma$ -MPS (2 g) was added in excess to a suspension of silica (1.9 g), in toluene (48 g). The mixture was stirred at room temperature for 30 minutes. The mixture was then heated to 110°C for 24 hours, during which time the  $\gamma$ -MPS methoxysilane groups interact and bond with the free silanol groups on the MSNs surface, concluding the grafting of  $\gamma$ -MPS to the MSNs. Finally, the  $\gamma$ -MPS grafted silica nanoparticles were washed three times by centrifugation with acetone and dried under vacuum (Pardal *et al* 2009).

The ormosil treated coupons were then immersed in a continuously stirred dispersion of silane grafted MSNs (0.1 g) in of MeOH (100 mL). The immersed coupons were left to stir for 1 hour, before removal and drying at ambient temperature. The treated textile coupons were washed three times with methanol, to ensure the MSNs were tightly bound to the fibres and allowed to dry before SEM analysis. Samples were cut into circles (10 mm diameter) and fixed to SEM sample stubs using 12 mm diameter conductive carbon loaded double-sided adhesive tape (Agar Scientific). Finally, samples were gold sputtered in preparation for SEM analysis (as described in Section 3.1.3.1).

#### 4.4.2.3 Layer by layer treatment

Three synthetic textile coupons were treated sequentially with the ormosil gel,  $\gamma$ -MPS and finally the MSNs, in MeOH. This method attempted to isolate the individual stages of MSN affixation to the synthetic textile fibres and so create a layered structure. Initially, ormosil gel was prepared using the method described

in (Section 4.4.1), with 3:1 precursor ratio (MTEOS:TEOS). Three synthetic textile coupons (65% polyester 35% cotton supplied by Alexandra®) measuring 20 mm x 20 mm were immersed and stirred continuously for 1 hour. The coupons were left to dry on a plastic tray at ambient temperature before further treatment.

The Ormosil treated coupons were then immersed in a solution of  $\gamma$ -MPS (20 mL) and MeOH, while being stirred continuously for 1 hour. The silane treated coupons were then immersed in a continuously stirred dispersion of blank MSNs (1 g) in MeOH (100 mL) for 1 hour. Samples were then left to dry on a plastic tray at ambient temperature. The treated textile coupons were washed three times with immersion in methanol to ensure the MSNs were tightly bound to the fibres and allowed to dry before SEM analysis. Samples were cut into circles of 1 cm diameter and fixed to SEM sample stubs as previously described. Finally, samples were sputtered with gold in preparation for SEM analysis (see Section 3.1.3.1). A schematic representation of the anticipated structure produced by this method is shown in (Figure 4.3).

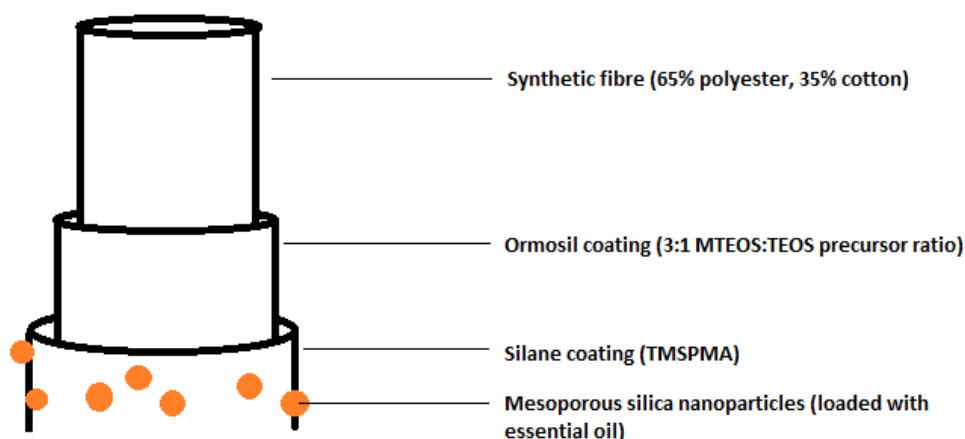


Figure 4.3. Schematic representation of the anticipated structure produced using the layer-by-layer method for chemically affixing MSNs to synthetic fibres.

#### 4.4.2.4 Analysis of optimal MSN coverage of synthetic fibres

Using the method described in (Section 4.4.2.3) to treat the textile coupons, nine textile samples were made to determine the effects of increasing concentration by weight of MSNs in suspension and increasing time of exposure on MSN coverage of the synthetic fibres. Briefly, coupons were stirred in MeOH (100 mL) dispersions with 0.1, 0.5 or 1 g of MSNs for 10 minutes, 1 hour or 18 hours (as summarised in Table 4.3).

Table 4.3. Summary of the amount of MSN and time of exposure textile samples encountered to determine optimal coverage of synthetic fibres.

Sample No.	MSN by weight (g)	Length of exposure (hours)
1	0.1	0.17
2	0.1	1.00
3	0.1	18.00
4	0.5	0.17
5	0.5	1.00
6	0.5	18.00
7	1	0.17
8	1	1.00
9	1	18.00

#### 4.4.3 EO release from loaded textiles

EO loaded (CIN:CLO 1:1) MSN treated textile coupons (20 mm x 20 mm, supplied by Alexandra®) and blank MSN control coupon were placed into separate 10 mL headspace vials (supplied by Sigma-Aldrich, UK with a 15 mm diameter screw-top and 8 mm diameter septum). The MSNs were loaded via EO immersion as described in (Section 3.4.3).

The vials were sealed and placed in an incubator at 25°C for 1 hour. A headspace sample of 1 mL was taken, using a gas syringe, for GC-MS analysis. Further samples were taken after 12 and 24 hours at 25°C. It should be noted the vials were left open between readings, in order to simulate the anticipated service environment for these antimicrobial textiles as closely as possible. The vials were sealed with a screw top an hour before headspace gas samples were taken.

The GC-MS system used is described previously in (Section 2.1.7). The temperature programme used for this method was as follows; the initial oven temperature of 60°C was ramped to 280°C at a rate of 10°C per minute. The temperature was held at 280°C for 15 minutes, with injector port temperature of 275°C and detector port temperature 250°C.

#### 4.4.4 Attenuated total reflectance (ATR) FTIR analysis of affixation layers

Synthetic textile coupons at each stage of the layer-by-layer affixation process (Table 4.4) were analysed using ATR FTIR. The samples were clamped using a pressure tower with specification 10,000 psi and analysed between 4000 and 500  $\text{cm}^{-1}$  wavenumbers. The Nicolet 380 was fitted with a Smart iTR ATR unit (Thermo), which is a single bounce unit, with a diamond window (ZnSe lens) and

DTGS detector. The resulting spectra were made up of 16 scans, no replicates, with resolution set to  $4\text{ cm}^{-1}$ .

Table 4.4. Displaying the five synthetic textile samples and their respective layer-by-layer treatment, for ATR FTIR analysis.

Sample	Stage of layer-by-layer treatment
1	Untreated
2	Ormosil
3	$\gamma$ -MPS
4	Blank MSNs
5	EO loaded MSNs

#### 4.4.5 SEM

*Vide Supra* Section 3.4.2.2

The synthetic textile samples were examined at different magnifications and areas to ensure coverage of the different treatments was consistent across the samples.

### 4.5 Results and discussions

#### 4.5.1 Ormosil treated textile stiffness

A standard synthetic textile of 65% polyester and 35% cotton (Figure 4.4) was chosen for use (supplied by Alexandra®). Ormosil was used to provide thin film coating of fibres onto the textile, thence allowing the silane-coupling agent ( $\gamma$ -MPS) to chemically bond MSNs to the synthetic textile. To achieve an ormosil gel that would form a thin film around the synthetic fibres it was necessary to experiment with a range of different ratios of MTEOS:TEOS precursor.

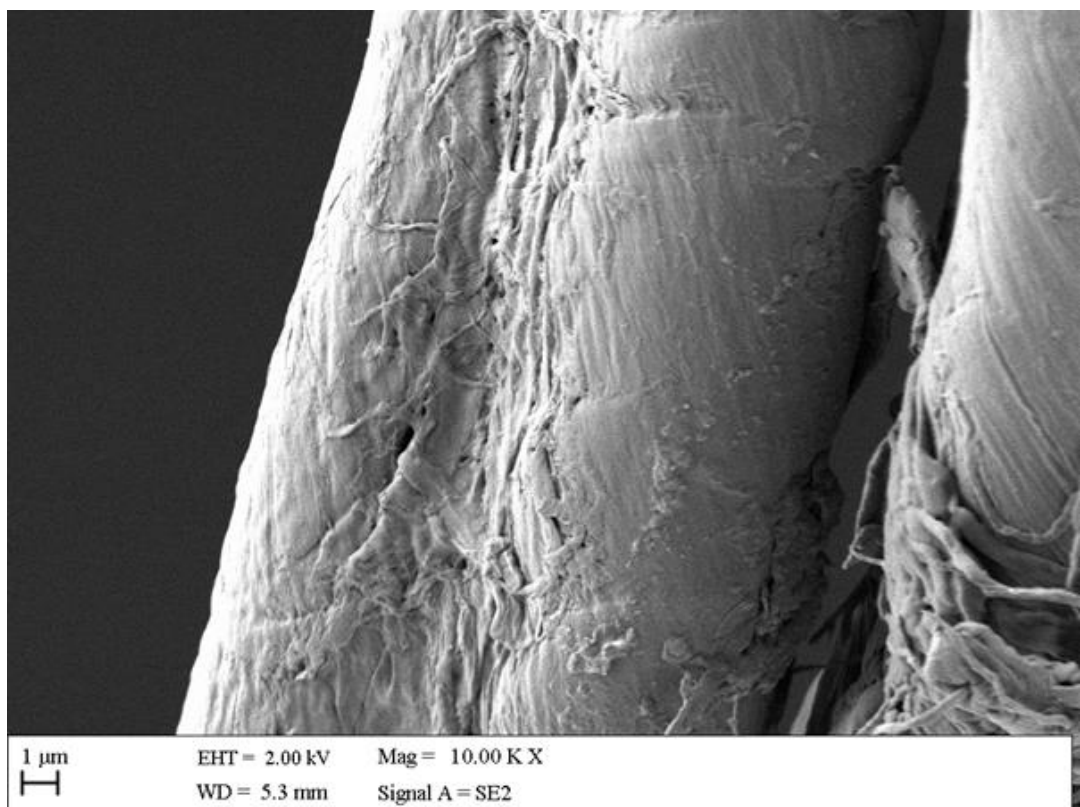
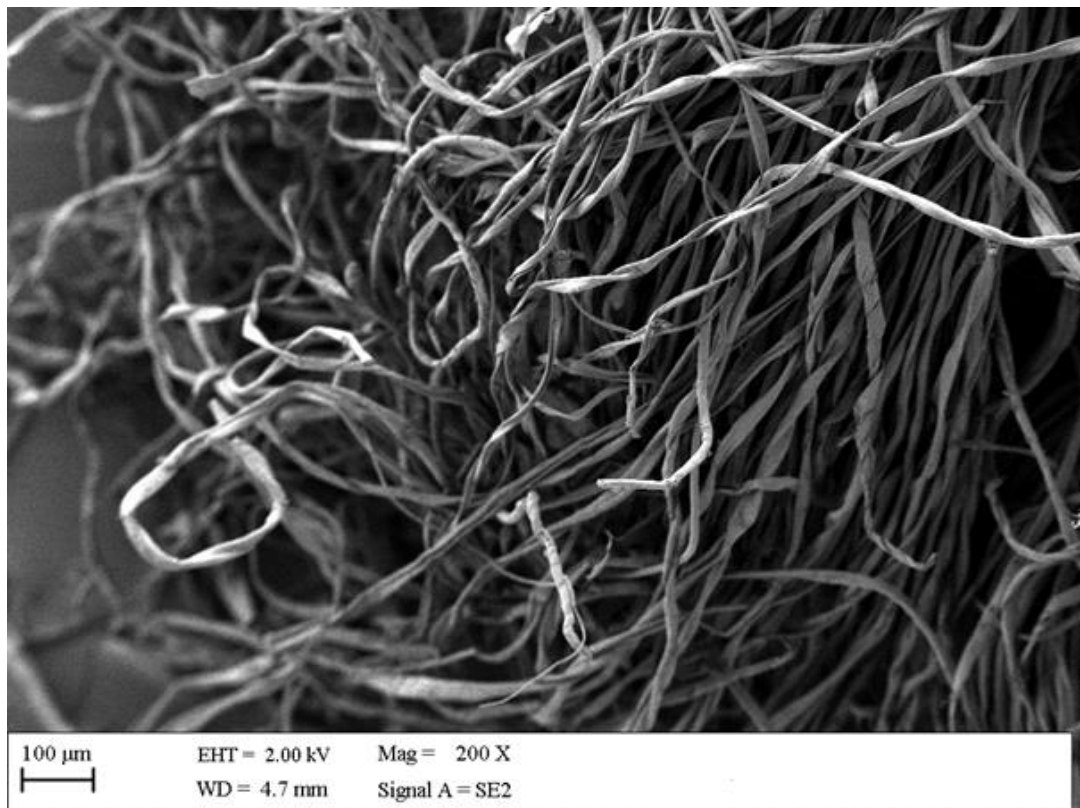


Figure 4.4. SEM images of untreated synthetic textile (65% polyester, 35% cotton).

A range of ormosil gels were synthesised using different ratios of MTEOS:TEOS precursor and to test the stiffness or ‘droop’ of the resultant treated textiles against an untreated control, results presented in (Table 4.5). The samples (200 mm x 50 mm) were cut from the treated textile sheets for purpose of this test, as described in (Section 4.4.1).

Table 4.5. Results of stiffness testing of synthetic textile coupons treated with ormosil gels ranging in MTEOS:TEOS concentration. Droop results an average of three repeats (n=3).

MTEOS:TEOS	pH	MeOH (mL)	Water (mL)	Droop from horizontal (mm)	Gelation time (hours)
Control (untreated textile)	na	na	na	45	18
1:1	2	25	5	20	18
2:1	2	25	5	28.67	18
3:1	2	25	5	38.93	18
1:2	2	25	5	27.93	18
1:3	2	25	5	20.5	18

The increase in the relative amount of MTEOS used in the synthesis of ormosil gels leads to a decrease in skeletal (crosslink) density (Estella *et al* 2006). The entry of methyl groups into the network leads to xerogels that are less dense, but more compact as the methyl groups are not hydrolysable. The reduction of the cross-linking leads to less rigid structures, which can bend without cracking, as shown in (Figure 4.5 – 4.7). Xerogels formed from a higher relative level of

MTEOS should have reduced porosity. Therefore, providing a more homogenous surface for coverage by MSNs (Rios 2011).

The 3:1 formulation was used for further experiments, as this gel provided a thin film coating round the synthetic textile fibres, without sticking or clumping the fibres together (Figure 4.8). In addition, this formulation produced the least stiffening of the treated coupons, relative to the untreated control, presented in (Figure 4.4).



Figure 4.5. SEM images of ormosil treated synthetic textile samples at differing precursor ratios MTEOS:TEOS A) 1:1.

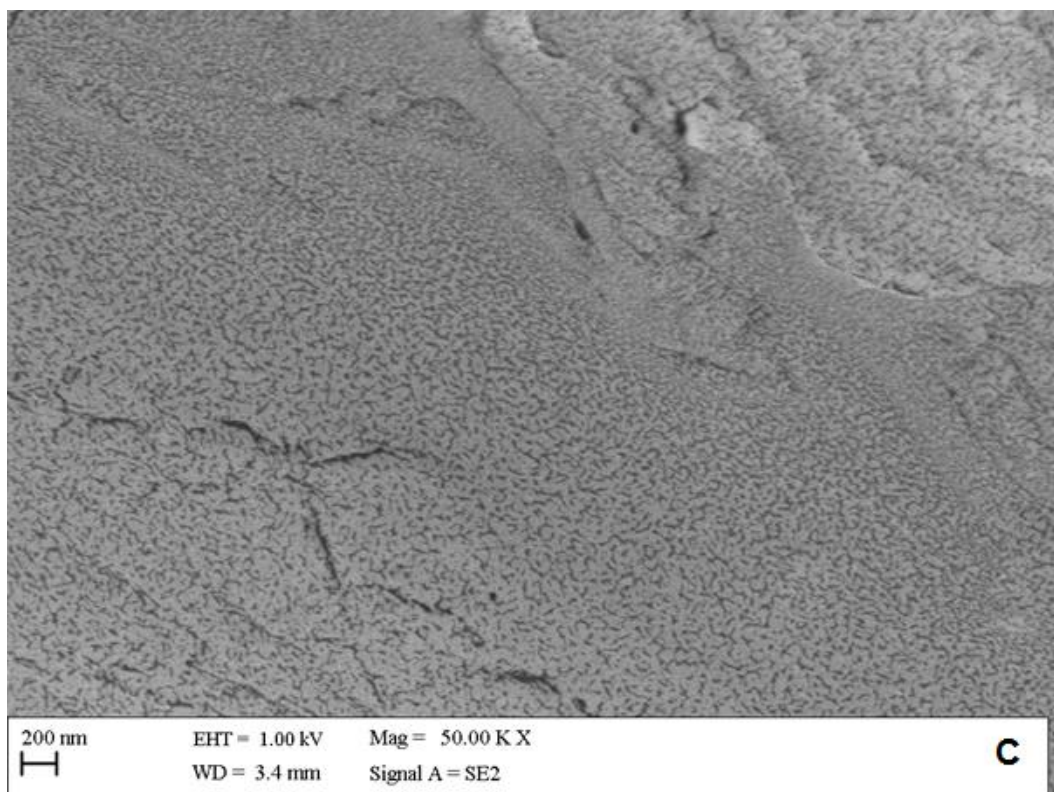
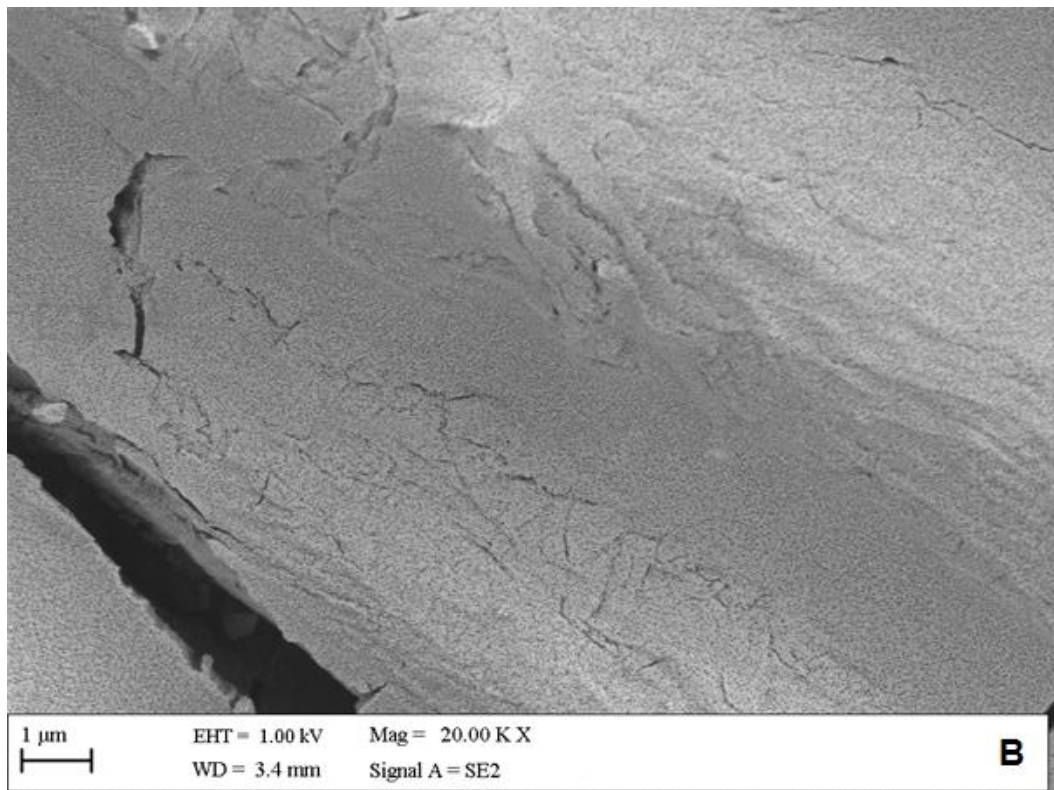


Figure 4.6. SEM images of ormosil treated synthetic textile samples at differing precursor ratios MTEOS:TEOS, B) 2:1 C) 3:1.

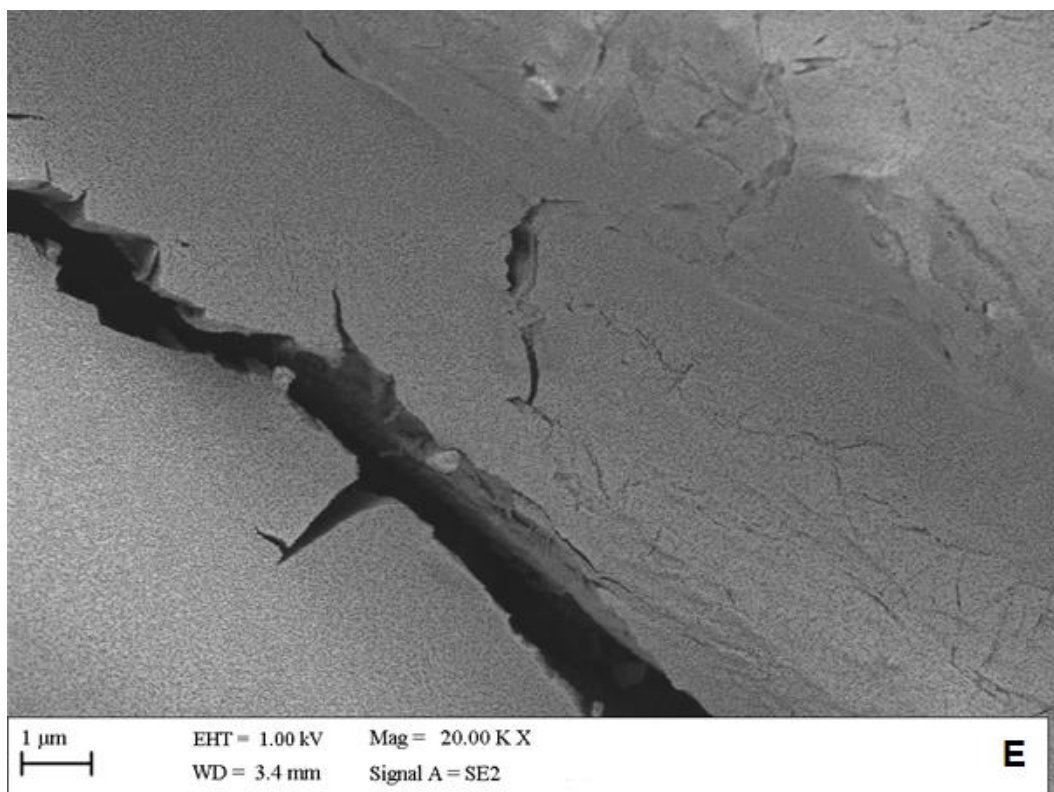
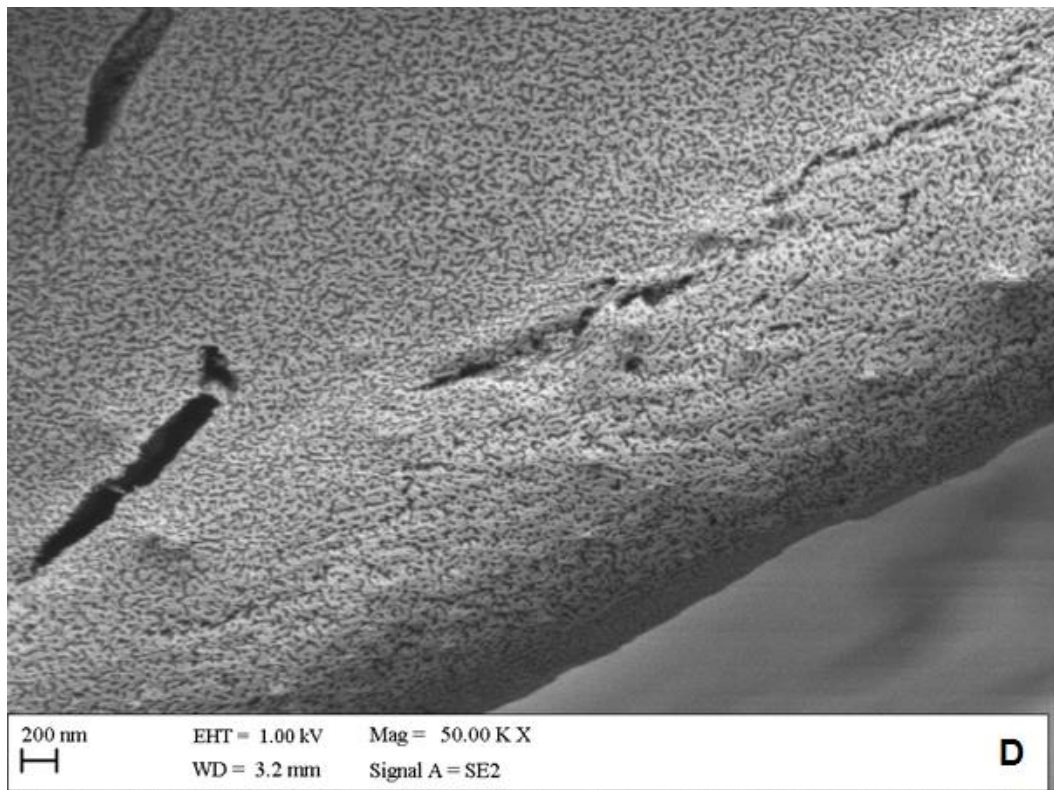


Figure 4.7. SEM images of ormosil treated synthetic textile samples at differing precursor ratios MTEOS:TEOS, D) 1:2 E) 1:3.

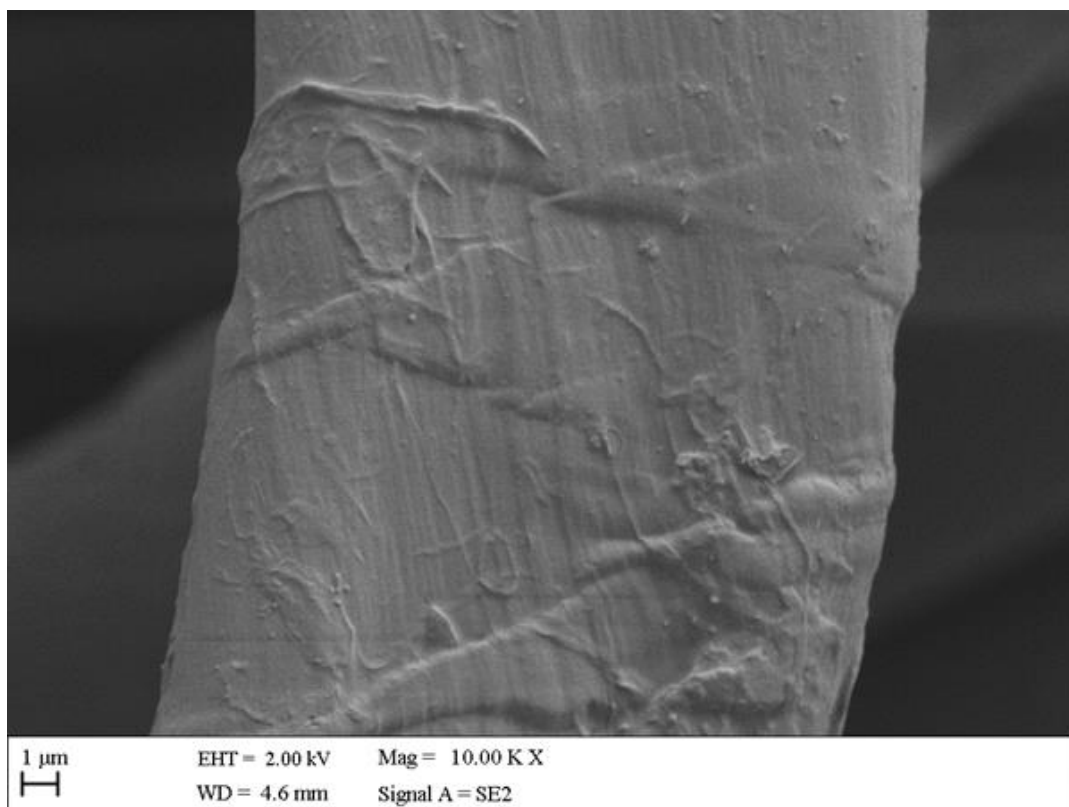
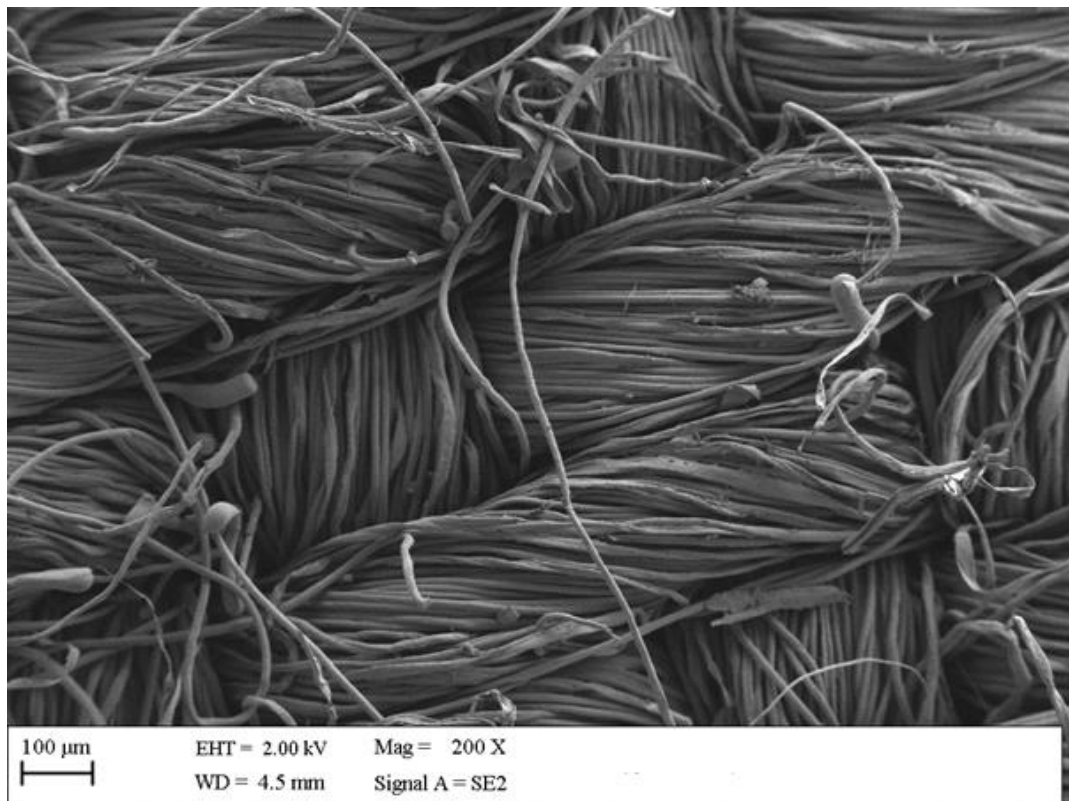


Figure 4.8. Ormosil treated sample 3:1 MTEOS:TEOS 1 hour stir, air dried.

In HCl-catalysed reactions, hydrolysis occurs at a faster rate than condensation (Meixner and Dyer 1999), and alkyl-substituted trialkoxysilanes hydrolyse faster than the corresponding tetraalkoxysilanes (Himmel *et al* 1990). In particular, MTEOS hydrolyses faster than the TEOS monomer during each sequential hydrolysis reaction (Jitianu *et al* 2003). The replacement of of an alkoxy species by a non-hydrolysable species leads to higher hydrolysis rates because the inductive effect of these radicals reduces the positive charge on the silicon atom and increases the negative charge on the oxygen atoms (Devreux *et al* 1990). Due to the rapid hydrolysis rate, the formation of siloxane bonds via silanol-alkoxy and silanol-silanol condensation is the rate-determining step, which in acidic media increases exponentially with time. The presence of methyl groups decreases the condensation rate as they reduce the net charge on the silicon atom, which is the key parameter for the nucleophilic condensation process above the isoelectric point of pH 2 (Iler 1979). As MTEOS concentration increases, condensation kinetics slow down because the dimerisation rate of hydrolysed species from MTEOS is slower than that of species from TEOS (Fyfe and Aroca 1997), which confers well with the SEM analysis of ormosil treated synthetic coupons with differing MTEOS:TEOS ratios.

#### 4.5.2 Affixation methods

The following experiments (4.5.2.1 – 4.5.2.4) were conducted using blank MSNs as SEM was used to analyse the treated textile coupons. The addition of EO was not carried out as it will evaporate in the high vacuum within the SEM chamber and potentially damage the instrument.

#### 4.5.2.1 One pot synthesis

As described in (Section 4.4.2.1) ormosil treated textile coupons were immersed in a sol containing  $\gamma$ -MPS and MSNs dispersed in MeOH. The samples were analysed using SEM (Figure 4.9). The SEM analysis shows agglomeration/aggregation of the MSNs, on the surface of the synthetic fibres. From this result, it is clear  $\gamma$ -MPS will bond to both the Ormosil coating on the fibres and the MSNs. However, there is no control over the distribution of MSNs on the surface of the fibres. The occlusion of the nanoparticle mesopores caused by the aggregation is likely to hinder the release of the EO blend. As such, it was thought the grafting of  $\gamma$ -MPS onto MSNs prior to exposure to ormosil coated coupons would produce a more uniform coverage of MSNs on the fibres.

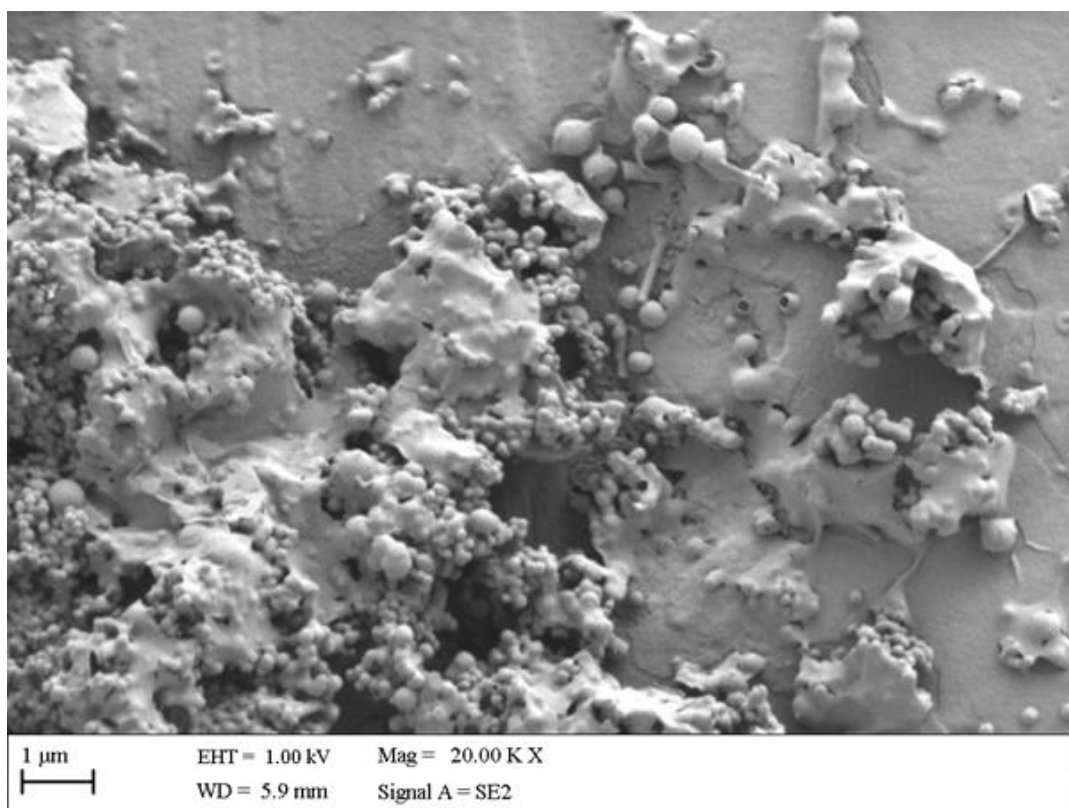


Figure 4.9. SEM image of one pot synthesis on synthetic textile.

#### 4.5.2.2 Silane grafted MSNs

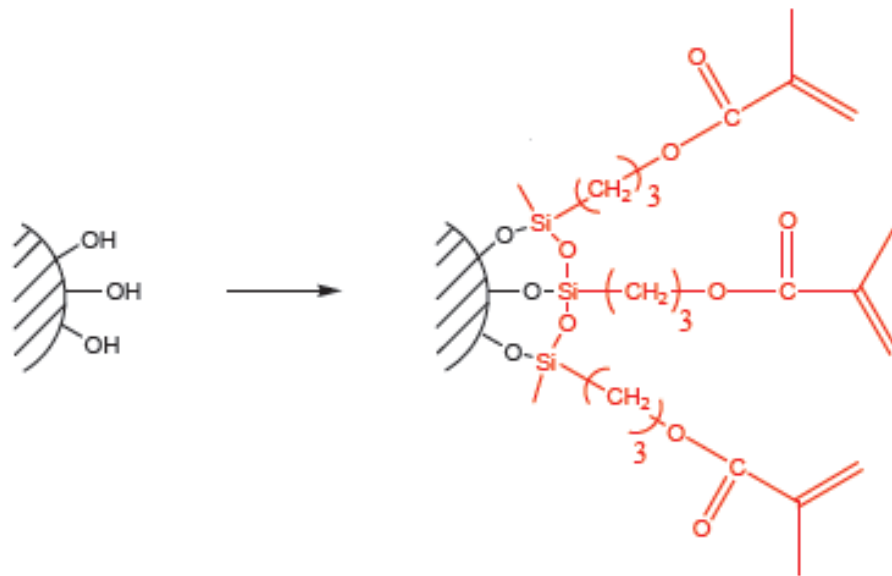


Figure 4.10. Grafting of silane coupling linkers onto MSNs based on (Pardal *et al* 2009, Bartholome *et al* 2003). Image reproduced from Pardal *et al* 2009.

Figure 4.10 shows the chemical formula of a  $\gamma$ -MPS molecule that contains a carbon-carbon double bond and methoxysilane groups ( $\text{SiOCH}_3$ ). The former group is suitable for free radical polymerisation and the latter group can form a three-dimensional silica network through hydrolysis and condensation reactions. In an attempt to improve the coverage of MSNs on the surface of the synthetic fibres,  $\gamma$ -MPS was grafted to the MSNs, as described in (Section 4.4.2.2).

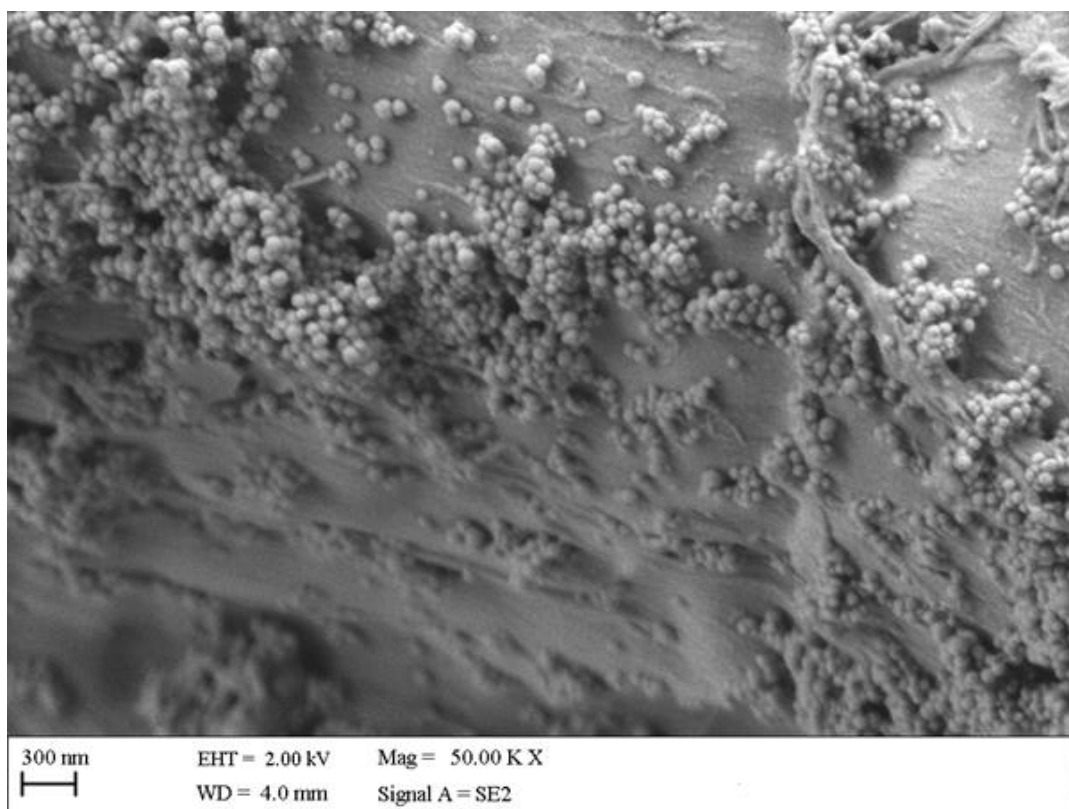


Figure 4.11. TMSPPMA grafted MSNs attached to ormosil coating on synthetic textile fibres.

The SEM results (Figure 4.11) suggest the MSN/ $\gamma$ -MPS grafted composites are composed of polymer that threads through the mesoporous silica particles and among the MSNs on the ormosil coated synthetic fibre surface. It can be said the MSNs serve as pseudo-cross-linking points within the MSN/ $\gamma$ -MPS composite. Hydrolysis and condensation of MSNs and  $\gamma$ -MPS in a solvent result in sols containing organically modified silicate species (Pardal *et al* 2009). Polymerisation of monomer surrounding and adsorbed within particles results in inhomogeneous, chemically bonded hybrid inorganic-organic composites. Since the polymerisation may occur within both the pore channels and among the particles, as-synthesised composites may contain dispersed particles with polymer chains threaded within their pore channels.

Figure 4.11 also shows aggregation of the silane grafted MSNs, leading to fewer open mesopores for release of the EOs, possibly harming the antimicrobial

efficacy of the textile. It was speculated that treating the ormosil dried textile samples alone with  $\gamma$ -MPS first and then with MSNs dispersed in MeOH using a layering approach would provide a more uniform affixation of the MSNs to the ormosil coating via the silane coupling linker.

#### 4.5.2.3 Layer-by-layer

The SEM analysis for the synthetic textile coupons treated via the layer-by-layer method (Section 4.4.2.3) produced good attachment of the MSNs to the fibres, (samples were washed three times in MeOH before analysis). The MSNs appear to be dispersed relatively uniformly on the surface of the fibres with minimal aggregation. The decision to initially isolate the coupling-linker from the MSNs and instead treat the ormosil coated textile coupons with  $\gamma$ -MPS appears to provide a favourable route to the chemical affixation of the MSNs to the fibres, as represented in (Figure 4.12).

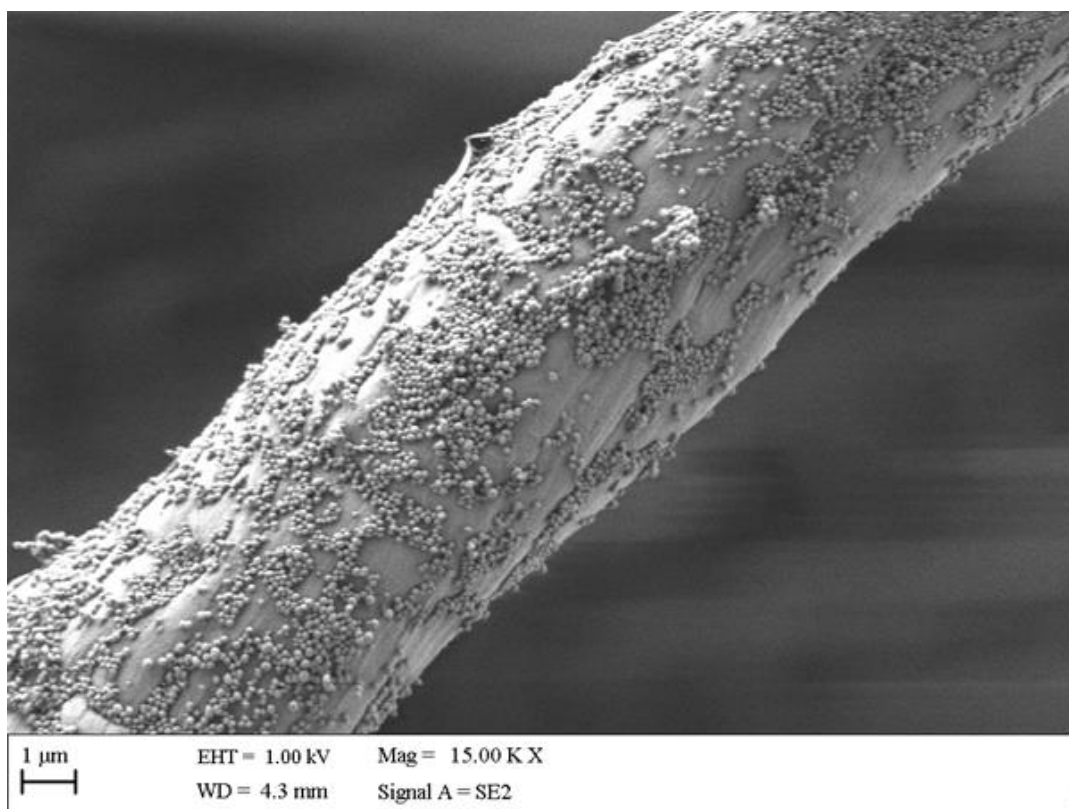


Figure 4.12. SEM image showing MSNs affixed to synthetic textile fibres after layer-by-layer treatment.

#### 4.5.2.4 Optimal MSN coverage of synthetic fibres analysis

SEM images, shown in (Figure 4.13) indicate the coverage of MSNs increases with increasing MSN concentration, and time exposure with stirring in MeOH, the method described in (Section 4.4.2.4). The coverage is clearly time and concentration dependant, with the best results occurring with dispersion of MSN (1g) in MeOH (100 mL) after 18 hours of stirring. With the ormosil coating formulation resolved and the layer-by-layer affixation process selected (Section 4.4.2.3); the next stage of the work was to affix EO loaded MSNs to the synthetic fibres. Following the latter, the release of the antimicrobial EO blend from the nanoparticle mesopores will be investigated.

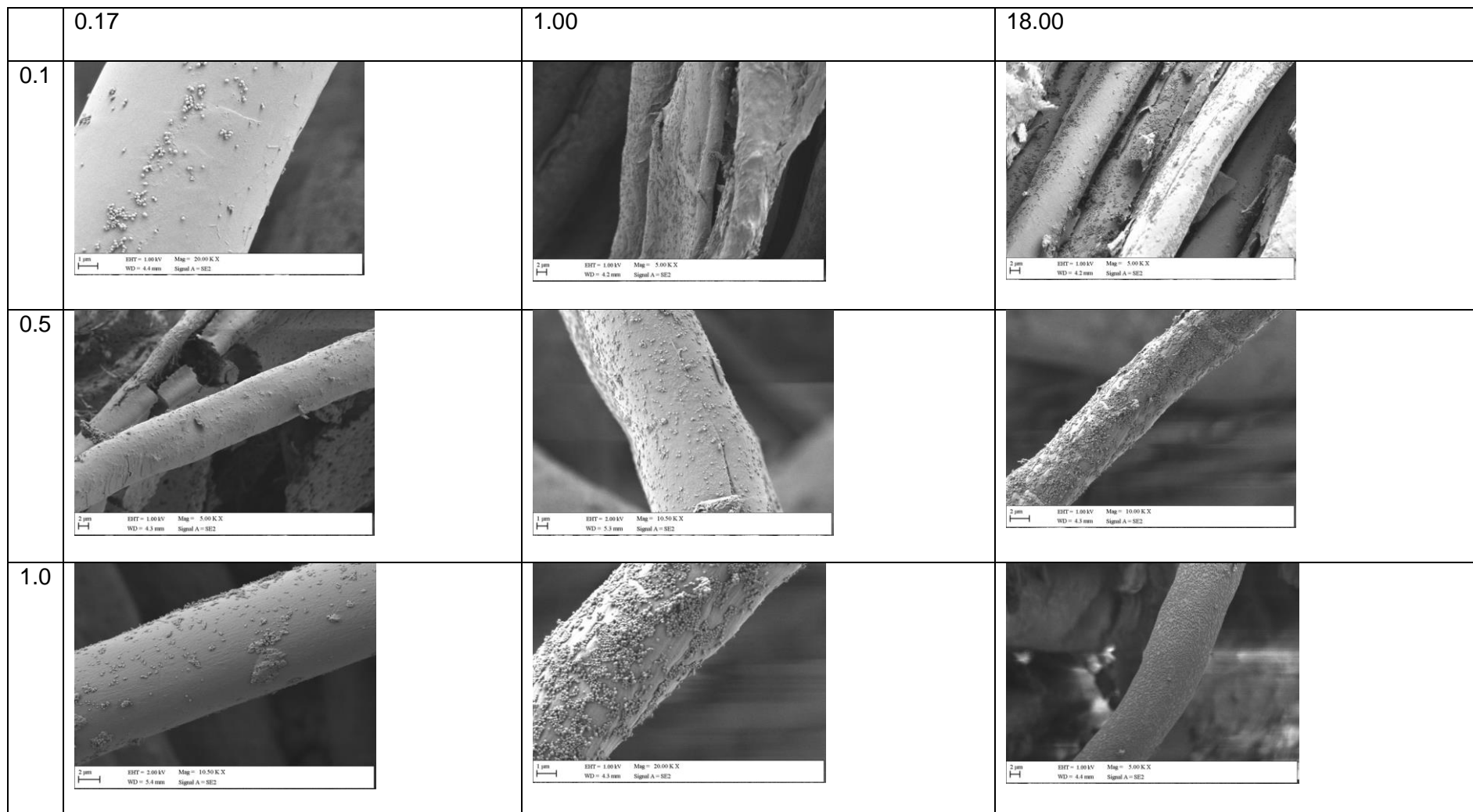


Figure 4.13. SEM images of MSN coverage on individual synthetic fibres, representative of coverage on textile coupons treated with three different concentrations of blank MSNs (0.1, 0.5 and 1g). With three different lengths of exposure (0.167, 1 and 18 hours).



### 4.5.3 EO release from loaded textile

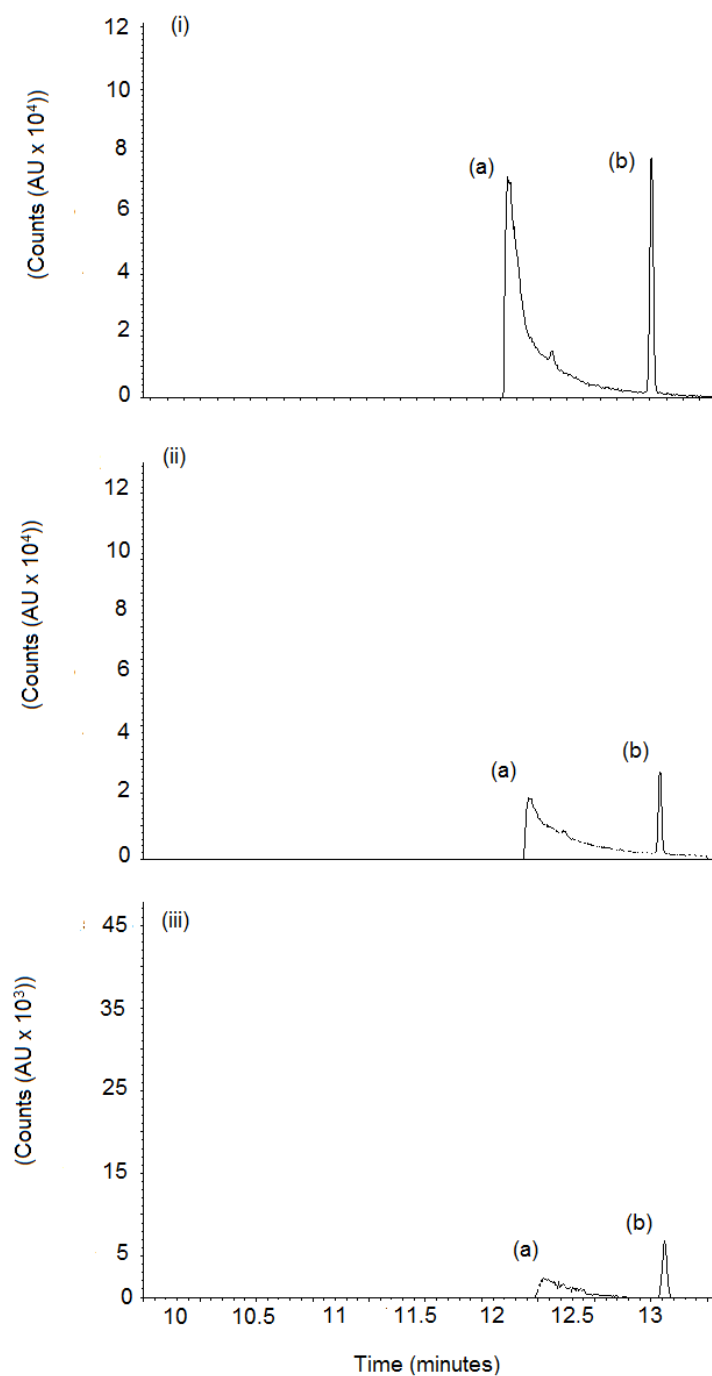


Figure 4. 14. Extracts from GCMS spectra showing EO release at three different time points from EO loaded MSNs affixed to synthetic fibres. (a) Eugenol, (b) eugenyl acetate. Gas samples were taken at 1 hour (i), 12 hours (ii), and 24 hours (iii). Y axis scales (i) and (ii) (Counts (AU x 10<sup>4</sup>)), (iii) (Counts (AU x 10<sup>3</sup>)).

The main function of using mesopores to adsorb the essential oil was to prolong the antimicrobial efficacy of the textile, by slowing the release of the EO molecules. In (Section 3.5.3.3) the EO loaded MSNs were studied for EO release from the mesopores, charting leaching of the EO molecules into an organic solvent. It was decided this was not desirable for the loaded textile coupons as it would not mimic real world conditions for the end product. A gaseous environment would be best suited to analyse the release of volatile EO molecules from the mesopores. However, traditional headspace sampling involves heating of the sample to quantify the molecules in a sample. Again, the real world conditions for the end product would most likely be room temperature. As such, samples were placed in an incubator set at 25°C to mimic a constant room temperature, with the glass vials being closed an hour before each reading to give an indication of the release of EO molecules from the mesopores over a 24 hour period, described in (Section 4.4.3). Again, 24 hours was chosen as the longest sampling time as any medical textile would likely be washed or discarded after a day of use.

Figure 4.14 shows a peak for eugenol, 70000 counts high, recorded after 1 hour, with a much reduced count at 12 hours and baseline levels after 24 hours. Interestingly, a greater peak for eugenyl acetate (4.75% in the CIN-CLO blend) was recorded at 12 and 24 hours compared to the most abundant molecule in the CIN-CLO blend (eugenol >94%). Considering the decline in the amount of eugenol evolved over the sampling period, it is possible that after an hour, the dual-point attached, multi-point attached or molecules attached in the pore entrance could have diffused, while those EO molecules deep in the pores or multi-point attached would not evolve from the sample.

#### 4.5.4 ATR FTIR analysis of affixation layers

The ATR FTIR spectra obtained, using the method described in (Section 4.4.4) for different stages of the layer-by-layer method followed the same basic pattern for all five samples, with some shifting and broadening of peaks. The following figures (4.15 – 4.18) show spectra for each stage of the chosen affixation method with the subsequent stage, for comparison.

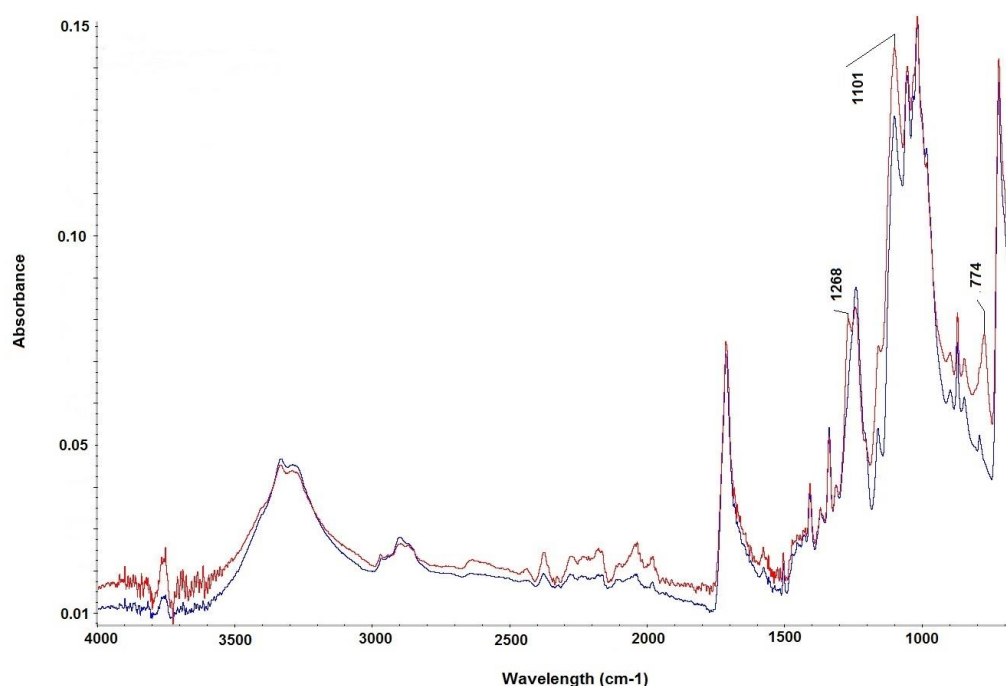


Figure 4.15. FTIR spectra for textile coupon samples at the first stage of treatment. Untreated (blue) and ormosil treated (red),

The FTIR spectra for the ormosil treated textile coupon (Figure 4.15, red line), displays some peak intensity differences from the untreated coupon around 1100-900 cm<sup>-1</sup>. These more intense peaks recorded for the ormosil treated layer could be attributed to the asymmetric stretching vibration of the Si-O-Si bond, which constitutes the skeletal SiO<sub>2</sub> network of the xerogel (Estella 2007).

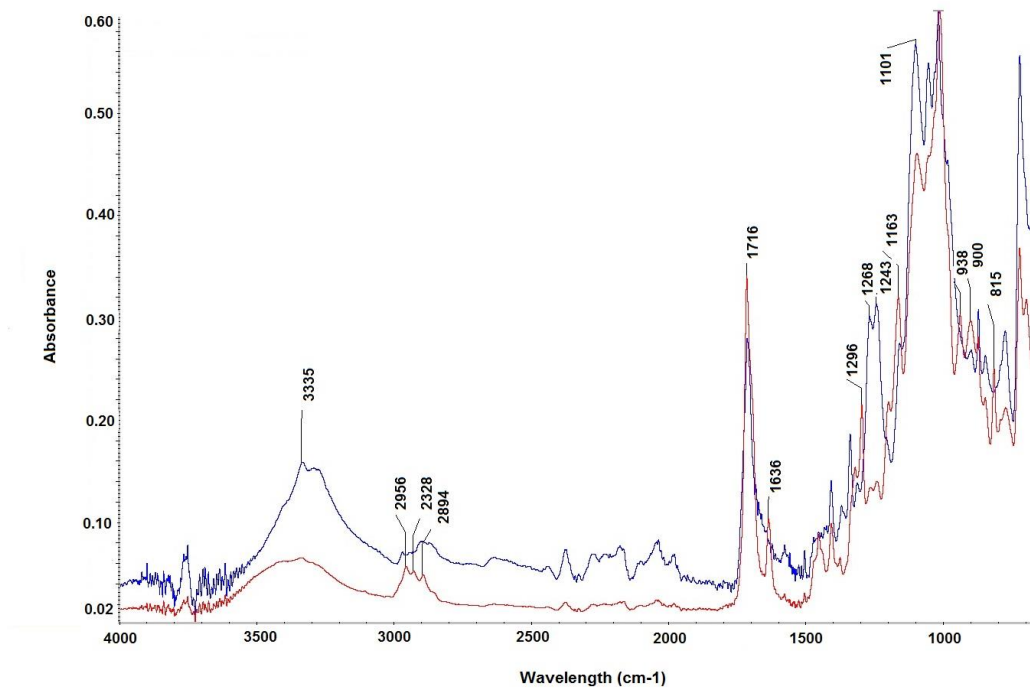


Figure 4.16. FTIR spectra for textile coupon samples at each stage of treatment. Ormosil treated (blue) and silane treated (red).

The FTIR spectra for the ormosil treated coupon and the  $\gamma$ -MPS -MPS treated coupon follow roughly the same pattern of absorbance (Figure 4.16), with some differences in peak intensity at 1716 cm<sup>-1</sup>. This could be attributed to  $\gamma$ -MPS -MPS C=O carbonyl groups and also, changes around 2900 cm<sup>-1</sup> corresponding to aliphatic carbons of  $\gamma$ -MPS -MPS moieties (Pardal 2009).

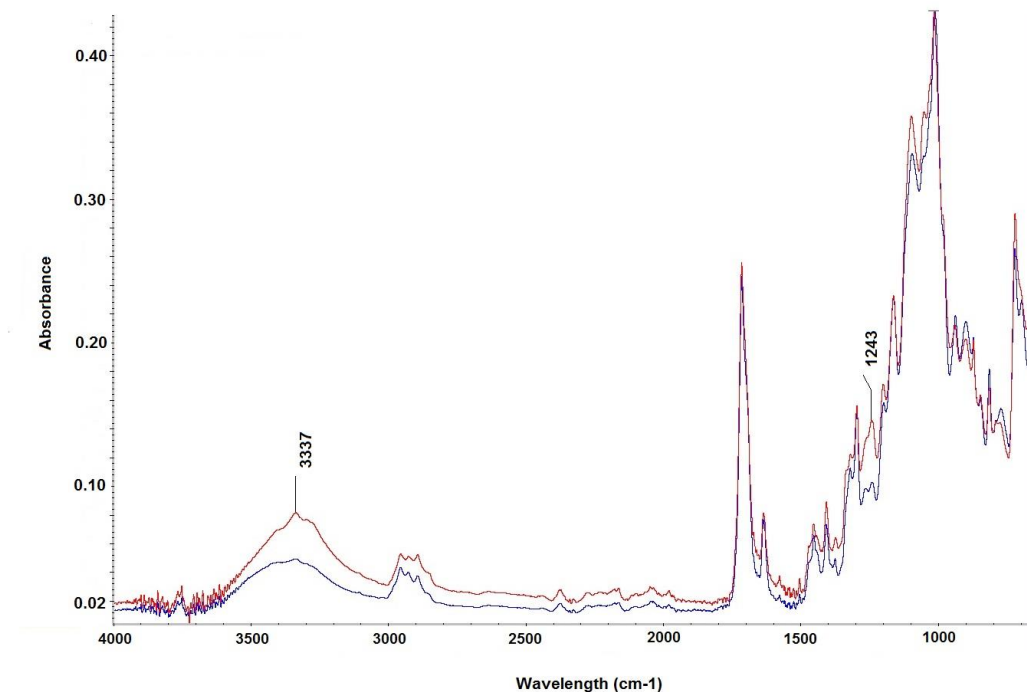


Figure 4.17. FTIR spectra for textile coupon samples at each stage of treatment. TMSPMA treated (blue) and blank MSN treated (red).

The spectra for TMSPMA and blank MSN treated textile coupons (Figure 4.17) do not display a great deal of variation, layer to layer. A very slight increase in intensity at 1243 cm<sup>-1</sup> can be seen for the coupons treated with blank MSNs, the relative decrease for  $\gamma$ -MPS -MPS can be attributed to the C(=O)-O-C stretch of the ester of the gamma MPS linker. The spectra comparing blank MSN and EO loaded MSN treated textile coupons (Figure 4.18) in theory would provide differences due to the addition of peaks characteristic of EO, in this case a blend of clove and cinnamon oil (>94% eugenol). The C-H stretch vibrations in the 3000 cm<sup>-1</sup> – 2800 cm<sup>-1</sup> range (CH<sub>2</sub> 2875 cm<sup>-1</sup> and CH<sub>3</sub> 2995-2936) could be attributed to the presence of EO in the MSN pores. In addition, the peak at 1600 cm<sup>-1</sup> for the EO loaded MSNs, is indicative of C-C stretching in phenyl ring containing structures, such as eugenol. Furthermore, the differences in spectra at 1243 cm<sup>-1</sup> can be assigned to the Ar-O-C stretch of the eugenol ether.

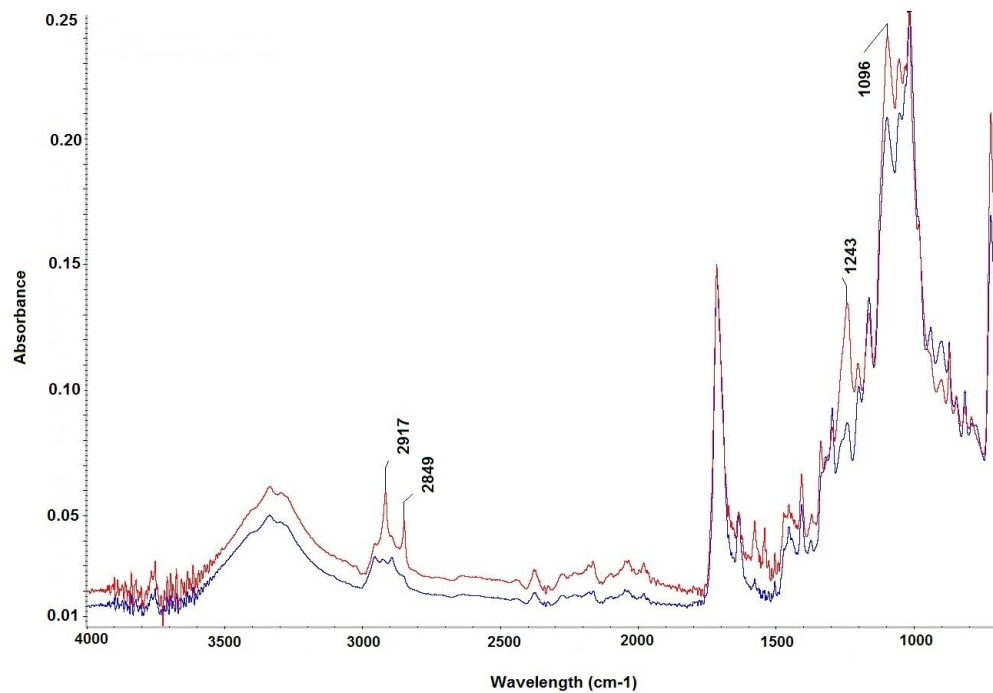


Figure 4.18. FTIR spectra for textile coupon samples at each stage of treatment. Blank MSN treated (blue) and EO loaded MSNs (red).

It was speculated that the individual layers were too thin to provide better defined spectra. ATR FTIR is noted for sample penetration between 0.5 – 2  $\mu\text{m}$ , although this is dependant on the wavelength of light, the angle of incidence and the indices of refraction for the ATR crystal and the medium being probed (Queiroz *et al* 2012).

#### 4.6 Conclusions

- A 3:1 formulation of ormosil precursors (MTEOS:TEOS) at pH 2 was chosen to provide a flexible yet robust thin film coverage of the synthetic fibres, allowing bending of the textile and a large surface area for MSNs to attach on to.
- $\gamma$ -MPS coupling linker allowed the MSNs to adhere and bond to the ormosil coating on the synthetic fibres.
- Although the reflux method for chemically affixing MSNs to  $\gamma$ -MPS in toluene was successful, the simpler, less time intensive and therefore more cost effective layer-by-layer method produced good MSN coverage on the synthetic fibres.
- MSN coverage on the synthetic fibres increased with increased MSN concentration and with increasing duration of exposure.
- Headspace gas samples from sealed bottles containing untreated, and EO loaded MSN treated textile coupons were analysed using GC-MS. EO was able to diffuse from the MSN pores after being affixed to the synthetic fibres.
- FTIR spectra characterising the different layers of the layer-by-layer affixation method were produced, displaying the changes in chemical environment between sequential treatments on the synthetic textile coupons.

## **Chapter 5**

### **Challenge testing and wash durability of antimicrobial textile**

## 5.1 Introduction

### 5.1.1 Textiles and the skin

Aside from clothing, textiles are used in household, medical and hygiene, agricultural, automotive, aeronautics and marine applications (Horrocks and Anand 2004). Development areas of the textile industry constantly focus on integrating improved physical features, such as insulation properties, elasticity, stiffening, or novel features, such as static, crease, water resistance, fire retardant, and antimicrobial properties into or onto textiles (Schindler and Hauser 2004). These are achieved by means of chemical or mechanical finishes given to fabrics. A trend in the fabrication of hygiene textiles has evolved with consumers seeking low maintenance textile products, which increases the market potential for durable antimicrobial finishes (Perera 2013). Antimicrobial finishes on fabrics are developed to protect the consumer, patient or carer against infection, disease or odour causing microorganisms. The growth of microorganisms not only cause hygiene (cross-infection) issues, but also affects the functional and aesthetic properties of the material by producing rot, mold or mildew (Gao and Cranston 2008). There is a significant need for antimicrobial finishes to meet the market demands in preventing unpleasant odours on intimate apparel, socks and sportswear. Most importantly, health care settings, schools, hotels or any other crowded public area where protection from diseases should be addressed (Windler *et al* 2013). Fabrics support temperature and humidity balance for the human body's comfort. The human skin and fabrics are in direct contact for prolonged periods. The human skin is a complex bionetwork, sheltering microorganisms such as bacteria, viruses and fungi that live in different habitats on the skin. The amount of bacteria present on the skin out-numbers the number of human skin cells by a factor of ten. (Elsner 2006).

While evidence exists that the use of antimicrobial substances may change the ecology of resident bacteria in the gut, leading to overgrowth of pathogenic bacteria, such as *E.coli*, there is no such data for the ecology of the skin (Sullivan *et al* 2001). Because of the direct contact of fabrics with human skin, most bacteria can transfer and propagate between the two. Further, bacteria can reside on fabrics causing fabric discoloration, skin diseases and unpleasant odours, providing necessity for antimicrobial finishes on clothing that is also appropriate for intimate contact with the skin for daily use. Indeed, it has been reported 60% of physician and nurse clothing carried disease-causing bacteria, including methicillin-resistant *S. aureus*, at a hospital in Israel (Wiener-Well *et al* 2011). Natural fibres such as cotton can act as a host to many microorganisms because of its hydrophilic nature, which means it easily picks up body sweat and water-borne stains. Synthetic fibres, such as polyester, can propagate microbes on the skin due to their hydrophobic nature as they block evaporation of sweat, making a wet environment on the skin, conducive to microbial growth (Elsner *et al* 2003). Therefore, there is great need for effective antimicrobial textiles that are skin friendly.

#### 5.1.2 Challenges faced by the use of natural agents on textiles

There are several common limitations expressed in the literature regarding the use of natural antimicrobial agents on textiles. The plant products are in their natural chemical structure, and not all the chemical components possess antibacterial activity. Therefore, the selective isolation of the active constituents is a possible solution to reducing the effective dose of the antimicrobial. The exact mechanism of bactericidal action of the different essential oils is still to be elucidated (Hylgaard *et al* 2012). The dissolution of the agents for textile application is also a major challenge as essential oils are not soluble in water.

This challenge is addressed by the use of MSNs in the present work. It is of vital importance that there is no loss of antimicrobial activity due to blocking of functional groups, during the textile attachment or finishing process, leading to diminished antimicrobial activity. Although synthetic antimicrobial agents are very effective against a range of microbes and provide a relatively long-lasting effect on textiles, they also exhibit a range of unwanted side effects, such as action on non-target microorganisms and water pollution (Joshi *et al* 2008). Hence, the need for antimicrobial textiles that utilise natural agents, such as essential oils to combat the negative/potentially harmful effects associated with microbial growth on or contamination of textiles (Joshi *et al* 2008).

### 5.1.3 Antimicrobial textile finishes

The antimicrobial activity of EOs has potential to be utilised to help reduce the bioburden of pathogenic microbes in healthcare environments. This may be achieved via application of EOs to textiles and surfaces that are frequently touched. Technical textiles, describe the growing variety of products and manufacturing techniques being developed primarily for their technical properties and performance rather than their appearance or other aesthetic characteristics (Milwich *et al* 2006). The rapid growth in technical textiles and their end uses has generated many opportunities for the application of innovative finishes. Antimicrobial textiles with improved functionality are useful in a wide range of applications, from infection control in a medical setting, to odour control for outdoor apparel (Nelson, 2001). A number of antimicrobial treatments are now available that can kill bacteria and enable garments to remain smelling fresh for longer (Holme 2007). Although there are many natural products rich in antimicrobial agents, including essential oils, research into their use in textiles is relatively limited and not extensively documented. Most of the published

research in this area tends to focus on synthetic antimicrobials, for example, textiles treated with triclosan (Orhan *et al* 2006).

Silver has also been used in antimicrobial products, either in the form of fibres / yarns, or as nanoparticles (Dubas *et al* 2006). Silver impregnated textiles are used as wound dressings for infected wounds or wounds at high risk of infection. Podycare™ is a product that contains silver particles, incorporated into the fibre during formation.

Quaternary ammonium salts have a positively charged nitrogen ion that can interact with the negatively charged groups of anionic dyes. These intermolecular interactions inside fibres serve as binding forces to enhance the durability of the biocidal agents once attached. Dye molecules can be used as bridges to bind functional antimicrobial groups to chemically stable synthetic polymers. Quantitative antimicrobial evaluation of these treated fabrics reveal significant reductions in bacterial load on surface contact (Kim & Sun, 2000). Amicor™ is an example of a polyacrylic fibre that has an organic biocide blended into the polymer before melt spinning of the fibres (Mahtig *et al* 2004).

Due to the volatile nature of EOs, it would be ineffective to simply apply them directly to fabrics as they would quickly evaporate, rendering the fabric unprotected. Encapsulation of the EO in organic, inorganic or organic-inorganic hybrid media, may lead to sustained release of the EO, and hence prolong the duration of antimicrobial activity. Research into the encapsulation of EOs predominantly focuses on using organic media. Maji *et al.* (2007) used gelatine to encapsulate *Zanthoxylum limonella* oil, the gelatine surrounded the oil in coacervates that were then cross-linked using gluteraldehyde. They were able to achieve a maximum encapsulation efficiency of 98% by varying the

proportions of the three components. This was calculated by dividing the actual amount of oil encapsulated in a known amount of microcapsules by the amount of oil introduced in the same amount of microcapsules. The release rate of 60% of the oil over 70 hours was determined by cumulative oil release from the microcapsules, analysed spectrophotometrically. The best release rate obtained was 90% oil release over 70 hours, with an encapsulation efficiency of 78% (Maji *et al* 2007).

Zein nanospheres, fabricated from a hydrophobic protein found in corn have been used to encapsulate oregano, red thyme, and cassia oils. This was achieved by adding the oil and zein to 85% ethanol and dispersing with high speed mixing into water containing 0.01% silicone fluid. The solution containing the encapsulated oil particles was lyophilised to obtain a dry powder. Release rates in phosphate buffered saline (PBS), and PBS with 24% ethanol, ranged from 60-80% over 50 hours depending on the EO (Pariss *et al* 2005).

When compared to organic polymer coatings and encapsulation media, the advantages of inorganic sol-gel coatings and encapsulation media are substantial. The advantages of the latter include good mechanical, chemical and thermal stability, high transparency and photo-stability, biological inertness controllable porosity and hence controllable release of encapsulated agents (Mahltig *et al* 2010). Interestingly, it is also possible to encapsulate / intercalate liquids, oils (or more viscous compounds) to loadings of up to 30 % wt., in sol-gel matrices and layered structures, by simple admixture with silica nanosols. After gelling and drying, they form dry, non-sticky composite materials. The release of encapsulated liquids from the silica film can be controlled by regulating the mass ratio of silica to agent, by chemically modifying the silica matrix, by adding soluble or swellable pore-forming substances and by

controlling the preparation conditions. The use of encapsulated products offers greater convenience and the controlled release of the encapsulated organic substances. For example, insect resistant treatments and flame retardant finishes demonstrate higher levels of performance if encapsulated. Ideally, the boiling points of the liquids to be encapsulated should be higher than 150°C and they must differ sufficiently to the boiling point of the sol solvent. When incorporating hydrophobic oils, the sol should have low water content. The inclusion of biocidal compounds into modified silica matrices using the sol-gel technique offers new interesting prospects for antimicrobial coatings with controlled release effects. Studies using sol-gel coatings encapsulating bioactive liquids, such as essential oils, have encountered problems with wash fastness and oxidation stability of the coated textiles whilst in storage (Haufe *et al* 2008). In order to increase the robustness of antimicrobial action to textile washing processes, a number of approaches can be utilised, dependent on the chemical nature and mode of action of the antimicrobial agent. Fibre treatment with resins, condensates or fibre crosslinking agents have been studied, along with microencapsulation of the antimicrobial agent and durable binding of the microcapsules to the fibre (Gao and Cranston 2008). For the present work, EOs (cinnamon and clove oil blend) were loaded into MSNs for slower release of the antimicrobial over time.

#### 5.1.4 Methods commonly used to test antimicrobial textile finishes

The American Association of Textile Chemists and Colorists (AATCC) antimicrobial test standards are used globally for demonstrating a product's performance against common microbial challenges. The antibacterial activity assessment of textile materials: Parallel Streak Method (AATCC 147) is a quick and relatively inexpensive method for determining if a textile sample displays antimicrobial activity. Textile samples are laid onto agar plates that have been

inoculated with test microorganisms, in parallel streaks across the width of the agar plate. A weakness of this method is its non-quantitative nature, making results difficult to compare to other antimicrobial finishes. However, it is an introductory method, designed to quickly establish if a textile sample has antimicrobial capability. Changing the method to incorporate spreading of the microbial inoculum across the surface of the agar plate allows for a zone of inhibition (ZOI) to be determined. This allows quantitative data to be recorded, and allows comparisons to be made between antimicrobial textile finishes. A clear weakness for both agar diffusion methods is that they cannot differentiate growth inhibition of the test microorganism from killing.

American Society for Testing and Materials (ASTM) E2149 and AATCC 100 methods allow quantitative testing of a samples capacity to kill test microorganism inoculum. Textile samples are saturated or immersed in dilute test inoculum, with bacterial enumerations recorded at the start of the experiment and usually after a 24 hour contact period. AATCC 100 is well designed in terms of including neutralisation of the antimicrobial agent controls, however, for both methods there are no clear standards for pass or fail.

AATCC 61 and AATCC 135 are used to condition samples prior to determine antimicrobial efficacy. Commonly used with AATCC 100 efficacy testing to show antimicrobial durability after specified rounds of washing cycles.

## 5.2 Objectives

- To screen the EO loaded synthetic textile coupons for bacteriostatic action using AATCC 147 parallel streak and zone of inhibition method.
- To determine the dynamic contact killing potential of the EO loaded synthetic textile coupons during a 24 hour exposure, using AATCC 100 and ASTM E 2149 methods as guides.
- To investigate the wash durability of the antimicrobial finish on the synthetic textile coupons using a method based on AATCC 61 and 135.

## 5.3 Materials

### 5.3.1 Synthetic textile coupons

White synthetic textile cut into 25 mm x 25 mm coupons (65% polyester, 35% cotton, supplied by Alexandra®) were used for experiments.

### 5.3.2 Culture media

*Vide supra* Section 2.3.1.1, in addition, phosphate buffered solution (PBS).

### 5.3.3 Microorganisms

All five test microorganisms were used.

*Vide supra* Section 2.3.1.2

### 5.3.4 Essential oils

Cinnamon and clove oil were used in a 1:1 blend (>94% eugenol and 4.75% eugenyl acetate content).

*Vide supra* Section 2.3.1.3

## 5.4 Experimental

Two antimicrobial testing methods are widely used; the first is based on measurement / examination of zones of inhibition on agar plates, and consists of the immersion of treated material in an agar culture media inoculated with microorganisms. The second method is based on quantification of bacterial populations and the effect the antimicrobial has on the latter. This is achieved via determination of bacteriostatic activity of the treated material that has been autoclaved and subsequently inoculated with a known quantity of microorganisms under investigation. The AATCC offers a variety of test methods that are useful for evaluation of antimicrobial finishes on textiles (Coman 2010).

### 5.4.1 Antibacterial activity assessment of textile materials: Parallel streak method (AATCC 147)

Cultures of the test microorganisms were incubated overnight at 37°C in ISB, and then adjusted to 0.1 OD wavelength, via dilution with ISB. An inoculation loop was fully loaded with the microbial culture; five, 1 cm spaced parallel streaks were then drawn across the surface of the agar in the petri dish. For each microorganism, textile coupons were tested in duplicate (n=2). 25 mm x 25 mm coupons were cut from the samples of synthetic textile. The samples assessed were as follows: untreated controls, 2% (v/v) EO (cinnamon and clove 1:1) loaded MSN layer-by-layer treated coupons (see Section 4.4.2.3), and untreated coupons that were immersed in 2% (v/v) EO blend (Clove and cinnamon 1:1) for 3 minutes and dried at 60°C for 30 minutes. The test coupons were gently pressed into the centre of the petri dish, across the five streaks of microbial culture, in order to ensure intimate contact between the textile coupon

and the inoculated agar surface. The test coupons were then incubated for 24 hours at 37°C before analysis. The test enables rapid assessment of whether (or not) a textile finish possesses bacteriostatic activity. A simple qualitative rating system was used to record results. The following numeric ratings were given for antimicrobial activity according to effect of the samples on the parallel streaks and the contact area of the sample with the agar:

- (1) Represents samples that were able to stop growth beyond the area of contact with the agar
- (2) Denotes no growth on textile samples contact area with the agar,
- (3) Denotes limited growth on the fabric sample contact area with the agar
- (4) Indicates that the fabric sample contact area with the agar is over-grown ( $\geq 50\%$  coverage).

#### 5.4.2 Zone of inhibition

A more advanced agar diffusion method was performed in order to provide a quantitative assessment of the bacteriostatic activity of the treated textiles. The test microorganisms were prepared as in (Section 5.4.1), after which, the selected culture (20  $\mu\text{L}$ ) was pipetted onto the ISA surface and evenly spread over it. 25 mm x 25 mm coupons were cut from the synthetic textile samples. Samples included, untreated controls, 2% (v/v) EO loaded MSN (applied using the layer-by-layer method (Section 4.4.2.3)) treated coupons and previously untreated coupons that were immersed in 2% (v/v) EO blend (Clove and cinnamon 1:1) for 3 minutes and dried at 60°C for 30 minutes. The latter coupons were gently pressed into the centre of their respective petri dish, ensuring intimate contact between the coupon and the microorganism inoculated agar surface. Coupons were assessed in triplicate (n=3). The plates were then incubated at 37°C for 24 hours.

### 5.4.3 Dynamic killing assay

This antimicrobial test method (AATCC 100 / ASTM E2149) provides a quantitative evaluation of the antimicrobial activity of the test coupons. It determines both bacteriostatic (inhibition of multiplication) and bactericidal activity (killing of bacteria) of the EO loaded synthetic textile test coupons.

Test microorganisms were prepared in stationary growth phase, as described in (Section 5.4.1), and also in exponential growth phase, as described previously in (Section 2.3.2.2). 25 mm x 25mm coupons were cut from the synthetic textile samples. As before the samples included; an untreated control, layer-by-layer 2% (v/v) EO loaded MSN treated coupons and untreated coupons that were immersed in 2% (v/v) EO blend (Clove and cinnamon 1:1) for 3 minutes and dried at 60°C for 30 minutes. Each test coupon was shaken at 230 rpm for 24 hours at 37°C, in ISB based microorganism culture (10 mL) which had been adjusted to 0.1 OD, or an PBS microorganism culture (also 10 mL) which had been adjusted to the same initial OD (i.e. CFU/mL). The antimicrobial activity of the test samples was expressed as the percentage reduction of the microorganisms in the test broth. The percentage reduction was calculated using (Equation 5.1).

Equation 5.1. Calculation to determine the percentage reduction in bacterial viability, after 24 hours exposure to antimicrobial textile.

$$R = \frac{(A - B)}{A}$$

Where A is the number of microorganisms in the broth inoculated with treated test coupons immediately after inoculation (zero contact time).

B is the number of microorganisms in the broth inoculated with treated test coupons after the contact period of 24 hours.

R is the percentage reduction.

These calculations were carried out for the test microorganisms in both stationary and exponential phases of growth. At time 0 and at 24 hours, a 1 mL aliquot was serially diluted in PBS and CFU/mL determined for each test microorganism. The experiment was performed once, with triplicate bacterial enumerations for CFU/mL reductions.

#### 5.4.4 Wash durability

The durability of the treated textile finish was tested after 1, 2, 5 and 10 washes, based on AATCC 61 and 135, as a guide. Samples were placed in a 250 mL beaker on a hotplate set to 30°C, with stirring set to level 4. A neutral soap (Bio-D non-biological perfume free washing powder) was added (0.1 g) to the beaker containing the test coupons, with the hotplate set at 30°C for 30 minutes, followed by rinsing in deionised water and drying in a fume cupboard at ambient temperature (air flow of  $0.53 \text{ m}^3 \text{ s}^{-1}$ ) for 30 minutes, with the test coupons spread flat on absorbent tissue. Samples were tested for antimicrobial activity after specified number of washing cycles (1,2,5 and 10) using the method described in (Section 5.4.3). The experiment was performed once, with triplicate bacterial enumerations for CFU/mL reductions.

## 5.5 Results and Discussion

### 5.5.1 Antibacterial activity assessment of textile materials: Parallel streak method (AATCC 147)

The antimicrobial activity of the finished synthetic textile samples were assessed qualitatively by parallel streak and agar diffusion methods. The Parallel streak method is designed to rapidly screen whether (or not) a coated / finished textile shows any bacteriostatic activity. A numeric grading system was used as described in (Section 5.4.1) and the footnote to (Table 5.1) where the data is presented.

Table 5.1. Summary table of test coupon outcomes for the parallel streak method

Fabric Treatment	Microorganism	Rating	
		Run 1	Run 2
Untreated coupons (Control)	<i>S.aureus</i>	3	3
	MRSA	3	3
	<i>E.coli</i>	3	3
	<i>P.aeruginosa</i>	4	4
	<i>C.albicans</i>	3	3
EO MSN treated textile coupons	<i>S.aureus</i>	1	1
	MRSA	1	1
	<i>E.coli</i>	1	1
	<i>P.aeruginosa</i>	2	2
	<i>C.albicans</i>	1	2
EO immersed textile coupons	<i>S.aureus</i>	1	1
	MRSA	1	1
	<i>E.coli</i>	1	1
	<i>P.aeruginosa</i>	2	2
	<i>C.albicans</i>	1	1

- (1) Represents samples that were able to stop growth beyond the area of contact with the agar
- (2) Denotes no growth on textile samples contact area with the agar,
- (3) Denotes limited growth on the fabric sample contact area with the agar
- (4) Indicates that the fabric sample contact area with the agar is over-grown ( $\geq 50\%$  coverage).

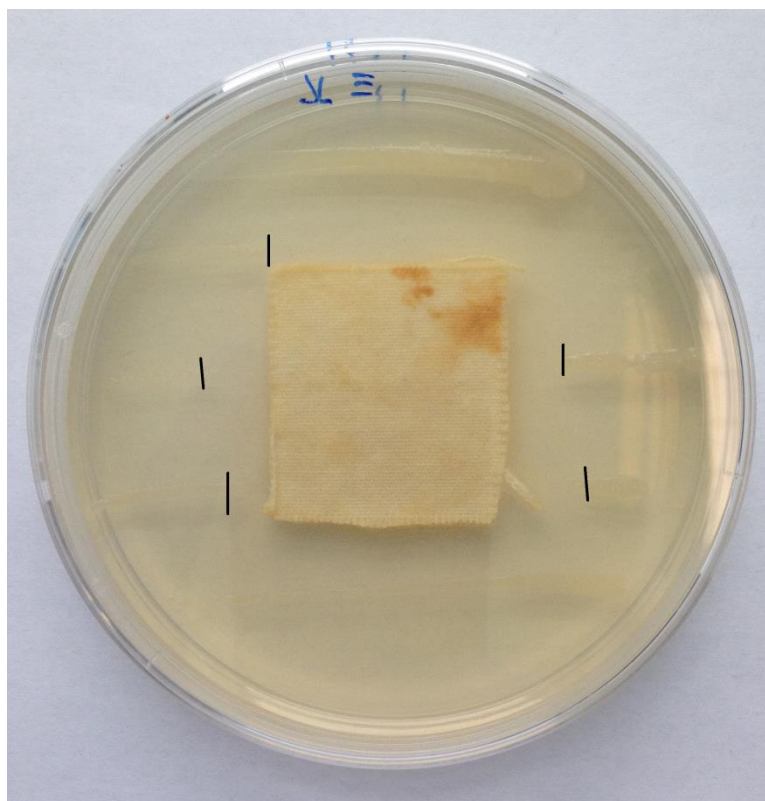


Figure 5.1. Showing an EO MSN treated textile coupon inoculated with *S.aureus* after 24 hour incubation. The black lines denote the zone of inhibition through the parallel bacterial streaks around the EO MSN treated synthetic textile coupon.

It is evident that the untreated control coupons displayed no antimicrobial activity, and hence failed to inhibit microbial growth within the contact area on the inoculated agar that is bounded by the textile coupon. In such cases scores between 3 and 4 were attained. Both EO treated textile coupons displayed bacteriostatic activity against the test microorganisms (Figure 5.1), only differing in efficacy against the yeast *C.albicans* by one rating score, on one replicate. In a study by Walentowska *et al*, a fabric based on a 55% linen, 45% cotton blend, treated with 8% thyme essential oil displayed no fungal growth, with a zone of inhibition around the sample. By comparison, the untreated reference sample was completely covered by mould spores (Walentowska and Foksowicz-Flaczyk 2013). The weaknesses of this method include the lack of quantitative analysis, making comparisons with other methods and textile finishes difficult.

Furthermore, the conditions in the sealed petri dish during the length of incubation are not generally representative of those during actual service of the textile.

### 5.5.2. Zone of inhibition

ZOI were recorded for untreated, EO MSN treated and EO immersed synthetic textile coupons (Figure 5.2)

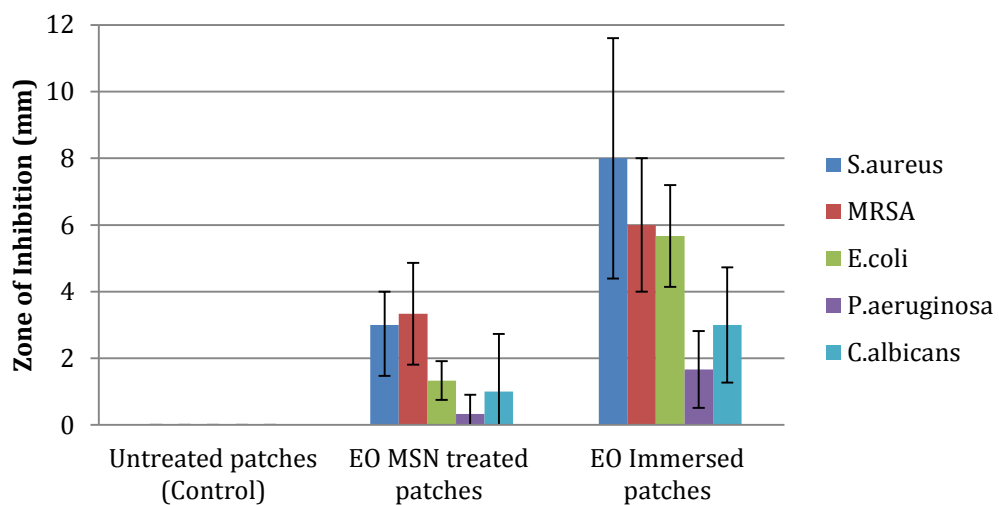


Figure 5.2. Zones of inhibition for untreated, EO MSN treated and EO immersed synthetic textile coupons against five test microorganisms.

Again, the untreated control coupons displayed no antimicrobial effect against the five test microorganisms. Interestingly, the EO immersed coupons, produced larger zones of inhibition, compared to the EO MSN coupons. This is likely to be due to greater diffusion of free EO and vapour in the confined and tape sealed petri dish during the elevated temperature of incubation (37°C). Gram-negative bacteria proved to be more resistant to the antimicrobial effect of the CIN-CLO blend, than Gram-positive bacteria. Chinta et al reported Zols for clove oil on 100% viscose hydroentangled non-woven fibre, at concentrations ranging from 1-10 wt% (Chinta *et al* 2012). At 2 wt% clove oil, Zols of 4 mm were reported for

*S.aureus* and *E. coli*. (Chinta *et al* 2012). Clove oil is comprised of roughly 70% eugenol, however, the EO blend used in this study is a 1:1 cinnamon / clove oil blend, comprising >94% eugenol (Section 2.4.6). This increase in eugenol level led to increased mean Zols of 8 mm and 6 mm, being observed for *S.aureus* and *E.coli* inoculated EO immersed textile coupons, respectively. The same EO blend encapsulated within layer-by-layer (4.4.2.3) fixed MSNs gave mean Zols of 3 mm (Figure 5.3) and 1 mm for for *S.aureus* and *E. coli*, respectively.

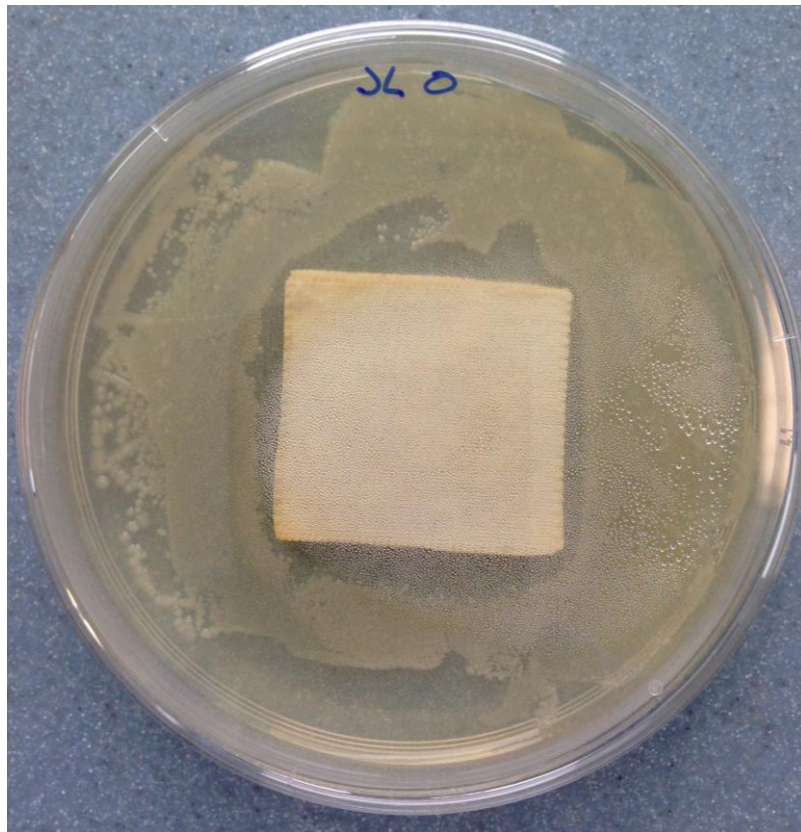


Figure 5.3. Showing an EO MSN textile coupon inoculated with *S.aureus* after 24 hours incubation.

Whilst it can be said both agar diffusion methods are relatively inexpensive and quick, Tanner noted fabrics must normally have considerable activity levels to demonstrate 'zones of inhibition' (Tanner, 2009). Although quantitative values can be assigned for ZOI, the nature of the method causes difficulties in terms of attempting comparison with other products or technologies. The method cannot

differentiate microbial cell death from inhibition of growth. The microbial inoculum generally only contacts the surface of the fabric, furthermore the wet surface of the agar artificially extends the time over which the microbial cells are in a wet and nutritive environment. As the latter is generally longer than expected under actual service conditions, it may be argued that the method is not entirely representative.

### 5.5.3 Dynamic kill assessment

Test and control fabric coupons were saturated with nutritive ISB media, but inoculated with a dilute suspension of microorganisms at a specific OD of 0.1, in static and exponential growth phases (Section 2.3.2.2). The method was based on (AATCC 100/ASTM E2149). Phosphate buffered saline (PBS) was also used as suspending medium for the microorganisms, as it provides the necessary buffered conditions for microorganisms to survive for a limited time, as there are no nutrients to support growth. It was considered this would provide a nutrient-deprived test environment for the EO treated test coupons, relative to the ISB. Microbial concentrations on the fabrics were immediately determined to provide a 'time 0' value and after a 24 h contact period. The percentage difference between the CFU/mL values at the two time periods was used to calculate an antimicrobial activity level (microbial reduction or growth inhibition). These values are displayed in (Figures 5.4 and 5.5).

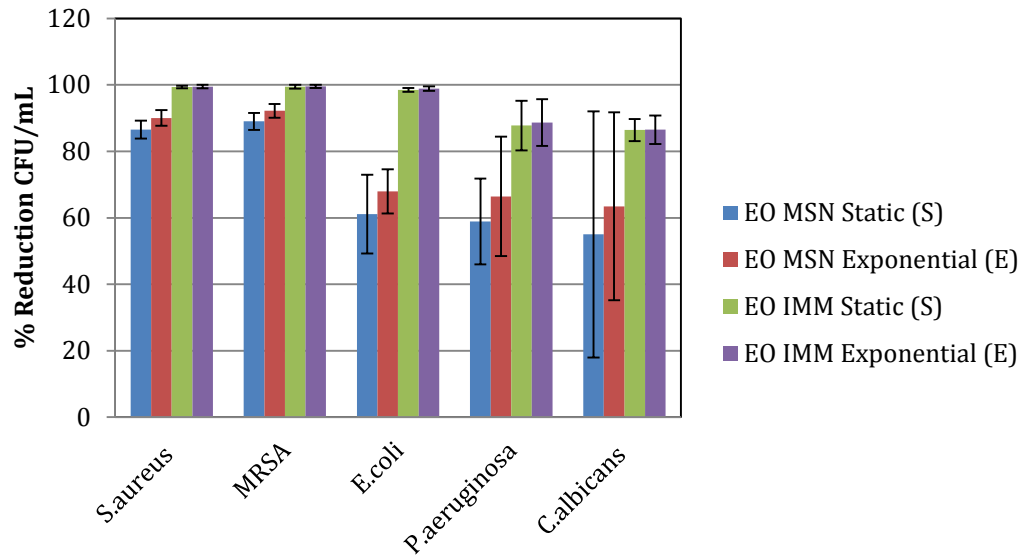


Figure 5.4. % CFU/mL reduction for unwashed EO MSN and EO immersed coupons (EO IMM) after 24 hours contact time in ISB, with test microorganisms in static (S) and exponential (E) phases of growth.

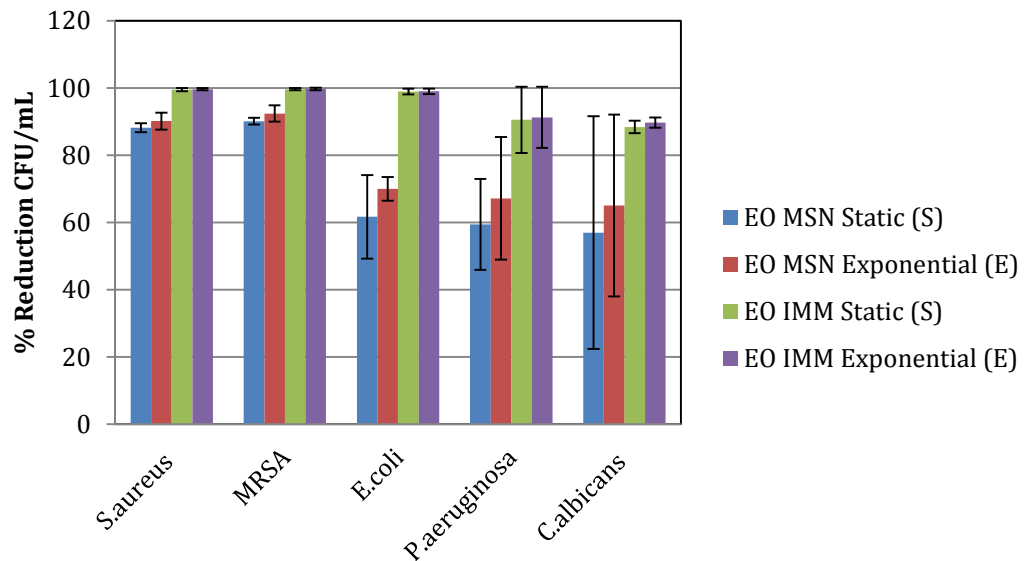


Figure 5.5. CFU/mL % reduction for unwashed EO MSN and EO immersed coupons (EO IMM) after 24 hours contact time in PBS, with test microorganisms in static (S) and exponential (E) phases of growth.

The data show slightly greater % reductions for the EO immersed coupons in comparison to the EO MSN coupons. This is not surprising, considering the free EO diffusion possible from the EO immersed coupons. The concept behind the EO loaded MSNs was to provide slower release of the antimicrobial, thereby allowing for greater durability of the antimicrobial effect, such that it can be maintained after cycles of washing. Un-washed textile coupons, treated using both EO application methods, led to percentage reductions (in CFU/mL) of over 90% for *S. aureus*, *MRSA* and *E.coli* (in both ISB and PBS). The same effect was observed at both phases of microbial growth and in nutritive and non-nutritive environments. It was considered that the latter changes may affect the post-washing efficacy of the two EO treatment methods. Use of such a time kill method for EO treated textiles has not been widely reported in the literature. However, Thilagavathi and Kannaian (2010) investigated woven 100% cotton fabrics with three different treatments; pure geranium extract, microencapsulated geranium by coacervation-spray drying and microencapsulated geranium by spray drying. With unwashed test coupons, reductions in *S. aureus* concentration of 100%, 92% and 94%, respectively, were reported for the three treatments. The respective reductions for *E. coli* were 78%, 55% and 60% (Thilagavathi and Kannaian, 2010). The latter trends are consistent with those observed in the present study for un-washed coupons. AATCC 100 and ASTM E2149 are quantitative methods that are well designed in terms of technicalities related to the testing of antimicrobial agents (Tanner 2009). It is worth noting that there are no clear standards set for 'pass' or 'fail' levels of performance in these method specifications. However, the test is very realistic in terms of prevention of microbial growth, or kill, of microorganisms in wet fabrics. Though if dry conditions are anticipated during service of the textile, it may be argued that the test is unrealistic as the fabrics are kept wet for the full contact period, as it is argued that most antimicrobial agents work best in the presence of liquid.

Furthermore, the incubation for 24 hours at elevated temperature, with agitation is also not realistic. Reductions in activity associated with dried microbial inoculum on textiles in real life may not be as strong as results might suggest for these experiments, as antimicrobials seem to be more efficacious in a liquid medium.

#### 5.5.4 Wash durability testing

The wash durability of the EO treated coupons was assessed based on AATCC 61 and 135 (see Section 5.4.4 for method). The EO encapsulated in MSNs by the layer-by-layer treatment (EO MSN) and free EO immersion (EO IMM) treated coupons were subjected to antimicrobial efficacy assessment (Section 5.5.3) after 1, 2, 5 and 10 washing cycles (Figures 5.6 – 5.13). As the untreated control textile coupons displayed no antimicrobial activity (Section 5.5.2), they were not subjected to wash durability testing.

##### 5.5.4.1 Reduction in %CFU/mL for five test microorganisms in static and exponential growth phase exposed to EO MSN and EO IMM in ISB

The trend of decreasing antimicrobial activity displayed by both EO MSN and EO IMM coupons with increasing washing cycles was consistent irrespective of the microorganisms phase of growth, or test media (ISB or PBS).

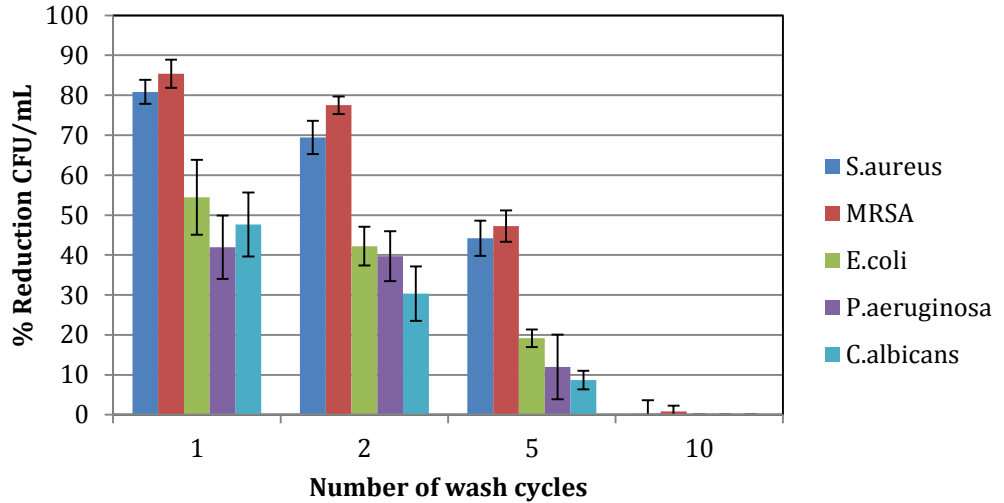


Figure 5.6. CFU/mL % reduction for test microorganisms in static growth phase, exposed to EO MSN coupons after 1, 2, 5 and 10 wash cycles, after 24 hours contact time in ISB.

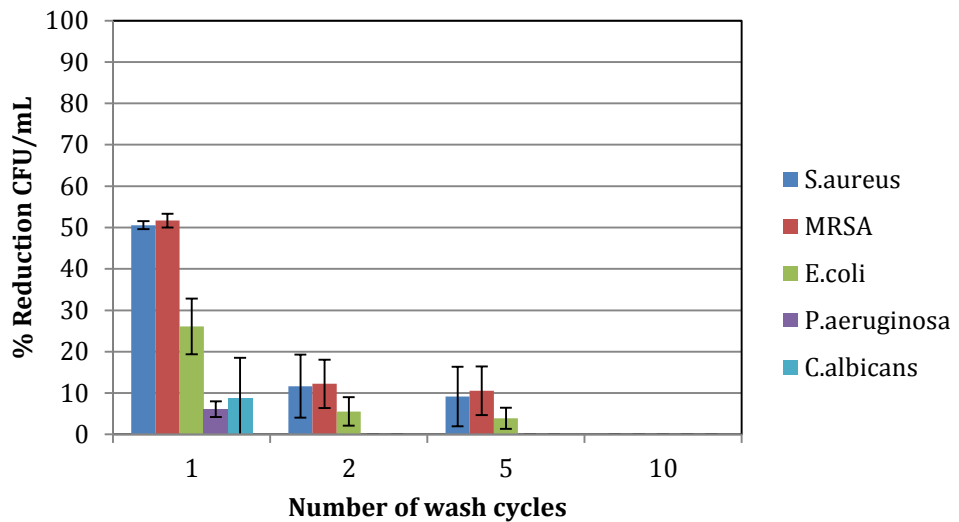


Figure 5.7. CFU/mL % reduction for test microorganisms in static growth phase, exposed to EO IMM coupons after 1, 2, 5 and 10 wash cycles, after 24 hours contact time in ISB.

After one washing cycle, the antimicrobial activity of the EO immersed coupons had clearly diminished in relation to the EO MSN treated coupons. The latter maintained a high level of activity, with %CFU/mL reductions ranging from 42% to 90% across all five microorganisms. In fact, for *S. Aureus*, MRSA, and *E. Coli* the levels of activity were only

slightly reduced relative to the unwashed samples (Figures 5.4 and 5.5). The differences in % CFU/mL reduction between static and exponential phase and nutritive versus non-nutritive test environments were not noticeable. It is possible the potential for differences between these parameters were negated by the length of contact time (24 hours).

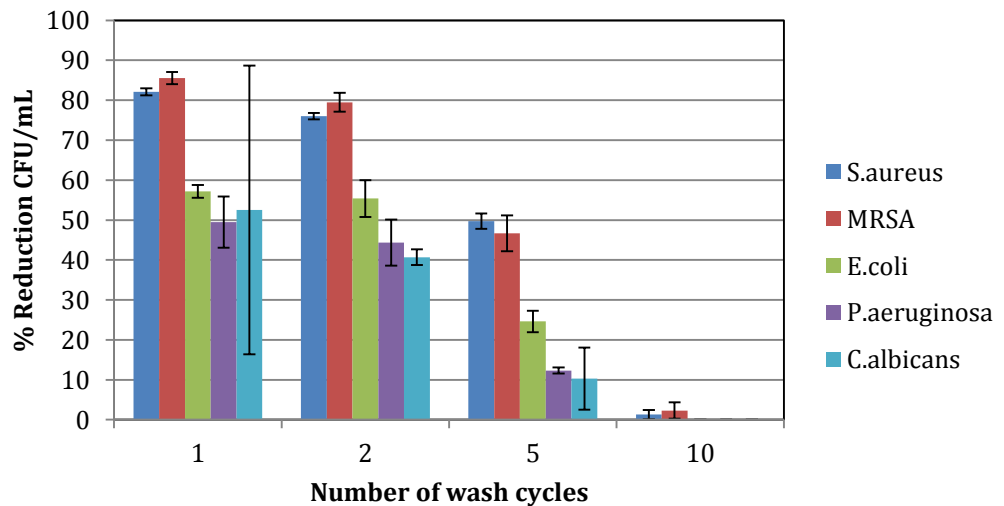


Figure 5.8. CFU/mL % reduction for test microorganisms in exponential growth phase, exposed to EO MSN coupons after 1, 2, 5 and 10 wash cycles, after 24 hours contact time in ISB.

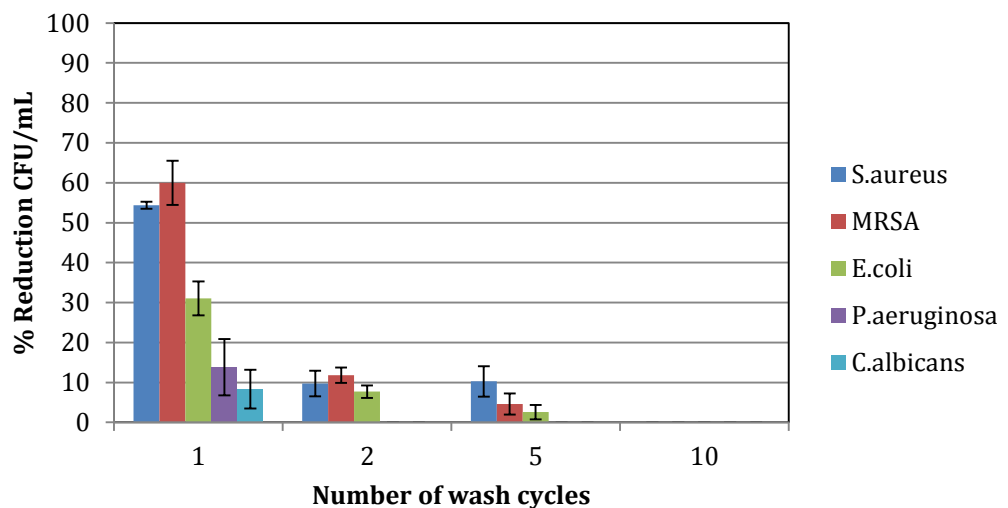


Figure 5.9. CFU/mL % reduction for test microorganisms in exponential growth phase, exposed to EO IMM coupons after 1, 2, 5 and 10 wash cycles, after 24 hours contact time in ISB.

The % reductions in CFU/mL show the Gram-positive bacteria are more susceptible to the EO blend, compared to the Gram-negative bacteria. This finding is documented in the literature for the antibacterial activity of EOs (Nazzaro *et al* 2013). The outer cell wall present in Gram-negative bacteria acts as a barrier to EO integration/penetration and subsequent cell wall lysis, seen with Gram-positive bacteria. This may be the reason for the lower % reductions in CFU/mL seen for *E.coli* and *P.aeruginosa* in comparison to the Gram-positive test bacteria. The yeast, *C.albicans* is also seen to be robust to the antimicrobial actions of the EO blend, relative to Gram-positive bacteria. This could be due to the protective effects of the cell wall, acting as a barrier to the cytoplasmic membrane, which Chen *et al* (2013) noted as the primary target of EO antifungal action.

#### 5.5.4.2 Reduction in %CFU/mL for five test microorganisms in static and exponential growth phase exposed to EO MSN and EO IMM in PBS

After five cycles of washing, Thilagavathi and Kannaian reported bacterial reduction percentages of 92% and 55% for *S. aureus* and *E. coli*, respectively, for microencapsulated geranium oil on 100% cotton test samples (Thilagavathi and Kannaian, 2010). By comparison, the EO MSN samples produced % reductions in CFU/mL of 44% and 19% after five wash cycles, for the same bacteria.

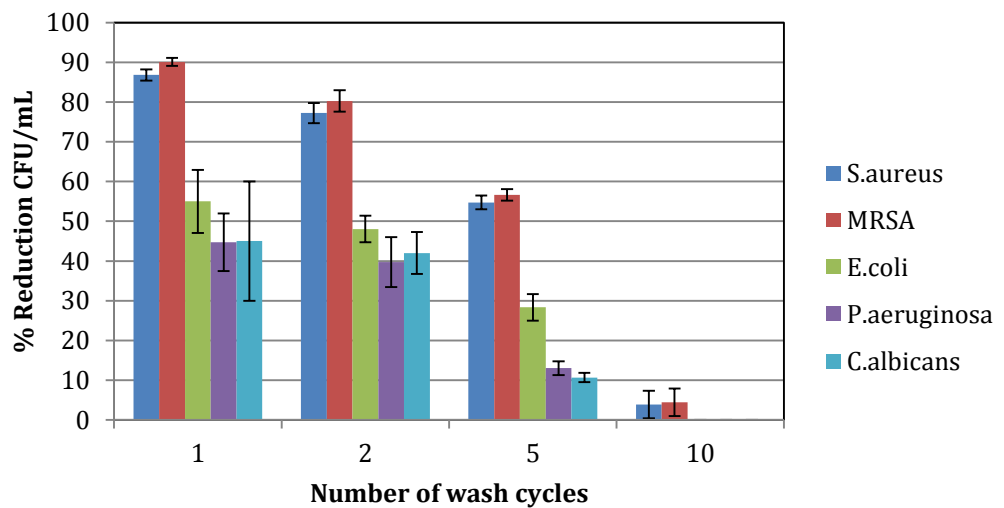


Figure 5.10. CFU/mL % reduction for test microorganisms in static growth phase, exposed to EO MSN coupons after 1, 2, 5 and 10 wash cycles, after 24 hours contact time in PBS.

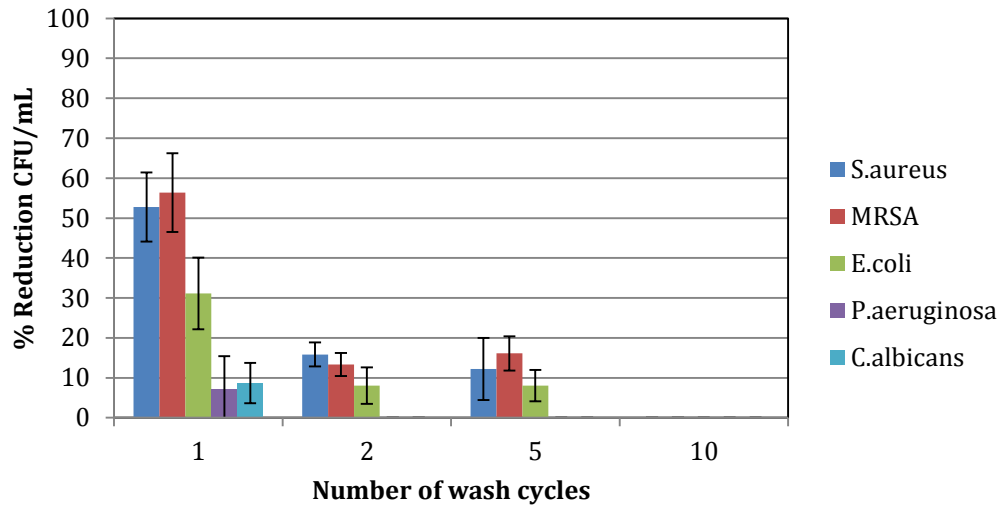


Figure 5.11. CFU/mL % reduction for test microorganisms in static growth phase, exposed to EO IMM coupons after 1, 2, 5 and 10 wash cycles, after 24 hours contact time in PBS.

The use of the cinnamon / clove oil blend in the present study and use of 100 % geranium oil in Thilagavathi and Kannaian's study renders direct comparison of performance impossible. However, the use of these three EOs (CIN, CLO and GER) individually at the same concentrations against the same microorganisms show they are similar in terms of antimicrobial activity (Section 2.4.3).

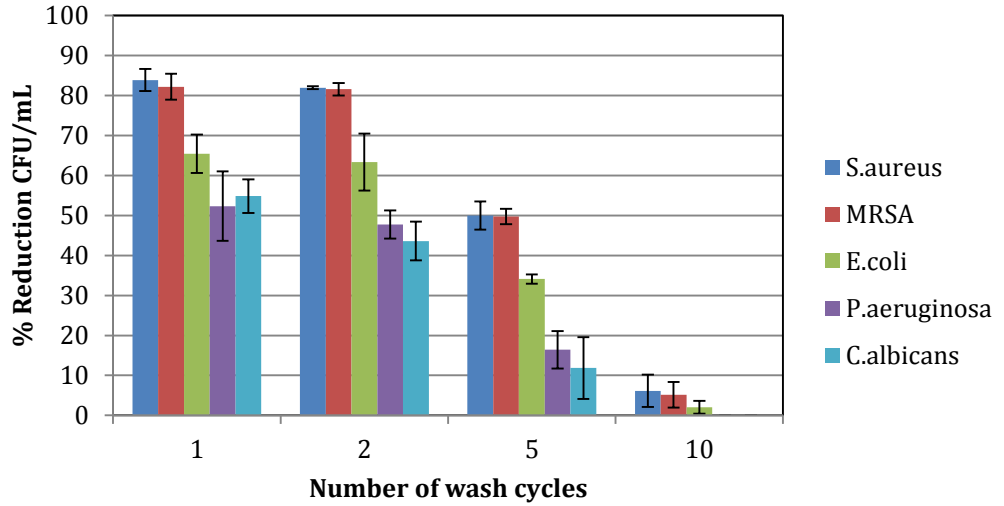


Figure 5.12. CFU/mL % reduction for test microorganisms in exponential growth phase, exposed to EO MSN coupons after 1, 2, 5 and 10 wash cycles, after 24 hours contact time in PBS.

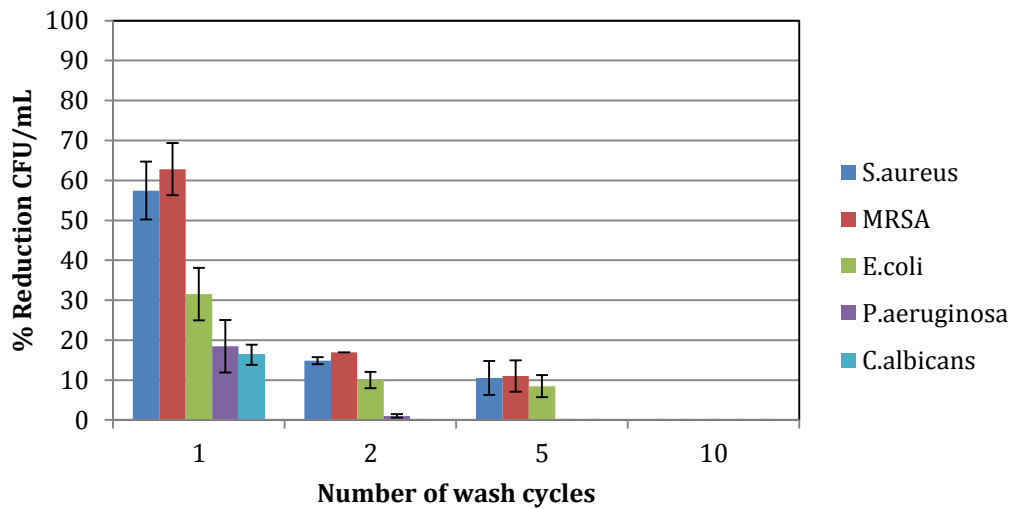


Figure 5.13. CFU/mL % reduction for test microorganisms in exponential growth phase, exposed to EO IMM coupons after 1, 2, 5 and 10 wash cycles, after 24 hours contact time in PBS.

Thilagavathi and Kannaian found that microencapsulated (coacervated and spray dried) geranium oil on cotton was effective against *S.aureus* and *E.coli* after 15 wash cycles. In comparison, cotton samples directly treated with geranium oil (non-encapsulated) displayed no antibacterial activity after 15 washes for both bacteria (Thilagavathi and Kannaian,

2010). There are few investigations of wash durability of EO treated textiles reported in the literature. In contrast, there are rather more reported investigations of silver and zinc oxide nanoparticle finishes on textiles and their wash durability. For example, Rajendran reported significant antimicrobial after 10 wash cycles for cotton coupons treated with ZnO nanoparticles. After 10 wash cycles, bacterial population reductions of 74% and 70% were reported for *S.aureus* and *E.coli*, respectively. Significant antibacterial activity was also observed after 20 wash cycles (Rajendran, 2010).

When investigating and reporting 'antimicrobial activity' it is important to define and understand the broad use of the term. For the current work, antimicrobial is understood to mean anything that has a negative effect on the unchecked growth of microorganisms (Tanner 2009). On the lowest end of the antimicrobial spectrum, in terms of different antimicrobials and their respective strengths or toxicity, a treated textile may slow the rate of growth of a few, or perhaps one microorganism. To deter growth may aid in the control of odour on textiles, or even the visual aesthetics of a garment, in terms of discolouration. However, it is not likely to impact the spread of potentially infectious or antimicrobial resistant microorganisms through a healthcare environment. More significant antimicrobial effects may cause microorganism growth to become static, with even stronger antimicrobials, which display low MICs, killing a percentage of microorganisms over time. The most potent end of the antimicrobial spectrum generally refers to toxic chemicals that disinfect, or render surfaces sterile within 10 minutes of contact, such as Quaternary ammonium compounds (QACs) and glutaraldehyde (Ballantyne and Jordan 2001). The latter will have broad-spectrum

activity against all viruses, bacteria and spore-formers. Few antimicrobial textiles kill large percentages of microorganisms in under ten minutes of contact. The standard methods of testing antimicrobial textile finishes, in general, analyse low level antimicrobial activity over a longer period of time (usually 24 hours), whereas methods used to test liquid chemical disinfectants and sterilisers, look for high level antimicrobial activity over a short period of time (usually up to 10 minutes).

The results show the EO MSN treated test coupons displayed good antimicrobial activity up to five wash cycles, with insignificant activity remaining after 10 wash cycles, whereas the antimicrobial activity of the EO immersed textile coupons diminished significantly over one to two washing cycles. The results show that coating of textile fibres with an MSN encapsulated EO blend (using the layer-by-layer application method, described in Section 4.4.2.3) leads to a much more sustained antimicrobial activity that is able to withstand several wash cycles.

## 5.6 Conclusions

- The test coupons were screened for bacteriostatic activity against the five test microorganisms qualitatively using parallel streak and quantitatively using zone of inhibition methods. The EO-MSN and EO immersion treated coupons displaying bacteriostatic activity against all five microorganisms and recording zones of inhibition.
- The EO-MSN and EO immersed test coupons (without being subjected to washing) were evaluated for CFU/mL reductions over a 24 hour period, with agitation. Both EO treatment methods led to high levels of reduction in CFU/mL after 24 hours exposure to the five test microorganisms. The microbial growth phase or liquid medium conditions (i.e. nutritive or non-nutritive) had no influence on the trends observed.
- The EO-MSN treated coupons showed useful antimicrobial activity after five wash cycles, though antimicrobial activity was barely noticeable after 10 wash cycles. In contrast, the antimicrobial activity of the EO immersed coupons (i.e. un-bound EO) was noticeably diminished after one to two wash cycles, though ca. 10 % CFU/mL reductions were observed for the more vulnerable organisms (*S. aureus* and MRSA) after five wash cycles.
- The results show that the EO-MSN coating (applied using the layer-by-layer method) confers sustained antimicrobial activity to the synthetic textile. Such sustained activity was not possible using un-bound EO.

## **Chapter 6**

### **Overall conclusions and further work**

## 6.1 Overall conclusions

There are concluding summaries given at the end of each preceding chapter. This section will provide overall conclusions and summarise the degree to which the original aims were achieved.

The primary objective of the work was to investigate the potential for the use of natural antimicrobials to add antimicrobial efficacy to synthetic textiles. Cinnamon, clove and lemongrass demonstrated good antimicrobial efficacy individually against the Gram-positive microorganisms and *E.coli* of the panel of microorganisms tested, as others have shown (Hammer 1999, Loughlin 2008, Cox 2001, Kwiecinski 2009), however lacked efficacy against the Gram-negative *P.aeruginosa* at less than 2% (v/v). It was thought blending the EOs may produce a synergistic effect against the microorganisms. Numerous blends displayed a reduction in the concentration (v/v) of oil necessary to inhibit microbial growth, and several blends displayed synergy against *P.aeruginosa*, which showed poor results with individual EOs. A 1:1 blend of Cinnamon-clove registered the best FIC results across the five microorganisms tested and producing the lowest MIC against the most robust microorganism, *P.aeruginosa*. For the selected blend of clove and cinnamon (1:1), the percentage of the main antimicrobial constituent increased from 82.85 and 76.39, respectively, to 94.84 when in combination.

MSNs were synthesised and investigated as potential encapsulants for the selected EO blend. Lu (2007) had shown hydrophobic compounds were able to load into MSN pores. A loading level of ca. 70% was

achieved using an immersion loading technique, after the initial solvent evaporation technique returned a loading level of roughly 30-35%. GCMS analysis of solvent washed EO loaded MSNs confirmed the ability of the EO antimicrobial components to leave the MSN pores. After confirming the blank MSNs exerted no antimicrobial effect, the EO loaded MSNs displayed bactericidal capacity against the five microorganisms tested between (25-50 mg/mL).

A range of different techniques were investigated to chemically affix the MSNs to synthetic fibres. A 3:1 formulation of ormosil precursors (MTEOS:TEOS) at pH 2 was chosen to provide a flexible yet robust thin film coverage of the synthetic fibres, allowing bending of the textile and a large surface area for MSNs to attach on to (Estella 2007, Perrera 2013). While one pot synthesis and silane grafted MSNs failed to affix the MSNs to the synthetic fibres without occluding the MSN pores (Pardal 2009), a layer-by-layer technique allowed the MSNs to be chemically affixed to the synthetic fibres with no occlusion of the MSN pores. The layer-by-layer treated samples were also subjected to headspace sampling to ensure the EO antimicrobial components could diffuse from the pores, with eugenol still diffusing after a sampling time of 24 hours.

The EO-MSN treated coupons showed useful antimicrobial activity after five wash cycles, though antimicrobial activity was barely noticeable after 10 wash cycles. In contrast, the antimicrobial activity of the EO immersed coupons (i.e. un-bound EO) was noticeably diminished after one to two wash cycles, though ca. 10 % CFU/mL reductions were observed for the more vulnerable organisms (*S. Aureus* and MRSA) after five wash cycles. The results show that the EO-MSN coating (applied using the layer-by-layer method) confers sustained antimicrobial activity

to the synthetic textile. Such sustained activity was not possible using un-bound EO, as found previously by (Thilagavathi and Kannaian 2010).

The project set out to investigate a controlled release system for EOs that could be used as a coating for synthetic textile fibres, and thereby confer antimicrobial activity to the textile. The successful product was targeted for use in healthcare environments to combat the spread of HCAs. The project was broken down into a number of key areas to enable fulfilment of the primary aims. EO MSN synthetic textile coupons (treated using the layer-by-layer method developed in this project) displayed good antimicrobial activity up to five wash cycles, whereas the antimicrobial activity of the EO immersed textile coupons diminished significantly over one to two washing cycles.

## 6.2 Further work

The initial antimicrobial screening investigated the efficacy of natural antimicrobial EOs individually and in blends. In addition, GC-MS was used to analyse their chemical composition. There was not time during the project to fully consider the changes in chemical composition when EOs are blended and subsequent changes in antimicrobial activity. GCMS analysis of EO blends ranging from synergistic to antagonistic should be undertaken to provide understanding of how the abundance of the main antimicrobial constituents for an individual oil change when blended. This may lead to understanding why certain EOs are more efficacious in their antimicrobial activity against microorganisms associated with HCAs. It would also be interesting to combine other liquid biocides with the EOs, in the quest to find antimicrobial synergy.

Antiseptics, such as triclosan, and polyhexamethylene biguanide could be used for this purpose.

The range of microorganisms tested in this study could be broadened, with anaerobic bacteria, such as *C.difficile*. In addition, the planktonic work could be complemented by challenging biofilms with the antimicrobials.

The antimicrobial activity of blank and EO loaded MSNs was investigated. It would have been worthwhile imaging the EO loaded MSNs and the test microorganisms in confinement, to gain an understanding of the MSN interaction with the bacterial or yeast cell wall, or capsule. Chemical fixatives used in such procedures would be toxic for the microorganisms and possibly cause lysing of the cells. It is possible dehydration via increasing concentrations of ethanol could be used, to preserve the microbial interaction with the MSNs. The work could again be broadened by the use of amorphous SBA-15 MSNs, or the use of different surfactants for the TEOS to adsorb on and polymerise. This would allow different pore size, surface area and antimicrobial loading levels, which could impact antimicrobial activity and the ability to control the release.

It has been shown in the literature that the skeletal structure and subsequent porosity of ormosil gels can be controlled via pH during synthesis. Producing gels of increased porosity, which could then be BET and BJH analysed, would possibly allow further investigation of loading these porous matrices with antimicrobials.

The EO MSN treated synthetic textile coupons were shown to have good antimicrobial activity for up to five washes, demonstrating the wash

durability of the antimicrobial finish. It was suggested the coupons could also have undergone challenge testing after increasing lengths of time, having been subjected to different environments commonly encountered in healthcare settings.

Finally, the initial aim of producing antimicrobial synthetic textiles intended for upholstery coverings or tunics / uniforms, could conceivably be used in wound dressings. Currently, expensive silver impregnated wound dressings are used (Boateng and Catanzano 2015), there could potentially be scope for wound dressings with natural antimicrobials encapsulated (Liakos *et al* 2014).

## References

1. Ahmed, I., Aqil, F. (2009), 'New Strategies Combating Bacterial Infection', (Wiley-Blackwell), 177-179.
2. Andrews, J., (2001), 'Determination of minimum inhibitory concentrations', Journal of Antimicrobial Chemotherapy, 48, 5-16.
3. Avrain, L., Mertens, P., Van Bambeke, F., (2013), 'RND efflux pumps in *P.aeruginosa*: an underestimated resistance mechanism', Clinical Laboratory International, 26-28.
4. Ballantyne, B., Jordan, S. L., (2001), 'Toxicological, Medical and Industrial Hygiene Aspects of Glutaraldehyde with Particular Reference to its Biocidal Use in Cold Sterilization Procedures', Journal of Applied Toxicology, 21, 131-151.
5. Bartholome, C., Beyou, E., Bourgeat-Lami, E., Chaumont, P., Zydowicz, N., (2003), 'Nitroxide-Mediated Polymerizations from Silica Nanoparticle Surfaces: "Graft from" Polymerization of Styrene Using a Triethoxysilyl-Terminated Alkoxyamine Initiator', Macromolecules, 36, 7946-7952.
6. Becerril, R., Nerin, C., Gomez-Lus, R., (2012), 'Evaluation of bacterial resistance to essential oils and antibiotics after exposure to oregano and cinnamon essential oils', Foodborne Pathogens and Disease, 9, 699-705.
7. Beck, J. S., Vartuli, J. C., Roth, W. J., Leonowicz, M. E., Kresge, C. T., Schmitt, K. D., Chu, C. T. W, Olson, D. H., Sheppard, E. W., (1992), 'A new family of mesoporous molecular sieves prepared with liquid crystal templates', Journal of American Chemistry Society, 1992, 114, 10834-10843.
8. Bescher. E., Mackenzie. J. D., (2003), 'Sol- Gel Coatings for the Protection of Brass and Bronze', Journal of sol-gel science and technology, 26, 1223-1226.

9. Blomquist, P. H., (2006), 'Methicillin resistant *Staphylococcus aureus* infections of the eye and orbit', *Transactions of the American Ophthalmic Society*, 104, 322.
10. Boateng, J., Catanzano, O., (2015), 'Advanced Therapeutic Dressings for Effective Wound Healing – A Review', *Journal of Pharmaceutical Sciences*, 104, 3653-3680.
11. Boyce, J. M. (2007), 'Environmental contamination makes an important contribution to hospital infection', *Journal of Hospital Infection*, 65, 50-54.
12. Brady, A., Loughlin, R., Gilpin, D., Kearney, P. and Tunney, M., (2006) 'In vitro activity of tea-tree oil against clinical skin isolates of methicillin-resistant and -sensitive *Staphylococcus aureus* and coagulase-negative staphylococci growing planktonically and as biofilms', *Journal of Medical Microbiology*, 55, 1375–1380.
13. Brenes, M., Medina, E., Romero, C., De Castro, A., (2007), 'Antimicrobial activity of olive oil', *Journal of Food Protection*, 70, 1194-9.
14. Brinker, C.J., Scherer, G.W., (1990), *Sol-Gel Science: The Physics and Chemistry of Sol-Gel Processing*. Academic Press, New York.
15. Burt, S., (2004), 'Essential oils: their antibacterial properties and potential applications in foods - a review', *International Journal of Food Microbiology*, 94, 223-253.
16. Camilli, A., Bassler, B.L., (2006), 'Bacterial small-molecule signaling pathways', *Science*, 311, 1113-1116.
17. Carson, C.F., Riley, T.V., (1993), 'Antimicrobial activity of the essential oil of *Melaleuca alternifolia*', *Letters in Applied Microbiology*, 16, 49-55.
18. Carson, C. F., Hammer, K. A., Riley, T. V., (2006), '*Melaleuca alternifolia* (Tea Tree) Oil: a Review of Antimicrobial and Other Medicinal Properties', *Clinical Microbiology Reviews*, 19, 50-62.

19. Cepeda, J. A., Whitehouse, T., Cooper, B., Hails, J., Jones, K., Kwaku, F., Taylor, L., Hayman, S., Cookson, B., Shaw, S., Kibbler, C., Singer, M., Bellingan, G., Peter, A., Wilson, R. (2005), 'Isolation of patients in single rooms or cohorts to reduce spread of MRSA in intensive-care units: prospective two-centre study', *Lancet* , 365, 295 – 304.
20. Chaieb, K., (2007), 'The chemical composition and biological activity of clove essential oil, *Eugenia caryophyllata* (*Syzgium aromaticum* L.Myrtaceae): A short review', *Phytotherapy*, 21, 501-506.
21. Chapman, J. S. (2003), 'Disinfectant resistance mechanisms, cross-resistance, and co-resistance', *International biodeterioration and biodisregulation*, 51, 271-276.
22. Chen, Y., Zeng, H., Tian, J., Ban, X., Ma, B., Wang, Y., (2013), 'Antifungal mechanism of essential oil from *Anethum graveolens* seeds against *Candida albicans*', *Journal of Medical Microbiology*, 62, 1175-1183.
23. Chinta, S. K., Landage, S. M., Abhishek, Sonawane, K. D., Jalkate, C. B., (2012), 'Medical textiles – application of essential oils as antimicrobial agent on nonwoven', *Global Journal of Bio-Science and Biotechnology*, 1, 75-80.
24. Chizzola, R., Michitsch, H., Franz, C., (2008), 'Antioxidative Properties of *Thymus vulgaris* Leaves: Comparison of Different Extracts and Essential Oil Chemotypes', *JOURNAL OF AGRICULTURAL AND FOOD CHEMISTRY*, 56, 6897-6904.
25. Cobben, N.A., Drent, M., Jonkers, M., Wouters, E.F., Vaneechoutte, M., and Stobberingh, E.E. (1996). Outbreak of severe *Pseudomonas aeruginosa* respiratory infections due to contaminated nebulizers. *J Hosp Infect* 33, 63-70.
26. Cohen, J. O., *Medical Microbiology*, (1986), S. Baron (Second Edition),

Menlo Park, Addison-Wesley.

27. Coman, D., Oancea, S., Vranceanu, N., (2010), 'Biofunctionalization of textile materials by antimicrobial treatments: a critical overview', *Romanian Biotechnological Letters*, 15, 4913-4921.
28. Cox, S. D., Gustafson, J. E., Mann, C. M., Markham, J. L., Liew, Y. C., Hartlans, R. P., Bell, H. C., Warmington, J. R., Wyllie, S. G., (1998), 'Tea tree oil causes K<sup>+</sup> leakage and inhibits respiration in *Escherichia coli*', *Letters in Applied Microbiology*, 26, 355-358.
29. Cox, S. D., Mann, C. M., Markham, J. L., Bell, H. C., Gustafson, J. E., Warmington, J. R., Wylie, S. G., (2000), 'The mode of antimicrobial action of the essential oil of *Melaleuca alternifolia* (tea tree)', *Journal of Applied Microbiology*, 88, 170-175.
30. Cox, S. D., Mann, C. M., Markham, J. L., (2001), 'Interactions between components of the essential oil *Melaleuca alternifolia*', *Journal of Applied Microbiology*, 91, 492-497.
31. Curran, M.D., Stiegman, A. E., (1999), 'Morphology and pore structure of silica xerogels made at low pH', *Journal of Non-Crystalline Solids*, 249, 62-68.
32. Curtis, L., Lawley, R., 'Micro-Facts, The Working Companion for Food Microbiologists', 5 ed. (2003), Surrey: Leatherhead Publishing.
33. Curtis, L.T. (2008). Prevention of hospital-acquired infections: review of non- pharmacological interventions. *Journal of Hospital Infections* 69, 204-219.
34. Damani, N. N. (2003). *Manual of Infection Control Procedures*. A. M. Ennmerson. 2nd Edition. London: Greenwich Medical Media Limited. ISBN 1841101079.
35. Deng, Y., Wei, J., Sun, Z., Zhao, D., (2013), 'Large-pore ordered mesoporous materials template from non-Pluronic amphiphilic block

- copolymers', *The Royal Society of Chemistry*, 42, 4054-4070.
36. Derakhshan, S., Sattari, M., Bigdeli, M., (2008), 'Effect of subinhibitory concentrations of cumin seed essential oil and alcoholic extract on the morphology, capsule expression and urease activity of *Klebsiella pneumoniae*', *International Journal of Antimicrobial Agents*, 32, 432-436.
  37. Derwich, E., Benziane, Z., Taouil. R., (2010), 'GC/MS Analysis of Volatile Compounds of the Essential Oil of the Leaves of *Mentha pulegium* growing in Morocco', *Chemical Bulletin of "Politehnica" University of Timisoara, Romania*, 55, 103-106.
  38. Devreux, F., Boilot, J.P., Chaput, F., Lecomte, A., (1990), 'Sol-gel condensation of rapidly hydrolyzed silicon alkoxides—a joint Si-29 NMR and small-angle X-ray-scattering study', *Physical Review A*, 41, 6901–6909.
  39. DiazGranados, C.A., Jones, M.Y., Kongphet-Tran, T., White, N., Shapiro, M., Wang, Y.F., Ray, S.M., and Blumberg, H.M. (2009). Outbreak of *Pseudomonas aeruginosa* infection associated with contamination of a flexible bronchoscope. *Infection Control Hospital Epidemiology* 30, 550-555.
  40. Donohue. M. D., Aranovich. G.L., (1998), 'Classification of Gibbs adsorption isotherms', *Advances in Colloid and interface Science*, 76-77, 137-152.
  41. Dorman, H. J., Deans, S. G., (2000), 'Antimicrobial agents from plants: antibacterial activity of plant volatile oils', *Journal of Applied Microbiology*, 88, 308-316.
  42. Dubas, S. T., Kumlangdudsana, P., Potiyaraj, P., (2006), 'Layer-by-layer deposition of antimicrobial silver nanoparticles on textile fibers', *Colloids and Surfaces*, 289, 105-109.
  43. Echeverria, J.C., Estella, J., Barberia, V., Musgo, J., Garrido, J.J., (2010),

- 'Synthesis- thesis and characterization of ultramicroporous silica xerogels', *Journal of Non-Crystalline Solids* 356, 378–382.
44. Elsner, P., Hatch, K., Wigger-Alberti, W., (2003), 'Textiles and the Skin', *Current Problems in Dermatology*, 31, 35-49.
  45. Elsner, P., (2006), 'Antimicrobials and the Skin Physiological and Pathological Flora', *Current Problems in Dermatology*, 33, 35-41.
  46. Estella, J., Echeverria, J.C., Laguna, M., Garrido, J.J., (2006), 'Silica xerogels of tailored porosity as support matrix for optical chemical sensors. Simultaneous effect of pH, ethanol: TEOS and water: TEOS molar ratios, and synthesis temperature on gelation time, and textural and structural properties', *Journal of Non-Crystalline Solids*, 353, 286–294.
  47. Estella, J., Echeverria, J.C., Laguna, M., Garrido, J.J., (2007), 'Effects of aging and drying conditions on the structural and textural properties of silica gels', *Microporous Mesoporous Materials*, 102, 274–282.
  48. Feng, Q. J., Wu, G., Chen, F., Cui, T., Kim J. Kim, (2000) 'A mechanistic study of the antibacterial effect of silver ions on *Escherichia coli* and *Staphylococcus aureus*', *Journal of Biomedical Materials Research*, 52, 662-8.
  49. Fernandes, R. M. F., Buzaglo, M., Regev, O., Marques, E. F., Furo, I., (2015), 'Surface Coverage and Competitive Adsorption on Carbon Nanotubes', *Journal of Physical Chemistry*, 119, 22190-22197.
  50. Flamini, G., Cioni, P. L., Puleio, R., Morelli, I., Panizzi, L., (1999), 'Antimicrobial activity of the essential oil of *Calamintha nepeta* and its constituent Pulegone against bacteria and fungi', *Phytotherapy Research*, 13, 349-351.
  51. Foster, J.W., (2004), '*Escherichia coli* acid resistance: tales of an amateur acidophile', *Nature Microbiology Review*, 2, 898-907.

52. Fux, C. A., Costerton, J. W., Stewart, P. S., Stoodley, P., (2005), 'Survival strategies of infectious biofilms', *TRENDS in Microbiology*, 13, 34-40.
53. Fyfe, C. A., Aroca, P. P., (1997), 'A kinetic analysis of the initial stages of the sol-gel reactions of methyltriethoxysilane (MTES) and a mixed MTES/tetraethoxysilane system by high-resolution Si-29 NMR spectroscopy', *Journal of Physical Chemistry B*, 101, 9504–9509.
54. Gao, Y., Cranston, R., (2008), 'Recent advances in antimicrobial treatments of textiles', *Textile Research Journal*, 78, 68–72.
55. Gayoso, C. W., Lima, E. O., Oliveira, V. T., Pereira, F. O., Souza, E. L., Lima, I. O. & Navarro, D. F., (2005), 'Sensitivity of fungi isolated from onychomycosis to *Eugenia caryophyllata* essential oil and eugenol', *Fitoterapia*, 76, 247–249.
56. Gende, L. B., Floris, I., Fritz, R., Eguaras, M. J., (2008), 'Antimicrobial activity of cinnamon essential oil and its main components against *Paenibacillus* larvae from Argentina', *Bulletin of Insectology*, 61, 1-4.
57. Giordoni, R., Trebaux, J., Masi, M., Regli, P., (2001), 'Enhanced antifungal activity of ketoconazole by *Euphorbia characias* latex against *Candida albicans*', *Journal of Ethno-pharmacology*, 78, 1-5.
58. Gobetti, M., de Angelis, M., di Cagno, R., Minervini, F., Limitone, A., (2007), 'Cell-cell communication in food related bacteria', *International Journal of Food Microbiology*, 120, 34-45.
59. Groen. J. C., Peffer. L. A. A., Pèrez-Ramírez. J., (2003), 'Pore size determination in modified micro- and mesoporous materials. Pitfalls and limitations in gas adsorption data analysis', *Microporous and Mesoporous Materials*, 60, 1- 17.
60. Gustafson, J. E., (1998), 'Effects of tea tree oil on *Escherichia coli*', *Letters in Applied Microbiology*, 26, 194-198.
61. Hajji, P., David, L., Gerard, J. F., Pascual, J. P., Vigier, G., (1999),

- 'Synthesis, structure, and morphology of polymer-silica hybrid nanocomposites based on hydroxyethyl methacrylate', *Journal of Polymer Science*, 37, 3172-3187.
62. Hammer, K. A., Carson, C. F., Riley, T. V., (1999), 'Antimicrobial activity of essential oils and other plant extracts', *Journal of Applied Microbiology*, 86, 985-990.
63. Haufe, H., Muschter, K., Siegert, J., Bottcher, H., (2008), 'Bioactive textiles by sol-gel immobilised natural active agents', *Journal of Sol-Gel Science and Technology*, 45, 97-101.
64. Health Protection Agency, (2009), 'Pseudomonas spp. and Stenotrophomonas maltophilia bacteraemia in England, Wales and Northern Ireland, 2004 to 2008'.
65. Health Protection Agency. (2012) English National Point Prevalence Survey on Healthcare Associated Infections and Antimicrobial Use, 2011: Preliminary data. Health Protection Agency: London.
66. Hench, L. L., West, J. K., (1990), 'The Sol-Gel Process', *Chemical Reviews*, 90, 33-72.
67. Hetrick, E. M., Shin, J. H., Stasko, N. A., Johnson, C. B., Wespe, D. A., Holmuhamedov, E., Schoenfisch, M. H., (2007), 'Bactericidal Efficacy of Nitric Oxide – Releasing Silica Nanoparticles', *American Chemical Society Nano Letters*, 2, 235-246.
68. Himmel, B., Gerber, T., Burger, H., (1990), 'Wax- investigations and saxes- investigations of structure formation in alcoholic SiO<sub>2</sub> solutions', *Journal of Non-Crystalline Solids*, 119, 1–13.
69. HIS (2007). Results of third national prevalence survey of healthcare associated infection in England released.
70. Hogberg, L.D., Heddini, A., and Cars, O. (2010). The global need for effective antibiotics: challenges and recent advances. *Trends*

Pharmacological Science 31, 509-515.

71. Holme, I., (2007), 'Innovative technologies for high performance textiles', *Coloration Technologies*, 123, 59-73.
72. Hong, C. Y., Li, Xin, Pan, C. Y., (2007), 'Grafting polymer nanoshell onto the exterior surface of mesoporous silica nanoparticles via the surface reversible addition-fragmentation chain transfer polymerization', *European Polymer Journal*, 43, 4114-4122.
73. Horcajada, P., Rámila, A., Pérez-Pariente, J., Vallet-Reg, M., (2004), 'Influence of pore size of MCM-41 matrices on drug delivery rate', *Microporous and Mesoporous. Materials*, 68, 105-109.
74. Horrocks, A. R., Anand, S. C., *Handbook of Technical Textiles*,(Cambridge: Woodhead Publishing Ltd, 2000), 1-559.
75. HPA (2011c). Quarterly Epidemiological Commentary: Mandatory MRSA & MSSA bacteraemia, and Clostridium difficile infection data (up to July – September 2011), pp. 3, 11.  
[http://www.hpa.org.uk/webc/HPAwebFile/HPAweb\\_C/1284473407318](http://www.hpa.org.uk/webc/HPAwebFile/HPAweb_C/1284473407318)
76. Hyldgaard, M., Mygind, T., Meyer, R. L., (2012), 'Essential oils in food preservation: mode of action, synergies, and interactions with food matrix components', *Frontiers in Microbiology*, 3, Article 12.
77. Iler, R. K., (1979), *The Chemistry of Silica*, Wiley, New York.
78. Iwami, Y., Kawarada, K., Kojima, I., Miyasawa, H., Kakuta, H., Mayanagi, H., (2002), 'Intracellular and extracellular pHs of Streptococcus mutans after addition of acids: loading and efflux of a fluorescent pH indicator in streptococcal cells', *Oral Microbiology and Immunology*, 17, 239-244.
79. Janssen, A. M., Scheffer, J. J. & Baerheim Svendsen, A., (1987), 'Antimicrobial activity of essential oils: a 1976–1986 literature review. Aspects of the test methods', *Planta Medica*, 53, 395–398.
80. Jitianu, A., Britchi, A., Deleanu, C., Badescu, V., Zaharescu, M., (2003),

- 'Comparative study of the sol-gel processes starting with different substituted Si-alkoxides', *Journal of Non-Crystalline Solids*, 319, 263-279.
81. Johnson, D., Lineweaver, L., and Maze, L.M. (2009). Patients' bath basins as potential sources of infection: a multicenter sampling study. *American Journal of Critical Care* 18, 31-38, 41; discussion 39-40.
82. Joshi, M., Wazed Ali, S., Purwar, R., (2008), 'Ecofriendly antimicrobial finishing of textiles using bioactive agents based on natural products', *Indian Journal of Fibre and Textile Research*, 34, 295-304.
83. Kealey, D., Haines, P. J., '*Instant notes: analytical chemistry*', BIOS Scientific Publishers Limited, (2002), 7, 1-342.
84. Khalaj, L., Farzin, D., (2006), 'Evaluation of antidepressant activities of rosewood oil and geranium oil in the forced swim test in mice', *European Neuropharmacology*, 16, 334-335.
85. Khan, M.S.A., Zahin, M., Hasan, S., Husain, F.M., Ahmad, I., (2009) 'Inhibition of quorum sensing regulated bacterial functions by plant essential oils with special reference to clove oil, *Letters in Applied Microbiology*', 49, 354-360.
86. Khan, A.P., Malki, A., Subhan Khan, H., (2012), 'Profile of candidiasis in HIV infected patients', *Iranian Journal of Microbiology*, 4, 204-209.
87. Kim, Y. H., Sun, G., (2000), 'Dye molecules as bridges for functional modifications of nylon: Antimicrobial functions', *Textile Research Journal*, 70, 728-733.
88. Kim, J., E. Kuk, K. Yu, J. Kim, S. Park, H. Lee, S. Kim, Y. Park, Y. Park, C. Hwang, Y. Kim, Y. Lee, D. Jeong., M. Cho, (2007) 'Antimicrobial effects of silver Nanoparticles'. *Nanomedicine*, 3, 95-101.
89. Kon, K., Rai, M., (2012), 'Antibacterial activity of *Thymus vulgaris* essential oil alone and in combination with other essential oils', *Bioscience*, 4, 50-56.

90. Kramer, A., Schwebke, I., Kampf, G. (2006), 'How long do nosocomial pathogens persist on inanimate surfaces?', *BMC Infectious Diseases*, 6, 130-138.
91. Krishnan, T. G., Shalini, V., Krishnaraj., (2015), 'Analysis of drug resistance *Pseudomonas aeruginosa* against the commonly used aminoglycoside antibiotic drugs, *Journal of Chemical and Pharmaceutical Research*, 7, 655-657.
92. Kwiecinski, J., Eick, S., Wojcik, K., (2009), 'Effects of tea tree oil on *Staphylococcus aureus* in biofilms and stationary growth phase', *Journal of Antimicrobial Agents*, 33, 343-347.
93. Lahlou, M., (2004), 'Methods to study the phytochemistry and bioactivity of essential oils', *Phytotherapy Research*, 18, 435-438.
94. Lambert, R. J. W., Skandamis, P. M., Coote, P. J., Nychas, G. J. E., (2001), 'A study of the minimum inhibitory concentration and mode of action of oregano essential oil, thymol and carvacrol', *Journal of Applied Microbiology*, 91, 453-462.
95. Langeveld, W. T., Veldhuizen, E. J. A., Burt, S. A., (2014), 'Synergy between essential oil components and antibiotics: a review', *Critical Reviews in Microbiology*, 40, 76-94.
96. Lanini, S., D'Arezzo, S., Puro, V., Martini, L., Imperi, F. (2011) 'Molecular Epidemiology of a *Pseudomonas aeruginosa* Hospital Outbreak Driven by a Contaminated Disinfectant-Soap Dispenser', *PLoS ONE*, 6, e17064.
97. Laureti, L., Matic, I., Gutierrez, A. (2013), 'Bacterial Responses and Genome Instability Induced by Subinhibitory Concentrations of Antibiotics', *Antibiotics*, 2, 100 – 114.
98. Liakos, I., Rizzello, L., Scurr, D. J., Pompa, P. P., Bayer, I. S., Athanassiou, A., (2014), 'All-natural composite wound dressing films of essential oils encapsulated in sodium alginate with antimicrobial

- properties', International Journal of Pharmaceutics, 463, 137-145.
99. Liauw, C.M. Hurst, S.J., Lees, G.C., Rother, R.N., Dobson, D.C., (1995), 'Investigation of the surface modification of aluminium hydroxide filler and optimum modifier dosage level', Plastics Rubber and Composites Processing and Applications, 24, 211-219.
100. Loughlin, R., Gimore, B. F., McCarron, P. A., Tunney, M. M., (2008), 'Comparison of the cidal activity of tea tree oil and terpinen-4-ol against clinical bacterial skin isolates and human fibroblast cells', Letters in Applied Microbiology, 46, 428-433.
101. Lu, G. T., Huang, Y., (2002), 'Synthesis of polymaleimide/silica nanocomposites', Journal of Material Science, 37, 2305-2309.
102. Lu, J., Liong, M., Zink, I., Tamanoi, F., (2007), 'Mesoporous Silica Nanoparticles as a Delivery System for Hydrophobic Anticancer Drugs', SMALL, 3, 1341-1346.
103. Mackenzie, J., Bescher, E. P., (1998), 'Structures, Properties and potential Applications of Ormosils', Journal of Sol-Gel Science and Technology, 1, 371-377.
104. Mahltig, B., Fiedler, D., Bottcher, H., (2004), 'Antimicrobial sol-gel coatings', Journal of SolGel Science and Technology, 32, 219-222.
105. Mahltig, B., Fiedler, D., Fischer, A., Simon, P., (2010), 'Antimicrobial coatings on textiles-modification of sol-gel layers with organic and inorganic biocides', Journal of Sol-Gel Science and Technology, 55, 269-277.
106. Maji, T. K., Baruah, I., Dube, S., Hussain, M. R., (2007), 'Microencapsulation of *Zanthoxylum limonella* oil (ZLO) in glutaraldehyde crosslinked gelatin for mosquito repellent application', Bioresource Technology, 98, 840-844.
107. Mann, C. M., Cox, S. D., Markham, J. L., (2000), 'The outer

- membrane of *Pseudomonas aeruginosa* NCTC 6749 contributes to its tolerance to the essential oil of *Melaleuca alternifolia* (tea tree oil)', Letters in Applied Microbiology, 30, 294-297.
108. McDonagh. C., MacCraith. B.D., McEvoy. A. K., (1998), 'Tailoring of sol-gel films for optical Sensing of Oxygen in Gas and Aqueous Phase', Analytical Chemistry, 70, 45-50.
109. Meixner, D. L., Dyer, P. N., (1999), 'Influence of sol-gel synthesis parameters on the microstructure of particulate silica xerogels', Journal of Sol-Gel Science Technology, 14, 223–232.
110. Meletiadis, J., Pournaras, S., Roilides, E., Walsh, T. J., (2010) 'Defining fractional inhibitory concentration index cutoffs for additive interactions based on self-drug additive combinations, Monte Carlo simulation analysis, and in vitro-in vivo correlation data for antifungal drug combinations against *Aspergillus fumigatus*', Antimicrobial Agents and Chemotherapy, 54, 602-609.
111. Milwich, M., Speck, T., Speck, O., Stegmaier, T., Planck, H., (2006), 'Biomimetics and Technical Textiles: Solving Engineering Problems With The Help of Nature's Wisdom', American Journal of Botany, 93, 1455-1465.
112. Musgo, J., Echeverria, J. C., Estella, J., Laguna, M., Garrido, J. J., (2009), 'Ammonia-catalyzed silica xerogels: Simultaneous effects of pH, synthesis temperature, and ethanol:TEOS and water:TEOS molar ratios on textural and structural properties', Microporous and Mesoporous Materials, 118, 280–287.
113. Muyldermans, G., de Smet, F., Pierard, D., Steenssens, L., Stevens, D., Bougateg, A., and Lauwers, S. (1998). Neonatal infections with *Pseudomonas aeruginosa* associated with a water-bath used to thaw fresh frozen plasma. J Hosp Infect 39, 309-314.

114. Naik, M. I., Fomda, B. A., Jaykumar, E., Bhat, J. A., (2010), 'Antibacterial activity of lemongrass oil against some selected pathogenic bacterias', *Asain Pacific Journal of tropical Medicine*, 535-538.
115. Nair, S., A. Sasidharan, V. Divya Rani, D. Menon, K. Manzoor. S. Raina, (2009) 'Role of size scale of ZnO nanoparticles and microparticles on toxicity toward bacteria and osteoblast cancer cells'. *Journal of Materials Science*, 20, 235- 41.
116. NAO (2009). *Reducing Healthcare Associated Infections in Hospitals in England*.
117. Nazzaro, F., Fratianni, F., De Martino, L., Coppola, R., De Feo, V., (2013), 'Effect of Essential Oils on Pathogenic Bacteria', *Pharmaceuticals*, 6, 1451-1474.
118. Nazer, A. I., Kobilinsky, A., Tholozan, J. L., and Dubois-Brissonnet, F., (2005), 'Combinations of food antimicrobials at low levels to inhibit the growth of *Salmonella* sv. Typhimurium: a synergistic effect?' *Food Microbiology*, 22, 391-398.
119. Nelson, G., (2001), 'Microencapsulation in textile finishing', *Coloration Technology*, 31, 57-64.
120. Orhan, M., Kut, D., Gunesoglu, C., (2006), 'Use of triclosan as antibacterial agent in textiles', *Indian Journal of Fibre and Textile Research*, 32, 114-118.
121. Othman. Z. A. AL., (2012), 'Areview: Fundamental Aspects of Silicate Mesoporous Materials', *Materials*, 5, 2874-2902.
122. Oussalah, M., Caillet, S., Saucier, L., Lacroix, M., (2006), 'Antimicrobial effects of selected plant essential oils on the growth of a *Pseudomonas putida* strain isolated from meat', *Meat Science*, 73, 236-244.
123. Pal, S., Y. Tak. J. Song, (2007) 'Does the antibacterial activity of silver

- nanoparticles depend on the shape of the nanoparticle? A study of the Gram-negative bacterium *Escherichia coli*'. *Applied Environmental Microbiology*, 73, 1712-20.
124. Pardal, F., Lapinte, V., Robin, J. J., (2009), 'Modification of Silica Nanoparticles by Grafting of Copolymers Containing Organosilane and Fluorine Moieties', *Polymer Chemistry*, 47, 4617-4628.
  125. Pariss, N., Cooke, P. H., Hicks, K. B., (2005), 'Encapsulation of essential oils in zein nanospherical particles', *Journal of Agricultural Food Chemistry*, 53, 4788-4792.
  126. Park, S. Y., Pendleton, P., (2012), 'Mesoporous silica SBA-15 for natural antimicrobial delivery', *Powder Technology*, 223, 77-82.
  127. Pauli, A., and Schilcher, H., (2010), '*In vitro* antimicrobial activities of essential oils monographed in the European pharmacopoeia 6<sup>th</sup> Edition', *Handbook of essential oils. Science Technology and Application*. Boca Raton, London. Taylor and Francis Group, 353-548.
  128. Pennycook, S. J., Nellist, P. D., '*Scanning transmission electron microscopy: imaging and analysis*', Springer New York, (2011), 1-762.
  129. Percival, S. L., Bowler, P. G., Russell, D., (2005), 'Bacterial resistance to silver in wound care', *Journal of Hospital Infection*, 60, 1-7.
  130. Perera, S., Bhushan, B., Bandara, R., Rajapakse, G., Rajapakse, S., Bandara, C., (2013), 'Morphological, antimicrobial, durability, and physical properties of untreated and treated textiles using silver-nanoparticles', *Colloids and surfaces A*, 436, 975-989.
  131. Petrovic, Z. S., Javni, I., Waddon, A., Banhegyi, G., (2000), 'Structure and properties of polyurethane-silica nanocomposites', *Journal of Applied Polymer Science*, 76, 133-151.
  132. Plummer, S., Weaver, M. A., Harris, J. C., Dee, P., Hunter, J., (2004), 'Clostridium difficile pilot study: effects of probiotic supplementation

- on the incidence of *C. difficile* diarrhoea', *International Microbiology*, 7, 59 – 62.
133. Prabuseenivasan, S., Jayakumar, M., Ignacimuthu, S., (2006), '*In vitro* antibacterial activity of some plant essential oils', *BMC Complementary and Alternative Medicine*, 6, 39.
134. Quieroz, J. R. C., Benetti, P., Ozcan, M., de Oliveira, L. F. C., Della Bona, A., Takahashi, F. E., Bottino, M. A., (2012), 'Surface characterization of feldspathic ceramic using ATR FT-IT and ellipsometry after various silanization protocols', *Dental Materials*, 28, 189-196.
135. Rahal, J.J., Urban, C., and Segal-Maurer, S. (2002). Nosocomial antibiotic resistance in multiple gram-negative species: experience at one hospital with squeezing the resistance balloon at multiple sites. *Clinical Infectious Disease* 34, 499-503.
136. Rajendran, R., Balakumar, C., Ahammed, H. A. M., Jayakumar, S., Vaideki, K., Rajesh, E. M., (2010), 'Use of zinc oxide nano particles for production of antimicrobial textiles', *International Journal of Engineering, Science and Technology*, 2, 202-208.
137. Renneberg, J., *Definitions of Antibacterial Interactions in Animal Infection Models*. *Journal of Antimicrobial Chemotherapy*, (1993), 31(Supplement D): p. 167-175.
138. Riedel, S., Beekmann, S. E., Heilmann, K, P., Richter, S. S., Garcia-de-Lomas J., Ferech M., (2007) Antimicrobial use in Europe and antimicrobial resistance in *Streptococcus pneumoniae*. *European Journal Clinical Microbiological Infectious Disease*, 26, 485-90.
139. Rios, X., Moriones, P., Echeverria, J. C., Luquin, A., Laguna, M., Garrido, J. J., (2011), 'Characterisation of hybrid Xerogels synthesised in acid media using methyltriethoxysilane (MTEOS) and tetraethoxysilane (TEOS) as precursors', *Adsorption*, 17, 583-593.

140. Rosato, A., Vitali, C., De Laurentis, N., Armenise, D., and Antonietta Milillo, M., (2007), 'Antibacterial effect of some essential oils administered alone or in combination with Norfloxacin', *Phytomedicine*, 14, 727-732.
141. Salonen, J., Kaukonen, A. M., Hirvonen, J., Lehto, V. P., (2008), 'Mesoporous silicon in drug delivery applications', *Journal of Pharmaceutical Sciences*, 97, 632-653.
142. Schindler, W. D., Hauser, P. J., *Chemical Finishing of Textiles* (Cambridge: Woodhead Publishing Ltd, 2004) 74.
143. Shaw, D. J., '*Introduction to Colloid & Surface Chemistry*', 4 ed, Butterworth Heinemann, (1992), 1-306.
144. Singleton, P., *Bacteria in Biology, Biotechnology and Medicine*. 6 ed. (2004), Chichester: John Wiley and Sons.
145. Sivropoulou, A., Kokkini, S., Lanaras, T., and Arsenakis, M., (1995), 'Antimicrobial activity of mint essential oils', *Journal of Agricultural and Food Chemistry*, 43, 2384-2388.
146. Sondi, I., B. Salopek-Sondi, (2004) 'Silver nanoparticles as antimicrobial agent: a case study on E. coli as a model for Gram-negative bacteria'. *Journal of Colloidal Interface Science*, 275, 177-82.
147. Stevens, D., (2006), 'Streptococcal and Staphylococcal Infections', *Tropical Infectious Diseases*, (Second Edition), 356-368.
148. Sullivan, A., Edlund, C., Nord, C. E., (2001), 'Effect of antimicrobial agents on the ecological balance of human microflora', *The Lancet Infectious Disease*, 1, 101-114.
149. Szabo, I. A., Varga, G. Z., Hohmann, J., Schelz, Z., Szegedi, E., Amaral, L., (2010), 'Inhibition of Quorum sensing signals by essential oils', *Phytotherapy Research*, 24, 782-786.
150. Talbot, G.H., Bradley, J., Edwards, J.E., Jr., Gilbert, D., Scheld, M., and Bartlett, J.G. (2006). Bad bugs need drugs: an update on the

- development pipeline from the Antimicrobial Availability Task Force of the Infectious Diseases Society of America. *Clinical Infectious Disease* 42, 657- 668.
151. Tangarife-Castano, V., Correa-Royero, J., Zapata-Londono, B., Duran, C., Stanshenko, E., Mesa-Arango, A. C., (2011), 'Anti-Candida Albicans activity, cytotoxicity and interaction with antifungal drugs and essential oils and extracts from aromatic and medical plants', *Infection*, 15, 160-167.
152. Tanner, B., (2009), 'Antimicrobial Fabrics – Issues and opportunities in the Era of Antibiotic Resistance', *Applied Technology Article*, 9, 30-33.
153. Tenover, F. C., (2006), 'Mechanisms of Antimicrobial Resistance in Bacteria', *The American Journal of Medicine*, 119, 53-510.
154. Thilagavathi, G., Kannaian, T., (2010), 'Combined antimicrobial and aroma finishing treatment for cotton, using micro encapsulated geranium leaves extract', *Indian Journal of Natural Products and Resources*, 1, 348-352.
155. Thompson, J. D., Chalchat, J. C., Michet, A., Linhart, Y. B., Ehlers, B., (2003), 'QUALITATIVE AND QUANTITATIVE VARIATION IN MONOTERPENE CO-OCCURRENCE AND COMPOSITION IN THE ESSENTIAL OIL OF *Thymus vulgaris* CHEMOTYPES', *Journal of Chemical Ecology*, 29, 859-880.
156. Tortora, G.J., Funke, B.R., and Case, C.L., *Microbiology an Introduction*. 9 ed. (2007), San Francisco: Pearson Benjamin Cummings.
157. Trewyn, B. G., Slowing, I. I., Giri, S., Chen, H. T., Lin, V. S. Y., (2007), 'Synthesis and Functionalization of a Mesoporous Silica Nanoparticle Based on the Sol-Gel Process and Applications in Controlled Release', *Accounts of Chemical Research*, 2007, 40, 846-853.

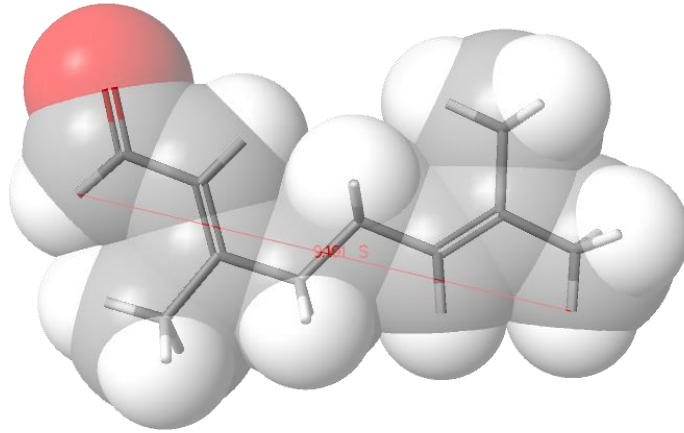
158. Trombetta, D., Castelli, F., Sarpietro, M. G., Venuti, V., Cristani, V., Daniele, C., Saija, A., Mazzanti, G., Bisignano, G. (2005), 'Mechanisms of antibacterial action of three monoterpenes', *Antimicrobial Agents and Chemotherapy*, 49, 2474-2478.
159. Utree, A., Kets, E. P. W., Smid, E. J. (1999), 'Mechanisms of Action of Carvacrol on the Food-Borne Pathogen *Bacillus cereus*', *Applied and Environmental Microbiology*, 65, 4606-4610.
160. Utree, A., Slump, R. A., Smid, E. J., (2000), 'Antimicrobial activity of carvacrol towards *Bacillus cereus* on rice', *Journal of Food Protection*, 63, 620-624.
161. Upadhyay, R. K., Dwivedi, P., Ahmad, S., (2010), 'Screening of Antibacterial Activity of Six Plant Essential Oils Against Pathogenic Bacterial Strains', *Asia Journal of Medical Sciences*, 2, 152-158.
162. Van de Braak, S.A.A.J., Leijten, G.C.J.J., (1999), 'Essential oils and oleoresins: a survey in the Netherlands and other major markets in the European Union', Rotterdam: CBI, Centre for the promotion of imports from developing countries, Rotterdam, 116.
163. Veerabadran, S., Parkinson, I. M. (2010), 'Cleaning, disinfection and sterilization of equipment', *Clinical Anaesthesia*, 11, 451 – 454.
164. Verhaegh N.A., van Blaaderen A., (1994), 'Dispersions of rhodamine-labeled silica spheres: Synthesis, characterization, and fluorescence confocal scanning laser microscopy', *Langmuir*, 10, 1427-1438.
165. Walentowska, J., Foksowicz-Flaczyk, J., (2013), 'Thyme essential oil for antimicrobial protection of natural textiles', *International Biodeterioration and Biodegradation*, 84, 407-411.
166. Wallace, R. J., (2004), 'Antimicrobial properties of plant secondary metabolites', *Proceedings of the Nutrition Society*, 63, 621-629.
167. Warnke, P. H. (2009), 'The battle against multi-resistant strains:

- Renaissance of antimicrobial essential oils as a promising force to fight hospital-acquired infections'. *Journal of Cranio-Maxillofacial surgery*, 37, 392-397.
168. Wencel. D., Higgins. C., Klukowska. B., MacCraith. B. D., McDonagh. C., (2007) 'Novel sol-gel derived films for luminescence-based oxygen and pH sensing', *Materials Science*, 25, 767-779.
169. Wiener-Well, Y., Galuty, M., Rudensky, B., Schlesinger, Y., Attias, D., Yinnon, A. M., (2011), 'Nursing and physician attire as possible source of nosocomial infections', *American Journal of Infection Control*, 39, 555-559.
170. WHO. Antimicrobial Resistance. Global Report on Surveillance.
171. Williams, D., *Lecture Notes on Essential Oils*. 1989, Long Melford: Bush Boake Allen Ltd.
172. Windler, L., Height, M., Nowack, B., (2013), 'Comparative evaluation of antimicrobials for textile applications', *Environment International*, 53, 62-73.
173. Xiangling, J., Hampsey, J. E., Hu, Q., He, J., Yang, Z., Lu, Y., (2003), 'Mesoporous Silica-Reinforced Polymer Nanocomposites', *Chemical Materials*, 15, 3656-3662.
174. Yamanaka, M., Hara, K., Kudo, J., (2005) 'Bactericidal actions of a silver ion solution on Escherichia coli, studied by energy-filtering transmission electron microscopy and proteomic analysis', *Applications in Environmental Microbiology*, 71, 7589-93.
175. Yanagisawa, T., Shimizu, T., Kuroda, K., Kato, C., (1990), 'The Preparation of Complexes and Their Conversion to Microporous Materials', *Bulletin of The Chemical Society of Japan*, 63, 988-992.
176. Yang, Y.L., (2003), 'Virulence factors of Candida species', *Journal of Microbiological Immunological Infection*, 36, 223–228.

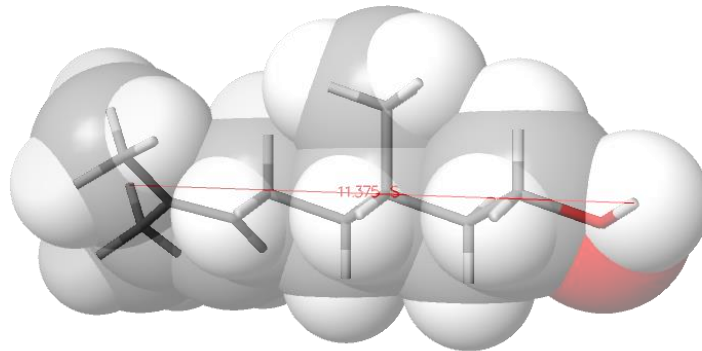
177. Zhang, M., O'Donoghue, M.M., Ito, T., Hiramatsu, K., Boost, M.V. (2011), 'Prevalence of antiseptic-resistance genes in *Staphylococcus aureus* and coagulase-negative staphylococci colonising nurses and the general population in Hong Kong', *Journal of Hospital Infection*, 78, 113 – 117.
178. Zou, L., Meng, J., McDermott, P. F., Wang, F., Yang, Q., Cao, G., Hoffmann, M., Zhao, S. (2014), 'Presence of disinfectant resistance genes in *Escherichia coli* isolated from retail meats in the USA', *Journal of Antimicrobial Chemotherapy*, 69(10), 2644 – 2649.

## Appendices

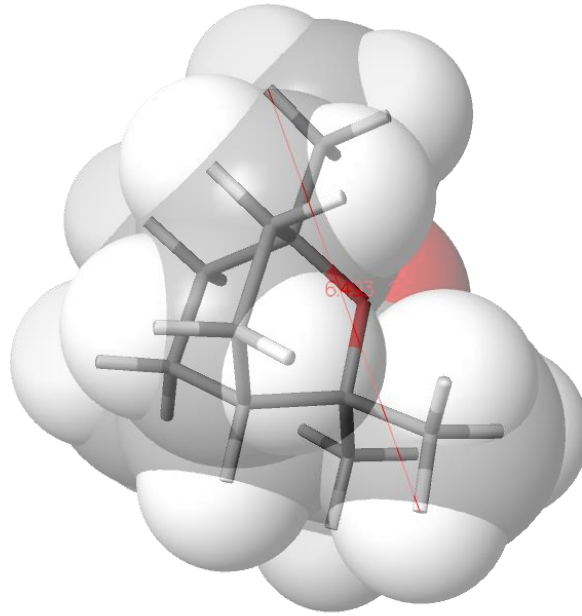
### Appendix I



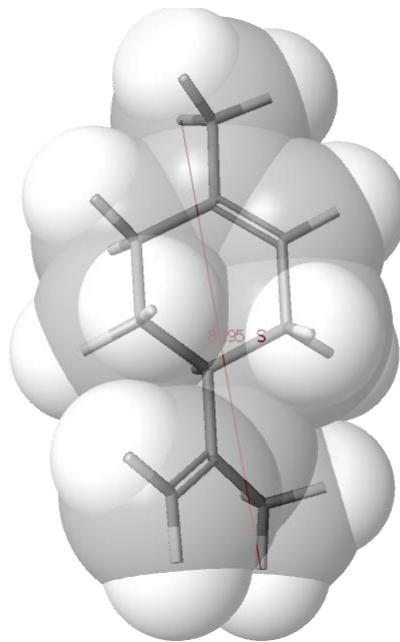
Citral, main constituent of lemongrass oil



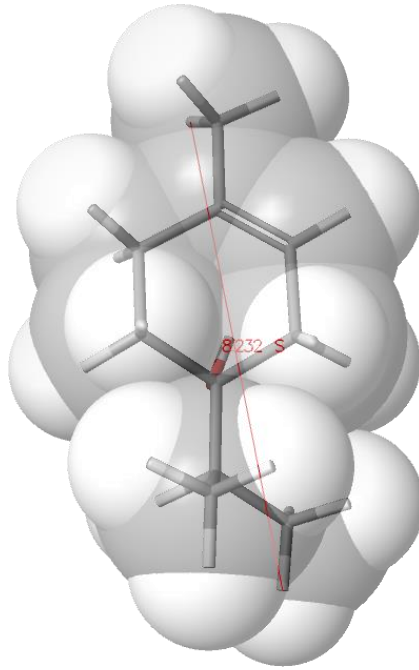
Citronellol, main constituent of geranium oil



Eucalyptol, main constituent of eucalyptus oil

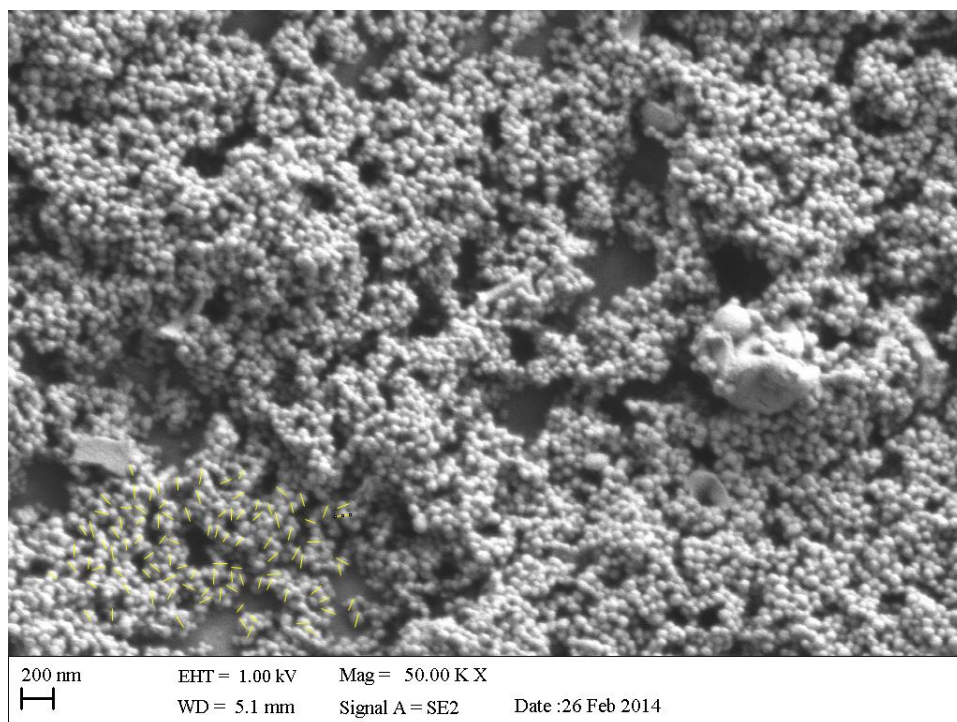


Limonene, main constituent of lime oil



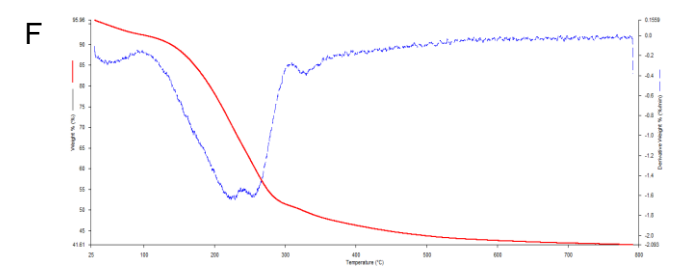
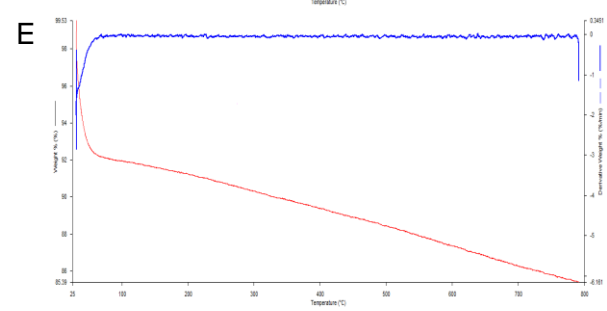
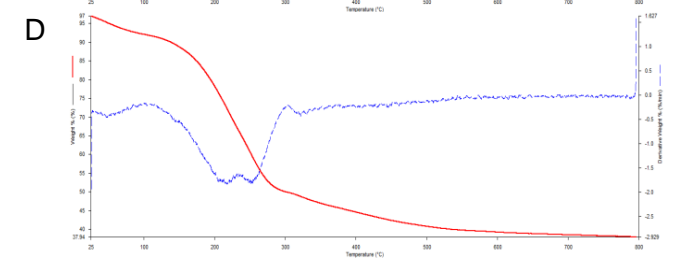
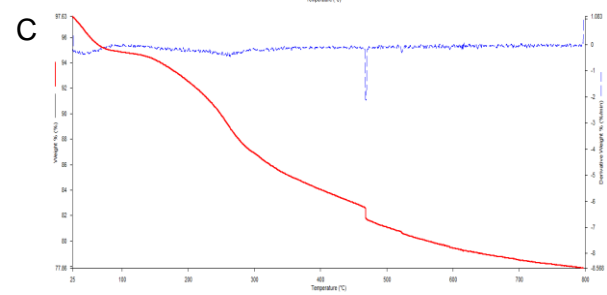
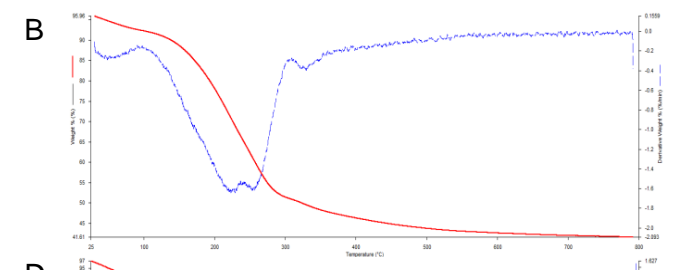
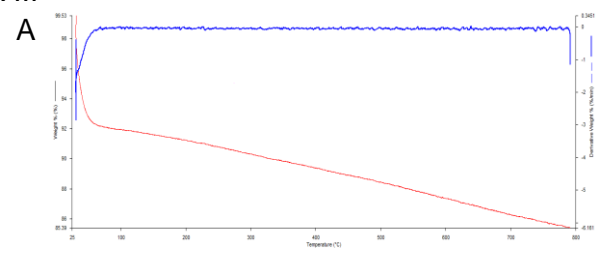
Terpinen-4-ol, main constituent of tea tree oil

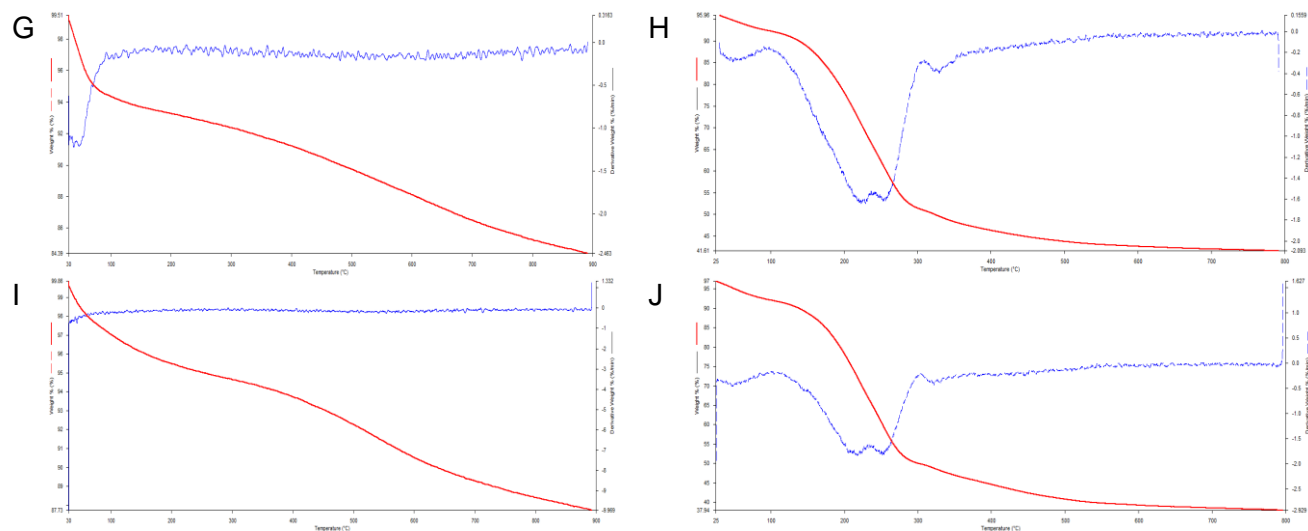
## Appendix II



Example of sizing MSN sample 1, using image J. The diameter of 100 nanoparticles (bottom left corner of the image) were recorded and averaged.

Appendix III





Thermogravimetric analysis (solid line) and derivative thermogravimetric curve (dotted line) of surfactant intact MSN samples 1-5 – A, C, E, G, I. Also, MSN samples 1-5 post calcination, B, D, F, H, J.